CARDIAC ENERGY METABOLISM IN ISCHAEMIA AND TYPE 1 DIABETES

Ross Thomas Lindsay

Jesus College

University of Cambridge

This dissertation is submitted for the degree of doctor of philosophy

August 2018

This dissertation is the result of my own work and includes nothing which is the outcome of work done in collaboration except as declared in the Preface and specified in the text.

It is not substantially the same as any that I have submitted, or, is being concurrently submitted for a degree or diploma or other qualification at the University of Cambridge or any other University or similar institution except as declared in the Preface and specified in the text. I further state that no substantial part of my dissertation has already been submitted, or, is being concurrently submitted for any such degree, diploma or other qualification at the University of Cambridge or any other University or similar institution except as declared in the Preface and specified in the text

It does not exceed the prescribed word limit for the relevant Degree Committee

ACKNOWLEDGEMENTS

My time working in the laboratories of Andrew Murray and Julian Griffin has been a fantastic experience. Andrew has always been very supportive, and his confidence and ability to let me learn and plan for myself rather than simply providing answers or directions has greatly enhanced my development over the last three years. Jules has always offered the enthusiasm and encouragement to keep this thesis going, has an incredible work ethic, and in taking me in for a summer project as an undergraduate was the first to show me how enjoyable and rewarding working in a lab could be. I've come to the end with the utmost regard for both of them, and wherever I go will always be their student.

In the Murray lab, the people I've worked with have been brilliant. Sophie Dieckmann spent a fantastic year in the lab, and the place still doesn't feel quite the same without her, whether it was whisky tastings, Deutsche Donnerstage, or just generally keeping me sane through hours of experiments. Dominic Manetta-Jones with an exceptional brand of dry wit was also a great lab partner, and I've never met anybody more ready to suggest a trip to Wetherspoons. James Horscroft did a fantastic job of showing me the ropes when I first started in the lab and Katie O'Brien has also always been a cheerful source of company and music. Jules Devaux and Mitchel Tate had all too short stays with the group, but made the place great fun while they were here, whether through throwing a rugby ball knee deep in the Welsh snow or through wise life advice and help depriving German brauhauses of their beer. All of the students who have come through the lab have also been great fun (and mostly called Alice, which has made the job of remembering their names considerably easier!)

In Jules' group, without a doubt the person I've spent the most time with over the years has been the long suffering James West, who has spent many an hour enlightening me on his multiple subjects of expertise. This project owes a great deal to the devotion of his time, and I'm grateful for both that and his company. The others who have been invaluable to this project are Ben McNally for his assistance with running samples, Steve Murfitt for doing his thing, Zoe Hall, and Cecilia Castro, whose initial observation during a pilot run was the spark for a whole chapter of this thesis. Everybody else in the group has also been great company, and it's been fun to be part of a group of people doing such a diversity of things.

First and foremost among the others in PDN who deserve a mention is Katie Davies, who has kept me company through hundreds of lunch breaks, days in the lab and other more sociable things. She has been and is a great friend who has made the whole PhD experience so much more fun. Yougiu Niu was an invaluable help when initially setting up and learning to use the rig in the lab, as was Christian Beck who also lent his expertise on top of being a great friend and introducing me to the finest of

Frankfurt's wein and schweinshaxe. Ana Mishel, Nozomi, Shani and Nadia have also all been great to have around, inducting me into their labs' social calendar when I had no labmates in PDN and making the whole place more fun. My work in the facility wouldn't have been possible without Chris, Julie, Hayley and Damian, and nothing at all would have been possible without the ever friendly assistance of Mick King and Debbie McQuillan. Alan Cattell with a multitude of talents and great humour always welcomed a challenge, and a special mention should go to Aileen Briggs for looking after all of the PhD students so well.

In Denmark, I had the fortune to work with a collection of talented and friendly people at Gubra. Special thanks should go to Lisbeth Fink, whose friendly style of management and insights throughout were an inspiration and whose arrangements made it both possible for me to get to Gubra, and feel very welcome when I did. The project would have gone nowhere without Louise, who led it and introduced me to many Danish foods such as risengrød and pingvin lakrids, and Nora, who designed it, taught me echo - and thankfully actually wanted to eat the lakrids! There are many to thank, including Keld for inviting me; Mette and Katrine for our sessions in the surgery room; the ever friendly Sisse for making sure I had a place to stay; Sebastian and Martin for their work with RNAseq; Bo, Simon, Annette, Lisbeth, Mathilde, Bente, Eva and Lotte for sharing their lab and helping me to get set up; and everybody in the office, in the "young Gubra" crowd and at lunch who were regularly kind enough to switch to English and have a great conversation.

Lisa Heather and Luz Sousa Fialho were kind enough to host me in Oxford three years ago, and to them I would like to extend a warm thank you for teaching me skills which have made all of this work possible.

Grateful thanks to the British Heart Foundation for funding this work and me, giving me the opportunity to have four fantastic years. Martin Bennett and Anthony Davenport do a fantastic job of heading up the finest PhD programme in Cambridge, and Suzanne deserves many thanks for keeping us right and administering for all of the students, which can't be easy and which she does with excellence.

Last but most importantly, thank you very much to my family and my friends for supporting me and helping make my life here so enjoyable.

SUMMARY

Ischaemic heart disease represents a restriction of blood, and therefore oxygen, supply to the myocardium. This leads to a remodelling of cardiac metabolism, which can exacerbate production of damaging reactive oxygen species and tissue necrosis upon reperfusion. In a different paradigm of metabolic disease, the type-1 diabetic heart becomes more dependent upon the oxidation of fatty acids (FAO) for ATP synthesis due to an inability to regulate blood glucose concentration. The work presented in this thesis aimed to further our understanding of substrate selection and metabolism in the ischaemic and type-1 diabetic hearts.

A mathematical network model for tracing universally-^{13}C labelled metabolic substrates through the Krebs cycle using mass spectrometry was developed and presented. Experimentally-observed isotopologue distributions of Krebs cycle intermediates and proxies were interpreted using this model to determine the percentage of acetyl-CoA oxidised in the Krebs cycle which originated from the U-^{13}C labelled substrate.

In the Langendorff perfused rat heart, perfusion with intralipid resulted in greater functional recovery following ischaemia/reperfusion. Supplementation with dietary nitrate ablated this cardioprotective effect, but this highlights the importance of fatty acid oxidation to recovery from ischaemia/reperfusion injury.

Ketogenesis was found to occur in the ischaemic heart, and was not specifically dependent upon either fatty acid or glucose oxidation. Its inhibition resulted in improved recovery of contractile function following ischaemia/reperfusion, suggesting the ketogenesis which occurs during cardiac ischaemia is a detrimental process.

Isoprenaline administration conserved mitochondrial respiratory capacity and energetics in the type-1 diabetic rat heart. 10 weeks following removal of 90% of the pancreas (Px), mitochondrial respiratory capacity was impaired, with a substrate switch towards fatty acid oxidation (FAO) observed alongside greater expression of FAO-related enzymes and evidence of oxidative stress. Isoprenaline administration also impaired respiratory capacity, but enhanced flux through glycolysis. In the hearts of isoprenaline treated Px rats, mitochondrial respiratory capacity and energetics were conserved.

In conclusion, cardiac ischaemia and type-1 diabetes both represent diseases where metabolic substrate oxidation is perturbed. FAO is not detrimental to the ischaemic or type-1 diabetic heart without associated loss of metabolic flexibility, and even appears beneficial to recovery following ischaemia/reperfusion.

CONTENTS

ABBREVIATIONS

ΔμH+	proton motive force
$\Delta G'^{ATP}$	free energy of ATP hydrolysis
ΔG^{OATP}	standard free energy of ATP
ΔS	entropy change
ACAD	acyl-CoA dehydrogenase
ADP	adenine diphosphate
AMP	adenine monophosphate
Amu	atomic mass unit
ANOVA	analysis of variance
ATP	adenine triphosphate
BDH	β-hydroxybutyrate dehydrogenase
BSA	bovine serum albumin
bpm	beats per minute
CACT	carnitine-acylcarnitine translocase
CoA	coenzyme A
CPT	carnitine palmitoyl transferase
Cr	creatine
ETC	electron transport chain
ETF	electron transferring flavoprotein
FAD	flavin adenine dinucleotide
$FADH_2$	reduced flavin adenine dinucleotide
FAO	fatty acid oxidation
G6PDH	glucose-6-phosphate dehydrogenase
GDP	guanine diphosphate
GMP	guanine monophosphate
GSH	reduced glutathione
GSSG	oxidised glutathione
GTP	guanine triphosphate
HMG-CoA	β-Hydroxy β-methylglutaryl-CoA

HOAD	3-hydroxyacyl-CoA dehydrogenase
HIF	hypoxia-inducible factor
HILIC	hydrophilic interaction liquid chromatography
HK	hexokinase
HR	heart rate
HRR	high-resolution respirometry
JO2	rate of O2 consumption
KH	Krebs-Henseleit
LDH	lactate dehydrogenase
LVDP	left ventricular developed pressure
MCKAT	medium chain 3-ketoacyl-CoA thiolase
MCT	monocarboxylate transporter
MetSO	methionine sulfoxide
mmHg	mm of mercury
mtDNA	mitochondrial DNA
MTP	mitochondrial trifunctional protein
mtPTP	mitochondrial permeability transition pore
m/z	mass to charge ratio
NAD+	nicotinamide adenine dinucleotide
NADH	reduced nicotinamide adenine dinucleotide
NMN	nicotinamide mononucleotide
NO	nitric oxide
NOS	nitric oxide synthase
Oxphos	oxidative phosphorylation
PCr	phosphocreatine
PDH	pyruvate dehydrogenase
PDK	pyruvate dehydrogenase kinase
PGC-1α	peroxisome proliferator-activated receptor-gamma coactivator 1-alpha
PHD	prolyl hydroxylase
PPAR	peroxisome proliferator-activated receptor
RCR	respiratory control ratio

RNA	ribose nucleic acid
ROS	reactive oxygen species
RPP	rate pressure product
SCOT	succinyl-CoA-3-oxaloacid CoA transferase
SEM	standard error of the mean
SUIT	substrate-uncoupler-inhibitor titration
UCP	uncoupling protein
VEGF	vascular endothelial growth factor

CHAPTER 1

Introduction

STATEMENT OF RELEVANCE

Myocardial infarction, the underlying cause of a heart attack, has a vast social and economic impact on the UK and is the largest single cause of mortality. 433000 hospital admissions and 66000 deaths are the result of a heart attack each year in the UK (BHF, 2018b, 2018a). Furthermore, even those who survive treatment following a heart attack are likely to face secondary complications and spend the rest of their lives taking drugs for symptoms. In the US those who have previously suffered a heart attack are 2.8 times more likely to be diagnosed with heart failure in future (Hugli et al., 2001), and between 10-20% of those hospitalised for heart failure have previously been admitted for a heart attack (Fang et al., 2008; Hugli et al., 2001). Direct costs of heart attack related healthcare in the UK are estimated to be around £3bn, while the total loss to the economy is thought to be as high as £7-10bn (Astrazeneca, 2009; Liu et al., 2002).

On top of the mortality it causes in its own right, Diabetes Mellitus represents a further cause of mortality through increasing susceptibility to several forms of heart disease. 40% of those presenting with acute heart failure syndrome have a history of diabetes (Gheorghiade and Pang, 2009), and the risk of suffering a heart attack is 3.5 times greater for sufferers of type 1 diabetes than for a non-diabetic individual (NHS, 2017). £51m and £31m are estimated to be spent annually on diabetic patients who contract ischaemic heart disease or heart failure, respectively (Hex et al., 2012).

Both ischaemia and diabetes are essentially metabolic diseases. Ischaemia stems from the occlusion of blood and oxygen supply to the heart, and as oxygen is directly involved in energy metabolism as the final electron acceptor of the electron transport chain this drastically disrupts metabolism. Diabetes mellitus meanwhile leads to dysregulation of blood sugar and fatty acid levels, and since these are both important metabolic substrates this also has a severe impact upon cardiac metabolism as is discussed in greater depth in **Chapter 6**. Study and manipulation of the heart's metabolism is therefore essential to further understanding the mechanisms of these diseases, and offers a direct opportunity for interventions which may lessen or reverse symptoms and hopefully in the long run improve the mortality statistics mentioned above.

This work is funded by the British Heart Foundation, who have a goal to eradicate all cardiovascular disease. Through helping understand the metabolic mechanisms behind ischaemia and type 1 diabetes in the heart, the work in this thesis aligns with this goal, and will hopefully lead to better understanding and identification of targets for treating these diseases in the future.

1.1 ENERGY, METABOLISM AND THE ROLE OF OXYGEN

Electrons and protons obtained from the catabolism of high energy substrates play a crucial part in generating the energy all organisms require to function. These are themselves generated through the sequential catabolism of macromolecules such as fatty acids, carbohydrates and proteins. However, whilst the generation and manipulation of these sub-atomic particles is key to the process of converting stored energy into a useable form, they can be highly damaging to the cell if allowed to accumulate.

Oxygen is therefore employed to facilitate safe excretion of subatomic catabolic products while enabling continuation of energy metabolism. Readily available as an atmospheric gas and highly electronegative, O_2 can react with protons and electrons to form water, a safe and stable vehicle molecule for electron disposal which may also be further be employed by the cell in catabolic reactions. Oxygen is the final electron acceptor of the respiratory chain, with its point of action coming after the electrons have passed along the mitochondrial electron transport chain (ETC) to drive oxidative metabolism **(Figure 1.1)**. When electrons reach complex IV, four of these electrons are accepted by oxygen, along with four protons, in order to form two molecules of H_2O.

Metabolic oxygen consumption is therefore directly related to the flow of electrons through the electron transport chain. Electrons harvested from catabolic metabolism are transferred via NADH or $FADH_2$, until entering the mammalian ETC through one of three main points. Complex I provides an interface for the acceptance of electrons carried by NADH, using the energy released to pump four protons into the intermembrane space. Meanwhile, complex II catalyses the removal of electrons from succinate via $FADH_2$. The $FADH_2$ which is generated from the β-oxidation of fatty acids donates its electrons similarly through the electron transferring flavoprotein (ETF). All three electron receptors transfer electrons to complex III via the ubiquinone pool, which passes them along to cytochrome *c* in a reaction further associated with protons being pumped into the intermembrane space. Cytochrome *c* oxidase (complex IV) pumps two further protons across the membrane upon receipt of these electrons, the energy for this being released during the acceptance of the electron by oxygen.

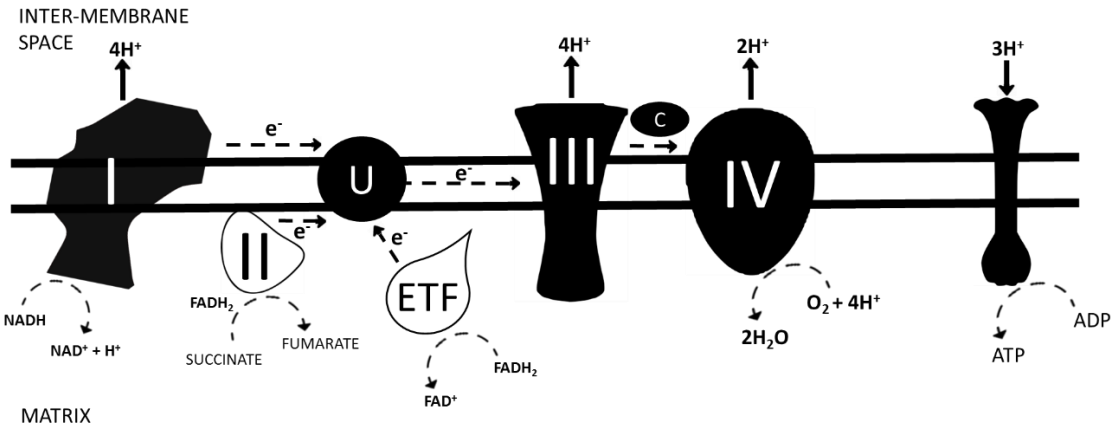

Figure 1.1: The Electron Transport Chain and Oxidative Phosphorylation. Schematic of mitochondrial respiratory chain consisting of complexes I, II, III, IV and V (ATP synthase). NADH supplies electrons to complex I, whilst complex II accepts electrons from the conversion of succinate to fumarate via $FADH_2$. The electrons are then shuttled to complex III via ubiquinone, before being accepted by cytochrome *c* and transferred to complex IV, at which point they are accepted by oxygen. Protons are pumped into the inter-membrane space at complexes I, III and IV, generating a proton-motive force which drives phosphorylation of ADP to ATP by ATP synthase.

1.1.2 Oxidative Phosphorylation

This cascade of electrons through the ETC generates a proton gradient, $\Delta\mu H^+$, which is harnessed by ATP synthase to generate the cellular energy currency (ATP) (Mitchel, 1961). The flow of protons from the intermembrane space back into the mitochondrial matrix is dependent upon the magnitude of $\Delta\mu H^+$, and drives the rotation of the ATP synthase subunits which catalyse phosphorylation of ADP to ATP (Jonckheere et al., 2012).

1.1.3 ATP as a Vector for Energy Transfer

Hydrolysis of the high energy phosphate bonds of ATP to produce ADP and an inorganic phosphate molecule serves to provide most cellular processes with the energy they require. The free energy yielded by ATP hydrolysis, $\Delta G'^{ATP}$, is a function of both the standard free energy of ATP (ΔG^{OATP}) and of the ratio of ATP/ADP in the cell, which is maintained at a high level by mitochondrial metabolism. $\Delta G'^{ATP}$ may thus be represented as $\Delta G'^{ATP} = \Delta G^{OATP} + RT\ln\frac{[ADP][Pi]}{[ATP]}$, where R is the gas constant and T temperature in degrees Kelvin (Veech et al., 2001)

The ratio of ATP to ADP in the cell is therefore crucial both to the availability of ATP to power reactions, and because it affects the amount of energy available from the hydrolysis itself (Veech et al., 2001). The amount of ATP generated per gram of metabolic substrate and per molecule of oxygen impacts upon this ratio, allowing metabolism of some substrates to reach functional levels of $\Delta G'^{ATP}$ more efficiently than the metabolism of others depending upon the amount of reducing intermediates they yield in the Krebs cycle and proceeding metabolic pathways.

1.1.4 The Krebs Cycle

Under oxidative conditions, the majority of the NADH and $FADH_2$ which provides reducing power to the ETC is yielded by the Krebs cycle. Conceptualised by Hans Krebs in 1937, the Krebs cycle constitutes a mitochondrial cycle of enzymatic reactions which harvest reducing power from carbon-based intermediates in a stepwise process (Kornberg, 2000; Krebs and Johnson, 1937, 1980). One of the major vectors for carbon input into the Krebs cycle is acetyl-CoA, which citrate synthase combines with oxaloacetate to form the six carbon molecule citrate (Krebs et al., 1938). Over a sequence of enzymes and intermediates detailed in **Figure 1.2**, CO_2 and reducing power are stripped from citrate and its derivatives, with the end result being regeneration of oxaloacetate and hence completion of the cycle.

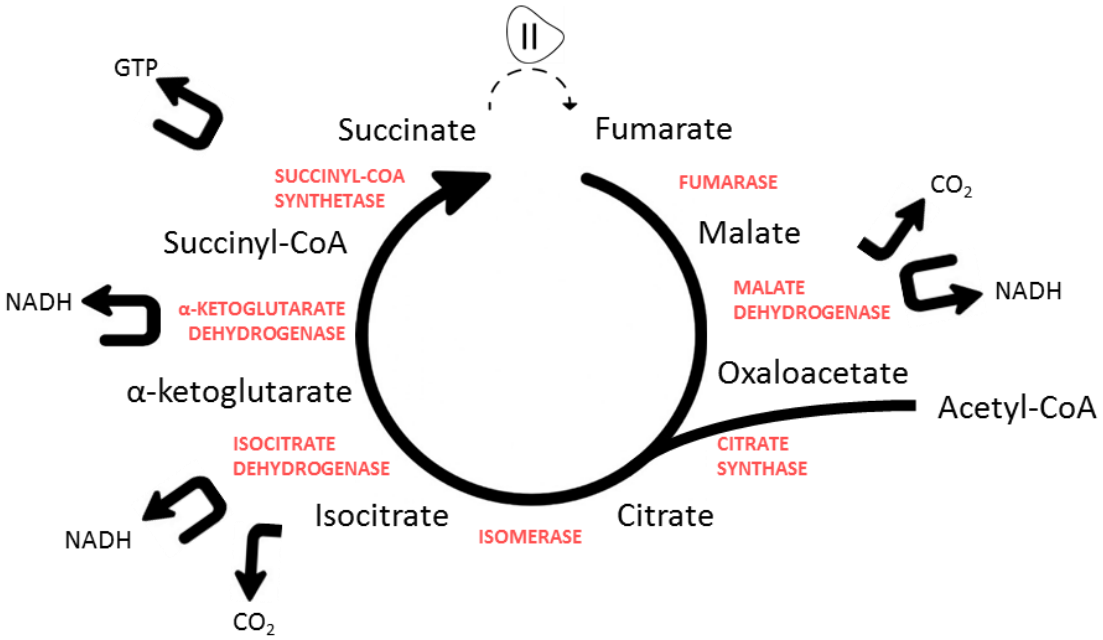

Figure 1.2: The Krebs Cycle. Acetyl-CoA is combined with oxaloacetate to form citrate by citrate synthase, initiating a cyclic series of reactions which culminate in the regeneration of oxaloacetate following the production of NADH, CO_2 and GTP. GTP is readily converted into ATP for cellular processes.

1.1.5 Metabolic Substrates

Catabolism of glucose, fatty acids, ketone bodies and amino acids can all yield high energy electrons for oxidative phosphorylation. Metabolic selection of which substrate to oxidise can depend upon many things, including current energetic demand of the tissue, substrate and oxygen availability. Generally, fatty acids, glucose and ketone bodies all feed into the Krebs cycle as acetyl-CoA, whilst amino acids are capable of entering following conversion to intermediates including pyruvate, glutamate and fumarate.

1.1.6 Fatty Acid Metabolism

The Carnitine Shuttle

Fatty acids are initially converted to acyl-CoAs via addition of coenzyme A by the enzyme acyl-CoA synthase. Conditional upon the length of their carbon chain, these acyl-CoAs are prepared for uptake to the mitochondria via conversion to acyl-carnitines by carnitine palmitoyl transferase 1 (CPT-1), the cardiac isoform of which is CPT-1b. Carnitine acylcarnitine translocase (CACT) subsequently transports the fatty acids into the mitochondria in their acyl-carnitine form, where CPT-2 reverses the transformation into acyl-CoA esters which may then undergo FAO (Houten and Wanders, 2010).

β-Oxidation

For the most part fatty acid oxidation (FAO) begins with the conversion of fatty acids to acetyl-CoA via β-oxidation **(Figure 1.3)**. Acyl-CoA dehydrogenases specific to the length of fatty acid (VL (Very Long chain), L (Long chain), M (Medium chain) and S (Short chain) ACAD) serve to prepare the Acyl-CoA for metabolism by the mitochondrial trifunctional protein (MTP) or cytosolic equivalents (Chegary et al., 2009). MTP performs hydration of the double bond for long chain CoAs, dehydrogenation of the resulting L-3-hydroxy-acyl-CoA to 3-keto-acyl-CoA, and thiolytic cleavage of the 3-keto-acyl-CoA to yield an acyl-CoA that is two carbons shorter and acetyl-CoA (Houten et al., 2018). Medium (< 10 carbons) and short chain acyl-CoAs (2-4 carbons) are metabolised by enoyl-CoA hydratase, the medium and short chain hydroxyacyl-CoA dehydrogenase HOAD, and medium chain 3-ketoacyl-CoA thiolase (MCKAT) instead of MTP. Following the release of each acetyl-CoA molecule, the newly shortened chain re-enters β-oxidation in a repetitive cycle until it has been completely metabolised to acetyl-CoA (Schulz, 1991).

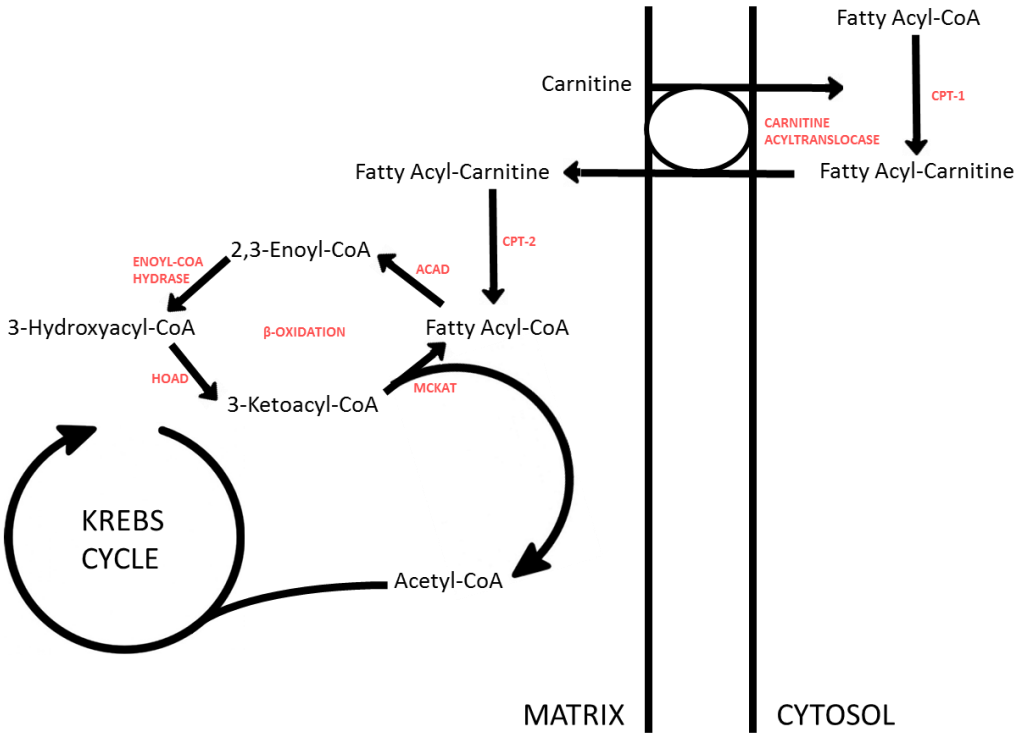

Figure 1.3: β-oxidation. Acetyl-CoA is yielded from the cyclic decomposition of fatty acyl-CoAs. Following import into the mitochondria via the carnitine shuttle, fatty acyl-CoAs are sequentially dehydrated, hydrated, dehydrated and thioytically cleaved by ACAD, enoyl-CoA hydrase, HOAD and MCKAT to generate acetyl-CoA and a shorter acyl-CoA which may undergo the process again.

1.1.7 Glucose Metabolism

The six carbon molecule glucose is either taken up from the bloodstream or catabolised from internal glycogen stores for metabolism. Glucose Transporter 1 (GLUT1) is constitutively expressed and allows a basal rate of glucose uptake, while upregulation of Glucose Transporter 4 (GLUT4) allows post-prandial adjustment of glucose uptake in response to the secretion of insulin by the pancreas when blood glucose levels are high. The initial phase in glucose metabolism, glycolysis, is triggered by hexokinase mediated phosphorylation of the glucose. Glucose is then sequentially converted to the three carbon molecule pyruvate **(Figure 1.4, overleaf)** (Li et al., 2015; Lunt and Heiden, 2011). Under aerobic conditions, pyruvate is decarboxylated to acetyl-CoA by pyruvate dehydrogenase following the transport of pyruvate into the mitochondria by the mitochondrial pyruvate carrier (Mccommis and Finck, 2016; Schell and Rutter, 2013). Under anaerobic conditions, glycolysis supplies some limited ATP, with pyruvate being converted to either lactate or alanine rather than entering the mitochondria (Folbergrová et al., 1974; Li et al., 2015; Zhou et al., 2005).

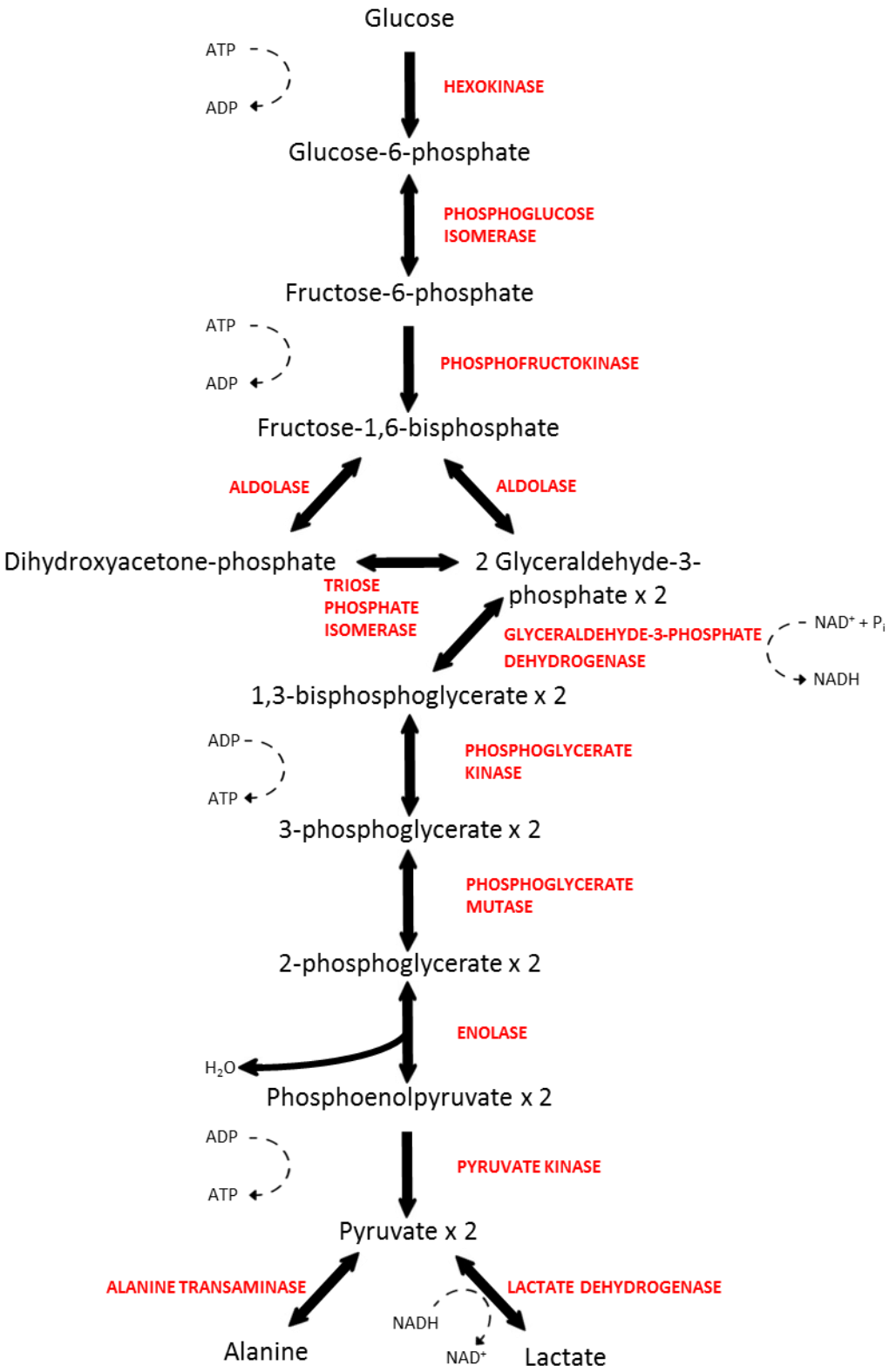

Figure 1.4: Glycolysis. Glucose is converted into pyruvate which can be taken up into the mitochondria via sequential enzyme catalysed reactions. The process consumes two moles of ATP per mole of glucose, but yields four. In anaerobic conditions, pyruvate is diverted to lactate and alanine in order to permit the continued production of this ATP.

1.1.8 Ketone Body Metabolism

The ketone bodies, β-hydroxybutyrate, acetoacetate and acetone, are another energy substrate which are typically produced by the liver and oxidised by other tissues including the heart during fasting or starvation (Grabacka et al., 2016). While acetone is metabolised through a different pathway, β-hydroxybutyrate is oxidised by the enzyme β-hydroxybutyrate dehydrogenase to acetoacetate, which is subsequently converted to acetoacetyl-CoA by the enzyme SCOT. Acetoacetyl-CoA can then be converted to acetyl-CoA for entry into the Krebs cycle (Grabacka et al., 2016). Alternatively, the interchange between acetoacetyl-CoA and acetoacetate may be mediated via a HMG-CoA intermediate by the enzymes HMG-CoA synthase and HMG-CoA lyase through a pathway which is commonly thought of as ketogenic rather than ketolytic and yet consists of enzymes which catalyse bidirectional reactions (McGarry and Foster, 1976). Ketone bodies are a very oxygen efficient fuel which increase the oxygen efficiency of the working heart by 25% when supplied in addition to 10mM glucose (Sato et al., 1995). They are oxidised preferentially to fatty acids and glucose through their inhibition of the other substrates' oxidation (Le Foll et al., 2014; Sato et al., 1995; Stanley et al., 2003).

For a more thorough introduction to cardiac metabolism of ketone bodies, see the introduction to **Chapter 5.**

1.2 SPECIFIC METABOLIC TRAITS OF THE HEART

The metabolic demands of the heart are amongst the greatest of any organ. With the human body's surface area to volume ratio being too low to support sufficient gas diffusion directly into the tissues, the survival of every organ is contingent upon the action of the heart to supply oxygen as well as other essential nutrients and components. Under normal physiological conditions this tonic contraction consumes about 35 kg of ATP per day (Taegtmeyer and de Villalobos, 1995; Ferrari *et al.*, 2018), but cardiac energy requirements must also be met under more strenuous conditions such as exercise, hypertension or chronic stress.

The heart is a metabolic omnivore because it can oxidise a range of different substrates for ATP. However, it relies heavily on FAO in its healthy state because fatty acids are the most energy dense metabolic substrate, producing ~2.4 times more ATP per gram dry substrate than glucose (Darvey, 1998). The healthy human heart can derive almost 100% of its ATP from fatty acids in appropriate circumstances, although on average the percentage of ATP derived from fatty acids is ~50-90% (Neely et al., 1972; Lopaschuk et al., 2010; Brinkmann *et al.*, 2002). The heart mostly oxidises exogenous substrate because its daily energy demands are greater than the amount of substrate it can store, but can also utilise internal stores of triglyceride (Lahey et al., 2014; Lopaschuk et al., 2010).

However, metabolic plasticity is a hallmark of cardiac function, and when circumstances dictate other substrates are just as readily oxidised. Glucose is a more oxygen-efficient fuel than fatty acids, so when oxygen is a limiting factor, for example during exercise induced exertion, or in the hypoxic and foetal hearts, it is common to find a shift towards glucose oxidation at the expense of fatty acids (Horscroft et al., 2015; Onay-Besikci, 2006; Opie and Sack, 2002; Taegtmeyer and Lubrano, 2014).

Such a shift can also be effected by alterations in the availability of substrates, as would occur due to a sustained dietary change. Generally, the heart takes up all of its oxidisable substrates from the blood, and, even though it has internal stores of both fatty acids and glucose, substrate selection is heavily influenced by the levels of circulating metabolites (Brinkmann et al., 2002). Long term dietary changes can have lasting influence upon what the heart can take up and therefore oxidise. For example, a high protein diet results in a lower rate of glucose oxidation (Linn et al., 2000), high fat diets suppress glucose oxidation and enhance FAO (An et al., 2013), and low-carbohydrate diets have similar effects while also enhancing the oxidation of ketone bodies (Manninen, 2004).

When ability to switch substrates for oxidation is impaired, the heart loses its ability to respond to metabolic stimuli, and this is often associated with pathology. Diabetes Mellitus, a group of metabolic diseases defined by high blood sugar levels over a prolonged period, represents one well characterised example of a condition which results in such an impairment of metabolic flexibility, and also increased mortality from cardiovascular disease (Bayeva et al., 2013). The diabetic heart becomes more reliant upon oxidation of fatty acids for ATP production due to the resultant dysregulation of glucose metabolism. The increased cardiovascular disease risk associated with diabetes highlights the importance of metabolic flexibility to the function of the heart, although it is unknown whether loss of metabolic flexibility is a symptom or a cause of heart disease in diabetics. This is addressed, and a more thorough introduction to metabolism in the diabetic heart presented in **Chapter 6.**

Regardless of the level of FAO, some oxidation of glucose is always required to facilitate Krebs cycle function (Paoli et al., 2013). As with any system which comprises bi-directional reactions, there can be a net loss of carbon molecules from the TCA cycle over time where reactions converting its intermediates to other molecules proceed at a greater rate than their reverse direction. This necessitates the replacement of carbon in order for production of sufficient levels of NADH and $FADH_2$ to continue. For regeneration of overall carbon levels in the Krebs cycle, acetyl-CoA cannot contribute for two reasons. The first is that for every acetyl-CoA molecule which enters the Krebs cycle, two carbons are subsequently lost as CO_2, meaning that there is no net gain or loss of carbon. Secondly, without entry of molecules larger than two carbons to the Krebs cycle the net carbon loss will mean that there are fewer molecules of oxaloacetate for the acetyl-CoA to bind to. The mitochondria metabolise fatty acids to acetyl-CoA, which can only fix two carbons into the Krebs cycle, and subsequently produces two molecules of CO_2. On the other hand, glucose is initially metabolised into the three carbon unit pyruvate, which may then supplement carbon levels in the Krebs cycle through conversion to oxaloacetate by the enzyme pyruvate carboxylase. This replenishment of Krebs cycle intermediates is an example of anaplerosis. Pyruvate carboxylase is the main anaplerotic enzyme, although certain amino acids may also contribute to anaplerosis (Manninen, 2004; Owen et al., 2002). Pyruvate and amino acids may function as anaplerotic substrates because they contribute more carbons to the Krebs cycle than the two which are removed as CO_2, whereas acetyl-CoA derived from FAO only contributes two carbons and so its incorporation does not represent a net gain of carbon for the Krebs cycle.

1.3 ISCHAEMIA

Cardiac ischaemia stems from the occlusion or cessation of blood flow, and therefore supply of oxygen and metabolic substrates, to an area of cardiac tissue. This is the most common cause of heart attacks. Cardiac ischaemia usually follows blockage of one or more coronary arteries which prohibits all, or more commonly, most, blood supply to the myocardium. For such an energetically demanding tissue, this loss of oxygen and therefore capacity for oxidative metabolism can be catastrophic. Time is a crucial factor during ischaemia as the longer an area of the heart is subjected to ischaemia, the greater the likelihood of the affected area of tissue undergoing necrosis and forming an infarct which can cause ongoing issues such as angina or heart failure even if reperfused with oxygenated blood (Debrunner et al., 2008).

1.3.1 Disruption of Contractile Function

Ischaemia has an instant effect upon contractile function of the heart. Contractile function is directly linked to metabolism, and therefore when oxygen supply is attenuated and metabolism affected, regular contractile function ceases. This has an immediate effect upon the rest of the body, since the supply of oxygen and nutrients to other tissues is disturbed.

Collapse of calcium homeostasis during ischaemia also contributes to the failure of contractile function. Ordinarily in the heart, calcium influx from the extracellular space leads to further release of calcium from the sarcoplasmic reticulum (SR), which binds to troponin C to potentiate the association of myosin and actin, the hydrolysis of ATP and generation of contractile force (Wier, 1990). This influx of calcium is then rapidly cleared in preparation for the next contractile cycle by the action of the Ca^{2+}/Na^{+} transporter, which harnesses the influx of Na^{+} to the cell down its concentration gradient to remove Ca^{2+} from the cytosol (Barry, 1991). However, the decreased ability to produce ATP in ischaemia impairs the activity of the cellular Na^{+}/K^{+} pump, leading to an increase in intracellular Na^{+} (Hasin and Barry, 1984). This initially decreases the Na^{+} gradient into the cell, and therefore the rate of calcium efflux, but eventually leads to calcium influx through reversal of the direction of the transporter. Increased intracellular Ca^{2+} decreases the response to SR calcium release in part due to a decreased gradient from SR to cytosol, but also due to desensitisation of the Ca^{2+} response (Lee and Allen, 2006).

1.3.2 Reactive Oxygen Species

The altered reductive environment in ischaemia can lead to the production of reactive oxygen species (ROS) (Becker, 2018). ROS are potentially-damaging free radicals and non-radical oxidising

agents most commonly including hydrogen peroxide (H_2O_2) and superoxide ($\bullet O_2^-$) (Panth et al., 2016), which may cause cellular damage and even direct necrosis via peroxidation of lipid membranes and damage to proteins (Becker, 2018). The process of ROS generation is highly oxygen dependent, occurring at both high and low oxygen tensions. Despite it being counterintuitive that in an oxygen-limited environment there is damaging levels of oxygen radical production, the process is observable via the use of fluorescent probes (Becker et al. 1999; Zhu & Zuo 2013; Panth et al. 2016). It appears therefore that in a redox-reduced cell the ETC is capable of "leaking" electrons to what little oxygen remains in order to produce reactive anions (Nohl and Werner, 1986).

The major source of ischaemic ROS is ETC complex III, with some contribution from other complexes (Bleier and Dröse, 2013; Guzy and Schumacker, 2006). While reverse electron flow has been postulated as a mechanism for ROS generation from complex I during ischaemia, it has been shown that reverse electron flow actually decreases through an ischaemic period due to uncoupling, making this unlikely (Ross et al., 2013). Complex I and complex II do have the ability to contribute some ROS production, although this is rendered negligible by mitochondrial antioxidant defences (Chen et al., 2003; Turrens, 2003). Blockade of electron flow at complex III, which occurs as a response to ischaemia and hypoxia, results in a much higher rate of ROS production, and this is further supported by evidence that inhibition of electron flow to complex III through complex I greatly reduces this ROS production and damage sustained to complex III (Chen et al., 2003, 2007; Guzy and Schumacker, 2006; Heather et al., 2010).

1.3.3 The Metabolic Response to Ischaemia

Ischaemia represents a severe and immediate effector of change to metabolism. Attenuation of oxygen supply to the myocardium leads almost immediately to a near total ablation of oxidative metabolism, and while a tiny amount of oxidative metabolism still occurs, the majority of the ATP which the cells need to survive must be generated anaerobically.

During ischaemia, there is a swift switch towards glycolytic metabolism. Ischaemia represents a disease where oxygen supply is limiting, and induces a diversion of pyruvate through lactate dehydrogenase (LDH) to form lactate (Li et al., 2015; Zhou et al., 2005) as part of anaerobic respiration. Glycolytic respiration produces far less ATP per glucose molecule than oxidation would, but is able to proceed in the absence of oxygen.

Accumulation of lactate itself can cause damage to the heart without blood flow to facilitate its excretion, however. Lactate is a proton donor, and can cause acidification of the cytosol, damaging cellular superstructures and interfering with pH dependent reactions (Kraut and Madias, 2014; Marcinek et al., 2010). During ischaemia, where there is low coronary perfusion, lactate is present to a high concentration in the coronary effluent (Goodwin and Taegtmeyer, 1994). Because of the accumulation of lactate and the associated low ATP yield, anaerobic respiration is not conducive to sustaining healthy cells over longer periods, but some ATP is preferable to none early during the insult. Whilst anaerobic respiration may therefore be beneficial during the early stages of ischaemia therefore, there comes a point at which the damage caused may outweigh the benefits.

Of the oxidative metabolism which does still occur, there is debate over whether fatty acid or glucose oxidation is favoured during ischaemia. While oxidation of both substrates is severely ablated relative to before the ischaemic insult, glucose oxidation has been documented in some sources to predominate that oxidation which does still occur (Yao et al., 2015). This would appear to make sense given it is a more oxygen efficient substrate than fatty acids. Moreover, the highly reductive environment during ischaemia, typified by enhanced NADH/NAD^+ ratios, would act to inhibit β-oxidation.

However, it has also been argued that fatty acid oxidation can come to dominate in the ischaemic heart due to dysregulation through malonyl-CoA. Malonyl-CoA is a product of the carboxylation of acetyl-CoA by acetyl-CoA carboxylase (ACC), and has an inhibitory effect upon uptake of fatty acids into the mitochondria via CPT-1 (Dyck et al., 2004; Stanley et al., 2005). In the ischaemic heart, AMP kinase (AMPK) is thought to be activated by the associated metabolic stresses, particularly the drop in ATP and PCr levels (Fillmore et al., 2014; Kantor et al., 1999). AMPK phosphorylates and inactivates ACC, compromising its inhibition of CPT-1 and thus making it possible that there is increased capacity for mitochondrial fat uptake/oxidation during ischaemia **(Figure 1.5)** (Lopaschuk et al., 2010).

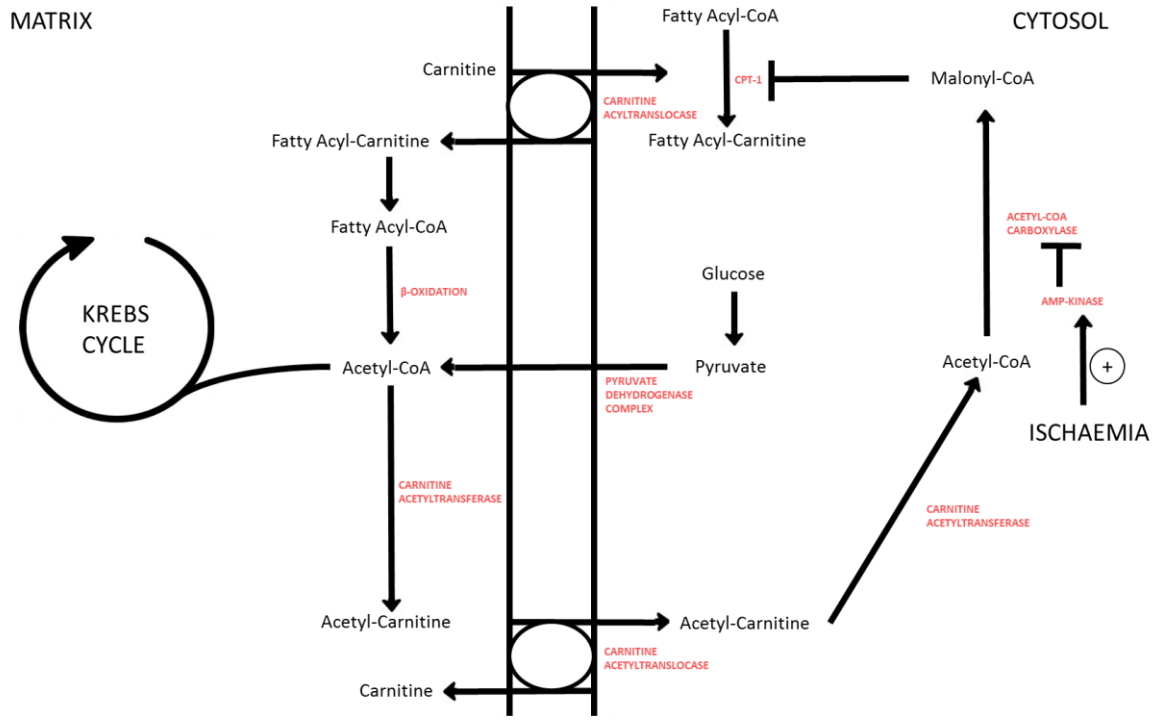

Figure 1.5: Inhibition of Fatty Acid Oxidation by Malonyl-CoA and Putative Release of Inhibition during Ischaemia. Acetyl-CoA from the mitochondrial matrix is exported from the mitochondria via an acetyl-carnitine intermediate by carnitine acetyl-translocase under aerobic conditions. In the cytosol it is converted to malonyl-CoA by acetyl-CoA carboxylase, and comes to inhibit further uptake of fatty acids to the mitochondria by inhibiting the action of CPT-1. However, during ischaemia, when AMP kinase is activated, Lopaschuk et al. hypothesise an inhibition of acetyl-CoA carboxylase, resulting in a lesser conversion rate of acetyl-CoA to malonyl-CoA and therefore greater capacity for fatty acid uptake to the mitochondria.

Whichever of glucose or fatty acid oxidation comes to dominate during ischaemia will inhibit the other via the Randle cycle. On a cellular level, the balance between glucose and fatty acid oxidation is given an extra dimension of control by this cycle of mutual inhibition (Hue et al., 2009). FAO leads to increased ratios of acetyl-CoA/CoA and of NADH/NAD^+, both of which are factors inhibiting the activity of PDH (Guo, 2015; Randle et al., 1963). Meanwhile, there is thought to be an increase in cytosolic citrate levels, leading to inhibition of 6-phosphofructo-1-kinase and a resultant increase of glucose-6-phosphate, which inhibits hexokinase (Hue et al., 2009). On the other hand, glucose oxidation leads to an inhibition of fatty acid oxidation through enhanced production of malonyl-CoA as described above (Lopaschuk et al., 2010).

In addition to the debate over whether fat oxidation is inhibited or potentiated during ischaemia, there is contention over whether it might be beneficial or pathological under these conditions. High levels of fatty acids detected clinically in circulation during ischaemia and reperfusion have

been correlated with the severity of the incident, and one suggestion has been that increased oxidation of fatty acids at the expense of glucose might promote higher rates of glycolysis at the expense of glucose oxidation and therefore acidification of the myocardium (Jaswal et al., 2011; Lopaschuk et al., 1993). However, in the absence of a previous severe ischaemic insult, presence of fatty acids in cardiac tissue has not been found to impair recovery of function post-reperfusion (Johnston and Lewandowski, 1991; Taegtmeyer and Stanley, 2011). In fact, with a variety of differing types of fatty acid in the perfusion buffer including both intralipid (a commercially available triglyceride mixture) and palmitate it has been found that functional recovery has actually been enhanced, suggesting that the presence of fatty acids is actually beneficial in restoring the ATP debt established during ischaemia (King et al., 2001; Liedtke et al., 1988; Lou et al., 2014a). It is even possible that rather than being a contributor to the damage sustained following ischaemia, the high levels of circulating fatty acids detected clinically may actually be a symptom or beneficial response – the liver and adipose tissue being stimulated to release more fatty acids to aid recovery or damaged heart tissue leaking more fatty acids the more severe the insult is. It is therefore currently unclear whether increased oxidation of fatty acids is beneficial or detrimental during ischaemia, and more definitive experiments are required before a consensus on this can be reached.

Genes related to FAO generally come under the direct transcriptional control of a set of enzymes known as the peroxisome proliferator associated receptors, or PPARs (Roberts et al., 2011). These transcription factors can up- or down-regulate enzymes involved in FAO in association with dietary or environmental stimuli. For this reason, these transcription factors have been identified as a potential avenue for therapeutic treatment in the diabetic and failing hearts, where there is an imbalance between FAO and glucose oxidation (Fillmore et al., 2014; How et al., 2007). PPAR agonists are of debateable use clinically due to side effects such as genotoxicity and heart failure (Home, 2011). However, PPAR agonists and NOx species such as nitrate have been documented to stimulate PPAR in a range of tissues, which could be of scientific interest across a broad range of cardiac metabolic perturbances (An et al., 2018; Ashmore et al., 2014a, 2015; Huang et al., 2017). However, another question to which the answer is not yet clear is whether modulation of FAO related gene transcription using such agents could be effective if used as a protective strategy against damage mediated by cardiac ischaemia.

1.4 REPERFUSION INJURY

Perhaps counterintuitively, the greater damage to the heart is actually mediated upon reperfusion following ischaemia. At this point, the most reactive oxygen species are produced, probably due to the damage sustained during ischaemia being put under greater strain by the sudden increase in oxidative phosphorylation associated with restored blood supply to the myocardium (Chen et al., 2007). Plentiful supply of oxygen also means there is greater capacity for the generation of radicals, and so immediately following reperfusion there is often a damaging burst of ROS (Granger and Kvietys, 2015). ROS are also produced from other cellular sources upon reperfusion, such as NADPH oxidase (NOX), which can further trigger ROS release from the mitochondria by stabilising opening of the mitochondrial permeability transition pore (mtPTP) (Granger and Kvietys, 2015).

The burst of ROS upon reperfusion overwhelms cellular antioxidant defences (e.g. superoxide dismutase, glutathione peroxidase etc.) (Kalogeris et al., 2014). Once this has occurred, apoptosis can be caused by ROS-induced lipid peroxidation and weakening of cellular membranes, leading to cell rupture as well as further damage to the mitochondria (Chen et al., 2003; Kalogeris et al., 2014) **(Figure 1.6)**.

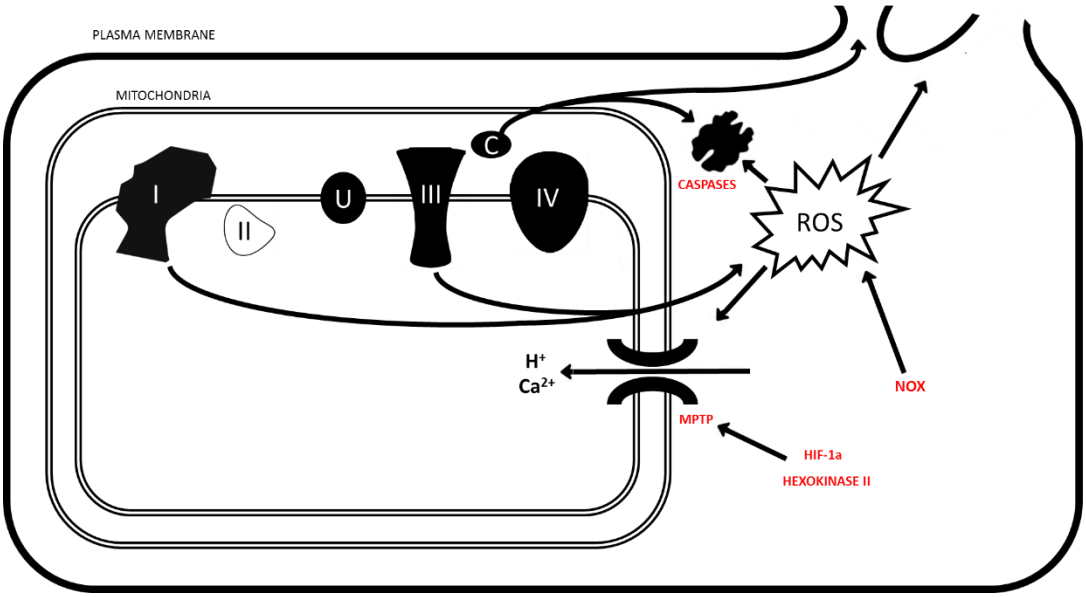

Figure 1.6: ROS mediated mechanisms of apoptosis upon reperfusion. ROS produced at complexes I & III of the ETC, or by NADPH oxidase (NOX) may trigger apoptosis via activation of the caspase pathway, necrosis via direct peroxidation of the plasma membrane, and ROS-induced ROS release through induction of mtPTP opening. Cytochrome *c* release from the mitochondria can further activate the caspase pathway, while Hypoxia Inducibe Factor 1a (HIF-1a) and Hexokinase II migrate to the mitochondria and stabilise the opening of the mtPTP in conditions of oxidative stress

Reperfusion is thought to lead to increased opening of the mitochondrial permeability transition pore (mtPTP), a phenomenon preceding leakage of pro-apoptotic factors and eventual cell death. The composition of the mtPTP remains contested, but is thought to involve a dimer of ATP synthase (Bonora et al., 2013). Its opening leads to a sudden permeability transition which permits ions and larger molecules to exit the mitochondria in an uncontrolled manner (Zorov et al., 2014). While mtPTP remains largely closed during the ischaemic period due to acidosis, reperfusion leads to its opening being mediated through ROS, HIF-1a and hexokinase-II (Kim et al., 2018). Opening mtPTP results in H^+ and Ca^{2+} entering the mitochondria, and prolonged opening leads to uncoupling and loss of the proton gradient. Cessation of ATP production is the consequence, and cytochrome-c efflux interacts with the caspase cascade to trigger apoptosis.

Myocardial ischaemia/reperfusion further induces an acute inflammatory response, both locally and in distal sites. Prolonged blockage of oxygen supply to the myocardium results in cell death and the release of their contents, which in turn recruits neutrophils and macrophages to the injury site (Von Hundelshausen and Weber, 2007). This is mediated by ROS released acutely during ischaemia, which induce leukocyte release of chemokines and also platelet aggregation (Canoso et al., 2018; Lakshminarayanan et al., 2001). These chemokines include interleukins and TNF, which may cause systemic inflammation and which correlate strongly with the severity of the insult (Debrunner et al., 2008; Prondzinsky et al., 2012). The recruited white blood cells may produce their own ROS, as well as degranulating proteases and cytokines which cause further cell death in the infarcted area and fibrosis which may then further impair contraction (Frangogiannis, 2015; Ruparelia et al., 2016). Reduction of damage sustained during ischaemia would therefore have the secondary advantage of preventing leukocyte recruitment, systemic inflammation and further cell death.

1.4.1 The Metabolic Response to Reperfusion

Metabolic pathways remaining adapted to low oxygen concentrations when oxygen and nutrients become re-available upon reperfusion is a key factor in reperfusion-injury. Since reperfusion is the major stimulant for mitochondrial ROS production, adaptation of metabolism to cope with this new availability affects how well the heart can recover.

The myocardium is thought to swiftly recover its ability to oxidise fatty acids post-reperfusion. Both enzyme activity studies and direct measurements indicate that fat oxidation capacity is maintained or higher relative to pre-ischaemic rates (Liedtke et al., 1988; Lopaschuk et al., 1990;

Nellis et al., 1991). FAO, as previously discussed, has a greater yield of ATP/g substrate than glucose, but also leads to a greater degree of uncoupling and ROS production (Boudina et al., 2005, 2007; Cole et al., 2011; Echtay et al., 2002; Murray et al., 2005, 2008). It is likely that the demand for ATP to sustain contraction and restore cellular ion balance influences this early drive to restore a high level of fat oxidation. Even those who have argued that FAO oxidation is decreased and glucose oxidation increased in the reperfused heart conclude that FAO still accounts for the majority of ATP production upon reperfusion (Myears et al., 1987).

Despite quickly restored FAO rates though, glycolysis after reperfusion continues to underlie the success of recovery. Hearts immediately after reperfusion display a much worse ability to cope with the inhibition of glycolysis than those which have never suffered an ischaemic insult or where glycolysis is inhibited further after reperfusion (Richmond et al., 1992). Initial high rates of glycolysis may be critical to provide cytosolic ATP, aiding homeostatic ion transport while the majority of mitochondrial ATP goes to support contractile function (Mcnulty et al., 2000; Weiss and Hiltbrand, 1985). Meanwhile, fat oxidation supports less efficient contraction than glucose respiration, so for the initial energy burst needed to get circulation re-started it may be the case that cardiac energy levels require supplementation from glucose (Johnston and Lewandowski, 1991).

These two statements are not necessarily contradictory despite appearances. FAO is dependent upon some glucose oxidation supplying carbon to the Krebs cycle through anaplerosis (Owen et al., 2002), so it makes sense that in a heart more dependent upon FAO high rates of glycolysis are critical to recovery. Furthermore, FAO inhibits glucose oxidation, but not glycolysis, via the Randle cycle (Randle et al., 1963), meaning more glucose metabolism will be anaerobic and able to satisfy the cytoplasmic ATP demand (Mcnulty et al., 2000). Also, despite FAO having been stated to account for the majority of ATP produced upon reperfusion (Lopaschuk et al., 1990; Myears et al., 1987; Nellis et al., 1991), this does not mean that this is the state of affairs most beneficial to functional recovery and could be a pathological response. Promoting glucose oxidation upon reperfusion could well enhance recovery then, as has been demonstrated by Lopaschuk et al. (1990), without contradicting any of these statements at all. **Figure 1.7** shows suggested figures for the breakdown of total ATP production in the “healthy” heart and upon reperfusion based upon these papers.

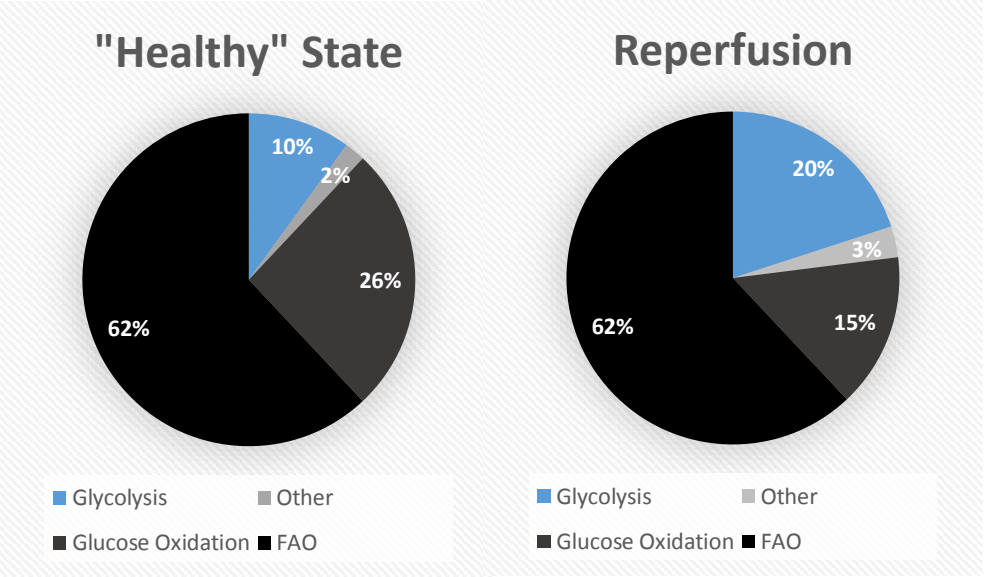

Figure 1.7: Graph Showing Suggested Figures for Percentage of Total ATP Production Accounted for by Each Source in a "Healthy" Heart and Immediately After Ischaemia/Reperfusion.

Whether it is most beneficial to promote FAO or glucose oxidation following reperfusion is a matter of controversy. Etomoxir inhibition of CPT-1 (and therefore FAO) during reperfusion stimulates glucose oxidation, and this has been shown to increase the rate of functional recovery (Lopaschuk et al., 1990). However, it has also been shown that presence of fatty acids in the perfusion buffer is protective against ischaemia/reperfusion injury, with improved recovery of contractile function following ischaemia (Lou et al. 2014 A; King et al. 2001). More conclusive evidence is needed before this controversy can be resolved.

1.4.2 Long Term Repercussions of Reperfusion Injury

Sustaining too much damage during ischaemia and/or subsequent reperfusion can lead to cell death – controlled (apoptotic) or uncontrolled (necrotic). Release of cytochrome *c* and ROS during reperfusion injury activates the caspase pathways and lead to apoptosis, providing radical mediated damage to the tissue doesn't first lead to tissue necrosis (Gottlieb, 2011; Piper and Ovize, 1998). A further mechanism of cell death can occur through the opening of the mtPTP, leading to exchange of mitochondrial pro-apoptotic factors with cytosolic water which causes swelling and lysis of the mitochondria (Halestrap, 1998). Following myocardial infarction, up to 1 billion myocytes can die (Laflamme and Murry, 2005), and cardiac tissue has a limited ability to

regenerate. Fibroblasts mediate fibrosis of the necrotic region, and reactive fibrosis can even lead to further fibrosis in the borderline region where the cells could otherwise have eventually recovered to viability (Shinde and Frangogiannis, 2014; Talman and Ruskoaho, 2016). The result is a non-contractile, refractory area of the heart.

Over longer periods an infarcted region may cause further complications. Even if the infarct size is small enough that overall cardiac function is not compromised and the heart can continue to supply the body with enough blood to survive, the excess strain upon the heart can lead to remodelling and heart failure (Dargie, 2005; Heusch and Gersh, 2018; Heusch et al., 2014). In the US those who have previously suffered a heart attack are 2.8 times more likely to be diagnosed with heart failure in future (Hugli et al., 2001). Heart failure is defined as the inability of the heart to pump sufficient blood to the tissues of the body (including the heart itself) to meet metabolic demands, and when a portion of myocardium is afunctional this means that the remaining viable myocardium must work harder to supply itself and the body with enough blood and oxygen. Working harder means that demand for oxygen increases, effecting uncoupling and alterations to metabolism (Murray et al., 2008). Infarct size correlates directly to the progression of heart failure (Stone et al., 2016), and therefore reducing I/R injury and damage will help to reduce the prospects of developing heart failure as well as immediate mortality.

Chronic infarctions may also underlie arrhythmias as a further complication. Healthy cardiac tissue conducts the electrical impulses generated by the sino-atrial node (SAN) to maintain synchronised contractility, yet a region of fibrotic tissue is incapable of passing these signals along (Francis et al., 2016). Further electrophysiological remodelling may occur in the border zone to the infarct, including reduction of conduction components and intracellular calcium mishandling, which can trigger malignant arrhythmias. The scar itself can lead to tachycardia (Ripplinger et al., 2009), while the disordered conductive structure of the border zone can lead to areas of blocked or cyclic conduction (Nguyen et al., 2014).

1.5 AIMS OF THE THESIS

The overall aims of this thesis were to investigate substrate oxidation in the heart, and how this is influenced by ischaemia and reperfusion as well as other metabolic perturbations.

In **Chapter 3**, the target was to develop a reliable model for determining the relative oxidation of glucose and fatty acids with respect to each other and other substrates in the Krebs cycle. A network model was generated to model the movement of ^{13}C labelled carbons through the Krebs cycle when different proportions of [1,2-^{13}C]acetyl-CoA enter the Krebs cycle. This model was developed to interpret the experimentally derived isotopologue distributions of key Krebs cycle intermediates and proxies in order to determine the proportion of glucose or FA oxidation in the experimental setup. In order to validate the model, the perfusion buffer for Langendorff perfused hearts was supplemented with a known percentage of U-^{13}C labelled glucose in order to follow the progress of labelled carbons derived from these substrates through the Krebs cycle. Following the achievement of steady state, the hearts were snap frozen, and the isotopologue distribution of key Krebs cycle intermediates or proxies were measured using LC-MS/MS.

Chapter 4 aimed to address the questions of whether dietary nitrate supplementation could protect against a future ischaemia/reperfusion insult, and whether FAO during and following ischaemia was beneficial or detrimental. Dietary supplementation with sodium nitrate has been shown to both protect the heart against hypoxia (Ashmore et al., 2014a), and enhance β-oxidation in a variety of tissues including the heart itself (Ashmore et al., 2014a, 2015; Roberts et al., 2015). This being the case, if FAO were beneficial to the ischaemic and reperfused heart then dietary nitrate supplementation might be expected to protect against ischaemia, an insult which has a strong hypoxic component. Hearts from rats fed either a sodium nitrate or sodium chloride (as a control) supplemented diet were perfused in the Langendorff mode either with or without intralipid, a triglyceride mixture, in the perfusion buffer. Following 32 minutes aerobic perfusion at 100 mmHg, 32 minutes low-flow ischaemia (0.32 ml/min/gww) and 32 minutes reperfusion at 100 mmHg, functional recovery of the hearts from ischaemia was assessed. Respirometry was used to assess oxygen consumption in the reperfused LV immediately at the end of reperfusion to determine whether there had been a protective effect upon the electron transport chain. Tissue frozen at the same stage was subsequently analysed using LC-MS/MS for energetics, oxidative stress markers and metabolite levels.

An interesting and surprising finding from **Chapter 4** was that the ketone body β-hydroxybutyrate was synthesised in the ischaemic heart, in a process previously thought only to occur in the liver. **Chapter 5** focussed on further characterising this ketogenesis and its impact upon the heart. LC-

MS was used to assess levels of β-hydroxybutyrate in both LV tissue and coronary effluent from Langendorff hearts pre-ischaemia, post-ischaemia and post-reperfusion. Oxygen consumption supported by the different ETC complexes and metabolic fluxes was measured alongside cardiac triglyceride uptake and the isotopologue distributions of β-hydroxybutyrate and Krebs cycle intermediates in order to assess whether ischaemic ketogenesis was a function of capacity for β-oxidation exceeding mitochondrial demand. Inhibitors of both LDH and of HMG-CoA synthase, an enzyme involved in the ketogenic pathway, were employed in order to manipulate ketogenesis and determine whether ischaemic ketogenesis was detrimental or beneficial to the heart.

Chapter 6 aimed at investigating cardiac substrate utilisation in a different paradigm of metabolic perturbation – the type-1 diabetic heart. As discussed above, the loss of metabolic flexibility in the heart has been associated with pathological consequences, and this chapter investigated whether altered flexibility impaired the capacity of the diabetic heart to respond to metabolic stress. Rats which had undergone either 90% pancreatectomy or a sham operation were administered 1 mg/kg isoprenaline, a β-adrenergic agonist, daily over a period of 10 days from 5 weeks post-operation, in order to determine how the type-1 diabetic myocardium coped with a metabolic stimulus. 10 weeks post-operation, and upon termination, fresh LV tissue was examined using high-resolution respirometry to assess function of the ETC and metabolic flux. LC-MS/MS was utilised to examine levels of energetic compounds in the tissue as well as markers of oxidative stress, while RNAseq gave an indication of left-ventricular gene expression. This chapter was undertaken as part of a larger concerted characterisation of the model at Gubra ApS, Horsholm, Denmark, which included measurements of cardiac function and morphology using echocardiography and histology by a team led by Louise Thisted, Dr. Nora Zois and Dr. Elisabeth Fink, and some of this data is also presented here to give an overview of the animal model.

CHAPTER 2

Methods

2 GENERAL MATERIALS AND METHODS

The methods outlined in this chapter are used throughout the thesis. For methods specific to Chapters 3, 4, 5 and 6, see the relevant sections in each chapter. All animal work detailed in Chapters 3, 4 and 5 was conducted in accordance with UK Home Office regulations under the Animals in Scientific Procedures Act. Protocols were performed by a personal licence holder under a project licence, and received prior approval from the University of Cambridge ethical review board. In Chapter 6, all animal work was carried out at Gubra ApS, Hørsholm, Denmark under the auspices of their ethical approval.

Materials

All reagents and chemicals were obtained from Sigma-Aldrich Ltd (UK or DK) unless otherwise stated.

2.1 LANGENDORFF PERFUSION

2.1.1. Concept of Langendorff Perfusion

Retrograde (Langendorff) perfusion is a technique initially developed by Oskar Langendorff for investigation of the function of the isolated heart. The technique involves supplying the *ex vivo* heart with a blood substitute through the aorta (Bell et al., 2011; Herr et al., 2015; Lateef et al., 2015). While the aorta is generally the vessel through which blood is pumped from the heart to supply the rest of the body, in a live mammal the mean arterial blood pressure generated in systole causes the closure of the aortic valve during diastole. This, coupled with diastolic relaxation of the myocardium which was constricting the coronary arteries during systole, allows pressure-driven flow of oxygenated blood through the coronary arteries in order to supply the myocardium **(Figure 2.1)**. The Langendorff preparation works on the principle that delivering a sufficient pressure of oxygenated fluid in reverse through the aorta will result in the same valve closure and thus provide a route of supply to the cardiac tissue through the coronary arteries **(Figure 2.2)**. When the oxygen and metabolic substrate demands of the heart are met in this manner, contraction will occur provided that the correct external concentrations of electrolytes are provided, as the sino-atrial node (SAN) generates and paces action potentials in the heart independently of the central nervous system.

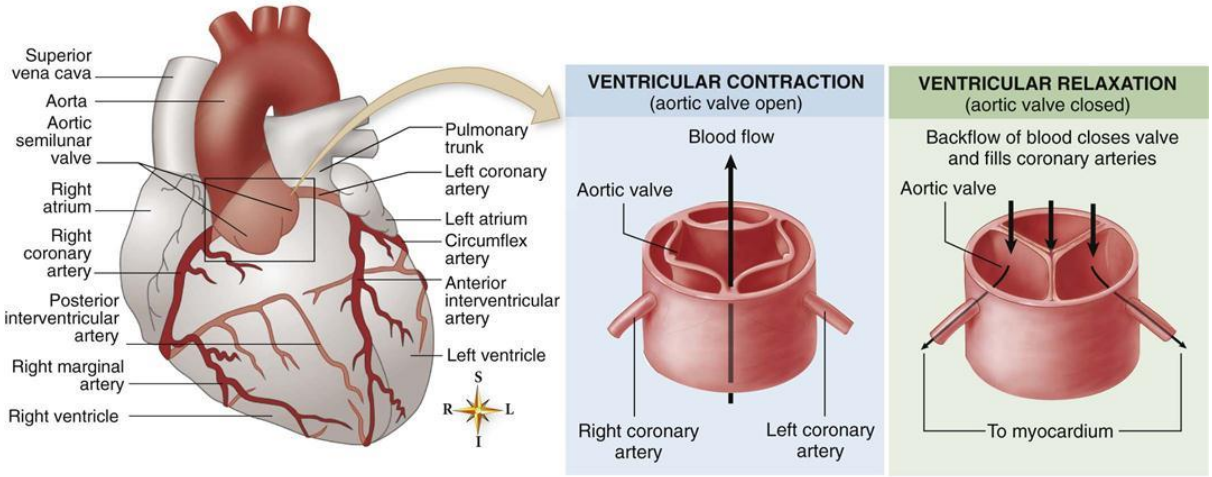

Image from Patton and Thibodeau, (2013)

Figure 2.1. Back-pressure generated by the elasticated aorta closes the aortic valve at the end of systole, diverting blood flow to supply the myocardium via the coronary arteries.

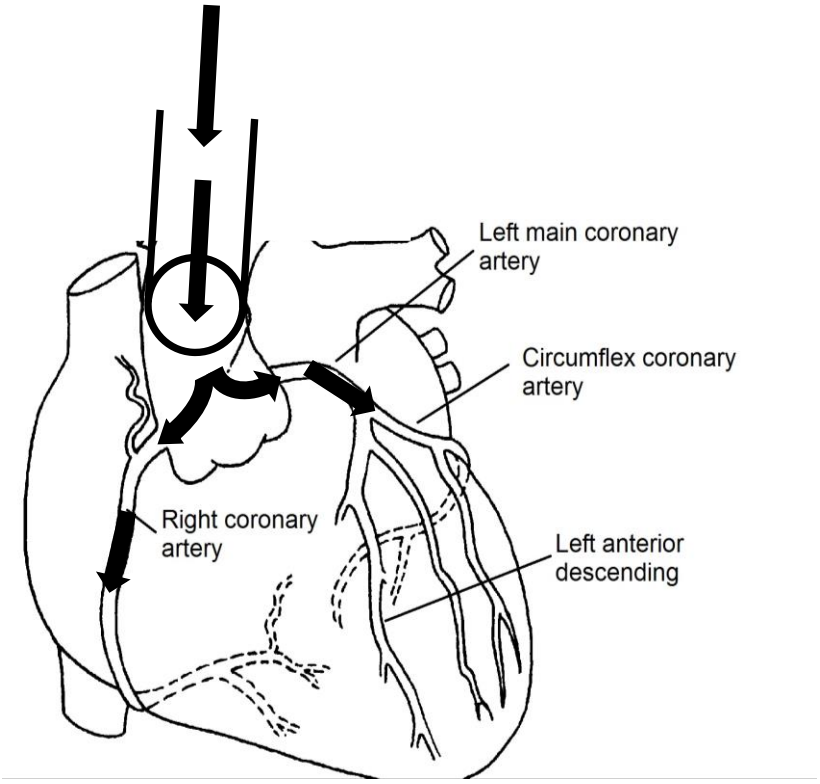

Figure 2.2. Diversion of perfusate into the coronary arteries of a heart perfused in Langendorff mode

2.1.2. Experimental Protocol

Preparation and mounting of the heart

The hearts used for Langendorff perfusion in this thesis came from rats which were between 300 and 350 g in bodyweight, and therefore had similar sized aortas which were wide enough to accommodate the cannula (4 mm in diameter). Rats were euthanised by rising CO2 levels and cervical dislocation, and, following removal from the chest cavity, the heart and thymus were swiftly transferred to a vessel of ice cold Krebs-Henseleit (KH) buffer **(Appendix II)**. Excess fat and any attached lung tissue and thymus was removed to expose the aorta, which was cut below the aortic branch **(Figure 2.4)**. Hearts were then mounted on the cannula via the aorta before undergoing retrograde perfusion at 38˚C (core body temperature for a rat (Lomax, 1966)) using KH buffer containing substrate combinations detailed

in the methods section of the appropriate chapter. The buffer was continually gassed with 95% O_2, 5% CO_2 gas at pH 7.4, recirculated, and filtered using an in-line pre-filter with 0.8 and 0.45 µm filters to remove any detritus washed out of the heart. The pulmonary artery was incised to prevent build-up of pressure in the right ventricle. All hearts were perfused at a constant pressure of 100 mmHg for lengths of time detailed in the individual chapters' methods sections, with the exception of during ischaemia when the hearts were perfused at a constant flow rate (again specified in the respective chapters' methods sections).

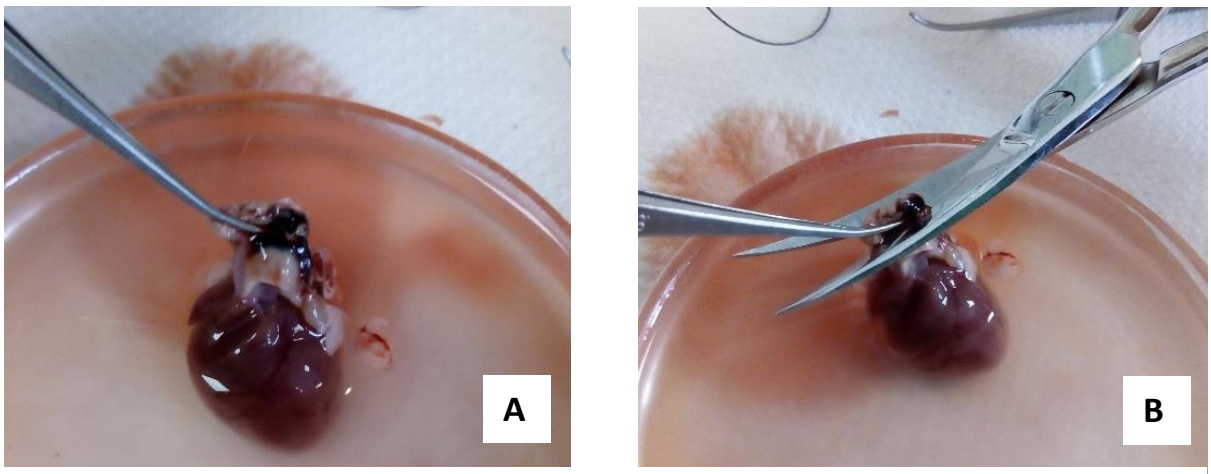

Figure 2.4. Preparation of the heart for perfusion in Langendorff mode. (A) The aortic branch is carefully exposed. (B) The aorta is cut below the aortic arch to allow insertion of the cannula

Measurement of Cardiac Function

Measurements of cardiac contractile function were made using a fluid filled PVC balloon inserted into the left ventricle (Liao et al., 2012; Transonic, 2018). The balloon was initially inflated to produce a left ventricular end-diastolic pressure (LVEDP) of ~4 mmHg, and was attached via a catheter to a pressure transducer (ADInstruments) which was regularly calibrated. The output from the pressure transducer was interpreted and recorded using a PowerLab and LabChart software (ADinstruments). Rather than constantly adjusting the LVEDP throughout the protocol as would have interfered with the measured results, the measured LVEDP was allowed to decrease naturally while the pre-ischaemic perfusion period progressed and the heart relaxed, therefore presenting a lightly loaded perfused heart model.

The pressure difference between the forces exerted by the heart on the balloon during systole and during diastole was calculated to give the left ventricular developed pressure (LVDP), and a measure of the force of contraction. The number of systole/diastole cycles per minute was recorded to give heart rate, in beats per minute (bpm), and through multiplication of LVDP and heart rate a measurement of RPP, or rate-pressure product, was obtained. In ischaemia/reperfusion experiments, recovery of LVDP and RPP were expressed as a percentage of pre-ischaemic LVDP and RPP respectively **(Figure 2.5)**.

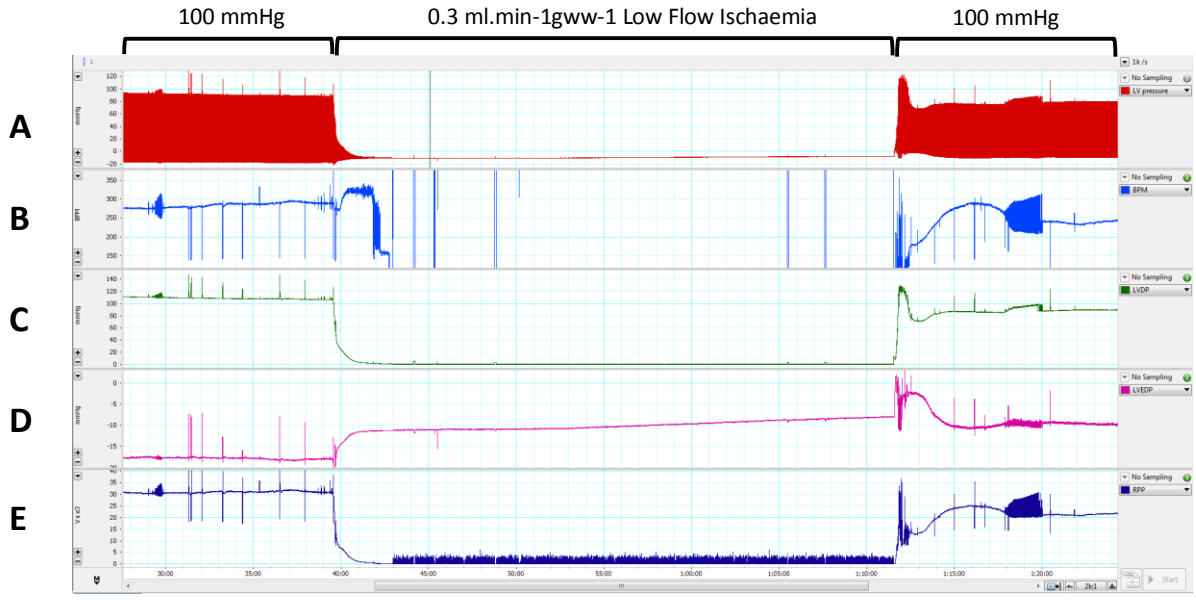

Figure 2.5. A sample trace of the measurements obtained during ischaemia and reperfusion. (A) Pressure exerted on the balloon by the left ventricle (mmHg). (B) Heart rate (Beats per minute, BPM). (C) Left Ventricular Developed Pressure (mmHg). (D) Left Ventricular End-Diastolic Pressure (mmHg). (E) Rate Pressure Product (mmHg/min).

2.1.3. Ischaemia Reperfusion Protocols

During this thesis, subjection of perfused hearts to ischaemia was employed for two purposes: assessment of metabolism in cardiac tissue during ischaemia; and assessment of the extent to which the heart recovered functionally from ischaemia following reperfusion. In all cases, low-flow ischaemia was implemented by using a three-way tap to divert the flow of oxygenated buffer to the heart through a low-flow peristaltic pump (Gilson Minipuls 3). Two separate ischaemic flow rates were employed during this thesis:

1) 30 min at 0.3 $ml.gww^{-1}min^{-1}$, which test runs had shown to yield a functional recovery of 65-70% pre-ischaemic LVDP and RPP following reperfusion, was used to assess functional recovery from ischaemia/reperfusion when different conditions were imposed.

2) 20 min at 0.56 $ml.gww^{-1}min^{-1}$, which resulted in 100% functional recovery following 20 min ischaemia and was used to assess metabolism during ischaemia and reperfusion while attempting to minimise the effect of differences in cardiac work-rate and structural damage caused by I/R upon the results.

Reperfusion of the hearts was achieved by returning the three-way tap to the pre-ischaemic position, restoring 100mmHg constant pressure perfusion for the desired period (specified in the individual results chapter methods sections).

Heart temperature was monitored by thermometer and maintained at 38°C throughout the ischaemia/reperfusion protocol.

2.1.4. The Langendorff Apparatus Used in this Thesis

The Langendorff apparatus used in this thesis (Figure 2.3) was designed, built and optimised by myself in accordance with the following specifications. Custom made glassware was obtained from Cambridge Glass Blowing, including a 1-litre reservoir for the perfusion buffer, from which Krebs-Henseleit (KH) buffer was pumped by a peristaltic pump (Watson Marlow 323S) to the oxygenation lung. Here it was gassed to saturation with 95% O_2, 5% CO_2 carbogen gas. The oxygenated buffer descended under the control of gravity to a stainless steel cannula (4 mm diameter) via a bubble trap designed to prevent any bubbles reaching and causing an embolism in the coronary arteries, producing a pressure of 100 mmHg at the end of the cannula. The heart itself was mounted upon this cannula. Cardiac temperature was measured using a type T thermocouple probe (Thermo Fisher), and maintained at a constant temperature of 38°C by a water-jacketed heart chamber. Flow into the bubble trap and cannula could be limited using a flow rate adjustor during the process of mounting the heart. The heart chamber also served to collect the coronary effluent which has passed through the heart, channelling it back to the reservoir or for sampling.

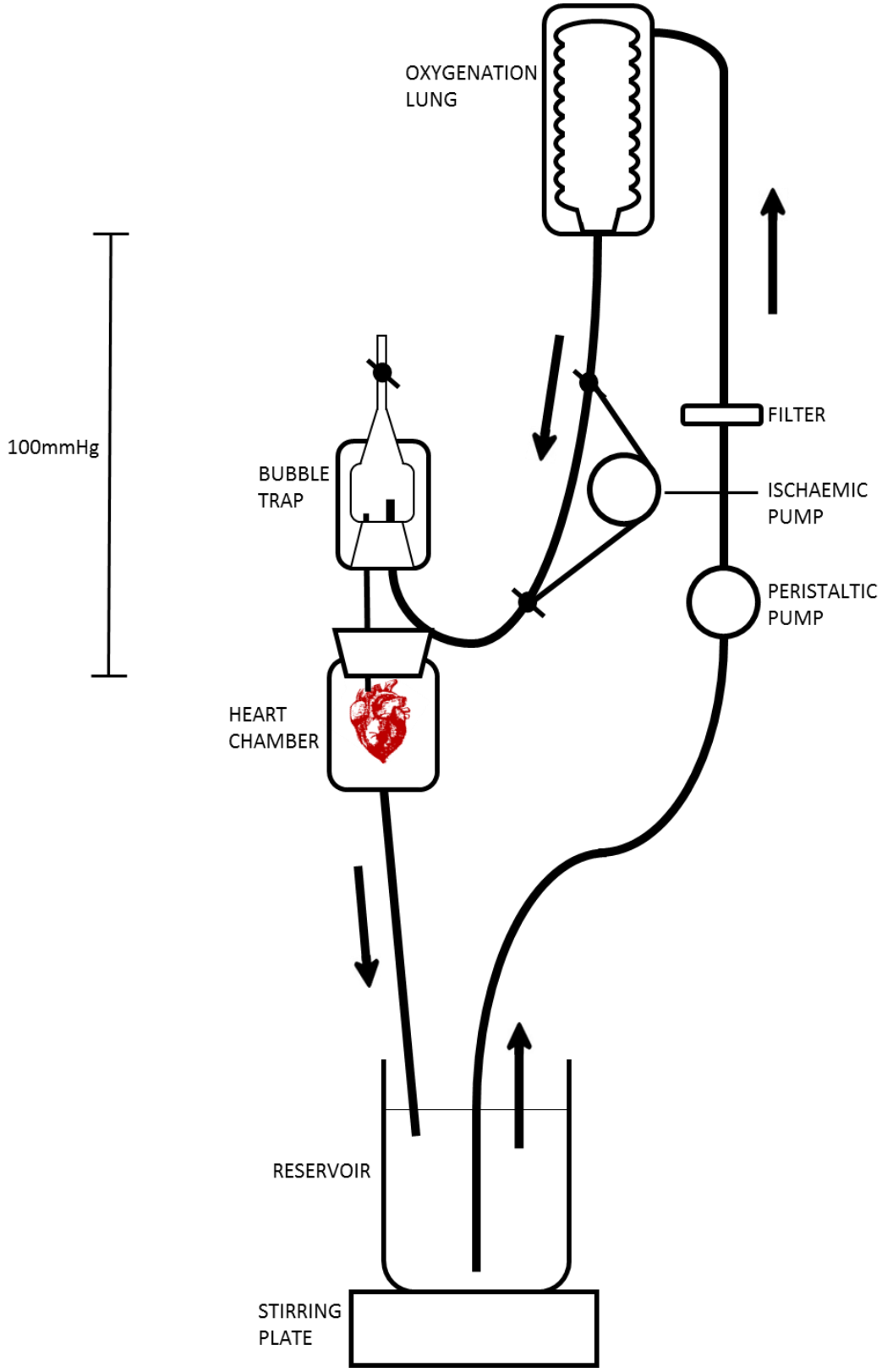

Figure 2.3. Schematic demonstrating the Langendorff rig used in this thesis. Krebs-Henseleit buffer from the reservoir was pumped by a peristaltic pump to the oxygenation lung, where it was continually gassed with 95% O_2/5% CO_2 carboxygen gas. A perfusion pressure of 100 mmHg to the heart was maintained by force of gravity from the level of buffer in the oxygenation lung.

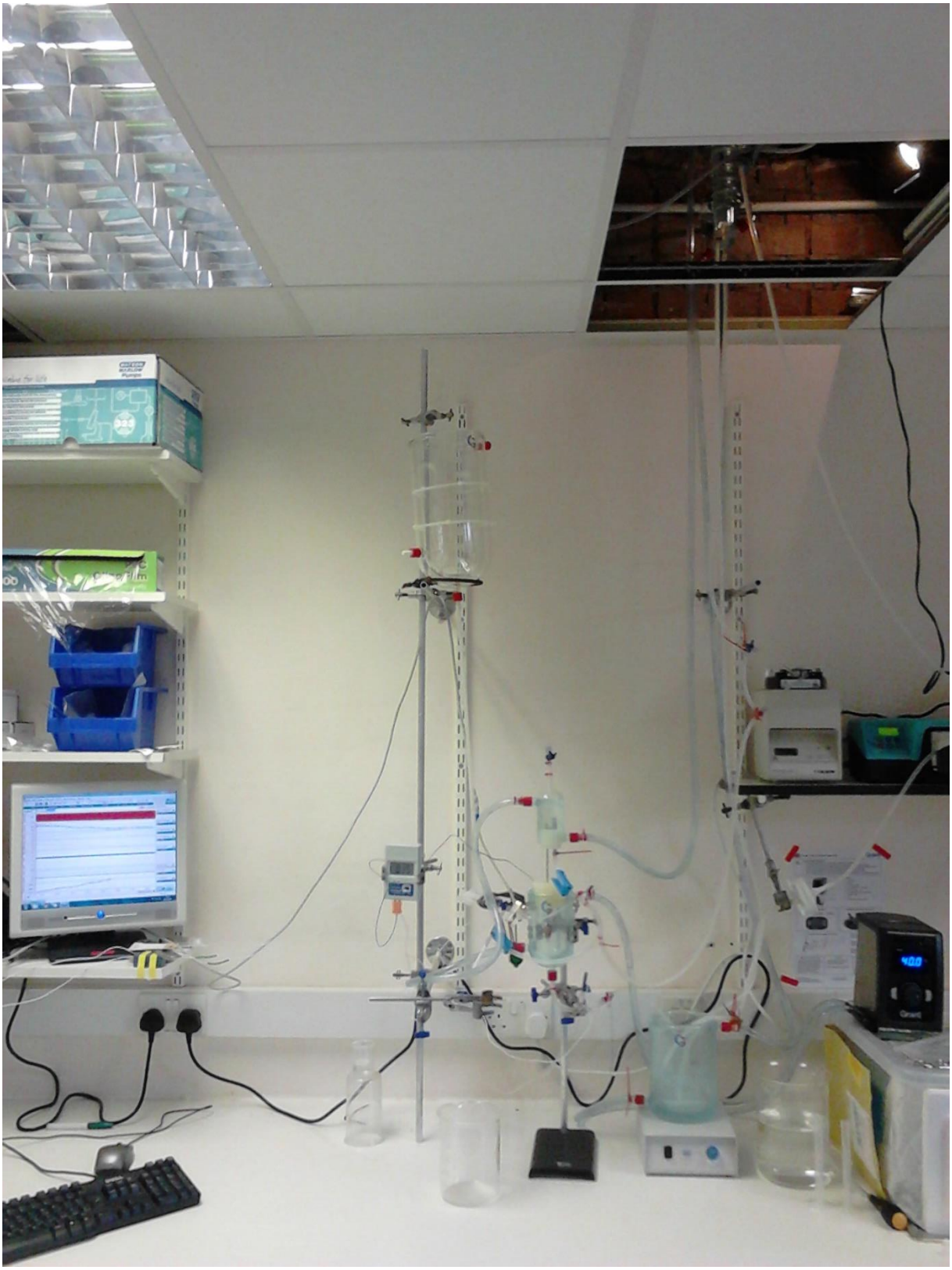

Figure 2.4. Photograph of the Langendorff perfusion apparatus setup used throughout this thesis.

2.2 HIGH RESOLUTION RESPIROMETRY

2.2.1 Concept of Respirometry

Mitochondrial respirometry measures the rate of oxygen consumption at the mitochondrial electron transport chain. It may be used to obtain an in depth analysis not only of broader oxidative capacity, but even of the functionality of individual ETC constituents.

Cellular consumption of oxygen, which as discussed in chapter one is the final electron acceptor of the ETC, is directly linked to the rate of mitochondrial metabolism. Despite other enzymes such as xanthine oxidase having the capacity to consume some oxygen, the predominant source of cellular oxygen consumption is at the ETC; unlike other metabolic indicators such as NADH and ATP which are consumed and regenerated in multiple cellular processes. Measurement of cellular oxygen consumption while controlling the metabolic conditions can therefore be used to accurately and sensitively make a measurement of electron flux through various components of the ETC.

2.2.2 Oxygen Sensing Apparatus

The respirometry conducted in this thesis employed the Oxygraph 2K (Oroboros Instruments, Austria), a highly sensitive set of oxygen detecting polarographic electrodes. The Oxygraph comprises two sealed 2 ml chambers, which are separated from the oxygen electrodes by a selectively permeable membrane. Behind the membranes, the electrodes themselves are in a 10 mM KCl electrolyte solution. At the gold cathode, oxygen reacts with water, while at the anode silver reacts with the chloride ions in the electrolyte solution as follows:

$$O_2 + 2H_2O + 4e^- \rightarrow 4OH^-$$

Reaction 2.1. At the cathode.

$$4Ag + 4Cl^- \rightarrow 4AgCl + 4e^-$$

Reaction 2.2. At the anode

The current passing between the electrodes is therefore directly limited by oxygen availability. The rate at which biological samples placed in the chamber consume oxygen can therefore be measured via the accompanying reduction in current.

Figure 2.5. An Oxygraph in use measuring mitochondrial function in Hørsholm, Denmark during data collection for chapter 6 of this thesis.

Oxygen consumption and current passed through the electrodes vary in a directly linear fashion through the experimental range, so a two point calibration was used to ensure that variations in conductivity over time did not affect the experimental results. The chamber was calibrated by equilibration firstly using air saturation as a known value (194.20 µM in MiR05 at 37˚C), and then by adding an oxygen scavenger, sodium dithionate, to the chamber to remove all oxygen from solution as the second calibration point.

The chambers were constantly maintained at 37°C by a copper heating block controlled by a feedback loop. Constant mixing ensured that substrate and oxygen concentration was maintained throughout the chamber. Periodic injections of pure oxygen into an introduced air gap were used to maintain the oxygen concentration of the buffer between 200µM and 400µM. The rate of oxygen consumption was calculated and acquired using DatLab data acquisition software (Oroboros Instruments, Austria).

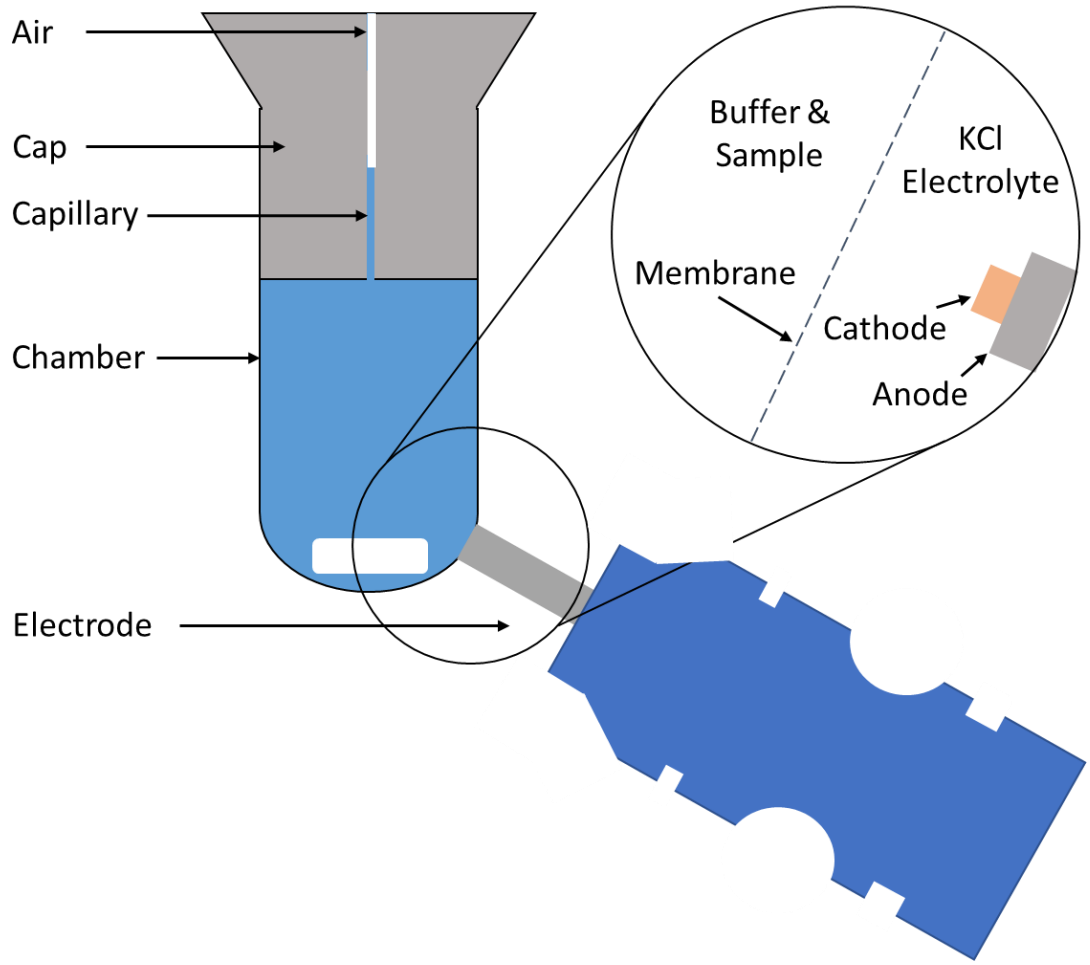

Figure 2.6. Configuration of the Oxygraph chamber

2.2.3. Preparation of the Biological Samples for Respirometry

It is possible to selectively permeabilise the plasma membrane, allowing access for substrates and inhibitors while maintaining overall tissue structure, and that is the method which has been employed in this thesis. The permeabilising agents saponin and digitonin bind cholesterol, which is present to a much higher concentration in the cellular membrane than the mitochondrial membranes, forming pores which allow passage of mitochondrial substrates and inhibitors into the cell while leaving the mitochondrial membranes intact (Kuznetsov et al., 2008). Washing the permeabilised tissue preparation in this state allows removal of all endogenous substrates and ADP, meaning that measurements could be made in the confidence that leftover metabolites from before the preparation were not affecting the results.

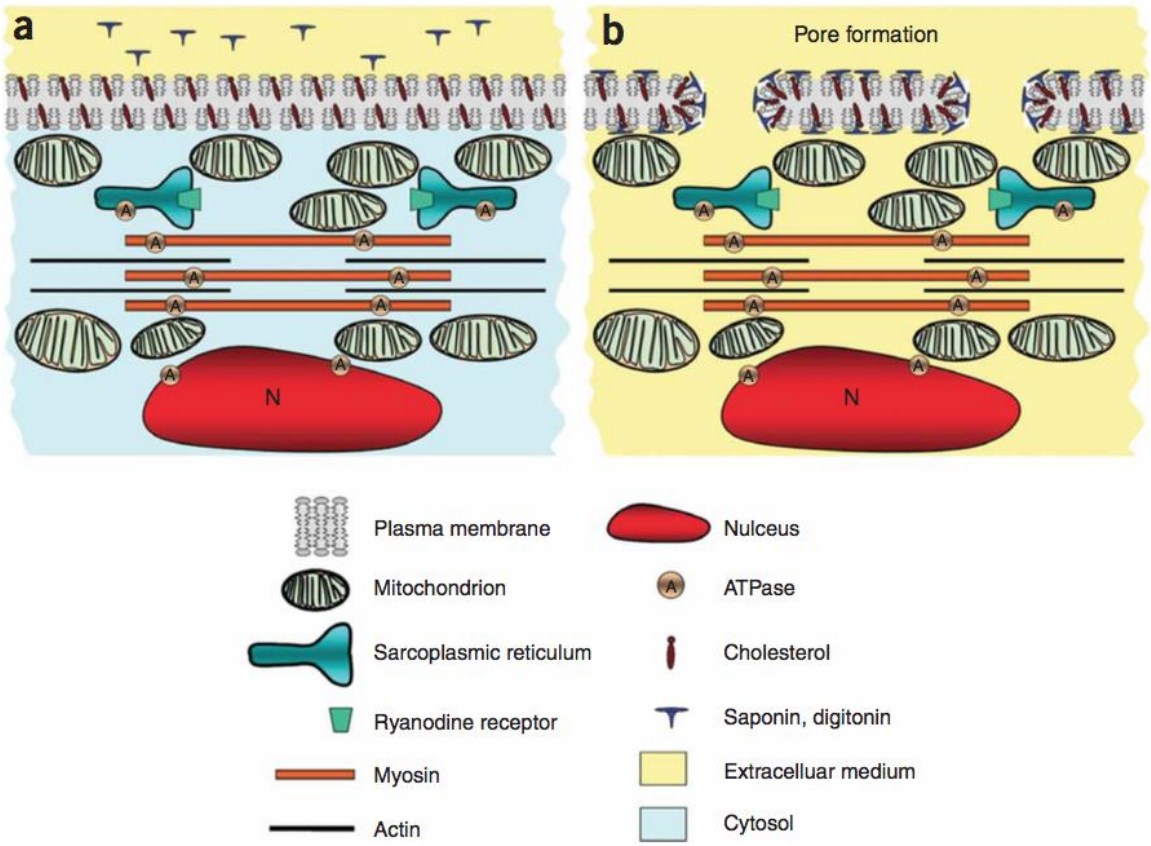

Figure 2.7. Schematic of the selective permeabilisation of the plasma but not mitochondrial membranes using saponin. Diagram from Kuznetsov et al. (2008)

Method for the Preparation of Permeabilised Cardiac Fibres

Sections of left ventricle were permeabilised for respirometry using previously described methods. Placed immediately in ice cold BIOPS solution **(Appendix II)**, the tissue was mechanically separated under a microscope using dissection forceps, so that individual myofibres of cardiac tissue were visible and medium would be able to move between them. The fibres were then incubated for 20 min, rocking on ice in the presence of 50 µg/µl saponin. The saponin was then washed out with 3 x 5 min washes with ice cold MiR05 **(Appendix II)**, after which fibres were blotted dry on filter paper and a known mass of around 2 mg was placed in each chamber.

2.2.4 Substrate Uncoupler Inhibitor Titration (SUIT)

In the permeabilised preparation, a substrate-uncoupler-inhibitor titration (SUIT) was employed to address the biological questions. Various contributing factors to mitochondrial electron flux rate, such as β-oxidation and the activity of various constituents of the ETC can be assessed through serial administration of saturating concentrations of compounds. In this thesis, the SUIT detailed in **Table 1** was employed, with injections of substrates and inhibitors in the following order:

Table 1. SUIT protocol used throughout this thesis

STATE	PATHWAY	ADDITION	CONCENTRATION	FIGURE
Leak		Malate	2 mM	**2.8**
Leak	β-oxidation	Octanoyl-Carnitine	0.2 mM	**2.9**
Oxphos	β-oxidation	ADP	5 mM	**2.10**
Oxphos	β-oxidation + Pyruvate	Pyruvate	20 mM	**2.11**
Oxphos	Complex I	Glutamate	10 mM	
Oxphos	Outer membrane integrity test	Cytochrome C	10 mM	**2.12**
Oxphos	Complex I + II	Succinate	10 mM	**2.13**
Oxphos	Complex II	Rotenone	0.5 mM	**2.14**

2.2.5 Explanation of the States and Mechanisms Investigated

Leak State Respiration

In the absence of ADP, ATP synthase cannot function to allow protons to flow from the inter-membrane space into the matrix. This means that any flux of protons (and therefore electron transit through the ETC to restore $\Delta\mu H^+$ and the associated oxygen consumption) corresponds to leakage of protons in other manners, either slippage through proteins, membrane uncoupling or the leakiness of the inner membrane itself. This measured oxygen consumption state reflects the inefficiency of the mitochondria.

Priming the Krebs Cycle with Malate

The initial addition of substrate for the experiments was malate, which primed the Krebs cycle for subsequent additions. The conversion of malate to oxaloacetate produces some NADH, which contributes to ETC flux through complex I (Gnaiger, 2008). However, the main advantage of adding it early in the protocol is because the subsequent production of oxaloacetate allows entry of acetyl-CoA to the TCA cycle through citrate synthase mediated combination of the two molecules to form citrate. Both β-oxidation and PDH yield acetyl-CoA as a product, so this allows subsequent assessment of their flux.

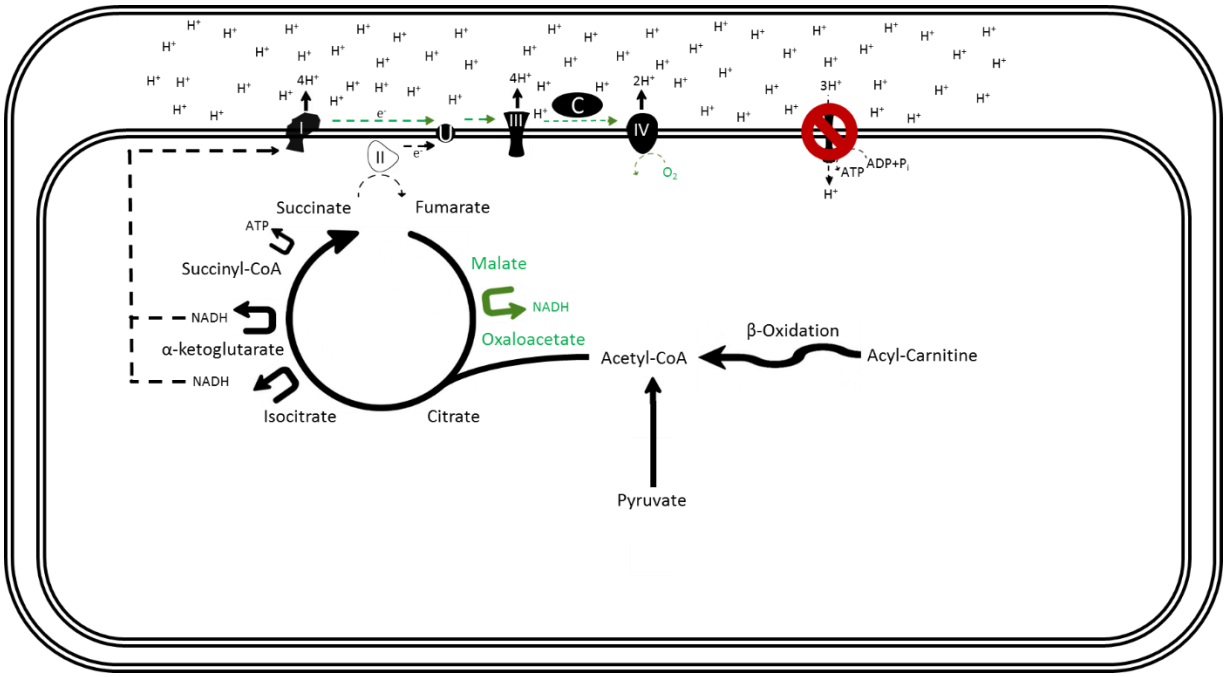

Figure 2.8. Leak State Respiration of Malate. Activated pathways are represented in green. In the absence of ADP, protons re-enter the mitochondrial matrix by leaking through the membranous proteins and the inner mitochondrial membrane itself, which allows O_2 to be consumed at complex IV at a low rate.

β-oxidation Limited ETC Function

Short to medium chain acyl carnitines, such as octanoyl carnitine which is used in this thesis, bypass CPT-I transport into the mitochondria through CACT and therefore allow assessment of the rate of function of the β-oxidation pathway directly. Both the cyclic oxidation of fatty acids and the combination of the resulting acetyl-CoA with malate to enter the TCA cycle result in the supply of electrons to the ETC, and so the rate limiting factor for oxygen consumption in the presence of octanoyl carnitine is β-oxidation capacity (Gnaiger, 2008).

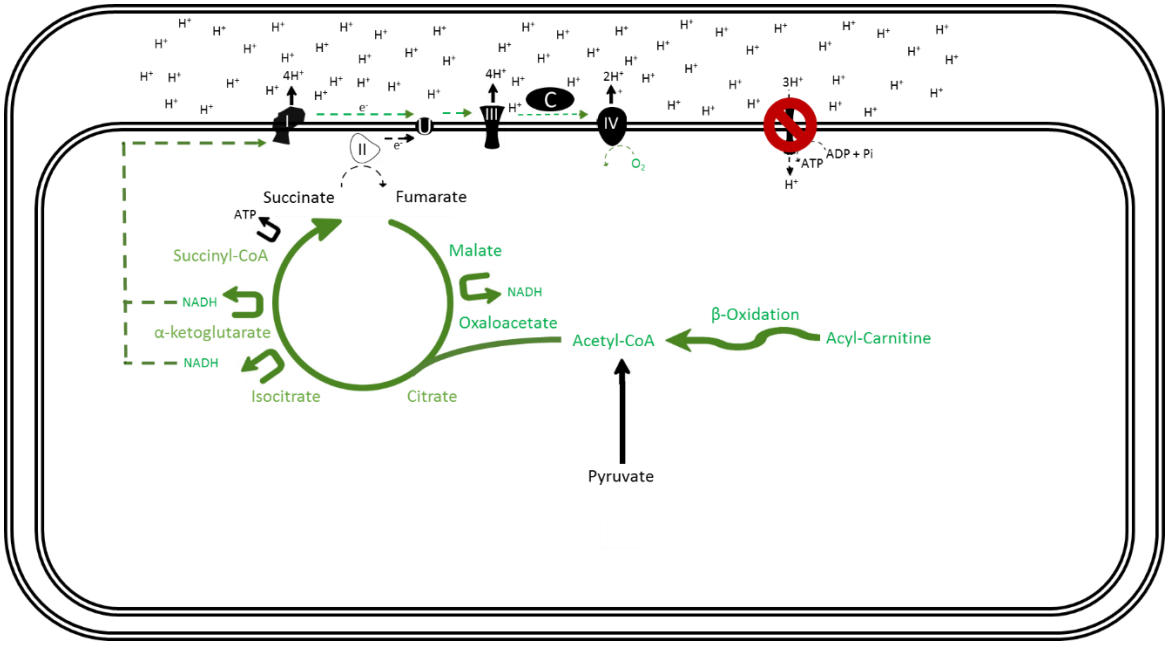

Figure 2.9. Leak State β-oxidation Supported Oxygen Consumption. Activated pathways are represented in green. Oxaloacetate formed from the dehydrogenation of malate allows acetyl-CoA produced by β-oxidation to enter the Krebs cycle. In the absence of ADP, protons continue to re-enter the mitochondrial matrix by leaking through the membranous proteins and the inner mitochondrial membrane itself, allowing a low rate of O_2 consumption at complex IV

Oxphos Limited Respiration

Oxidative phosphorylation was activated through the addition of saturating concentrations of ADP (Gnaiger, 2008). This potentiated flux through ATP synthase, allowing a much higher rate of ETC flux and therefore oxygen consumption to occur. Comparison of fluxes after and before addition of ADP allows an assessment of how coupled $\Delta\mu H^+$ is to ATP synthesis, with the ratio of post to pre-ADP addition therefore yielding an approximation of the respiratory acceptor control ratio (RCR), an indicator of mitochondrial coupling.

Once ADP is present, the addition of saturating concentrations of various substrates and inhibitors can be used to address the maximal contribution of different pathways and ETC components to overall ETC flux.

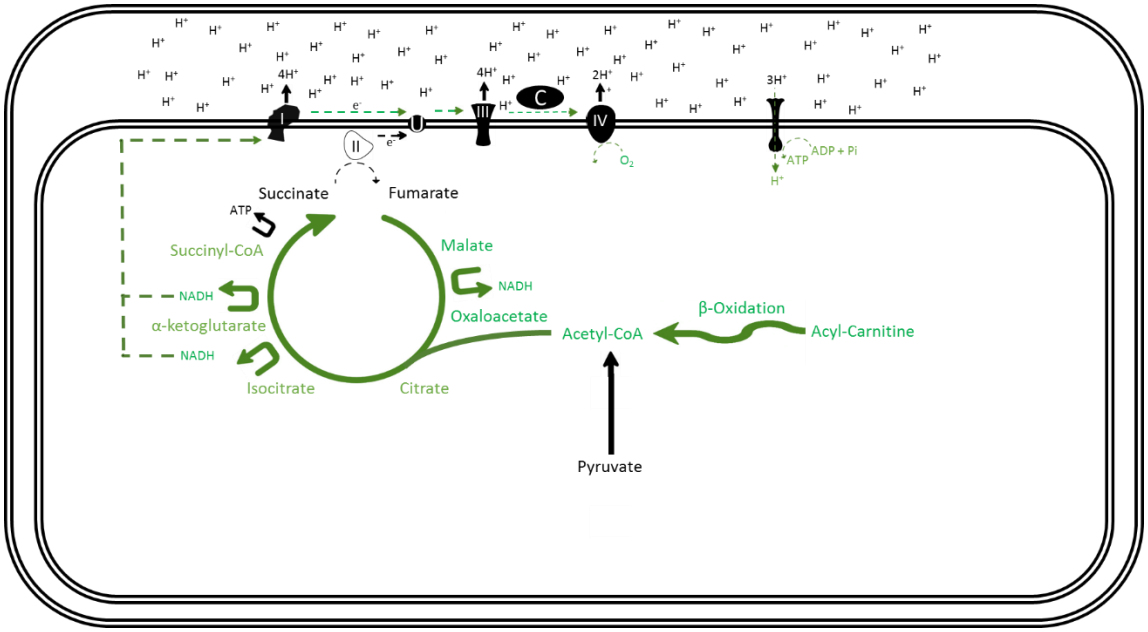

Figure 2.10. β-oxidation Supported Oxphos. Activated pathways are represented in green. ADP allows the activation of ATP-synthase, and a higher rate of ETC activation and oxygen consumption at complex IV

Pyruvate

Pyruvate, which enters the mitochondria via the mitochondrial pyruvate carrier, is converted to acetyl-CoA by pyruvate dehydrogenase for entry into the Krebs cycle. Addition of pyruvate therefore assesses the maximal contribution of pyruvate to complex I via the Krebs cycle (succinate is cell permeable and so the respiratory rate supported by complex II cannot be assessed without saturating concentrations). Further, in combination with previous assessment of β-oxidation this allows determination of how much of the total Krebs cycle oxidation capacity β-oxidation is capable of accounting for through division of the β-oxidation supported oxphos respiration rate by the β-oxidation + pyruvate supported oxphos respiration rate (Horscroft et al., 2015).

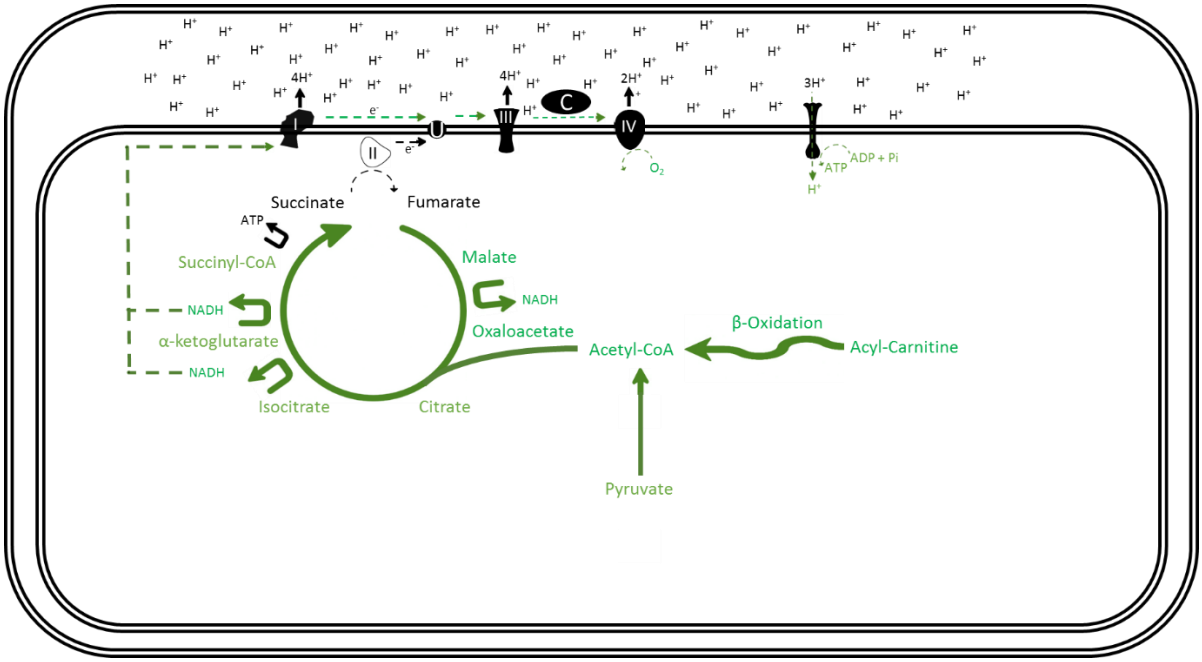

Figure 2.11. β-oxidation and Pyruvate Supported Oxphos. Activated pathways are represented in green. Pyruvate is also metabolised to acetyl-CoA, meaning the concentration of acetyl-CoA available to the Krebs cycle is no longer limited by β-oxidation.

Complex I Linked Respiration

In tandem with the previous addition of malate, addition of glutamate saturates complex I to achieve a measure of maximal complex I activity. Glutamate enters the mitochondria via the glutamate/aspartate antiporter and is rapidly converted to aspartate and α-ketoglutarate through reaction with oxaloacetate, thereby driving further NADH-producing conversion of malate to oxaloacetate. α-ketoglutarate is then further dehydrogenated in the Krebs cycle to produce more NADH. All of the NADH produced transfers its electrons to the ETC via complex I, saturating it and providing a measurement of total complex I activity.

Validation of the Condition of the Mitochondrial Membranes

To be assured that the mitochondrial membranes have not been damaged during the permeabilisation protocol, two tests were performed. The first, a test of inner membrane intactness, was performed intrinsically with the addition of ADP; if the inner mitochondrial membrane had been disrupted, the proton gradient would have dissipated with resultant loss of mitochondrial coupling. Therefore, any observation of an ADP response demonstrates that the mitochondrial inner membrane is intact.

The second test, of outer membrane integrity, was performed through the addition of reduced cytochrome *c*. If the outer membrane were damaged, then some cytochrome *c*, an electron carrier of the ETC which operates in the inter-membrane space, would have been lost. In this scenario, addition of cytochrome *c* would result in a dramatic increase in oxygen consumption, and so lack of response to cytochrome *c* acts as an assurance that the outer membrane is intact (Gnaiger, 2008).

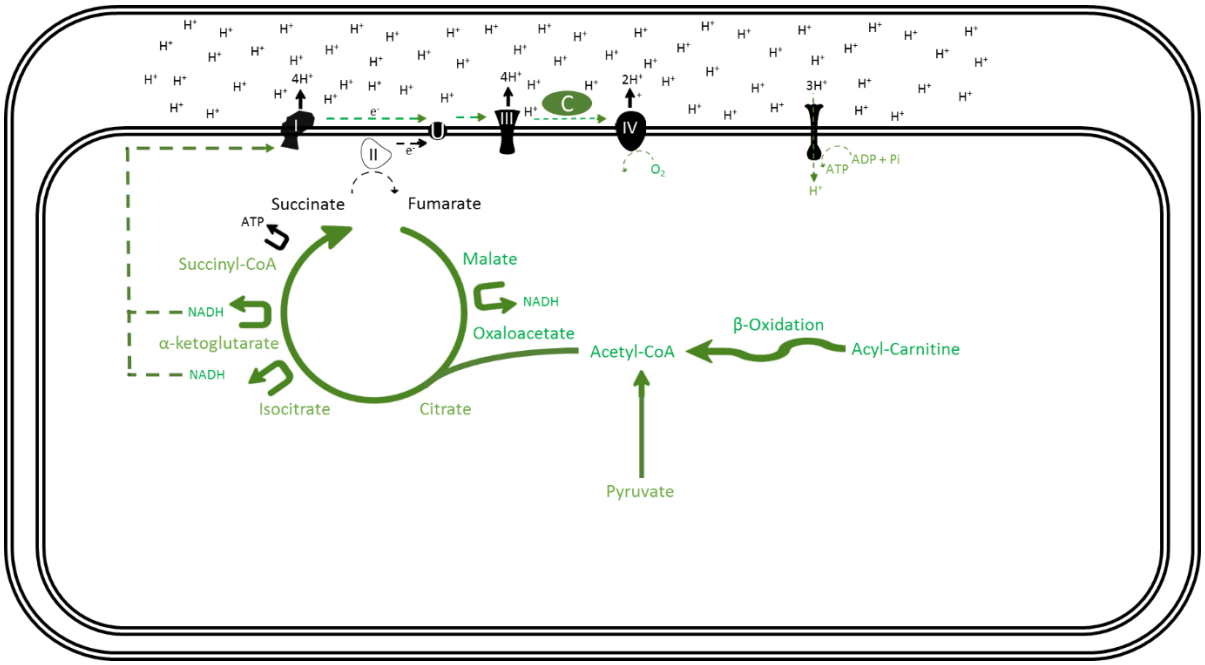

Figure 2.12. Cytochrome *c* Test of Membrane Integrity. Activated pathways and additions are represented in green. If there has been outer membrane rupture and loss of cytochrome *c*, addition of cytochrome *c* will enhance electron transfer and rate of oxygen consumption.

Total Oxphos

Addition of succinate in excess saturated the activity of complex II. Succinate is converted to fumarate by complex II (succinate dehydrogenase) reducing FAD^+, at which point the electrons this reaction yields enter the Krebs cycle via $FADH_2$. Oxygen consumption in the presence of malate, glutamate and succinate in tandem therefore reflects the maximal capacity for the ETC to support oxphos, because complex I and complex II are each individually capable of enabling more electron flux into the ETC than complex III will allow when both are maximally supplied with electrons (Gnaiger, 2008).

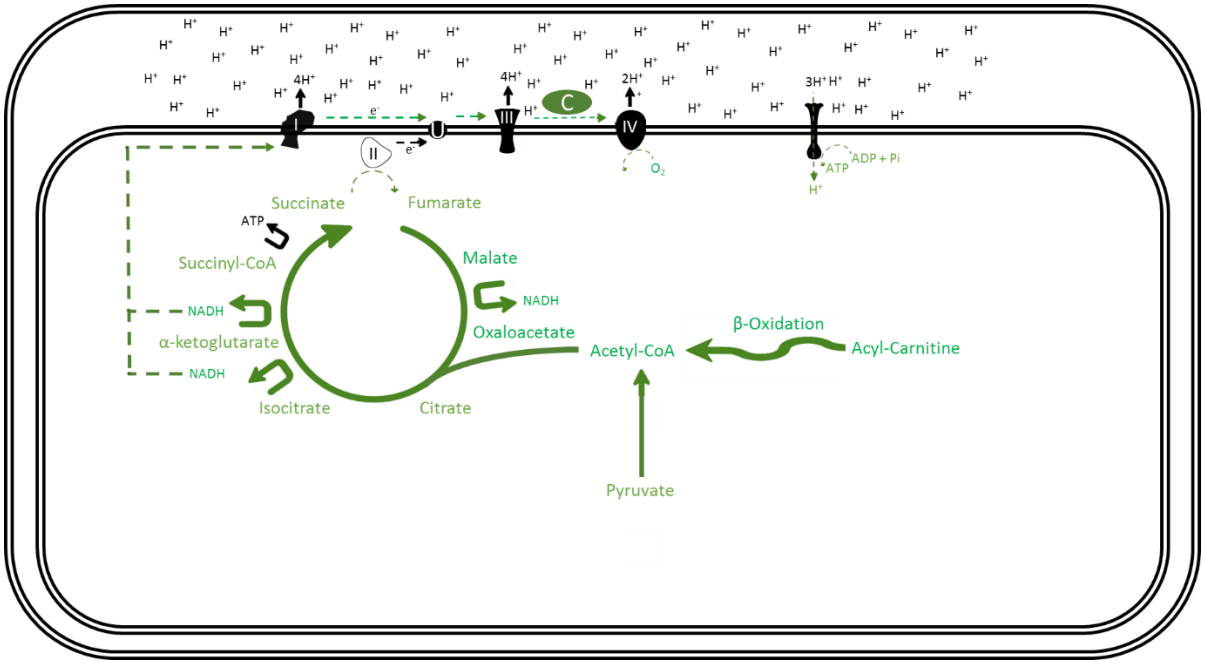

Figure 2.13. Total Oxphos. Activated pathways and additions are represented in green. Succinate activates complex I in addition to the previously activated complex I, resulting in full input of electrons to the ETC.

Complex II Linked Respiration

Since total oxphos represents a lower rate than the maximal complex I and maximal complex II respiration added together, subtracting complex I activity from complex I + II activity does not give the rate of saturated complex II activity. Instead, inhibition of complex I can be used to determine the maximal rate of complex II linked respiration. This was achieved using the complex I inhibitor rotenone, leaving succinate as the sole contributor of electrons to the ETC via complex II (Gnaiger, 2008).

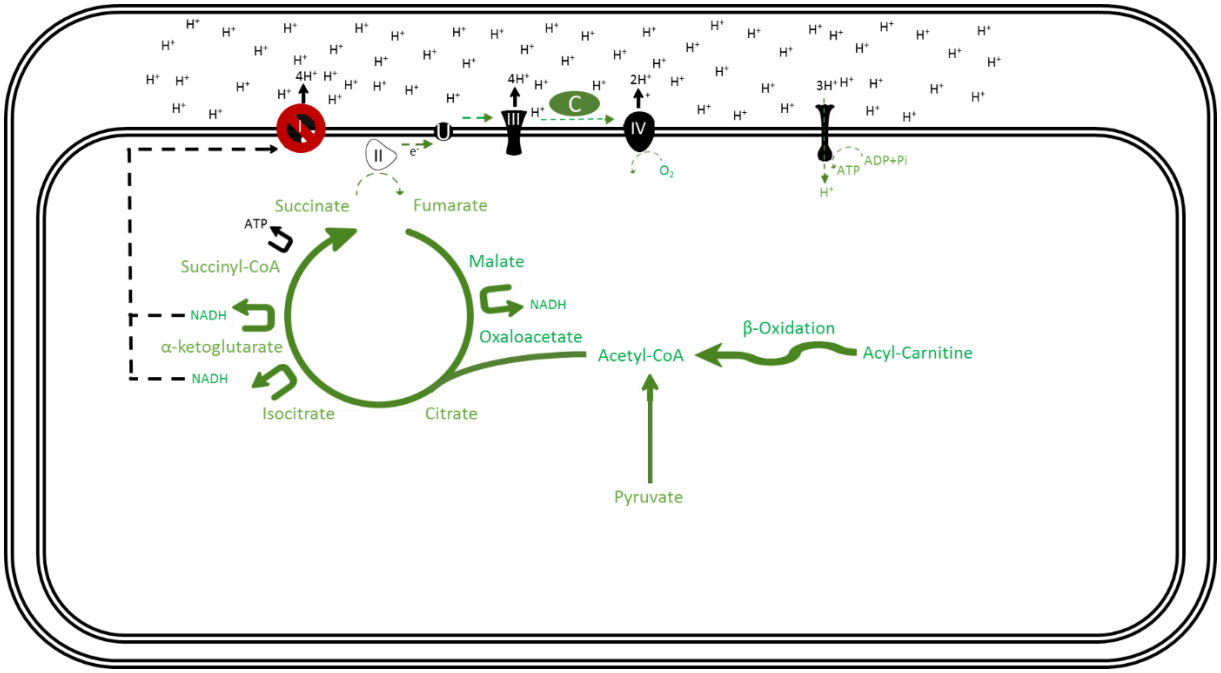

Figure 2.14. Complex II Function. Activated pathways and additions are represented in green. Inhibition of complex I with rotenone results in complex II becoming solely responsible for electron contribution to the ETC.

2.3 LIQUID CHROMATOGRAPHY COUPLED MASS SPECTROMETRY

2.3.1 Concept of Mass Spectrometry

Mass spectrometry is the effective discrimination of compounds based upon their resultant mass/charge ratio (m/z) following ionisation. It can be performed in analytical chemistry on both single purified compounds and complex mixtures of compounds, such as that represented by a biological sample, and allows the high throughput detection of the concentrations of many metabolites present in a tissue or buffer sample (Heather et al., 2013).

2.3.2 Tissue Extraction for Assessment Using Mass Spectrometry

Metabolites were extracted from heart samples using a methanol/chloroform/water extraction method (Le Belle et al., 2002). Frozen tissues were added to 600 µL methanol/chloroform (2:1; v/v), and the samples were homogenized with a Tissuelyser (Qiagen, UK) for 5 min at a frequency of 20/s before 15 minutes of sonication. Water (200 µL) and chloroform (200 µL) were then added to the samples prior to centrifugation at 17000 g for 7 min. The resulting aqueous and organic phases were collected, and the extraction procedure was repeated for a second time on the protein pellets. Aqueous phases were dried down using an evacuated centrifuge, while the organic phase was dried by evaporation. Dried samples were stored at −20°C until further analysis.

2.3.3 Separation of Compounds through Liquid Chromatography

In order to gain extra resolution, compounds can be separated by factors such as solubility, size, charge and shape through liquid chromatography (LC). This has the advantage of both separating compounds out when they arrive at the detector to enable greater sensitivity of detection, and also allowing more accurate identification of compounds with different retention times (especially those with the same m/z, termed isobaric species). Liquid chromatography is conducted at high pressure by injecting a small volume of tissue extract in solution into a mobile phase, which carries the sample through a solid phase, or column, to separate compounds by their affinity for the solid phase. The mobile phase composition may also be altered through the run time for each sample, which varies both the solubility of compounds in the mobile phase and the pressure they experience across the column to further separate compounds arriving at the detector.

In this thesis, two main liquid chromatography methods have been employed. The first, using a BEH amide column, has been developed to separate highly polar compounds and works best for separation of compounds including ATP and malonyl-CoA. The BEH amide column separates compounds using hydrophilic interaction chromatography (HILIC) to differentially retain polar compounds within the

column, allowing separation of these compounds and greater detection capacity. The second method implements a C18pfp column to separate compounds. The C18 chain interacts with hydrophobic components of molecules to separate compounds using Van der Wall's forces, while the pentafluorophenyl (pfp) component of the column is used for the separation of aromatic compounds and those with shape constraints.

BEH Amide LC Methodology

Aqueous extract fractions were reconstituted in an acetonitrile: 10 mM ammonium carbonate solution (7:3 v/v, 100 µl) containing a 10 µM mixture of internal standards (Appendix B). The column used was a 1.7 µm BEH amide column (150x2.1 mm), coupled to a Vanquish UHPLC+ series (Thermo Scientific, UK) LC system and a TSQ Quantiva Triple Quadrupole Mass Spectrometer (Thermo Scientific). The mobile phase was pumped at 600 $\mu l min^{-1}$ with mobile phase A 0.1% ammonium carbonate solution, and mobile phase B acetonitrile. Mobile phase A was held at 20% for 1.5 min, linearly increased to 60% over the next 2.5 min, held at 60% for 1 min, before being decreased back to the initial conditions (20% mobile phase A) in the next 0.1 min. The total run time was 6 min. Nitrogen at 48 mTorr, 420°C was used as a drying gas for solvent evaporation and the UPLC column was conditioned at 30°C.

C18pfp LC Methodology

Following reconstitution in a 10 mM ammonium acetate solution/internal standard mixture (200 µL; phenylalanine d5, Valine d8, leucine d10), samples were run for 6 min on either a Thermo Vanquish (coupled to a Thermo Quantiva triple quadrupole mass spectrometer) or a Thermo Dionex Ultimate 3000 (coupled to a Thermo Elite orbitrap mass spectrometer) LC system using an ACE Excel-2 C18-PFP 5 µm column (100 A, 150x2.1 mm, 30°C). Mobile phase A was 0.1% formic acid, while mobile phase B was acetonitrile plus 0.1% formic acid. The LC gradient was as follows: 0% B for 1.6 min followed by a linear gradient up to 30% B for 2.4 min. There was a further linear increase to 90% B for 30 s, following which B was held at 90% for 30 s before re-equilibration for 1.5 min. Drying gas was as used in the BEH amide method.

2.3.4 Mass Spectrometry

Mass spectrometry effectively utilises three stages to separate and quantify molecules by mass to charge. The first is ionisation of the compounds, the second is separation of the resultant ions by m/z ratio and other methods, and the third is detection of the separated ions. In this thesis, two different

types of mass spectrometer have been utilised: a triple quadrupole mass spectrometer (Thermo Quantiva), and an orbitrap (Thermo Orbitrap Elite).

Triple Quadrupole Mass Spectrometry (MS/MS)

In this thesis, triple quadrupole mass spectrometry was used to assess levels of a known collection of compounds involved in metabolism, energy transduction and the response to oxidative stress. These compounds had been previously characterised, and so rather than scanning across the whole range of ions, greater discrimination was achieved by scanning known SRM transitions for the parent and fragmented ions. A table of the SRM values acquired for each of the methods used in this thesis can be found in **Appendix II**.

An electrospray ionisation source was utilised, operated simultaneously in both negative and positive ionisation modes. The Thermo Quantiva uses an Ion Max NG ion source to spray electrons and convert the compounds into ions by either knocking off or adding on an electron. It is capable of rapidly switching between these two ionisation modes, allowing compounds which ionise in both manners to be detected in a single run. Varying the voltage rapidly switches the speed with which electrons collide with the sample molecules, determining whether an electron is knocked off or added on to induce positive or negative charged ionisation. In this instance, electrospray voltages of 3.5 kV and -2.5 kV were used to induce positive and negative ionisation, respectively.

Triple quadrupole mass spectrometers make use of two quadrupoles and an intervening collision cell (the second “quadrupole”) to separate and aid in the identification of ions. Quadrupoles work on the principle of having two sets of interspaced charged cylinders (the poles), which alternate in charge. Depending upon the m/z ratio of the ion passing through, the alternating charge impedes their passage to differing extents, achieving separation of the ions. The collision cell promotes further fragmentation of the ions, allowing compounds to be identified by their fragmentation pattern. Finally, the ions arrive at a detector, an electron multiplier which measures analyte concentration as a function of the current passed across it.

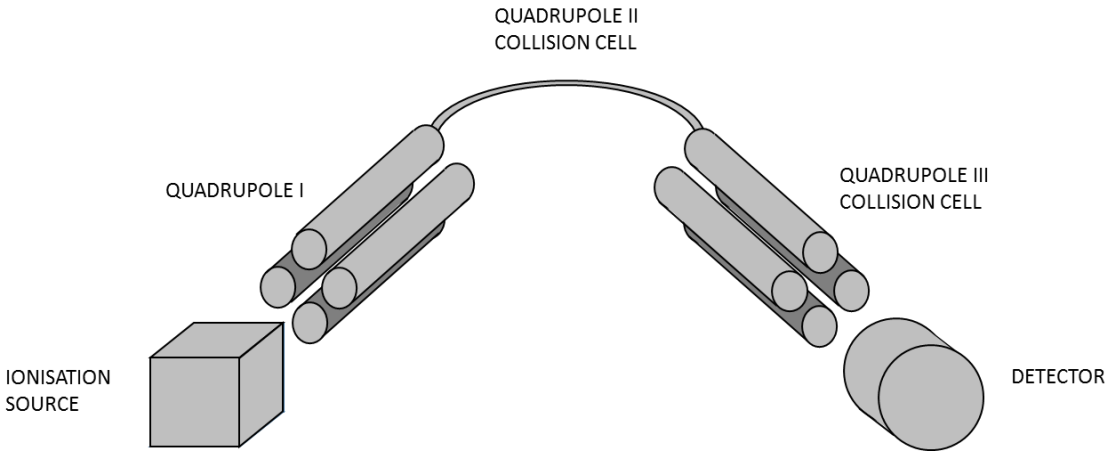

Figure 2.15. Configuration of a Triple Quadrupole Mass Spectrometer.

Orbitrap Mass Spectrometry

The Thermo Orbitrap Elite is an orbitrap based mass spectrometer which produces high resolution mass spectrometry (capable of discriminating ions with a few ppms m/z difference). This makes it more suited to open-profiling analysis where the target compounds to be measured are unknown, as well as measurement of compounds which do not easily fragment, as it does not need to be set to scan only specific mass ranges.

Instead of the quadrupoles, the Elite separates ions using an orbitrap, a charged spindle which differentially traps ions due to their m/z specific flight patterns. This achieves greater separation of ions by m/z ratio, if slightly lower chromatographic resolution.

In this thesis, the Thermo Orbitrap Elite was utilised for the measurement of β-hydroxybutyrate, which does not fragment easily, and lactate, as well as for the measurement of triolein levels in the coronary effluent and perfusion buffer as described in **Chapter 5.** Briefly, for the measurement of β-hydroxybutyrate and lactate, run parameters were as follows: Heater temp 420˚C, sheath gas flow rate 60 units, Aux gas flow rate 20 units, Sweep gas flow rate 5 units. The spray voltage was -2.5, capillary temp 380˚C and S-lens RF level 60%.

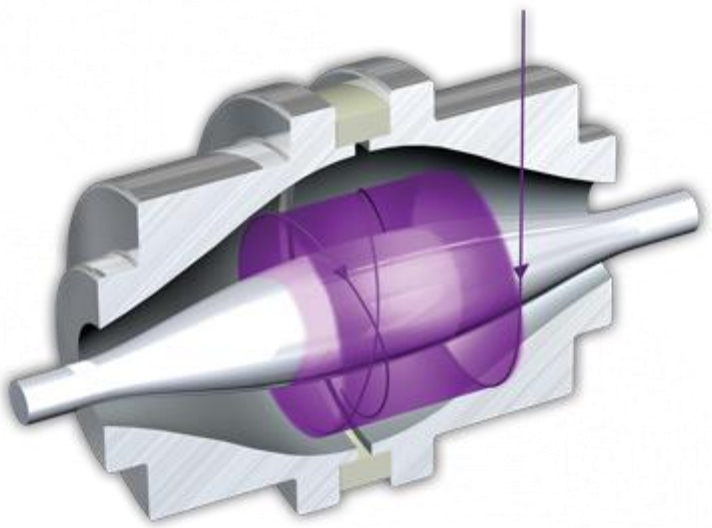

Figure 2.16. An Orbitrap Ion Trap. Upon entry, the molecular ions establish an orbital pattern around the spindle specific to their individual m/z ratios, becoming differentially separated by mass.

2.3.5 Analysis of Data

Peaks obtained using the above described LC-MS and LC-MS/MS methods were detected and analysed using Thermo Xcalibur software, and normalised to both internal standard values and the wet weight of tissue.

2.4 STATISTICAL ANALYSIS

Results are expressed throughout as the mean ± the standard error of the mean (SEM). Data was visualised in Excel before either Student's T-test or 2-way analysis of variance (ANOVA) was used to determine statistical significance alongside any appropriate post-hoc test as detailed in the methods sections of the individual chapters.

CHAPTER 3

A Model for Determining Mitochondrial Substrate Utilisation using ^{13}C-labelled Metabolites

ABSTRACT

As a sequence of enzymatic reactions which represent a major source of reducing potential for oxidative phosphorylation, the Krebs cycle is a focal point of oxidative metabolism. The relative oxidation rates of different substrates via the Krebs cycle varies both physiologically and pathologically, and it therefore constitutes an important area for investigation. Use of ^{13}C labelled substrates has become a key tool for studying this - although the challenge of interpreting the data arising from such experiments has to date often been underestimated. Here, a network model is presented for the prediction of Krebs cycle intermediate isotopologue distributions yielded by any given proportion of ^{13}C labelled acetyl-CoA entering the Krebs cycle, which may be used in conjunction with mass spectrometry to determine the relative contribution of the labelled substrate to the Krebs cycle. The model was validated *ex vivo* using isotopic distributions measured from isolated hearts in which the labelled fraction of the total glucose content in the perfusion buffer had been varied by known amounts. Consistent prediction of the fraction of acetyl-CoA which was labelled was demonstrated across the whole range of possible fractions. The model was further employed to determine the relative contributions of glucose and triglyceride production of acetyl-CoA for oxidation in the Krebs cycle in an experiment in which both were present in the perfusion buffer (11 mM Glucose, 0.4 mM equivalent intralipid triglyceride mixture). Metabolism of glucose and triglyceride in the perfusion buffer were determined to contribute 58 ± 3.6% and 35.6 ± 0.8% of acetyl-CoA oxidised in the Krebs cycle, respectively. These results demonstrate the accuracy of a functional model of Krebs cycle metabolism and can lead to greater scientific value being derived from ^{13}C substrate labelling experiments in the future.

3.1 BACKGROUND

Stable isotope carbon labelling has proven to be an invaluable tool for studying metabolic fluxes. An important use of ^{13}C labelled metabolites has been to investigate the proportional contribution of different substrates to the Krebs cycle in varying conditions and tissues, particularly in the heart which can metabolise a range of substrates (Aubert et al., 2016; Liu et al., 2016; Lloyd et al., 2004; Lloyd et al., 2003). However, interpreting the isotopic distribution of Krebs cycle intermediates arising in such studies is far from trivial, and over-simplified attempts to analyse labelling data have led to incorrectly analysed data in several previous publications.

3.1.1 Current Methods of Analysing Labelling in the Krebs Cycle

For many years Nuclear Magnetic Resonance (NMR) spectroscopy studies formed the basis of work tracking labelled carbons through the Krebs cycle. NMR can detect not only the labelled state of a given carbon but also its chemical environment, which has enabled studies to determine which carbon on the molecule is labelled (Lopaschuk, 1997). However, the sensitivity of detection with NMR remained an issue, with many metabolites including most of the Krebs cycle intermediates proving undetectable, and this led to the measurement of proxies which were assumed to be in chemical equilibrium (Burgess et al., 2001). Furthermore, NMR is based upon detection of individual carbons and their environments rather than the entire molecule; this means that the sensitivity of detection for two different carbons in a molecule could be different and that therefore it could be slower to detect incorporation of ^{13}C in a particular location than in others (Lopaschuk, 1997).

Mass spectrometry is an increasingly utilised approach to the measurement of levels of Krebs cycle intermediates and provides much more sensitivity, albeit without the insight into which carbon has been labelled (Katzs et al., 1993; Yang et al., 2008). Separating individual metabolites through chromatography allows the mass spectrometer to offer an accurate measurement of the atomic mass of individual Krebs cycle intermediates. The proportion of each of these which are 1-6 units heavier due to ^{13}C labelling is then directly detectable, but a number of studies have misinterpreted this data and obtained an incorrect rate of labelling through neglecting to consider which carbon it is which has become labelled.

3.1.2 Movement of Carbon labelling in the Krebs Cycle: Considerations for an Accurate Model

^{13}C originating from metabolism of $U^{13}C$ labelled fatty acids and carbohydrates primarily enters the Krebs cycle in identical units of two carbons as [1,2-$^{13}C_2$]acetyl-CoA. However, the stereochemistry

and cyclic nature of the intermediates leads to a complex distribution of different isotopomers (molecules with equivalent numbers of labelled and unlabelled carbon atoms, but differing in their positions) and isotopologues (molecules with different numbers of labelled and unlabelled carbons) being produced at equilibrium. This means that incorporation of 2+ amu acetyl-CoA (labelled with two ^{13}C atoms) into the Krebs cycle, which leads to an m/z + 2 isotopologue of citrate initially, does not lead in a straightforward manner to the production of 2+ amu succinate, malate and other Krebs cycle intermediates when the tissue is analysed. It is therefore not sufficient to say, for example, that all isotopomers of citrate with 1+ amu result from a metabolic substrate which has been labelled to yield acetyl-CoA with 1+ amu, and that all citrate with 2+ amu isotopomers stem from acetyl-CoA with 2+ amu, as the full range of citrate isotopologues with 1-6 + amu can result from an input of acetyl-CoA with 2+ amu.

The cyclic nature of the Krebs cycle (Krebs et al., 1938) leads to amplification of labelling at equilibrium. While the greatest mass increase an intermediate could gain from one turn of the cycle with [1,2-$^{13}C_2$] acetyl-CoA would be 2+ amu, metabolites recirculate continuously; so if a fraction of the oxaloacetate pool has been labelled 2+ in the first turn of the cycle this will result in 2+ and 4+ labelled citrate when combined with unlabelled and [1,2-$^{13}C_2$]acetyl-CoA respectively. Over a number of cycles towards steady state, this can increase carbon labelling in the Krebs cycle, complicating the situation much further than if entry of [1,2-$^{13}C_2$]acetyl-CoA to the Krebs cycle led only to the accumulation of 2+ amu citrate.

Carbon loss also occurs during the cycle, with some carbons removed as CO_2 with each turn indiscriminately of their atomic mass (Krebs et al., 1938). Following scrambling of label between the 1,2 and 3,4 positions when fumarate is hydrated to malate **(Figure 3.1)**, and further migration of ^{13}C labelled carbons between positions when acetyl-CoA is complexed with a labelled oxaloacetate molecule by citrate synthase, each turn some ^{13}C carbons arrive in positions where they are lost as $^{13}CO_2$. The outcome of this is that there is single ^{13}C loss from labelled intermediates. The mass shift of each Krebs cycle intermediate when there is [1,2-$^{13}C_2$]acetyl-CoA input to the Krebs cycle is therefore not exclusively in multiples of 2+ amu gains, with 1+, 3+ or 5+ amu (depending upon the size of the Krebs cycle intermediate) isotopologues also generated.

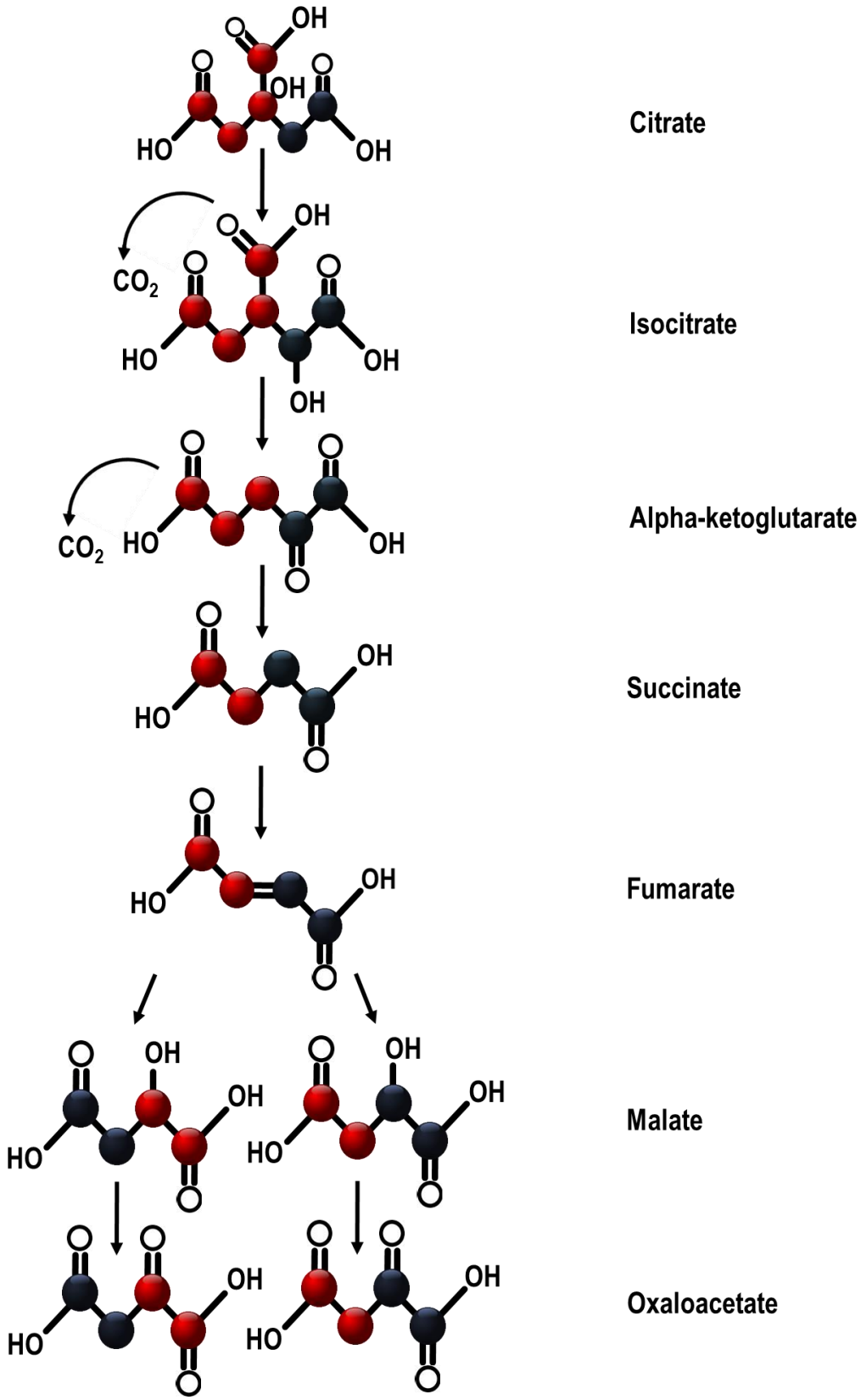

Figure 3.1: Movement of labelled carbons during one turn of the Krebs cycle. Black represents a ^{13}C labelled carbon, and red represents an unlabelled one. Labelled citrate with +2 amu, formed from oxaloacetate and labelled acetyl-CoA with +2 amu, is equally likely to produce one of two different isotopologues of oxaloacetate with +2 amu.

This is made possible through generation and loss of stereochemical centres during the Krebs cycle. During the hydration of fumarate, which has no stereochemical centre, to malate, which does, there is an equally likely probability of the hydroxyl group being added to either carbon 2 or carbon 3 of fumarate. This controls whether carbon 1 or carbon 4 becomes the alpha carbon of oxaloacetate which is fated to be removed in the next turn of the cycle during the conversion of isocitrate to α-ketoglutarate.

The distribution of Krebs cycle isotopologues which results from administering ^{13}C labelled substrates is therefore complex. To address this issue, this chapter presents a mathematical model capable of mapping ^{13}C accumulation within the cycle to steady state, and calculating the relative oxidation of different metabolites in a perfused heart model.

3.2 MATERIALS AND METHODS

Materials

All reagents and chemicals were obtained from Sigma-Aldrich Ltd (UK) unless otherwise stated.

3.2.1 Generation of the Model

Initial Conditions

The initial proportion of ^{13}C labelled Krebs cycle intermediates before the commencement of the labelling study was taken to be 0, and the proportion of entirely unlabelled intermediates 1. The proportion of the acetyl-CoA input which was [1,2-$^{13}C_2$]acetyl-CoA was designated α.

Mapping the Relationships of Krebs Cycle Isotopomers

The initial iterations of the Krebs cycle were worked through until every isotopomer possible for each intermediate had been introduced, and all were assigned a tag (C1,C2,… for citrate; A1, A2,… for α-ketoglutarate etc.). Four metabolites were crucial to the modelling model – the six-carbon intermediate citrate; the 5-carbon intermediate α-ketoglutarate; the non-stereochemical 4-carbon succinate, and the stereochemical 4-carbon malate. The isotopologue or isotopomer distributions of each of the other intermediates were identical to one of these 'crucial' metabolites, and therefore did not need to be incorporated into the model for calculating enrichments.

The relationships of each isotopomer at time T to the isotopomers of the preceding crucial metabolite in the cycle at time T-1 were drawn up as a set of differential equations. For example, if 1+ malate labelled on the alpha-carbon is designated M_1, M_1(T)= 0.5 S_6 (T-1), where S_6 corresponds to the 1+ succinate isotopomer labelled on the carbon at the end of the chain. The fate of the 50% of S_6 which is not converted to M_1 is to become 1+ malate labelled at the carbon on the opposite end of the chain to the α- carbon, which we can designate M_2 to get the equation M_2(T)= 0.5 S_6 (T-1) and so on.

Next, a network model was generated with the programming assistance of Demetris Demetriou. This was done by multiplying a 1 by 78 vector comprising the 78 isotopomers of citrate, α-ketoglutarate, succinate and malate at time T with a 78 by 78 network matrix comprising the relationships of those isotopomers to each other.

Experimentally obtained data could then be fitted to the model by running iterations to determine at which value of α the discrepancy between the predicted and experimental isotopic distributions was smallest.

3.2.2 Validation of the Model in the Isolated Rat Heart

Perfusion Protocols

Male Wistar rats (300-350 g) were obtained from a commercial breeder (Charles River, UK). All procedures involving live animals were carried out by a licence holder in accordance with UK Home Office regulations, and underwent review by the University of Cambridge Animal Welfare and Ethical Review Committee.

Hearts were excised and perfused in the Langendorff mode as described in Chapter 2. The perfusion medium was 250 mL of recirculated KH buffer with the basic composition 118 mM NaCl, 4.7 mM KCl, 1.2 mM $MgSO_4$, 1.3 mM $CaCl_2$, 0.5mM EDTA, 25 mM $NaHCO_3$ and 1.2 mM KH_2PO_4; pH 7.4.

To determine α with differing input percentages of $U^{13}C$ labelled glucose, the KH buffer was supplemented with glucose and $U^{13}C$ labelled glucose in the following proportions:

- For the 0% $U^{13}C$ labelled glucose hearts (n=3), with 11 mM unlabelled glucose
- For the 25% $U^{13}C$ labelled glucose hearts (n=3), with 8.25 mM unlabelled glucose and 2.75 mM $U^{13}C$ glucose
- For the 50% $U^{13}C$ labelled glucose hearts (n=3), with 5.5 mM unlabelled glucose and 5.5 mM $U^{13}C$ glucose
- For the 75% $U^{13}C$ labelled glucose hearts (n=3), with 2.75 mM unlabelled glucose and 8.25 mM $U^{13}C$ glucose
- For the 100% $U^{13}C$ labelled glucose hearts (n=3), with 11 mM $U^{13}C$ labelled glucose

To determine the relative input of triglyceride and glucose from the perfusion buffer to the TCA cycle, hearts were perfused with either 25% U-^{13}C labelled glucose or 25% U-^{13}C labelled triglyceride (Cambridge Isotopes Laboratories) alongside 75% unlabelled substrate in each case. The KH buffer for the ^{13}C glucose perfused hearts (n=6) contained 8.25 mM unlabelled glucose, 2.75 mM U-^{13}C labelled glucose (Cambridge Isotopes Laboratories) and 0.4 mM Intralipid; while for the ^{13}C triglyceride perfused hearts (n=6) it contained 11mM unlabelled glucose, 0.1 mM U-^{13}C mixed triglycerides (Cambridge Isotopes Laboratories) and 0.3 mM unlabelled Intralipid. All hearts were perfused at a constant pressure of 100 mmHg for 32 min following an initial stabilisation period.

Following the end of the perfusion protocol, the left ventricle was rapidly sectioned in transverse and snap frozen for analysis by LC-MS/MS

3.2.3 Liquid Chromatography-Coupled Mass Spectrometry (LC-MS/MS)

Metabolites were extracted from the frozen left ventricle, and isotopologue distributions of malate, citrate, glutamate (the cellular pool of which is in rapid interconversion with α-ketoglutarate) and succinate were determined using LC-MS/MS as described in Chapter 2.

α-ketoglutarate was unable to be measured accurately, perhaps due to resistance to fragmentation or ionisation, and so glutamate was measured instead. Glutamate is interconverted rapidly with α-ketoglutarate and therefore their labelling distributions are identical (Risa et al., 2011; Yu et al., 1995), so this was a convenient and accurate proxy.

Likewise, the 6+ amu isotopologue of citrate also had a high limit of detection, and therefore in conditions where the 6+ amu isotopologue of citrate was expected citrate has not been considered in the fitting of the model.

3.3 RESULTS

3.3.1 Prediction of Isotopologue Distribution in Krebs Cycle Metabolites

In order to visualise the model, bifurcation plots were generated for the four key Krebs cycle intermediates **(Figure 3.2)**. The model predicted the unlabelled isotopologue of each intermediate to decrease as the proportion of 2+ amu acetyl-CoA entering the cycle increases, eventually reaching 0. Meanwhile, the fully labelled isotopologue increased with rising α. Each of the other isotopologues are predicted to reach their own peak as α increases, and to then decrease again as the proportion of [1,2-$^{13}C_2$]acetyl-CoA entering the Krebs cycle continues to rise.

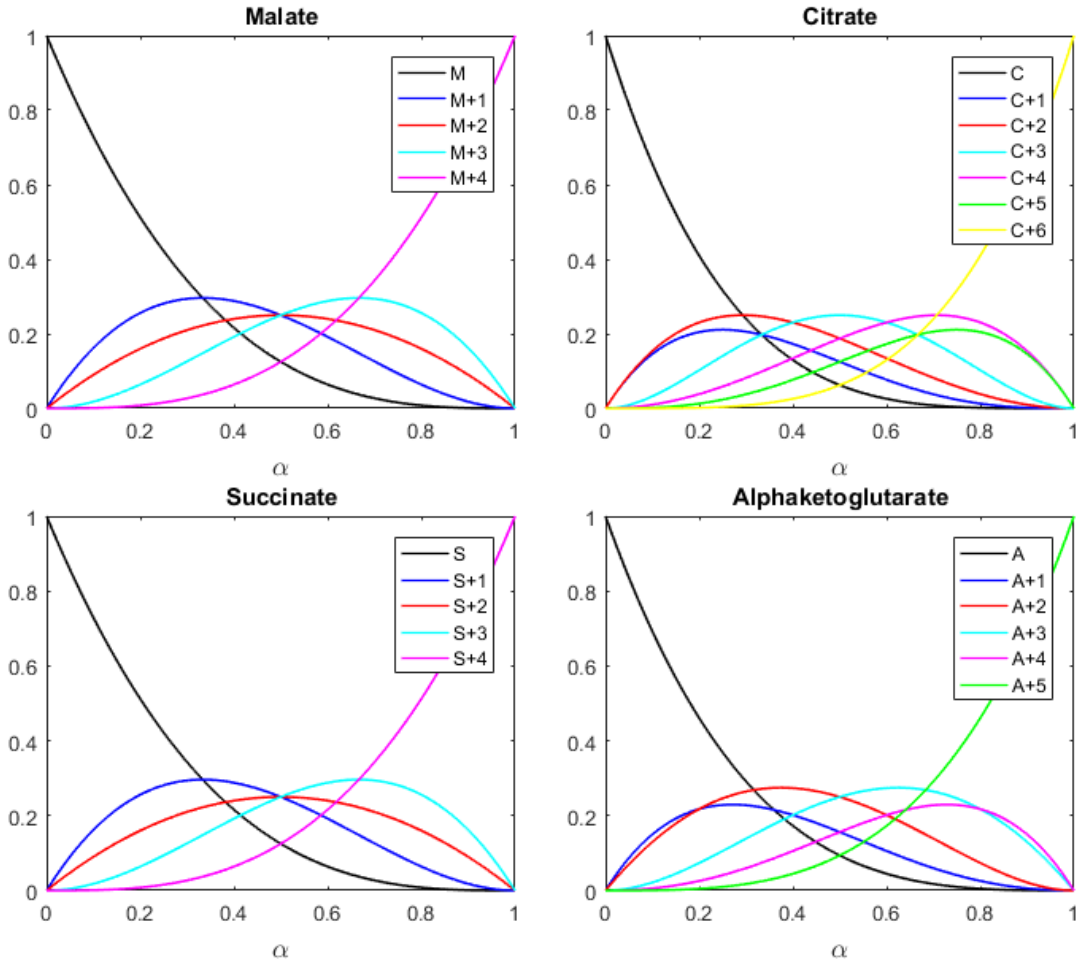

Figure 3.2: Bifurcation plots showing how the relative proportions of key Krebs cycle intermediate isotopologues vary at equilibrium as the proportion of [1,2-$^{13}C_2$]acetyl-CoA entering the Krebs cycle (α) increases, as predicted by the model.

The model allows us to predict the steady state isotopologue distributions of Krebs cycle intermediates resulting from different levels of acetyl CoA ^{13}C enrichment. **Figure 3.2** shows the

bifurcation diagrams generated by plotting alpha, the proportion of acetyl-CoA entering the Krebs cycle which is 2+ amu labelled, against the isotopologue distributions of the key Krebs cycle intermediates once steady state has been achieved. This allows us to visualise how the labelling density of each intermediate would change according to label input, useful both in the interpretation of data resulting from an unknown influx and in optimising the design of experiments to achieve a certain labelling pattern.

3.3.2 Validation of the Model

Next, the model was validated experimentally. Glutamate, succinate and malate isotopologue distribution was measured using mass spectrometry in extracts from frozen tissue from hearts perfused to steady state with a known percentage of $U^{13}C$ labelled glucose in the buffer (Figure 3). The value for α obtained through iteration for each of these intermediates at each percentage of $U^{13}C$ buffer glucose is displayed in **Figure 3.3**, as is the value that gives the overall % buffer glucose oxidation in the Krebs cycle when extrapolated to account for all glucose in the buffer (labelled and unlabelled).

The total percentage of glucose oxidation determined from analysis of the MS data with the model is largely consistent, ranging between 75 and 85%, and when factoring in SEM mostly encompassing 78-80% glucose oxidation. When assessed by 2 way ANOVA, there was no effect of the percentage of buffer glucose which was $U^{13}C$ labelled, of metabolite assessed (succinate, glutamate or malate), or of any interaction between the two factors (all $p>0.05$) upon the predicted percentage of acetyl-CoA being oxidised in the Krebs cycle which was derived from glucose. This demonstrates that the α values predicted by the model from isotopologue distributions of each of the measured metabolites at each known percentage of $U^{13}C$ labelled glucose in the buffer are all from the same population. Therefore, it seems the model is a good representation of the way in which [1,2-$^{13}C_2$]acetyl-CoA is metabolised in the Krebs cycle across the whole range of labelled input. The remaining ~20% of acetyl-CoA entering the TCA cycle which was not accounted for by buffer glucose oxidation most likely stems from catabolism of the heart's triglyceride and glycogen stores, which would be unlabelled in this scenario.

0% $U^{13}C$ Buffer Glucose	25% $U^{13}C$ Buffer Glucose	50% $U^{13}C$ Buffer Glucose	75% $U^{13}C$ Buffer Glucose	100% $U^{13}C$ Buffer Glucose
Glutamate				
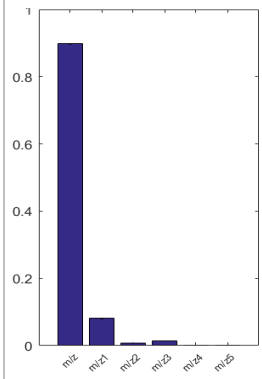	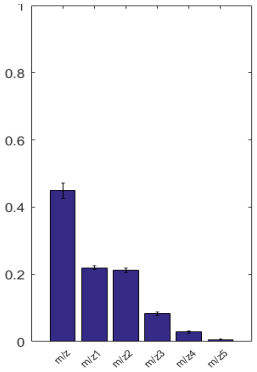	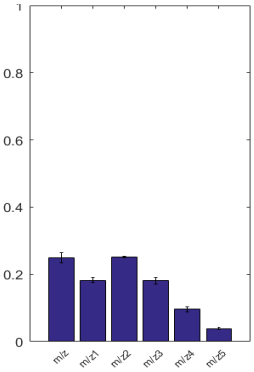	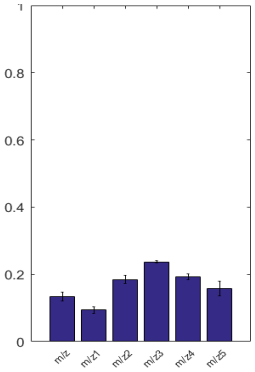	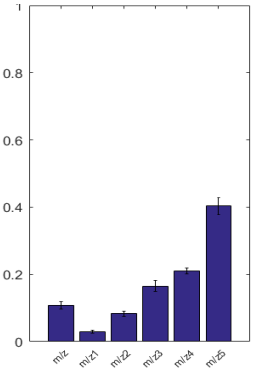
α	0.198 ± 0.011	0.372 ± 0.01	0.597 ± 0.023	0.779 ± 0.013
% Glucose Oxidation	79.2 ± 4.4	74.4 ± 4.0	79.6 ± 3.1	77.9 ± 1.3
Succinate				
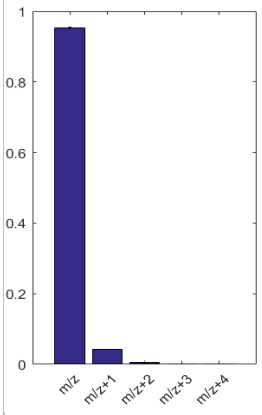	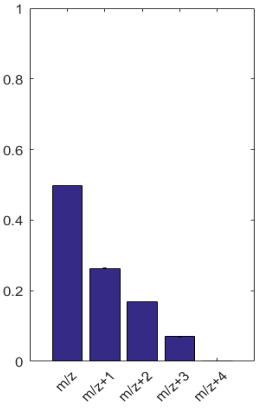	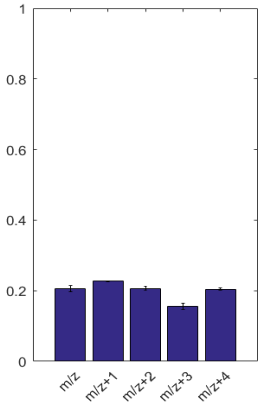	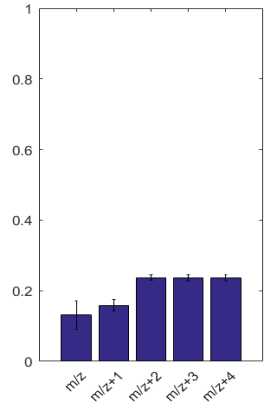	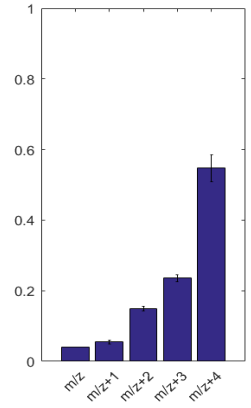
α	0.190 ± 0.009	0.381 ± 0.007	0.633 ± 0.025	0.833 ± 0.008
% Glucose Oxidation	76.1 ± 3.7	76.2 ± 1.4	84.4 ± 1.1	83.3 ± 1.3
Malate				
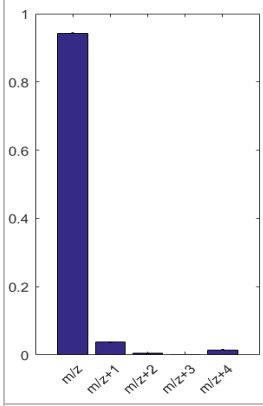	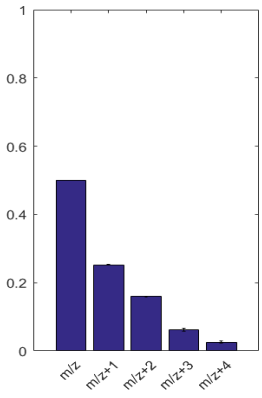	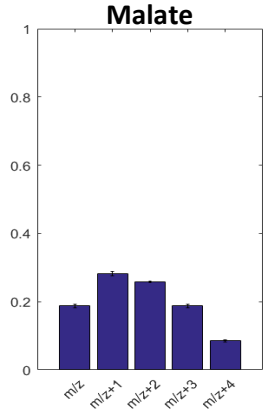	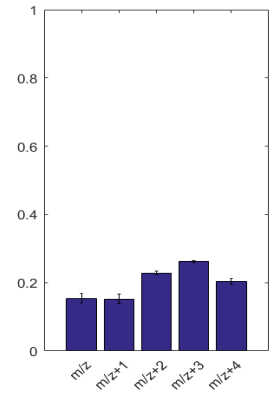	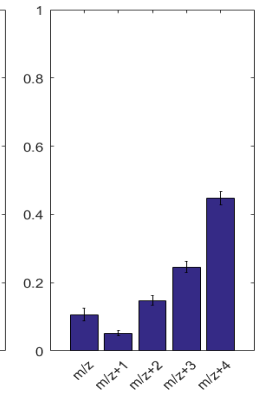
α	0.189 ± 0.0006	0.41 ± 0.006	0.615 ± 0.02	0.784 ± 0.011
% Glucose Oxidation	75.6 ± 0.2	82.0 ± 1.2	82.0 ± 2.7	78.4 ± 1.1

Figure 3.3: Isotope distribution plots showing the labelling distribution of glutamate, succinate and malate when the percentage of glucose in the perfusion buffer which was U-^{13}C labelled is varied through 0%, 25%, 50%, 75% and 100% (n=3).

3.3.3 Determination of the Relative Oxidation of Substrates in the Isolated Heart

Cardiac Function Throughout the Protocol

Table 1 shows cardiac function was consistent between all hearts perfused with 11mM glucose and 0.4 mM intralipid, in terms of developed pressure, heart rate, and rate pressure product. The perfused rat hearts (n=12) had a rate pressure product of 35500 ± 2500 mmHg/min.

Table 1: ***Pre-Ischaemic Cardiac Function***

LVDP (mmHg)	*Heart Rate (bpm)*	*RPP (mmHg/min)*
119 ± 7	300 ± 12	35500 ± 2500

Determining the Contribution of Glucose to the Cardiac Krebs Cycle

Figure 5B shows the LC-MS measured isotopologue distributions of the key Krebs cycle intermediates in cardiac tissue following 32 min of perfusion with 11 mM glucose (25% $U^{13}C$ labelled, 75% unlabelled), and 0.4 mM intralipid in the buffer. Again, as expected, the proportions of labelled Krebs cycle intermediates are lower than would be predicted if α were 0.25 due to competition for oxidation with acetyl-CoA derived from other substrates such as the perfused triglycerides, endogenous triglycerides, glycogen and amino acids.

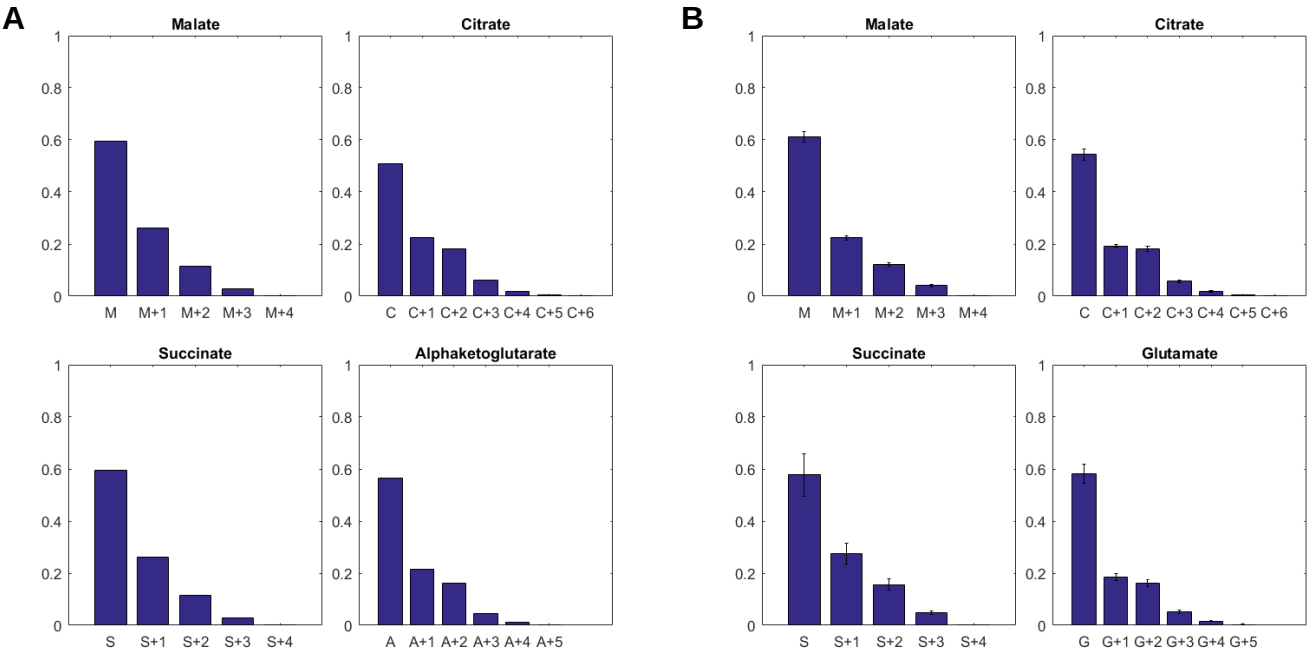

Figure 3.4: (A) Isotopologue distributions predicted by the model at α=0.145 for malate, citrate, α-ketoglutarate and succinate. (B) Isotopologue distributions for malate, citrate, glutamate and succinate measured in heart tissue perfused with 25% $U^{13}C$ labelled glucose by LC-MS

Fitting the experimentally observed isotopic distributions to the model tells us that the observed values for the isotopologue distribution in our heart tissue most closely fits the distribution predicted by the model when α = 0.145 (± 0.009). As we can see from Figure 5, the isotopologue distributions predicted for the key Krebs cycle metabolites with α = 0.145 closely matches the experimental data. The relative contribution of glucose to the Krebs cycle when 0.4 mM intralipid is present in the buffer is therefore 58 ± 3.6%

Determining the Contribution of Fatty Acid Oxidation to the Cardiac Krebs Cycle

The accuracy of the model in determining the contribution of glucose to the Krebs cycle could then be corroborated by using it to determine the value of alpha when the labelled acetyl-CoA originated from triglycerides in the perfusion buffer. Labelling 25% of the triglyceride available in the perfusion buffer resulted in a smaller proportion of labelled isotopologues than with the labelled glucose hearts when measured by LC-MS (Figure 6B), and the model determined α to be 0.089 ± 0.002 (a 35.6 ± 0.8% total contribution of perfusion buffer intralipid to the TCA cycle). As can be seen from Figure 6, the predicted isotopologue distribution for α=0.089 again closely matches the observed experimental data.

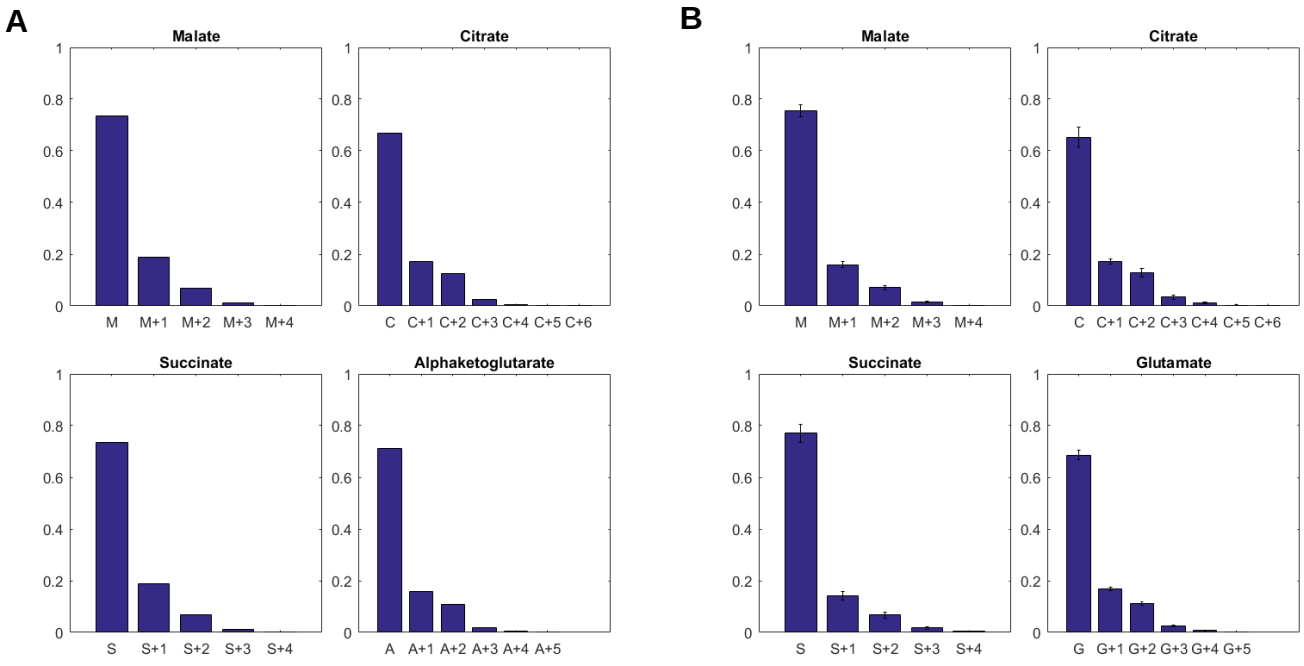

Figure 5. A: Isotopologue distributions predicted by the model at α=0.089 for malate, citrate, α-ketoglutarate and succinate. **B:** Isotopologue distributions for malate, citrate, glutamate and succinate measured in heart tissue perfused with 25% $U^{13}C$ labelled triglycerides by LC-MS.

This helps confirm the validity of the model, as together triglyceride oxidation (35.6%) and glucose oxidation (58%) account for almost 100% of the acetyl-CoA oxidised in the Krebs cycle. The remaining 6-7% of oxidised acetyl-CoA is likely to correspond to oxidation of endogenous lipid and glycogen stores. Despite FAO being thought to dominate in the heart, glucose is present at a much higher concentration in the perfusion buffer in order to facilitate uptake, and therefore it is not surprising to see it accounting for the greater proportion of oxidation here.

3.4 DISCUSSION

This mathematical model for analysis of ^{13}C labelling patterns has been developed to track labelled carbon through the Krebs cycle, and has been demonstrated to accurately predict isotopologue distribution across the whole range of different labelling inputs from $U^{13}C$ labelled substrates.

3.4.1 Strengths and Limitations of the Model

A great strength of this model relative to previous attempts to quantify substrate oxidation through Krebs cycle labelling is that it takes isotopologue distributions and the fate of the labelled carbons into account. Rather than assuming that more of a specific labelled isotopologue means more oxidation of the labelled substrate, as many studies have done (for example, Aubert et al., 2016; Liu et al., 2016; Lloyd et al., 2004; Lloyd et al., 2003), it is possible to see with this model that as α increases, the proportion of some labelled Krebs cycle intermediates (such as 2+ amu isotopomers) actually decreases. Indeed, the model also illustrates that most levels of 2+ amu intermediates can correspond to more than one value of α **(Figure 3)**, and that it is therefore necessary to take into account the whole isotopologue distribution rather than only specific individual isotopologues when determining the proportion of labelled substrate oxidation a labelling pattern corresponds to. This averts the potential for the misinterpretation of data which could occur if it were assumed that greater 2+ amu labelling meant greater oxidation of the labelled substrate in one group, where in practice it may actually mean there is a lower oxidation of the labelled substrate as shown in the bifurcation plots in the results section.

The use of mass spectrometry rather than NMR spectroscopy is also a strength of this study. The detection of the whole molecular ion and its fragments with LC-MS/MS negates any effects of certain carbon positions being detected with more sensitivity than others by NMR. This has potentially led to an assumption that late-stage Krebs cycle intermediates have been labelled before earlier intermediates via a back-flux through pyruvate carboxylase (Jones, 2014; Reed et al., 2016), with these carbons potentially more easily detectable early in the labelling process. The isotopologue distributions seen in this study do not show an enhanced number of the 3+ amu late Krebs cycle intermediates and citrate which would have to accompany significant flux through the pyruvate carboxylase pathway, suggesting that there isn't significant flux through pyruvate carboxylase in the heart under these conditions. The findings in this chapter concur with previous studies (Kowalski et al., 2015; Tran-dinh et al., 1996), which show pyruvate carboxylase flux to be negligible and operating purely to top up Krebs cycle carbon when the circulating organic acids are depleted.

One potential weakness of the study has been the difficulty in measuring some of the less well fragmenting Krebs cycle intermediates with enough resolution for a labelling study. While the total pool size of both α-ketoglutarate and oxaloacetate are sufficiently detectable with our method for inter sample comparisons, there is a high limit of detection (most likely due to the ketone group on a carbon neighbouring to a carboxylic acid group which is present on both molecules and may interfere with fragmentation or ionisation). This means that when the pool was split by differential labelling of isotopologues, some of the isotopologues present in lower concentrations weren't easily enough detectable for accurate fitting of isotopologue distribution to the model. With α-ketoglutarate, this was relatively easy to circumvent, as the cellular glutamate pool is interconverted rapidly with α-ketoglutarate and therefore their labelling distributions are identical (Risa et al., 2011; Yu et al., 1995), allowing its measurement as a proxy. However, it is still an indirect measurement and it would have been more ideal to be able to measure both metabolites.

Two limitations of the model currently are its lack of ability to account for anaplerosis and that in its current state it only calculates labelling assuming that the input acetyl-CoA is 2+amu labelled. It could be programmed to account for unknown rates of anaplerotic flux, but this would greatly complicate the maths and amount of computing power required; and in the context of ischaemia in which it is used in this thesis, anaplerotic flux is known to be negligible so this does not impair the study (Kowalski et al., 2015; Tran-dinh et al., 1996). If however, the model were to be used in the context of another organ or model where anaplerotic flux were significant, this would first have to be adjusted. Likewise, no 1+amu acetyl-CoA was used in his thesis, but in future work where it was required this could easily be adjusted. Within these limitations which can be expected though, the model has shown itself to be a robust indicator of labelling in the Krebs cycle.

3.4.2 Significance of Results

Validation of the Model

The model appears to offer a robust tool for determining the percentage oxidation of ^{13}C labelled metabolic substrates in the mitochondria from the isotopologue distribution of different Krebs cycle intermediates. A consistent answer as to the percentage of total Krebs cycle oxidation accounted for by glucose oxidation was given even when the percentage of U-^{13}C labelled glucose was varied, demonstrating that the model was accurate in predicting the proportion of oxidised acetyl-CoA which was [1,2-$^{13}C_2$]acetyl-CoA from the resultant isotopologue distributions in the Krebs cycle.

The Predominance of Glucose Oxidation in the Langendorff Heart

The heart is well documented to oxidise fatty acids to generate most of its ATP in physiological conditions, so it is interesting that in this preparation glucose oxidation accounts for the majority of Krebs cycle oxidation. When 0.4 mM equivalent intralipid was supplied in the perfusion buffer, glucose oxidation still accounted for 58 ± 3.6% of the total acetyl-CoA oxidised in the Krebs cycle. Two possible explanations for this discrepancy between previously measured physiological substrate oxidation ratios and that seen in this Langendorff preparation are that there may have been differences in tissue oxygenation or the proportions in which the substrates were delivered to the heart.

KH buffer has a lower oxygen delivery capacity than blood or red blood cell supplemented buffer (Schenkman et al., 2003), which could suggest that the heart may favour glucose oxidation as a more oxygen efficient fuel (Opie and Sack, 2002; Taegtmeyer and Lubrano, 2014). However, several studies have shown that O_2 delivery is not limiting in similar Langendorff heart preparations. When KH buffer oxygenated with 95% O_2 carbogen gas was delivered at 80 mmHg coronary flow and fractional oxygen extraction were sub-maximal, while lactate was not being produced (Edlund and Wennmalm, 1981). Fisher & Williamson (1961) demonstrate that it is feasible to supply considerably more O_2 to the Langendorff heart than the basal oxygen demand, while both Neely et al. (1967) and Wengrowski et al. (2014) show that their Langendorff preparation can further increase oxygen consumption in response to increased stimulation or pressure. Taken together, this suggests that O_2 delivery should not be such a limiting factor upon cardiac metabolism that it drives a preference for glucose oxidation over FAO.

Glucose concentration in the KH buffer is almost double that in the blood of a typical rat (Bell et al., 2011) in order to assure sufficient uptake in the absence of insulin, and this may lead to higher proportions of glucose oxidation to FAO. Increasing KH buffer glucose concentration past 11 mM leads to no further uptake of glucose in the Langendorff heart (King and Opie, 1998), meaning that cardiac glucose uptake is at its maximum non-insulin stimulated rate with this delivery concentration. This in turn means that glucose uptake could be exceeding that observed *in vivo,* possibly leading to further inhibition of FAO through the Randle cycle (Hue et al., 2009), and accounting for the greater glucose oxidation:FAO ratio in the Langendorff heart relative to *in vivo*. One way of investigating this further would be to lower the concentration of glucose present in the buffer and see whether that altered the proportion of substrate oxidation.

3.4.3 Future Directions

While in the healthy heart fatty acids can constitute up to 100% of the substrate oxidised (Lopaschuk et al., 2010), in pathophysiological states such as oxygen deprivation, metabolic syndrome or dietary manipulation the contribution of glucose and other substrate derived acetyl-CoA to the Krebs cycle is thought to be increased (Atherton et al., 2011; Mansor et al., 2013; Veech, 2004). Fat oxidation requires 15% more oxygen per gram ATP produced than glucose (Neely et al., 1972; Lopaschuk et al., 2010), which can offer the cardiac mitochondria incentive to vary the relative contributions of fats and glucose to the Krebs cycle when oxygen is a limiting factor (Heather et al., 2012; Horscroft et al., 2015). Furthermore, varying the availability of different substrates to the heart which can occur in conditions such as diabetes and fasting also dictates the ratio of substrates oxidised (Heather and Clarke, 2011). This model offers an accurate way to monitor mitochondrial substrate selection, and could be used to investigate cardiac substrate switching in each of these scenarios.

As a specific example of a further application which could be of great interest, the model could be used to assess the proportion of glucose to fatty acid oxidation in the failing heart. In heart failure, the heart is incapable of supplying itself with enough blood, and oxygen, to sustain contractile function (Dargie 2005). This is thought to lead to an overall reduction of substrate oxidation, but an increase in the proportion of glucose:fatty acids oxidised (Neubauer, 2007). If rats with and without heart failure were either given $U^{13}C$ labelled glucose in the diet, or the hearts were mounted on a Langendorff rig upon termination and perfused with $U^{13}C$ labelled glucose it would be possible to freeze the tissue at a steady state and assess the percentage contribution of glucose oxidation to total substrate oxidation by the Krebs cycle. This could even be performed at various stages of heart failure in order to track the progression of metabolic dysfunction.

CHAPTER 4

Dietary Nitrate Supplementation and the Role of Fatty Acid Oxidation in Ischaemia/Reperfusion

ABSTRACT

BACKGROUND Dietary supplementation with sodium nitrate protects cardiac mitochondrial complex I against hypoxic injury, and increases fatty acid oxidation (FAO) capacity.

OBJECTIVES The focus of this chapter was to investigate whether the protective effects of dietary nitrate supplementation could translate from protection against hypoxia to protection against ischaemia/reperfusion, and whether any protective effect was conditional upon substrate supply, specifically fatty acid availability.

METHODS Male Wistar rats had diets supplemented with 0.7 mM NaCl or 0.7 mM $NaNO_3$ for two weeks. Hearts excised from these rats were perfused in the Langendorff mode (100 mmHg, 32 min) before 32 min low-flow ischaemia (0.3 $ml.min^{-1}gww^{-1}$), with (n=7 per group) or without (n=7 per group) intralipid in the perfusion buffer. Recovery of contractile function was then assessed following 32 min reperfusion, before 10 mg left ventricle was permeablised with saponin and mitochondrial respiratory function assessed using respirometry. Tissue metabolite levels were measured in coronary effluent and myocardium frozen at the end of the reperfusion period using LC-MS/MS and LC-MS.

RESULTS Intralipid in the perfusion buffer resulted in greater recovery of LVDP following ischaemia/reperfusion, yet this was worsened if the rat's diet had been supplemented with sodium nitrate (Interaction, $p<0.05$). Meanwhile, intralipid decreased the coupling of the mitochondria assessed at the end of reperfusion ($p<0.01$), but neither intralipid nor dietary nitrate supplementation resulted in greater recovery of complex I supported oxygen consumption. Intralipid presence in the buffer also resulted in greater levels of ATP being present in the myocardium at the end of reperfusion, while nitrate supplementation counteracted this (Interaction, $p<0.05$) and also resulted in lower myocardial levels of PCr (Nitrate effect, $p<0.01$). Intralipid in the perfusion buffer resulted in higher myocardial levels of malonyl-CoA ($p<0.01$) and of alanine ($p<0.01$) post-reperfusion, suggesting that presence of intralipid results in greater substrate oxidation and perhaps increased glycolysis.

CONCLUSIONS While the presence of intralipid in the perfusion buffer appears to result in greater functional recovery of the heart following ischaemia/reperfusion, the cardioprotective potential of dietary nitrate supplementation remains unclear.

4.1 BACKGROUND

In recent years, the metabolic effects of dietary supplementation with sodium nitrate have started to become apparent (Carlström *et al.*, 2010; Larsen *et al.*, 2011). Nitrate supplementation has been associated with protection of heart and skeletal muscle against hypoxia (Ashmore et al., 2014a), induction of adipose tissue browning (Roberts et al., 2015) and enhancement of cardiac contractile function (Pironti et al., 2016), traits which suggest that its employment in the treatment of ischaemia may be beneficial. The protective effects of nitrate supplementation against a hypoxic challenge show particular promise in this regard, given ischaemia includes a severe hypoxic element.

4.1.1 Protection of the Mitochondrial Electron Transport Chain

To a certain extent during ischaemia, and especially during any subsequent reperfusion, excess generation of reactive oxygen species (ROS) can cause damage to the mitochondrial electron transport chain (ETC) (Chen et al., 2003; Kalogeris et al., 2014). Predominantly thought to be produced at ETC complex III, ROS mediated damage to this and other ETC complexes as well as to the mitochondrial DNA can lead to mitochondrial dysfunction and apoptosis (Halestrap, 1998; Kim et al., 2018). ROS production upon reperfusion follows maladaptation to the lack of oxygen supply during ischaemia, and could potentially be managed through the manipulation of substrate supply to the mitochondria upon reperfusion.

Supplementation of the diet with nitrate has been shown to protect the function of ETC complex I, which otherwise sustains damage during hypoxia. Complex I supported respiration, activity and expression were impaired by 14 days exposure to hypoxia at 13% O_2, but with nitrate supplementation (0.7 mM) full function continued to be observed following the same level of exposure (Ashmore et al., 2014a). The same study also reported an ablation of hypoxia-induced protein carbonylation (a marker of oxidative stress) when the rats' diets had been supplemented with nitrate, a finding corroborated by Monaco et al. (2018), who detected a reduction in H_2O_2 production. Increased mitochondrial efficiency has also been reported in skeletal muscle and heart tissue with dietary nitrate supplementation, as well as a lower demand for oxygen and increased mitochondrial biogenesis (Carlström et al. 2010; Larsen et al. 2011; Ashmore, Fernandez, Branco-price, et al. 2014).

Some of the action of nitrate is thought to stem from nitrite and NO activity, which are breakdown products of nitrate during hypoxia (Feelisch et al., 2008). This could be a key trait with regards to ischaemia and reperfusion, as nitrite in particular is thought to mediate s-nitrosylation of mitochondrial complex I whilst also protecting against reperfusion injury (Shiva et al. 2007; Shiva & Gladwin 2009). NO is also implicated in cardiovascular signalling through s-nitrosylation (Lima et al.

2010), the action of which is thought to protect complex I against ischaemia reperfusion injury (Chouchani et al. 2014).

4.1.2 Control of Metabolic Substrate Utilisation

In its healthy state, the heart gains between 70 and 100% of its ATP through oxidation of fats (Fillmore et al., 2014). To consider a heart fully recovered from ischaemia therefore, it might seem logical to expect that this metabolic pattern, along with the capacity for metabolic flexibility must be restored.

Whether maintenance of FAO prior to and following reperfusion is protective against further injury or a limit upon the healthy function of the heart is a matter for debate. Etomoxir inhibition of FAO through CPT 1 has been shown to boost glucose oxidation on reperfusion and be beneficial to functional recovery (Lopaschuk et al., 1990), and there is an argument that FAO is detrimental to recovery upon reperfusion (Fillmore et al., 2014). FAO is associated with mitochondrial uncoupling and the loss of efficiency and energetics (Cole et al., 2011; Murray et al., 2008), something which the reperfused heart with an impaired ETC might be ill able to afford. However, it has also been shown that presence of fatty acids in the perfusion buffer is protective against ischaemia/reperfusion injury, with improved recovery of contractile function following ischaemia (Lou et al. 2014 A; King et al. 2001).

Dietary nitrate supplementation has been shown to promote fatty acid metabolism. This has been observed across a variety of tissues, including heart, skeletal muscle and adipose tissue (Ashmore et al., 2014a, 2015; Roberts et al., 2015). In particular, nitrate has been found to rescue CPT-1 activity and FAO in the hypoxic heart (Ashmore et al., 2014a). In skeletal muscle, nitrate has been shown to activate PPARα, the “master regulator” of fat metabolism (Ashmore et al., 2015), expression of which is downregulated by HIF in response to impaired cardiac oxygen delivery (Papandreou et al. 2006; Ravingerova et al. 2011; Cole *et al.*, 2016). It may therefore be that dietary nitrate supplementation could reverse hypoxia driven suppression of FAO. If this reversal occurs, nitrate supplementation prior to ischaemia and reperfusion may therefore be an ideal vehicle to address the paradigm of whether or not an enhanced FAO capacity is cardioprotective.

4.1.3 Indications for Cardioprotection

Whilst a more oxidative state in the healthy heart could conceivably be a desirable clinical outcome, suppression of oxidative metabolism on reperfusion, both pharmacologically, with agents such as isofluorane and morphine, and through ischaemic post-conditioning, has been shown to reduce I/R injury (Chiari et al., 2005; Weihrauch et al., 2005; Zhao et al., 2003). Potentially therefore, when oxygen is limiting during reperfusion it may not be desirable to increase oxidative metabolism in the heart, which may even lead to greater ROS mediated damage or destruction of the ETC.

The protection of the electron transport chain and modulation of metabolic substrate usage which dietary nitrate supplementation mediates could therefore show promise as a preventative treatment against ischaemia/reperfusion injury. Certainly its metabolite nitrite has been shown in several studies to improve recovery of cardiac function following ischaemia/reperfusion (Bryan et al., 2007a; Pride et al., 2014; Shiva and Gladwin, 2009; Shiva et al., 2007). However, there are few studies demonstrating a cardioprotective effect of dietary nitrate. One of these was conducted using Langendorff apparatus and demonstrates improved recovery of LVDP following ischaemia, yet there were no fatty acids present in the perfusion buffer (Jeddi et al., 2016a). With an intervention such as nitrate which has extensive metabolic effects as detailed above, this is likely to have overlooked some of its effects in the ischaemic heart. The second study was conducted *in vivo*, and reported a reduced infarction size following dietary nitrate supplementation (Bryan et al., 2007b).

4.1.4 Objectives

The objective of this chapter was to establish whether dietary supplementation with sodium nitrate could protect the rat heart against subsequent ischaemia/reperfusion injury, and if so whether it depends upon the availability of exogenous fatty acids. The study was set up to investigate functional recovery following ischaemia, with and without intralipid, a triglyceride mixture, in the perfusion buffer.

4.2 METHODS

4.2.1 Animal Housing and Dietary Supplementation

Male Wistar rats (300-350 g) were obtained from a commercial breeder (Charles River, UK). All procedures involving live animals were carried out by a licence holder in accordance with UK Home Office regulations, and underwent review by the University of Cambridge Animal Welfare and Ethical Review Committee. Rats were housed in a temperature, humidity and light controlled environment (23°C) with a 12 h/12 h light/dark cycle.

Upon the completion of a one week wash-out period where distilled water and a quality-controlled diet were provided *ad libitum*, the rats' water was supplemented with either sodium nitrate or sodium chloride as a control to account for the concentration of sodium uptake (both 0.7 mM) for two weeks preceding termination. This represented a concentration and duration of treatment which had previously been shown to alter metabolism in rats (Ashmore et al., 2014a, 2014b, 2015; Roberts et al., 2015). During this time, the volume of water consumed was measured daily. Rats were terminated following the two weeks of water supplementation, and the hearts excised either for perfusion in the Langendorff mode as previously described in **Chapter 2** (n=7 x 4 groups), or for respirometry (n=5 x 2 groups) as also described in **Chapter 2**.

4.2.2 Langendorff Perfusion

Hearts were perfused in retrograde as described in **Chapter 2 (Section 2.1)**, and subjected to 32 min perfusion at 100 mmHg, followed by 32 min low flow ischaemia (0.32 ml/min/gww) and 32 min reperfusion at 100 mmHg.

For the Chloride/Glucose and Nitrate/Glucose groups (n=7), the perfusion medium was 250 mL of recirculated KH buffer (118 mM NaCl, 4.7 mM KCl, 1.2 mM $MgSO_4$, 1.3 mM $CaCl_2$, 0.5mM EDTA, 25 mM $NaHCO_3$, 1.2 mM KH_2PO_4, 11mM Glucose; pH 7.4). The Chloride/Intralipid and Nitrate/Intralipid groups (n=7) were perfused with an identical buffer which also contained 0.4 mM equivalent intralipid **(Appendix III.1)**. At the end of the perfusion protocol, the left ventricle was rapidly sectioned in transverse and snap frozen, with the exception of ~10 mg of left ventricle which was permeablised for respirometry. Samples of coronary effluent were collected and snap frozen at 4 minute intervals throughout the protocol.

Follow up groups of hearts (n=5) were perfused with identical buffer conditions to those described above, yet the experiment was terminated at the end of the ischaemic period without reperfusion and the hearts sectioned and frozen for future analysis with LC-MS

4.2.3 High-Resolution Respirometry

Tissue permeabilisation and High-Resolution Respirometry was conducted on fresh sections of LV from both pre-Langendorff perfusion nitrate and chloride treated hearts, and the post-reperfusion hearts as described in **Chapter 2 (Section 2.2)**. The respiratory control ratio (RCR) was calculated as an indicator of mitochondrial uncoupling by dividing the rate of oxygen consumption supported by malate and octanoyl carnitine in the oxphos state by that supported by the same substrates in the leak state.

4.2.4 Mass Spectrometry

Metabolites were extracted from frozen left ventricle using a Bligh-Dyer method as described in **Chapter 2 (2.3.2)**. Levels of metabolites in the post-reperfusion hearts (Krebs cycle intermediates, amino acids and malonyl-CoA) were assessed by LC-MS/MS using the C18pfp chromatography method coupled to the Thermo Quantiva, while levels of β-hydroxybutyrate and lactate in the ischaemic hearts were assessed by LC-MS/MS using the C18pfp method coupled to the Thermo Elite, all as described in sections **2.3.3** and **2.3.4**.

Coronary effluent samples (20 µl plus 80 µl 10 mM ammonium acetate/internal standard mix) were also analysed for β-hydroxybutyrate and lactate using the c18pfp chromatography method coupled to the Thermo Elite.

4.2.5 Presentation and Statistics

Unless otherwise stated, all statistical analysis was performed using two-way ANOVA with Nitrate supplementation and Intralipid as the variables. Wherever there was an interaction between the two factors, it was further examined through the use of post-hoc T-tests.

Graphically, the following representations were used for significant effects:

Effect of nitrate

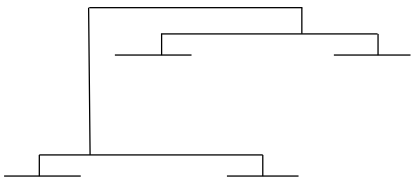

Effect of intralipid

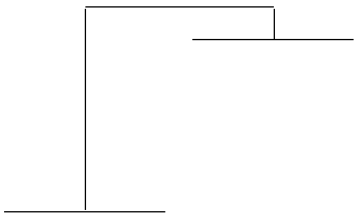

Interaction

Significance was denoted as * $p < 0.05$, ** $p < 0.01$, *** $p < 0.001$.

For data where there was more than one significant effect, both are instead noted upon the graph.

Significance by post-hoc t-test was denoted on graph using the following notation:

Ω = Relative to Chloride/Glucose

Δ = Relative to Nitrate/Intralipid

Θ = Relative to Chloride/Intralipid

Where: Ω/Δ/θ = p < 0.05, ΩΩ/ΔΔ/θθ = p < 0.01, ΩΩΩ/ΔΔΔ/θθθ = p < 0.001

4.3 RESULTS

4.3.1 Dietary Supplementation

Total intake of water across two weeks, and therefore sodium ions and either choride or nitrate ions, was identical between the sodium nitrate and sodium chloride supplemented groups of rats **(Figure 4.1).**

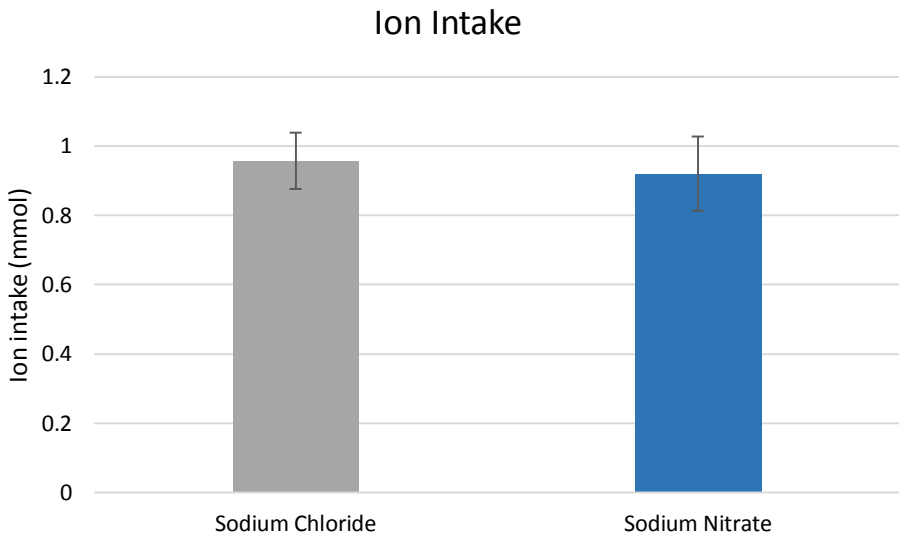

Figure 4.1: Total intake of sodium chloride or sodium nitrate across the two weeks of dietary supplementation ±SEM.

4.3.2 Functional Recovery of the Heart

Hearts from rats with diets supplemented either with sodium nitrate or sodium chloride were subjected to low-flow ischaemia (32 min at 0.3 $ml.min^{-1}gww^{-1}$) and reperfusion (32 min at a constant pressure of 100 mmHg). Pre-ischaemic contractile function was the same across all groups **(Table 4.1)**.

When intralipid was present in the perfusion buffer, recovery of LVDP in the hearts of nitrate-supplemented rats was 75% of that exhibited by the control rat hearts following 32 min reperfusion (interaction, $p < 0.001$ **(Table 4.2)**; post-hoc t-test, $p < 0.001$) **(Figure 4.2)**. Intralipid/chloride hearts recovered 33% greater levels of LVDP than glucose/chloride hearts (post-hoc t-test, $p < 0.01$).

Meanwhile, the heart rate recovered to the same extent across all four groups **(Figures 4.3 & 4.6)**.

The rate-pressure product also recovered to a lesser extent in the nitrate/intralipid hearts than in chloride/intralipid hearts **(Figure 4.4),** but there was no difference between the nitrate/glucose and chloride/glucose hearts **(Figure 4.7)** (Interaction, $p < 0.05$ **(Table 4.2)**).

Table 4.1: ***Pre-Ischaemic Cardiac Function***

	LVDP (mmHg)	Heart Rate (bpm)	RPP (mmHg.bpm)
Chloride/Glucose	136.7 ± 7.7	280.1 ± 10.9	37500 ± 2100
Nitrate/Glucose	129.6 ± 9.6	272.8 ± 13.1	36100 ± 4100
Chloride/Intralipid	130.4 ± 8.6	277.3 ± 15.6	35700 ± 2200
Nitrate/Intralipid	131.7 ± 9.7	277.1 ± 8.7	36400 ± 2900

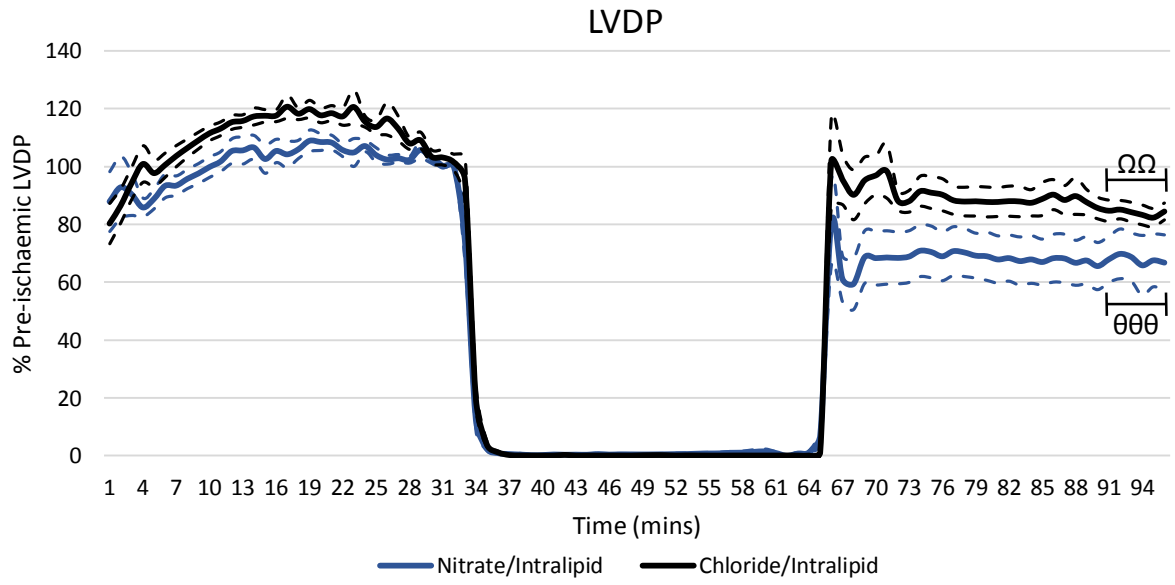

Figure 4.2: Recovery of left-ventricular developed pressure as a percentage of pre-ischaemic levels following 32 min at 0.3 $ml.min^{-1}gww^{-1}$ low flow ischaemia, ±SEM. ΩΩ = $p < 0.01$ relative to chloride/glucose; θθθ = $p < 0.001$ relative to chloride/intralipid

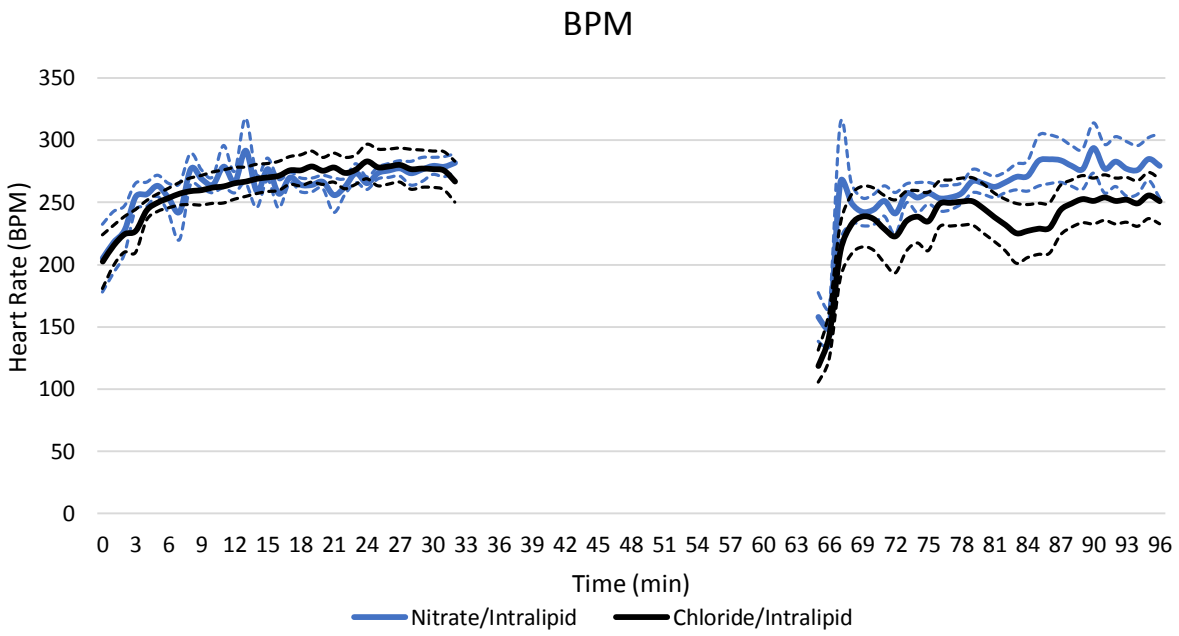

Figure 4.3: Heart rate preceding and following 32 min 0.3 ml.min^{-1}gww^{-1} low flow ischaemia, ±SEM.

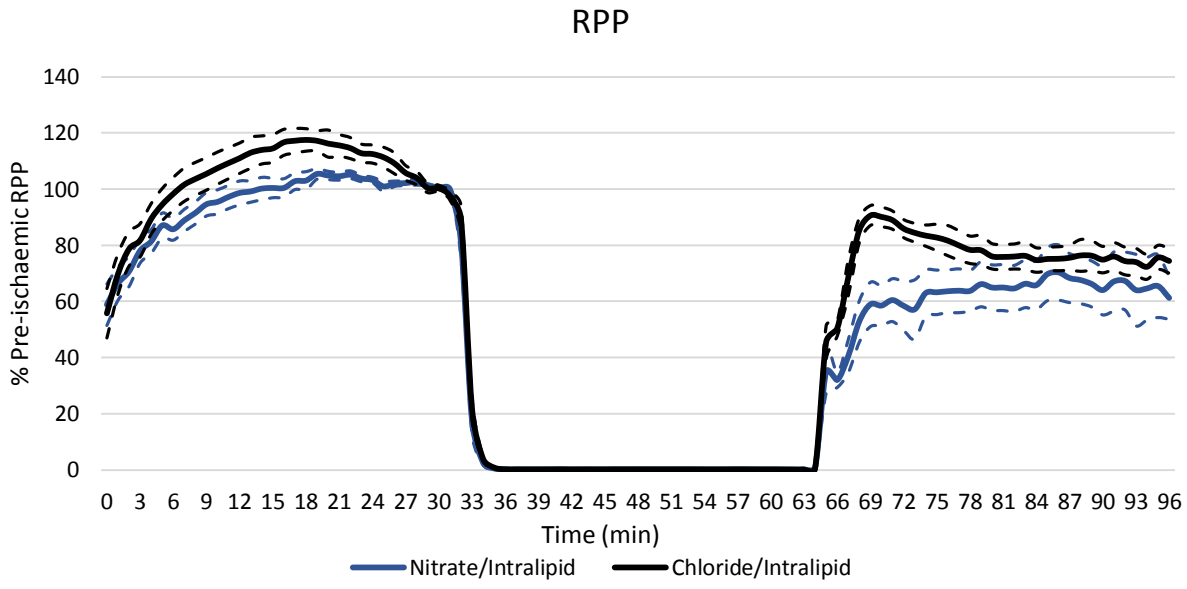

Figure 4.4: Recovery of rate-pressure product as a percentage of pre-ischaemic levels following 32 min 0.3 ml.min^{-1}gww^{-1} low flow ischaemia, ±SEM.

In the hearts perfused without intralipid in the buffer, nitrate did not influence recovery of LVDP at 32 min reperfusion **(Figure 4.5)**. The nitrate/glucose hearts did however recover LVDP to 18% higher levels than nitrate/intralipid hearts (post-hoc t-test, $p < 0.05$).

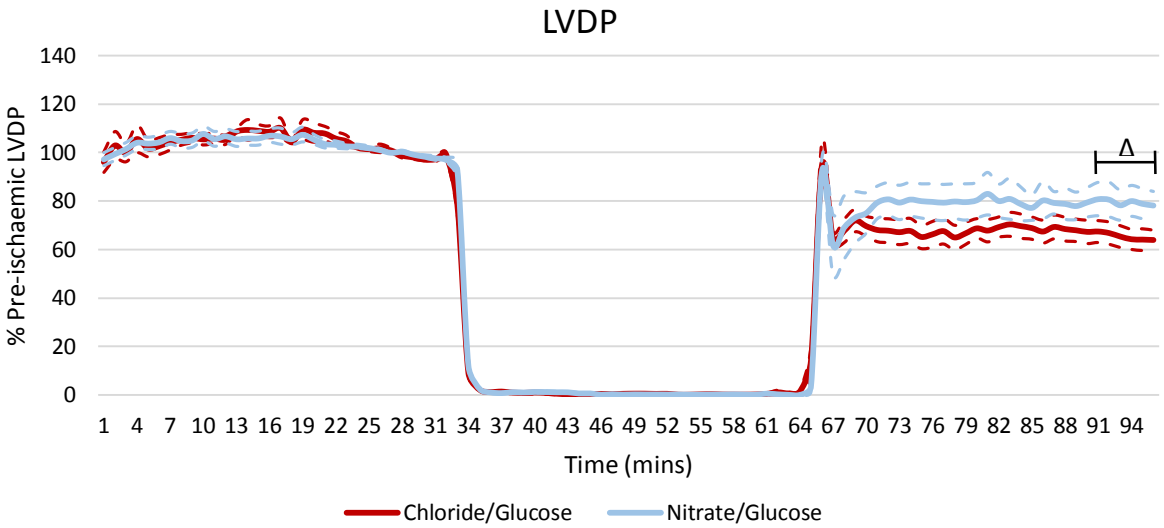

Figure 4.5: Recovery of left-ventricular developed pressure as a percentage of pre-ischaemic levels following 32 min at 0.3 ml.min^{-1}gww^{-1} low flow ischaemia, ±SEM. Δ = $p < 0.05$ relative to nitrate/intralipid.

Heart rate **(Figure 4.6)** and RPP **(Figure 4.7)** recovered to the same extent following ischaemia in both the Chloride/Glucose and Nitrate/Glucose groups.

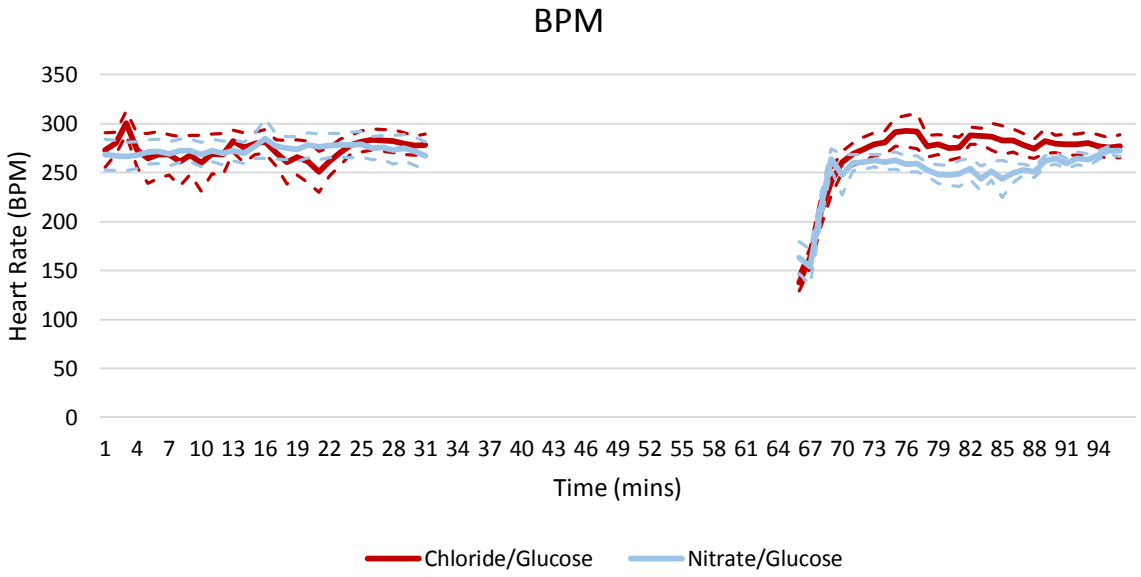

Figure 4.6: Heart rate preceding and following 32 min at 0.3 ml.min^{-1}gww^{-1} low flow ischaemia, ±SEM.

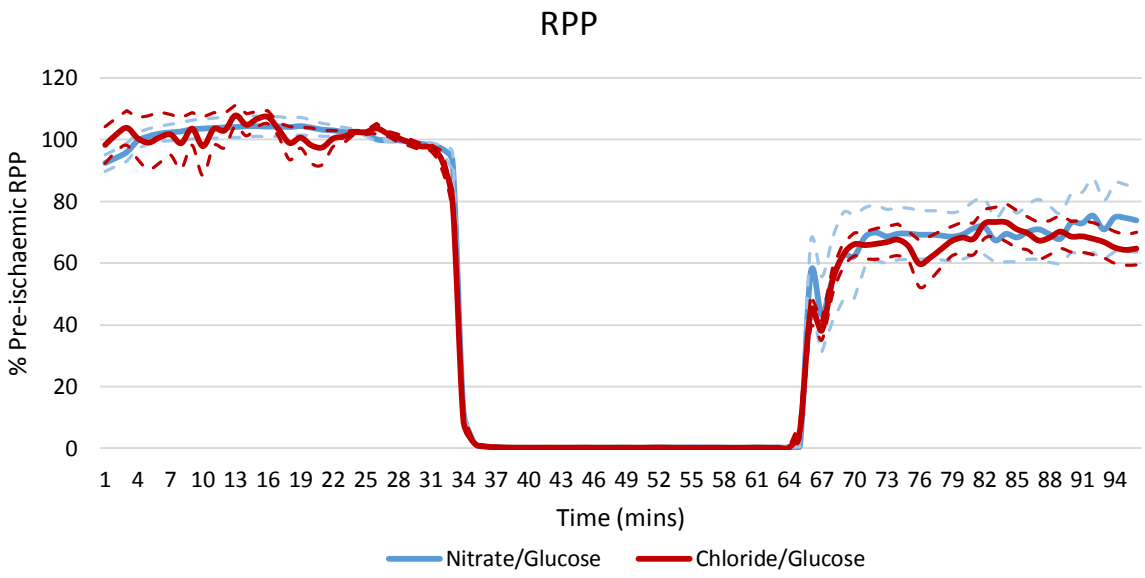

Figure 4.7: Recovery of rate-pressure product as a percentage of pre-ischaemic levels following 32 min at 0.3 ml.min^{-1} gww^{-1} low flow ischaemia, ±SEM.

The percentage recovery of LVDP and RPP for each group, as well as heart rate, at the end of the ischaemic period, is summarised in **Table 4.2:**

Table 4.2: ***Functional Recovery Following Ischaemia/Reperfusion***

	Chloride/ Glucose	**Nitrate/ Glucose**	**Chloride/ Intralipid**	**Nitrate/ Intralipid**	**2-way ANOVA**
%Pre-ischaemic LVDP	63.1± 4.3	77.3± 6.2	83.5± 2.8	63.6± 9.2	Interaction, p<0.001
Heart Rate (bpm)	277.7± 10.7	270.3± 4.9	251.9± 18.0	279.6± 16.9	
%Pre-ischaemic RPP	63.5± 5.5	72.1± 1.0	75.8± 4.8	65.1± 11.4	Interaction, p<0.05

4.3.3 Buffer Lactate

Levels of the ischaemic marker lactate, a product of anaerobic glycolysis, were assessed in the coronary effluent over the ischaemic period using LC-MS **(Figure 4.8)**. Production of lactate was negligible pre-ischaemia, and returned towards baseline following reperfusion, yet rose sharply at the onset of ischaemia and was maintained throughout this period. There was no overall difference between the groups in the concentration of lactate exuded during ischaemia.

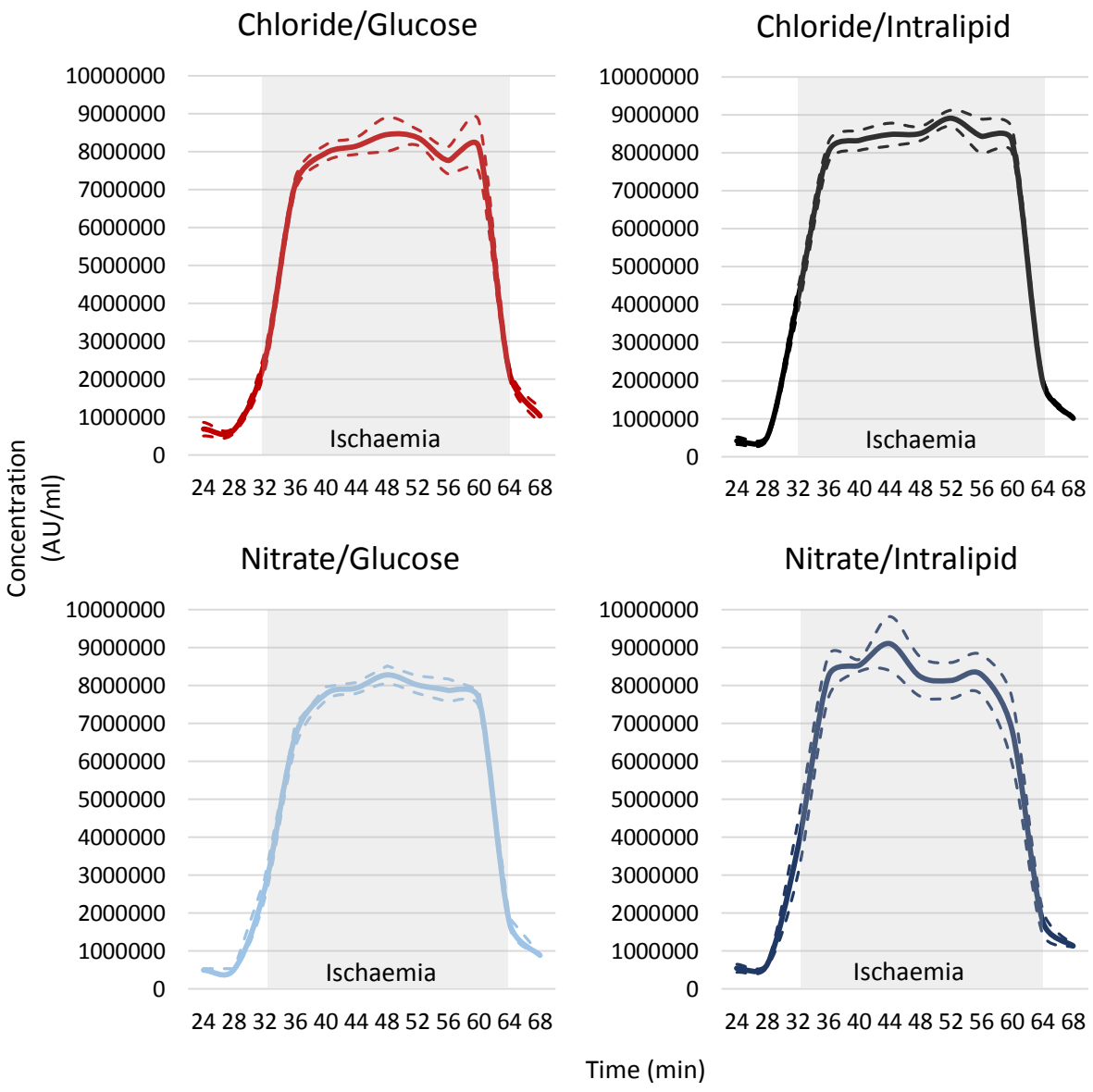

Figure 4.8: Levels of lactate in the coronary effluent. Ischaemic period is highlighted in grey. Results shown as mean ± SEM

4.3.4 Buffer β-hydroxybutyrate

A surprising finding was that the ketone body β-hydroxybutyrate was also present in the coronary effluent during ischaemia **(Figure 4.9)**. This appeared to follow a broadly similar pattern to lactate, with none present in the buffer pre-ischaemia and levels returning swiftly towards baseline post-ischaemia, yet a sharp rise at the onset of ischaemia and maintenance of this level of production through the ischaemic period. There was no overall difference between the groups in concentration levels of β-hydroxybutyrate secreted during ischaemia.

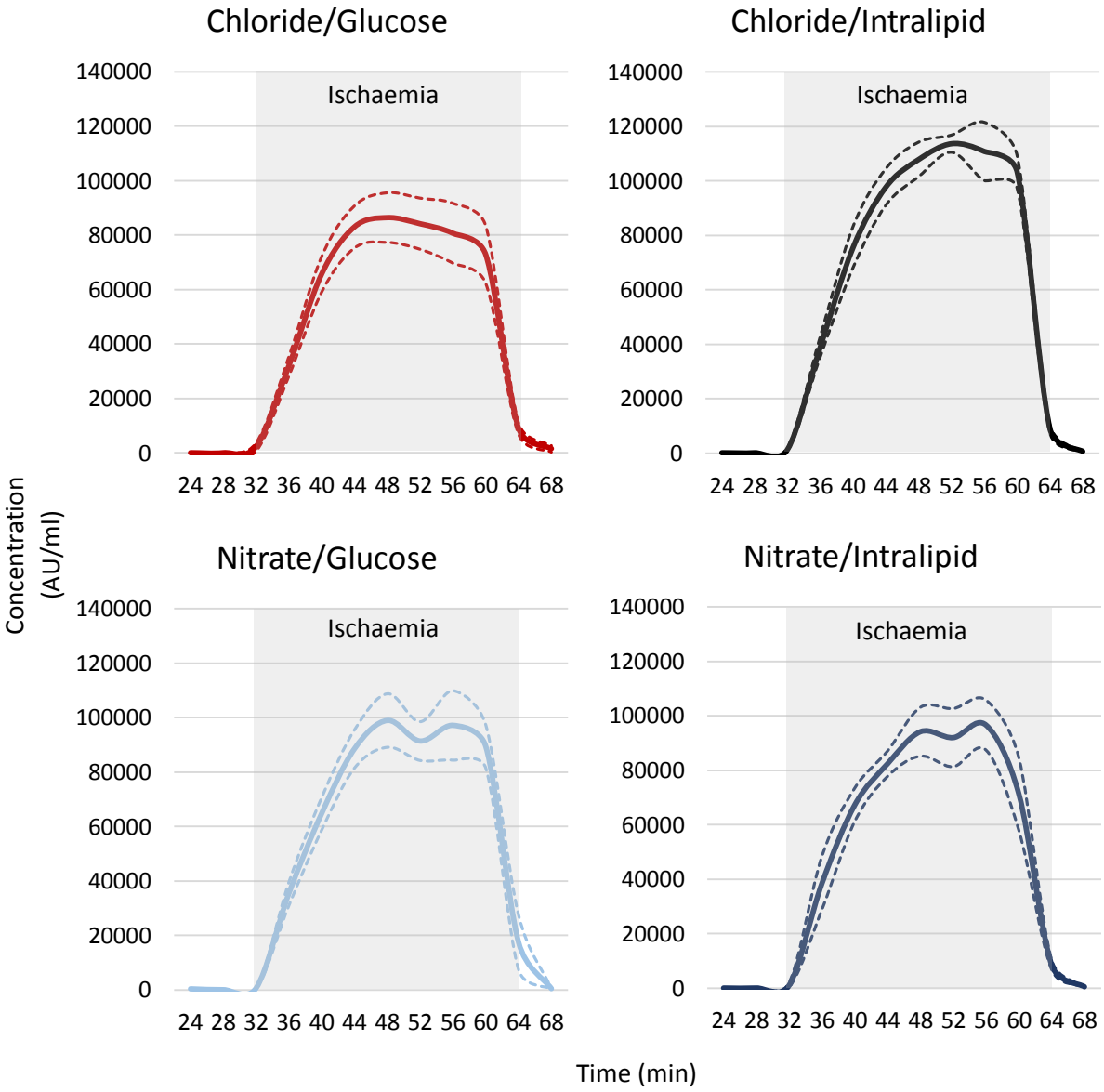

Figure 4.9: Levels of β-hydroxybutyrate in the coronary effluent. Ischaemic period is highlighted in grey. Results shown as mean ± SEM.

4.3.5 Cardiac Mitochondrial Function

In LV directly extirpated from sodium nitrate and sodium chloride supplemented rats, and examined via respirometry (without ischaemia/reperfusion), there was no difference in leak state respiration supported by malate and octanoyl-carnitine **(Figure 4.10)**. β-oxidation and complex I supported respiration were also unchanged by nitrate supplementation, however complex II supported respiration was 35% higher in nitrate supplemented rat hearts compared with those of chloride supplemented rats ($p<0.05$). There was no difference in the respiratory control ratio (RCR) or FAO ratio between groups.

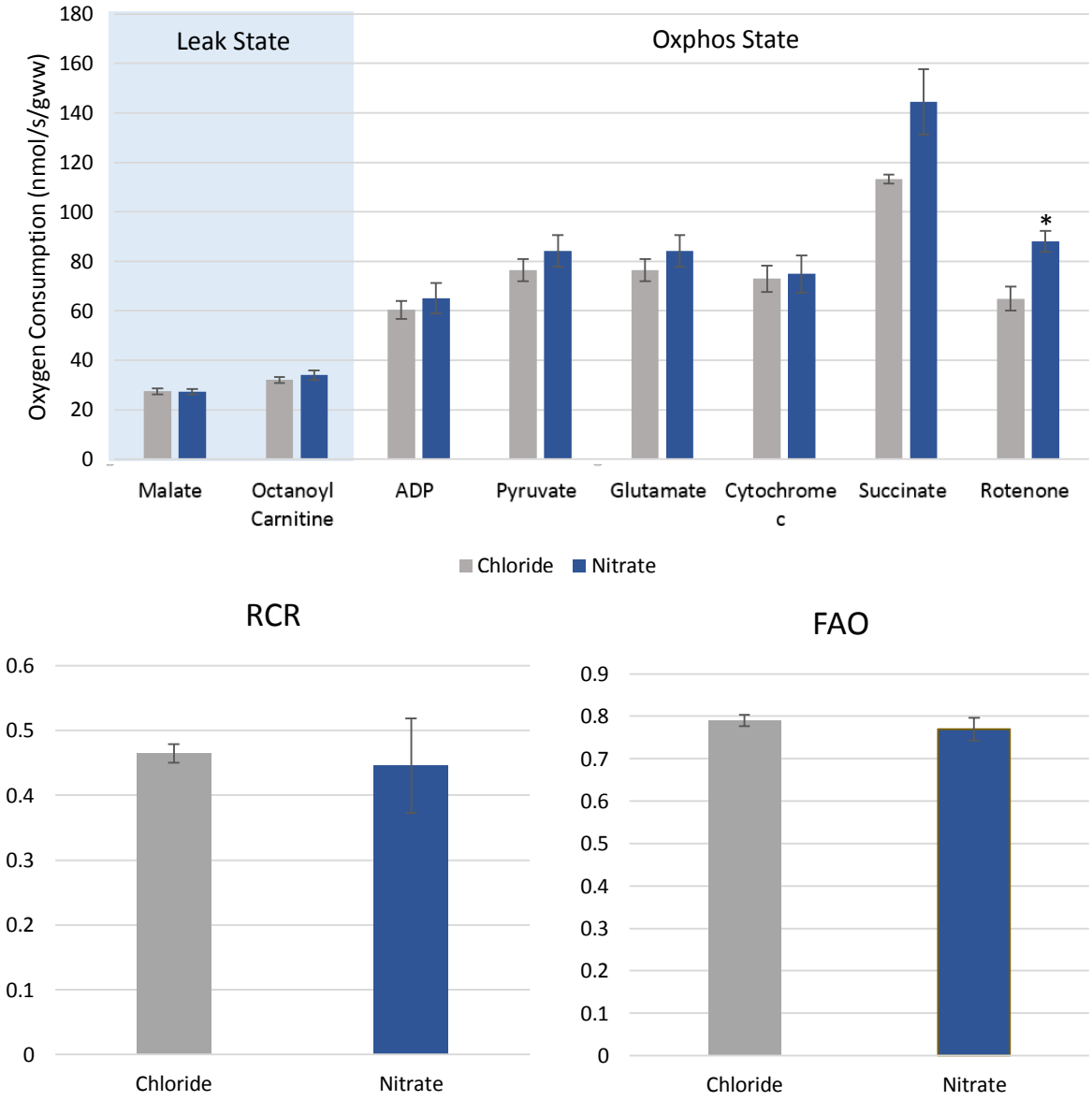

Figure 4.10: (A) Respiration rates in non-perfused hearts, corrected for wet mass. Malate and octanoyl carnitine were added initially to stimulate leak respiration, ADP to stimulate β-oxidation supported Oxphos, glutamate to saturate complex I, cytochrome *c* as a test of membrane integrity, succinate to activate complex II, and rotenone to inhibit complex I. (B) The respiratory control ratio (RCR) and (C) the FAO ratio. All results displayed as mean ± SEM. Statistical difference between nitrate and chloride with Student's T-test denoted as * = $p< 0.05$

Permeabilised LV muscle fibres from hearts which had been subjected to ischaemia/reperfusion were then analysed by respirometry to assess how mitochondrial function and metabolism was affected by ischaemia and reperfusion. The presence of intralipid in the buffer during ischaemia/reperfusion resulted in compromised β-oxidation and complex I function (Intralipid effect, $p<0.05$), along with a decreased respiratory control ration (RCR) (**Figure 4.12, overleaf**; Intralipid effect, $p<0.01$). Complex II supported respiration and total (complex I + II supported) respiration following reperfusion was unaffected by either intralipid or nitrate supplementation **(Figure 4.11, overleaf)**. There was no alteration in the mitochondrial FAO preference ratio between groups.

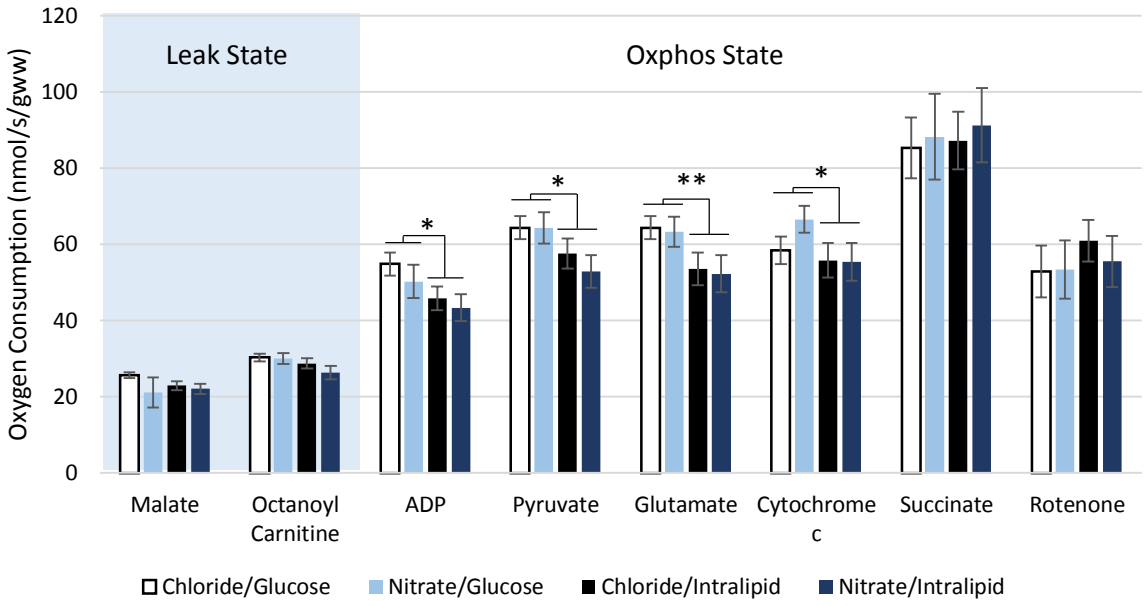

Figure 4.11: Respiration rates post-ischaemia/reperfusion, corrected for wet mass. Malate and octanoyl carnitine were added initially to stimulate leak respiration, ADP to stimulate β-oxidation supported Oxphos, glutamate to saturate complex I, cytochrome *c* as a test of membrane integrity, succinate to activate complex II, and rotenone to inhibit complex I. All results displayed as mean ± SEM. 2-way ANOVA * = p<0.05, ** = p<0.01

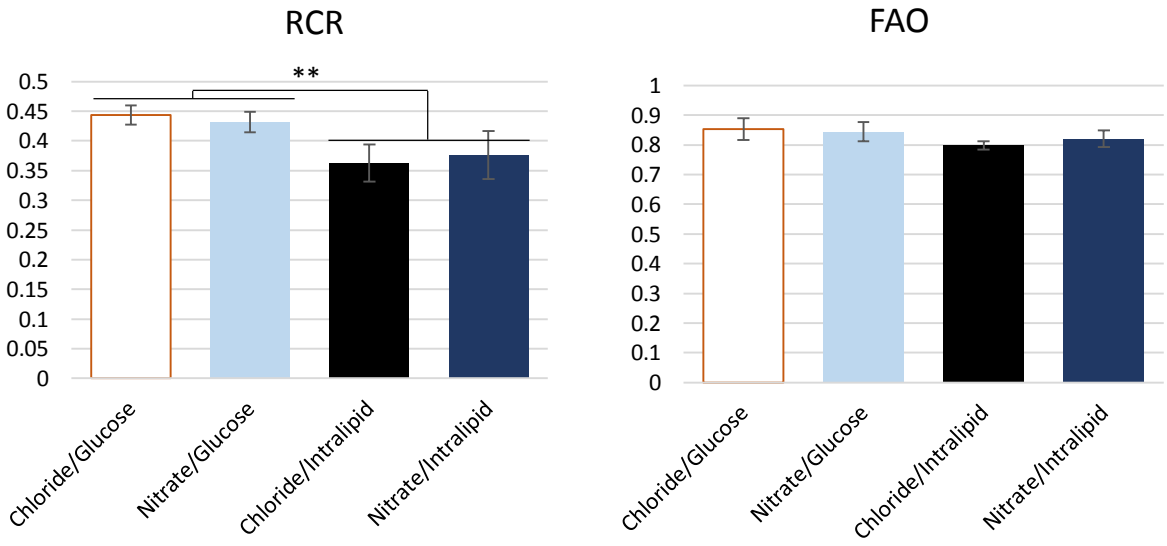

Figure 4.12: Respiratory control ratios (RCR), and FAO preference. All displayed as mean ± SEM. 2-way ANOVA ** = p<0.01

4.3.6 Recovery of Cardiac Energetics

ATP and PCr were assessed at the end of reperfusion by LC-MS/MS. Tissue levels of ATP were 1.8 fold higher in LV from the intralipid perfused chloride supplemented hearts relative to those perfused only with glucose, demonstrating a possible energetic component to intralipid mediated cardioprotection **(Figure 4.13A)**. Nitrate supplementation meanwhile resulted in 1.3 fold greater levels of ATP relative to chloride when there was no intralipid in the buffer, yet a 30% lower level of ATP relative to chloride when intralipid was present in the buffer. This manifested as an effect of nitrate ($p<0.05$), and an interaction between nitrate and intralipid ($p<0.05$). Chloride/intralipid hearts displayed 1.83 fold greater levels of ATP than chloride/glucose hearts (post-hoc t-test, $p < 0.05$).

PCr levels meanwhile were similar to chloride/glucose in the chloride/intralipid hearts, but nitrate depressed them in both buffer composition types **(Figure 4.13B)**. The effect of nitrate was stronger here ($p<0.01$), while there was also an interaction between nitrate and intralipid ($p<0.05$).

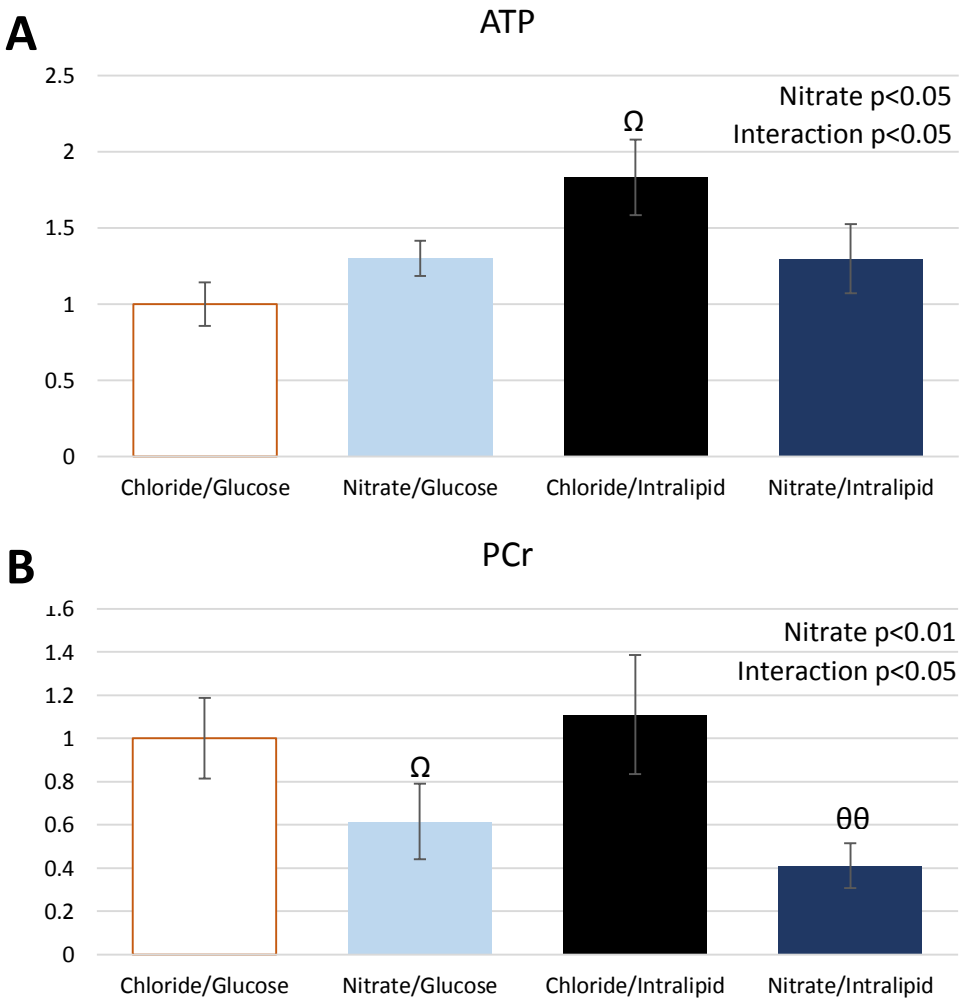

Figure 4.13: Cardiac levels of (A) ATP and (B) PCr displayed relative to chloride/glucose hearts. Results displayed as mean ± SEM**.** 2-way ANOVA outcomes denoted on graph. Ω = $p < 0.05$ relative to chloride/glucose, θθ = $p < 0.01$ relative to chloride/intralipid.

4.3.7 Malonyl-CoA Regulation of FAO

In order to investigate mitochondrial fatty acid uptake, levels of malonyl-CoA, the CPT-1 inhibitor, were investigated using LC-MS/MS **(Figure 4.14)**. Malonyl-CoA levels were 1.7-fold higher in hearts perfused with intralipid relative to those which had only glucose in the buffer (Intralipid effect $p<0.01$), suggesting there was an increased inhibition of CPT-1 post-reperfusion.

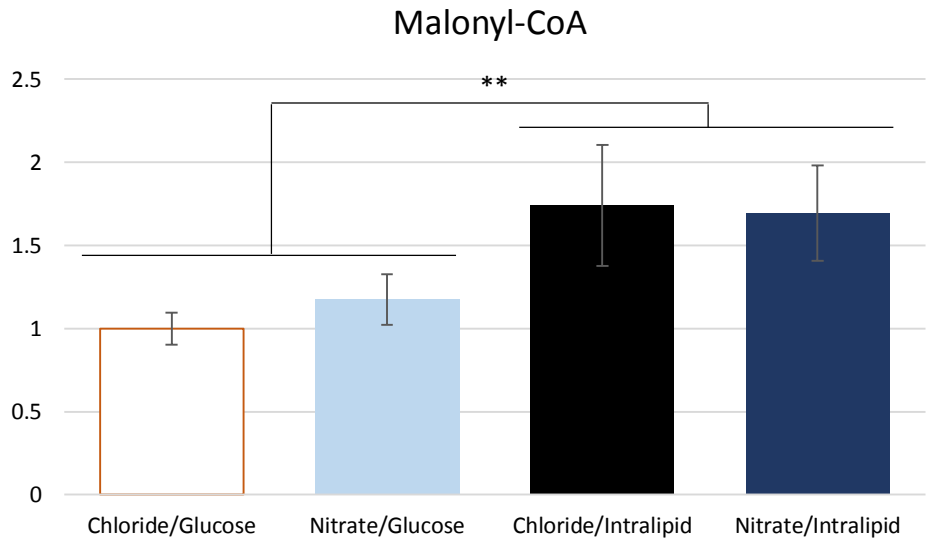

Figure 4.14: Cardiac levels of Malonyl-CoA relative to chloride/glucose hearts. Results displayed as mean ± SEM. 2-way ANOVA ** = $p<0.01$

4.3.8 Krebs Cycle Intermediates

Krebs cycle intermediates and acetyl-CoA were measured using LC-MS/MS **(Figure 15)**.

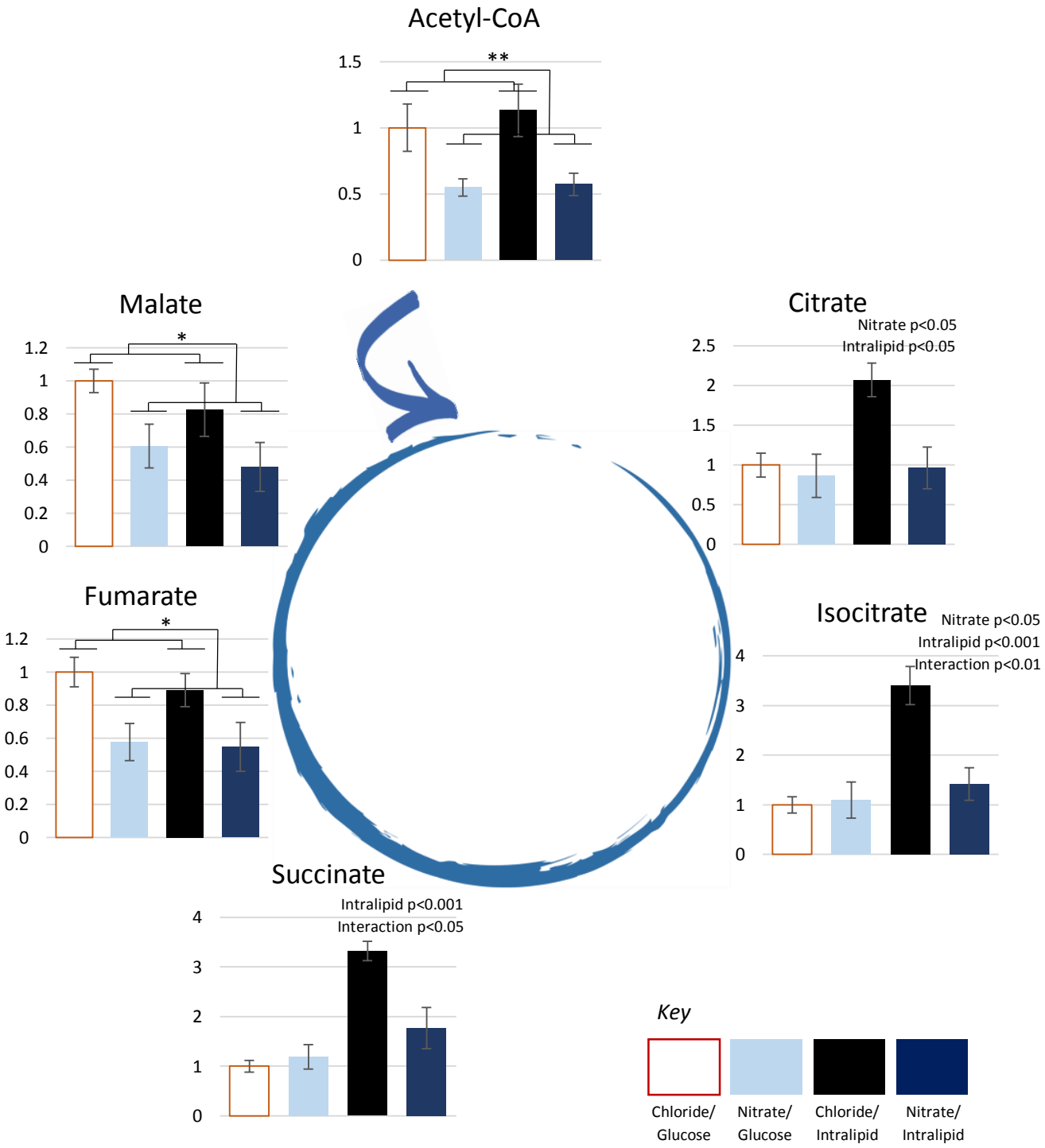

Figure 4.15: Concentrations of Krebs cycle intermediates relative to chloride/glucose hearts. Results displayed as mean ± SEM. 2-way ANOVA * = p<0.05, ** = p<0.01

Cardiac levels of acetyl-CoA were 45% lower in reperfused hearts from nitrate-supplemented rats relative to chloride-supplemented rats, a pattern similar to that seen with the late-Krebs cycle intermediates malate and fumarate (Nitrate effect, $p<0.01$, 0.05 and 0.05, respectively).

However, the early Krebs cycle intermediates citrate and isocitrate, as well as the complex II substrate succinate, were not lower following dietary nitrate supplementation relative to the chloride/glucose hearts. They were however markedly raised in the chloride/intralipid hearts compared with chloride/glucose hearts, ~2 fold, 3.5 fold and 3.25 fold for each respective intermediate (Intralipid effect of $p<0.05$, $p<0.001$ and $p<0.001$, respectively). This effect was not seen in the nitrate/intralipid hearts (An effect of both nitrate and intralipid for citrate (both $p<0.05$); an effect of nitrate ($p<0.05$), intralipid ($p<0.001$) and an interaction between the two factors ($p<0.01$) for isocitrate; and an effect of intralipid ($p<0.001$) and an interaction ($p<0.05$) for succinate).

4.3.9 Post-Reperfusion Alanine Levels

LV concentration of the amino acid alanine, measured by LC-MS/MS, was 2.25-fold higher in hearts where intralipid had been present in the perfusion buffer (**Figure 16**; Intralipid effect, $p<0.01$). Alanine is synthesised from pyruvate by alanine aminotransferase, and increased levels can often be interpreted as a sign of increased anaerobic metabolism, or decreased pyruvate uptake to the mitochondria.

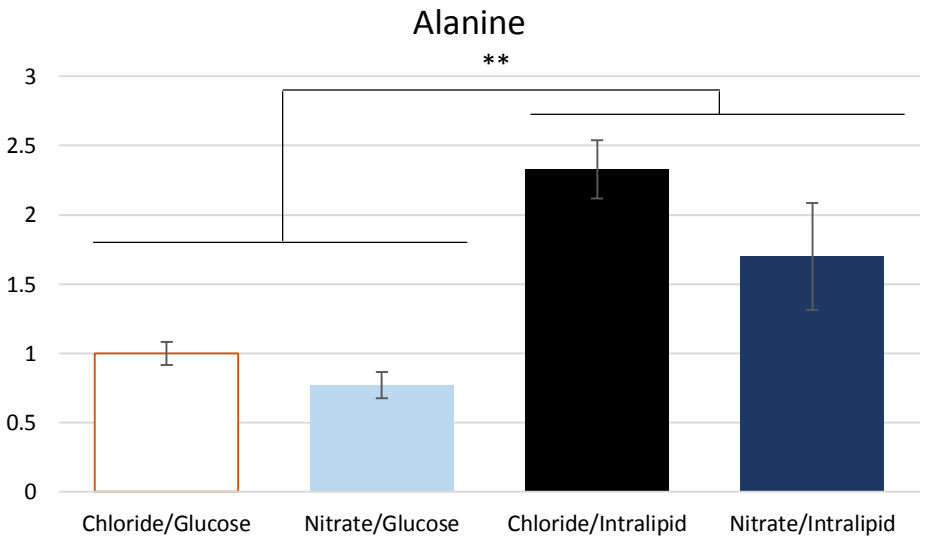

Figure 4.16: Cardiac levels of alanine displayed relative to chloride/glucose hearts. Results displayed as mean ± SEM 2-way ANOVA ** = $p<0.01$

4.3.10 Oxidative Stress Markers

Levels of oxidative stress markers in the reperfused heart were interrogated using LC-MS/MS (**Figure 17**). Contrasting effects of nitrate supplementation and intralipid delivery were observed in the different oxidative stress markers. Hydroxylysine levels were reduced ~40% when intralipid was present in the buffer ($p<0.05$). Meanwhile, intralipid mediated a roughly 30% increase in hydroxytyrosine levels (not significant) and methionine sulphoxide ($p<0.05$), markers which were present in lower levels in hearts which had been supplemented with sodium nitrate ($p<0.05$ for hydroxytyrosine, not significant for methionine sulphoxide). Hydroxyproline levels appeared affected by nitrate supplementation, which effected a 20-25% decrease in their presence, although this did not manifest as being significant.

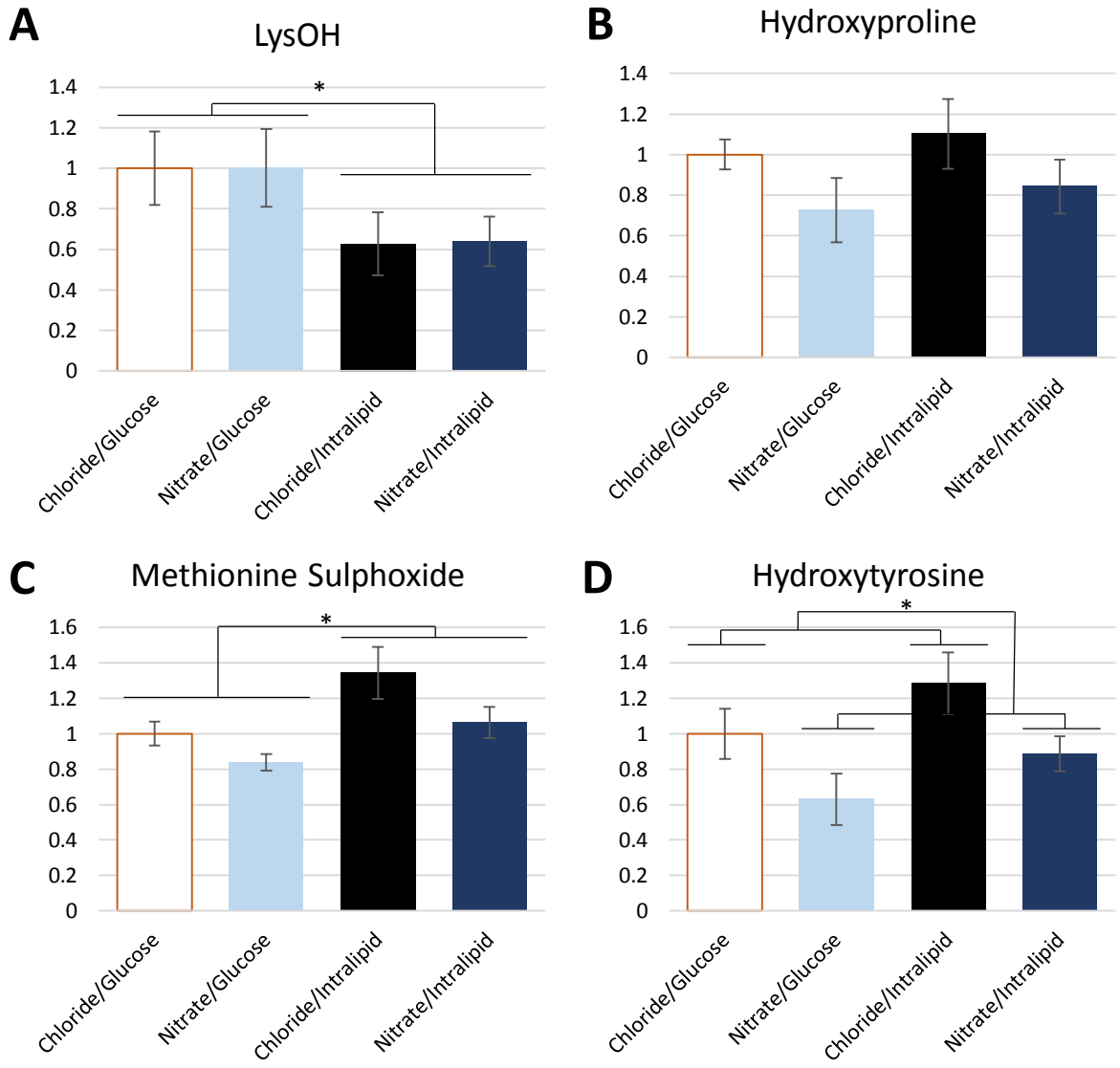

Figure 4.17: Cardiac levels of (A) hydroxylysine, (B) Hydroxyproline, (C) Methionine Sulphoxide and (D) Hydroxytyrosine relative to chloride/glucose hearts. Results displayed as mean ± SEM 2-way ANOVA * = $p<0.05$

4.3.11 Ischaemic Levels of Lactate and β-hydroxybutyrate

In order to further investigate the finding of increased β-hydroxybutyrate in the ischaemic coronary effluent, LC-MS was used to analyse tissue from hearts frozen at the end of the ischaemic period for lactate and β-hydroxybutyrate **(Figure 4.18)**. Lactate accumulated to a greater extent in hearts from the nitrate supplemented groups during ischaemia ($p<0.001$). This effect was mirrored for β-hydroxybutyrate ($p<0.01$), suggesting that its production is perhaps linked to anaerobic metabolism in the ischaemic heart.

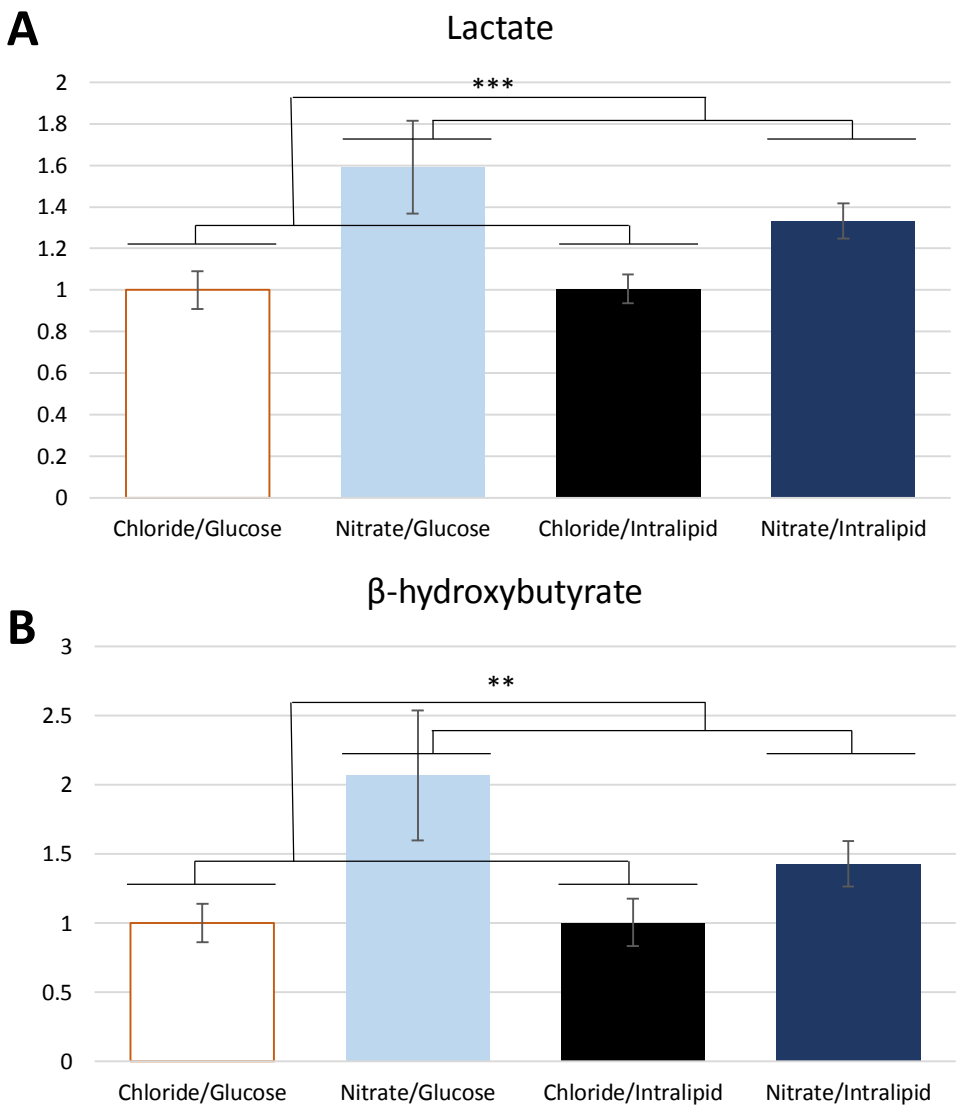

Figure 4.18: Ischaemic LV levels of (A) lactate and (B) β-hydroxybutyrate displayed relative to chloride/glucose hearts. Results displayed as mean ± SEM**.** 2-way ANOVA ** = $p<0.01$, *** = $p<0.001$

4.4 DISCUSSION

Whether dietary nitrate supplementation could have a beneficial effect upon recovery from an ischaemic insult remains unclear, but results in this chapter suggest a metabolic effects of nitrate beyond effects at the electron transport chain, for example through the greater production of lactate and β-hydroxybutyrate post-reperfusion. Intralipid meanwhile resulted in greater recovery of contractile function following ischaemia/reperfusion, protective effects which reaffirm the contested assertion that FAO can be beneficial in recovery from ischaemia/reperfusion. This intralipid mediated cardioprotection was reversed by dietary nitrate supplementation.

4.4.1 Strengths and Limitations of the Study

The ability to see these metabolic effects illustrated one of the big advantages of using Langendorff perfusion as an investigatory tool during this chapter and throughout this thesis. The ability to vary which metabolic substrates were available in the buffer in a highly controlled manner allowed the interaction between dietary nitrate supplementation and fat oxidation to be detected during cardiac recovery following ischaemia. Dietary supplementation with sodium nitrate reversed the cardioprotective effects perfusion with intralipid had upon hearts from animals on the control diet, even though without triglyceride in the buffer there was no nitrate effect. This kind of effect would not be visible in vivo, where the exact proportions of metabolic substrates supplied to the heart in the bloodstream are less controlled. Thus, the present study provides mechanistic insight to a previous study with dietary nitrite conducted *in vivo* which reported a reduction of infarct size (although no functional data) (Bryan et al., 2007b), and it would be interesting to know how this would alter if the proportions of metabolites in the bloodstream were varied.

Conducting the study ex vivo does have some potential drawbacks however. This study was conducted using the Langendorff apparatus partially with the intention of removing the complication non-cardiac effects would present, but the effects of dietary nitrate can be systemic rather than purely cardiac (Webb et al., 2008). The systemic effects of dietary nitrate supplementation may have unseen implications for cardiac recovery, such as the reduction of peripheral tension and therefore work the recovering heart is required to perform. Along with any invoked substrate level changes in the blood, higher levels of circulating NOx species seen with dietary nitrate supplementation (Pannala et al., 2003) were also removed from the study once the hearts were excised. The differences observed in this study were therefore due only to the more chronic changes that dietary nitrate supplement had evoked, which may include protein expression changes, possible angiogenesis and any structural remodelling; and which of these occur during nitrate supplementation deserves further elucidation.

4.4.2 Significance of Results

Previous studies have recorded two main effects of dietary nitrate supplementation upon the rat heart which were likely to have an impact on recovery from ischaemia/reperfusion; protection of mitochondrial complex-I against hypoxia and enhanced FAO (Ashmore et al., 2014a, 2015; Roberts et al., 2015).

Protection of complex-I supported respiration was observed in hypoxia, yet this effect did not appear to translate into ischaemia. Previously, hearts of rats exposed to reduced oxygen conditions exhibited reduced complex-I supported respiration rates unless their diet had been supplemented with nitrate, in which case complex-I function was preserved (Ashmore et al. 2014). However, here there was no indication that dietary nitrate supplementation had protected any of the ETC complexes from ischaemia. This may be a matter of the hearts in the present study having been subjected to more considerable oxidative stress than in the hypoxic study, which negated any protective effect of nitrate against less intense insults to complex I. Alternatively, protection of complex I may be a more acute effect of nitrate, and may not occur without circulating nitrate/nitrite in the perfusion buffer. It would be enlightening to further investigate this to determine whether complex I protection is dependent upon circulating NOx species.

In this study, dietary supplement with sodium nitrate had no effect upon complex I supported respiratory capacity in non-perfused hearts. This concurred with other studies which have suggested little or no impact of nitrate supplementation upon the mitochondrial complexes (Hezel et al., 2015; Monaco et al., 2018), and further suggests that the protection of complex I from hypoxia could be due to acute effects of nitrate in circulation. There was an observed increase in complex II supported respiration here however, which had not been reported previously.

The investigation was conducted with and without intralipid in the buffer because dietary nitrate supplementation is suggested to enhance FAO, yet no difference in the mitochondrial FAO capacity was observed here in either non-perfused hearts or following ischaemia/reperfusion. Previously, increased FAO capacity was observed in several tissues, including the heart, following dietary nitrate supplementation (Roberts et al. 2015; Ashmore et al. 2014; Ashmore et al. 2015). There is still an interaction between nitrate supplementation and intralipid supply on functional recovery from the heart however, with nitrate reversing intralipid mediated cardioprotection, so nitrate appears to be exerting some effect upon fat metabolism. Respirometry gives a measure of the total capacity for FAO rather than the experimentally occurring rate, so it is possible that it is capacity but not rate which is unaltered by nitrate supplementation. It is also the case that a different carnitine was given in this study to assess β-oxidation supported respiration (octanoyl carnitine), compared with the Ashmore et

al. (2014) study, which used palmitoyl carnitine to achieve the same purpose, and this may have affected the FAO capacity observed.

Nitrate supplementation appears to have boosted glycolytic metabolism and the production of lactate at the expense of generation of acetyl-CoA upon reperfusion **(Figures 4.15 & 4.18)**. This has then led to depletion of Krebs cycle intermediates. Since carbon from glucose metabolism is required in order to metabolise acetyl-CoA from fatty acids (Owen et al., 2002), and these fatty acids would usually be preferentially oxidised upon reperfusion (Myears et al., 1987), it is possible that this is how nitrate supplementation has cancelled out the cardioprotective effects of having intralipid in the perfusion buffer.

The cardioprotective effects of intralipid in the absence of nitrate appear to corroborate previous observations. In this study it was used primarily to mimic a physiological mixture of circulating non-esterified fatty acids and to ensure any effects of nitrate supplementation upon FAO were not missed, yet several studies have reported that presence of intralipid in the reperfusion buffer or infusion *in vivo* is cardioprotective (Li et al., 2013; Lou et al., 2014b, 2014a; Mamou et al., 2015; Rahman et al., 2012).

Lou et al (2014) suggest that intralipid acts through the inhibition of ETC complex IV, decreasing O_2 consumption; while the findings in this chapter support the observation that intralipid is cardioprotective (at least in the absence of nitrate), they differ to this in observing no intralipid mediated loss of total respiratory capacity, which would be visible if complex IV functionality was impaired. Instead, intralipid enhanced loss of complex I function following reperfusion, which could be a potentially cardioprotective mechanism given that complex I inhibition with amytal has previously been reported to result in decreased ROS production during ischaemia and improved functional recovery following reperfusion (Aldakkak et al., 2008). Intralipid also decreased coupling of the mitochondria, possibly due to FAO having been shown to be associated with uncoupling of the mitochondria (Cole et al., 2011).

It is also possible that, if as suggested intralipid confers cardioprotection through ROS mediated effects (Lou et al., 2014a), this pathway may be blocked by the antioxidant properties of nitrate. Since it appears here that dietary nitrate supplementation reduces several markers of oxidative stress which accumulate following reperfusion, it is possible that dietary nitrate supplementation abrogates any intralipid stimulated ROS signalling. Nitrate supplementation has also been reported to reduce oxidative stress in several other publications (Ashmore et al. 2014; Hendgen-Cotta et al. 2012; Monaco et al. 2018; Jeddi et al. 2016), which lends credence to the concept that this could be an interference between two ROS-related signalling pathways.

The main mechanistic story from this chapter appears to be one of cardiac metabolic substrate utilisation. The enhanced production of the metabolic by-product malonyl-CoA upon reperfusion suggests that intralipid is enhancing substrate oxidation. It is thought that this increased oxidation of triglycerides inhibits PDH via the Randle cycle (Hue et al., 2009; Randle et al., 1963), which would tally with the increased accumulation of alanine seen here and by Taegtmeyer *et al.* (1977), suggesting an inhibition of complete glucose oxidation. Many studies have previously suggested that fatty acids are the preferred metabolic substrate upon reperfusion when available (Liedtke et al., 1988; Lopaschuk et al., 2009; Nellis et al., 1991), and these findings support that notion. That this should be protective is perhaps more controversial, with extensive literature claiming that ischaemic oxidation of fatty acids is pathological (Fillmore et al., 2014; Jaswal et al., 2011; Lopaschuk et al., 2009). The evidence in this chapter appears to refute this assertion, offering a different aspect upon the debate. It is also possible that this is a result of the heart performing better when intralipid is in the buffer simply because it has more available substrate than when perfused with glucose alone, and this helps it restore its ischaemic ATP debt.

Perhaps the most interesting substrate level finding in this study is the detection of β-hydroxybutyrate production during ischaemia. The ketone body was observed both being excreted from the heart in the coronary effluent, and accumulating in the ischaemic myocardium, yet since it was not present in the buffer being delivered to the heart must be generated in the heart during ischaemia. This is interesting because ketogenesis is primarily considered to occur in the liver (Cotter et al., 2014), and while the heart is known to consume ketone bodies as an metabolic fuel (Aubert et al., 2016; Sato et al., 1995), it has never previously been reported that β-hydroxybutyrate is generated in the heart, except from when ETC complex I was inhibited using amytal (Krebs et al., 1961). In the ischaemic myocardium β-hydroxybutyrate accumulated to the greatest levels in the nitrate supplemented groups, in the coronary effluent however it was secreted to the highest level by hearts in the chloride/intralipid group, which also recovered LVDP to the greatest extent post-reperfusion. It could therefore be possible that generation and excretion of β-hydroxybutyrate during ischaemia is beneficial to recovery, a phenomenon which warrants further investigation in order to better determine what is driving it to occur.

4.4.3 Future Directions

With the conflicting results generated here it is unclear whether dietary nitrate supplementation would protect against ischaemia or impair recovery. However, *in vivo* it may yet prove to be protective, given nitrate has more systemic effects including improvement of vascularisation (Hendgen-Cotta et al., 2012; Webb et al., 2008). It would be interesting in the future to see a real time investigation of

the effects of nitrate/nitrite upon ROS release during ischaemia reperfusion perhaps using fluorescent markers of these compounds, and it would also be interesting to see a proteomic study which measured protein nitrosothiols formed as a result of dietary nitrate supplementation, as this would give an indication of which metabolic and signalling pathways it had an effect upon.

The implications for intralipid as a possible mediator of cardioprotection appear more conclusive. FAO has been painted as a villain during ischaemia/reperfusion (Lopaschuk et al., 2010), yet including this chapter a growing amount of evidence points to it having a positive role in recovery of function upon reperfusion (King et al., 2001; Lou et al., 2014c, 2014a; Rahman et al., 2012). Intralipid perfusion is already routinely used for restoring blood triglyceride content in those with deficiencies, so is safe clinically and could be easily administered upon presentation with the symptoms clinically given that its proposed signalling effects come post-reperfusion (Lou et al., 2014a). One possible future avenue for exploration would be to investigate whether the apparent protective effects of intralipid were due to preferential trigyceride oxidation during or after ischaemia, perhaps using isotopic labelling or hyperpolarised MRI techniques. It would also be interesting to run a dose-response experiment where the concentration of intralipid in the buffer was varied, as this would elucidate whether the protective effects seen during this chapter were concentration dependent.

CHAPTER 5

Ketogenesis in the Ischaemic Heart

ABSTRACT

BACKGROUND The enzymes that catalyse ketogenesis – a pathway thought to occur only in the liver when fat oxidation exceeds demand – are also present in the heart. In the previous chapter, I found that β-hydroxybutyrate (β-OHB) accumulated in the Langendorff-perfused rat heart during low-flow ischaemia, and hypothesised that altered redox state and acetyl-CoA accumulation during ischaemia could drive cardiac ketogenesis.

OBJECTIVES This chapter aimed to investigate ketogenesis in the ischaemic rat heart and the underlying mechanism.

METHODS Hearts were perfused in the Langendorff mode (100 mmHg, 32 min) before 20 min low-flow ischaemia (0.58 $ml.min^{-1}gww^{-1}$) and 20 min reperfusion, with some hearts snap-frozen after each stage. ^{13}C-labelled glucose or triglyceride were used to determine the source of metabolites, with frozen myocardium analysed using LC-MS. In subsequent experiments, hearts were subjected to 32 min of ischaemia (0.3 $ml.min^{-1}gww^{-1}$) and 32 min reperfusion, in order to investigate a mechanism. Initially, the NAD precursor NMN (nicotinamide mononucleotide, 200 μM) was added to alter redox balance. Next, the LDH inhibitor oxamate (50 mM) was added to enhance acetyl-CoA availability. Finally, hymeglusin (1 μM), an inhibitor of HMG-CoA synthase, was added to directly inhibit the ketogenic pathway.

RESULTS β-hydroxybutyrate (β-OHB) accumulated in the ischaemic heart to 0.5 mol/g ($p<0.01$), and was secreted into coronary effluent. Acetyl-CoA derived from fat and glucose oxidation contributed equally to β-OHB synthesis. NMN increased β-OHB levels by 37% ($p<0.01$), with no change in NAD, suggesting a role for altered NAD/NADH. Oxamate increased β-OHB levels 7-fold ($p<0.001$) and slowed the recovery of contractile function post-ischaemia. Inhibition of ketogenesis with hymeglusin resulted in a 33% greater recovery of contractile function post-ischaemia compared with controls.

CONCLUSIONS Ketogenesis occurs in the ischaemic rat heart and is associated with worsened functional recovery upon reperfusion.

5.1 BACKGROUND

In **Chapter 4**, I found that the ketone body β-hydroxybutyrate was present in both the coronary effluent and LV tissue from the ischaemic heart, yet not that from the aerobically perfused heart. This raised interesting questions: Is the β-hydroxybutyrate being produced in the heart, what is the metabolic mechanism which underlies this, and how beneficial or detrimental is the process to recovery of cardiac function following reperfusion?

5.1.1 Ketogenesis

Canonically, β-hydroxybutyrate is thought to be synthesised and secreted predominantly by the liver. It has only previously been documented to occur in cardiac tissue following pharmacological inhibition of complex I by sodium amytal (Krebs et al., 1961). The process of synthesising ketone bodies, which include acetoacetate, acetone and β-hydroxybutyrate, is called ketogenesis. This is commonly thought to occur in liver mitochondria when β-oxidation of fats exceeds mitochondrial demand for oxidation (McGarry and Foster, 1976). The excess acetyl-CoA produced is amalgamated into acetoacetyl-CoA, β-Hydroxy β-methylglutaryl-CoA (HMG-CoA) and then acetoacetate, which can be further reduced to β-hydroxybutyrate **(Figure 5.1)**.

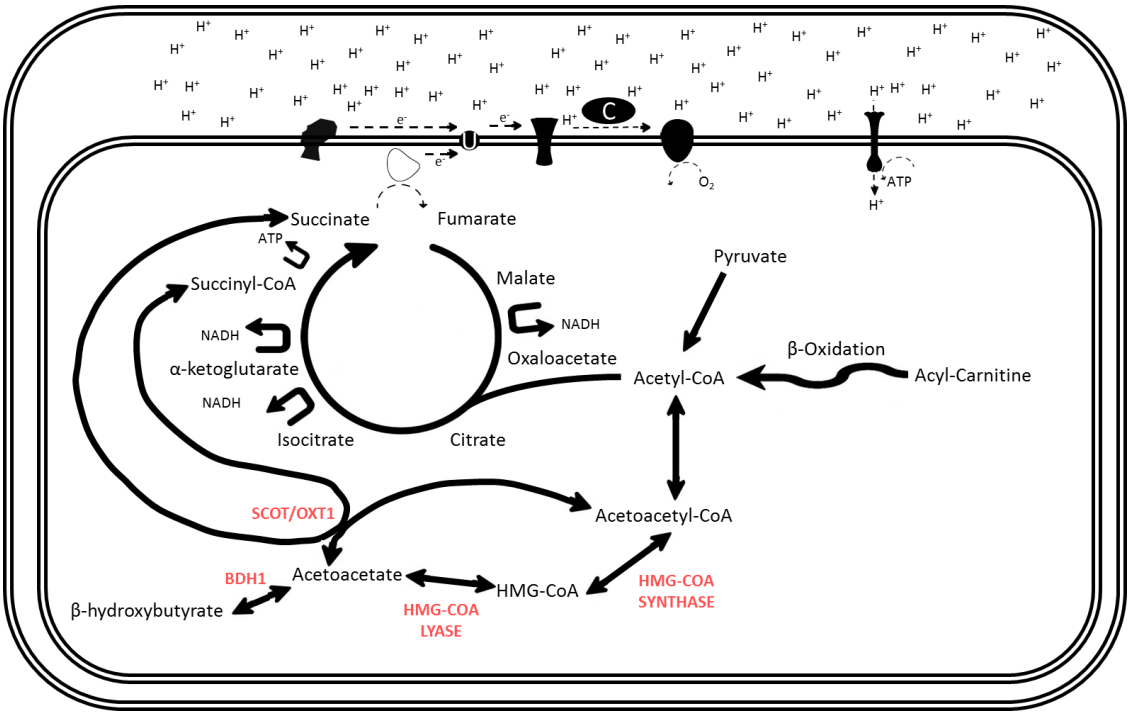

Figure 5.1: Ketogenesis and Ketolysis. Acetyl-CoA is converted to acetoacetyl-CoA, β-Hydroxy β-methylglutaryl-CoA (HMG-CoA), Acetoacetate and β-hydroxybutyrate in a series of reversible reactions. The enzymes which catalyse this are HMG-CoA synthase, HMG-CoA lyase, and β-hydroxybutyrate dehydrogenase (BDH1). HMG-CoA can be bypassed when conversion of acetoacetate to acetoacetyl-CoA is combined with succinyl-CoA to succinate by the enzyme succinyl-CoA-3-oxaloacid CoA transferase (SCOT).

Despite not being thought of as a ketone-producing organ, the requisite enzymes are present in the heart (Cook et al., 2017); yet net ketogenesis has not been shown to occur without artificial stimulation. In the perfused rat heart, ^{14}C label originating from palmitate is incorporated into β-hydroxybutyrate despite no net ketogenesis (Fink et al., 1988), in a process the researchers termed pseudoketogenesis. This demonstrates that the enzyme pathway is present and active even if there is not a clearly observed function.

5.1.2 Ketogenesis Could be Favoured by Reductive Ischaemic Conditions

It has however been demonstrated that ketogenesis can be activated in the heart if the conditions are manipulated in the right way. In the 1960s, Krebs et al observed ketone synthesis in heart homogenate following the addition of several substrates, including the ETC complex I inhibitor sodium amytal (Krebs et al., 1961). They linked this to probable levels of NADH, which normally transfers electrons from the Krebs cycle to complex I, a process inhibited by sodium amytal. NADH is also involved in the reduction of acetoacetate to β-hydroxybutyrate, and so increased concentrations could underpin sodium amytal-driven cardiac ketogenesis. Crucially, rate of electron flux through the ETC is also depressed during ischaemia due to low oxygen availability, and as such this could present an analogous environment to the one generated by complex I inhibition.

The heart is also found to accrue late-Krebs cycle intermediates, including succinate, at the expense of early intermediates during ischaemia and hypoxia (Bittl and Shine, 1983; Folbergrová et al., 1974; Hohl et al., 1987; Sato et al., 1995), and this could help drive ketogenesis. Succinyl-CoA-3-oxaloacid CoA transferase (SCOT), the enzyme thought to be primarily responsible for ketone body utilisation in the heart, converts acetoacetate and succinyl-CoA to acetoacetyl-CoA and succinate (Dedkova and Blatter, 2014). The presence of excess succinate during ischaemia could favour the reverse reaction of the reaction, with the concentration gradient forcing the production of acetoacetate and β-hydroxybutyrate. This would appear to be supported by observations that the stimulated reduction of acetoacetate to β-hydroxybutyrate occurs at its optimal rate only in the presence of succinate (Krebs et al., 1961; Schönfeld et al., 2010), further suggesting that the ischaemic heart might present an environment conducive to ketogenesis.

5.1.3 Link to Fat Oxidation

Ketogenesis in the liver is considered to be inextricably linked to fat oxidation (Cook et al., 1978). Oxidation of fatty acids produces around 2.4 times more ATP per gram of substrate than glucose oxidation (Darvey, 1998), and is therefore a major source of energy. However, some organs, including the brain, cannot take up and oxidise fatty acids for energy (Schönfeld and Reiser, 2013; Zhao et al.,

2015). This is circumvented by the liver converting fatty acids into circulating ketone bodies, which may be transported across the blood brain barrier by the monocarboxylic acid carrier and are consumed preferentially by several organs including the heart (McGarry and Foster, 1976; Veech, 2004).

It therefore would appear to follow that if there is cardiac ketogenesis occurring during ischaemia, it may result from FAO exceeding cardiac mitochondrial oxidation capacity under these conditions. It has been argued that FAO is pathologically stimulated by activation of AMP-activated protein kinase (AMPK) during ischaemia, which leads to a decrease in malonyl-CoA, an inhibitor of mitochondrial fat uptake via CPT-1 (Lopaschuk et al., 2009). This increase in FAO coupled with cessation of oxidative phosphorylation during ischaemia could lead to fat oxidation exceeding the mitochondrial capacity to utilise the resulting acetyl-CoA; analogous conditions to that of β-hydroxybutyrate production in the liver.

Oxidation of fatty acids in the heart has been linked to improved recovery from ischaemia/reperfusion as documented in **Chapter 4** and in other studies (King et al., 2001; Li et al., 2013). It is possible that this could be in part be facilitated by an increased production of β-hydroxybutyrate, which may be available upon reperfusion.

However, a confounding factor to this theory is that β-hydroxybutyrate has been shown to inhibit cardiac fatty acid oxidation. Independently of malonyl-CoA, β-hydroxybutyrate administration suppressed oxidation of fatty acids in the pig heart *in vivo*, even following infusion of a fat emulsion (Stanley et al., 2003). If FAO is inhibited by β-hydroxybutyrate and FAO is considered protective, then there is also an argument to be made that presence of β-hydroxybutyrate may be damaging during ischaemia and/or reperfusion.

5.1.4 Oxidation of β-hydroxybutyrate in the Heart

Unstimulated ketogenesis may be as yet unreported in the heart, but oxidation of β-hydroxybutyrate is well documented and has several beneficial effects upon the function of the healthy heart. In the working heart, its administration increases cardiac oxygen efficiency both by itself and in combination with insulin (Sato et al., 1995). ATP yielded from β-hydroxybutyrate oxidation is thought to have a greater $\Delta G'_{ATP}$ than ATP produced from the metabolism of different metabolic substrates due to it being a more oxygen efficient fuel (Lammerant et al., 1985; Veech, 2004).

It is perhaps for these reasons that β-hydroxybutyrate is thought to be taken up and oxidised preferentially over glucose in heart tissue (Gormsen et al., 2017). This could also be explained through

its action to inhibit glycolysis (Kashiwaya et al., 1994), which allows it to come to predominate oxidation in the heart and effectively occupy a dominant position in the Randle cycle.

β-hydroxybutyrate has also been recently documented to be consumed preferentially during heart failure. Aubert et al (2016) observed increased expression of β-hydroxybutyrate dehydrogenase (BDH1) and increased oxidation of β-hydroxybutyrate in a transverse aortic constriction and infarcted mouse model of heart failure, although it should be noted that BDH1 is a bi-directional enzyme and since they were administering β-hydroxybutyrate this does not conclusively prove whether ketogenesis or ketolysis is occurring *in vivo*. In human patients with type 2 diabetes , inhibition of glucose reuptake in the kidney resulted in increased levels of β-hydroxybutyrate and almost a 40% decrease in mortality rate (Ferrannini et al., 2016). Further, increased rates of β-hydroxybutyrate oxidation and increased SCOT expression were seen in the left ventricle of humans with advanced stage heart failure (Bedi et al., 2016). Taken together, this suggests β-hydroxybutyrate oxidation finds favour in the failing heart, where myocardial blood supply is insufficient to support its own requirements.

5.1.5 A Cardioprotective Role for β-hydroxybutyrate?

Whilst the presence of β-hydroxybutyrate has been shown to increase cardiac efficiency and function, there is no consensus on its effects upon recovery from ischaemia. King et al. (2001) claim that while free fatty acids are beneficial, β-hydroxybutyrate itself does not augment recovery from ischaemia, and this is supported to an extent by the work of Goodwin and Taegtmeyer (1994), which demonstrated no cardioprotective effect upon rats fed a control diet. However, Goodwin and Taegtmeyer do note a cardioprotective effect when the rats have been fasted, a result corroborated by Zou et al. (2002). A separate study observed a beneficial effect of β-hydroxybutyrate on recovery of contractile function only in rats fed a high fat-low-carbohydrate diet and not in controls (Liu et al., 2016). Fasting increases the expression of enzymes for ketone body oxidation (Grabacka et al., 2016; Wentz et al., 2010), while the high fat-low-carbohydrate diet increases HMGCS2 expression, so it is possible that any beneficial effects of β-hydroxybutyrate upon functional recovery are only visible when there is a greater capacity for, or dependency upon, its oxidation. Cumulatively this evidence suggests that metabolic state and ratios of metabolic substrates help to determine the role of β-hydroxybutyrate in the heart.

.

5.1.6 Signalling roles of β-hydroxybutyrate

β-hydroxybutyrate has emerged as a signalling molecule involved in the response to oxidative stress in recent years. Administration of β-hydroxybutyrate was shown to inhibit histone deacetylases, enhancing production of acetylation stimulated genes FOXO3a and MT2, which have antioxidative properties (Newman and Verdin, 2017; Newman et al., 2015; Shimazu et al., 2013). β-hydroxybutyrate is also a ligand for both the nicotinic acid receptor HCAR2 and free fatty acid receptor 3 (FFAR3) (Newman et al., 2015). As well as limiting lipolysis, HCAR2 modulates macrophage function, while FFAR3 has suppressive effects upon heart rate and overall sympathetic tone. It therefore seems plausible that the production of β-hydroxybutyrate during ischaemia could represent an antioxidant and damage limiting response.

5.1.7 Objectives

The objective of this chapter was to investigate the mechanisms underlying the ischaemic accumulation of β-hydroxybutyrate seen in **Chapter 4**, and whether it has any implications for recovery from ischaemia/reperfusion.

5.2 METHODS

Male Wistar rats (300-350 g) were obtained from a commercial breeder (Charles River, UK) and pair-housed in a temperature (21°C), humidity (46%) and light (12 h/12 h light/dark cycle) controlled environment. A standard diet RM1P (65% carbohydrates, 14% crude protein, 3% crude protein, 3% fatty acids, Special Diets Services, UK) and water were provided ad libitum.

All procedures involving live animals were carried out by a licence holder in accordance with UK Home Office regulations, and underwent review by the University of Cambridge Animal Welfare and Ethical Review Committee.

5.2.1 Isolated Heart Perfusion

Rats were anaesthetised and terminated by use of rising CO_2 levels and cervical dislocation. Hearts were immediately excised into ice cold KH buffer, and perfused on the Langendorff rig as described in **Chapter 2 (2.1).**

Protocol for the Initial Assessment of Ischaemic Ketogenesis

All hearts were perfused for 32 min at a constant pressure of 100 mmHg following an initial acclimatisation period. Following this, the protocol was terminated for the first group (termed pre-ischaemic), while the second (ischaemic) and third (reperfused) groups were progressed to a period of low flow ischaemia at a flow rate of 0.56 $ml.min^{-1}gww^{-1}$ for 20 min. Only the third group underwent reperfusion for 20 min at conditions identical to those used pre-ischaemia.

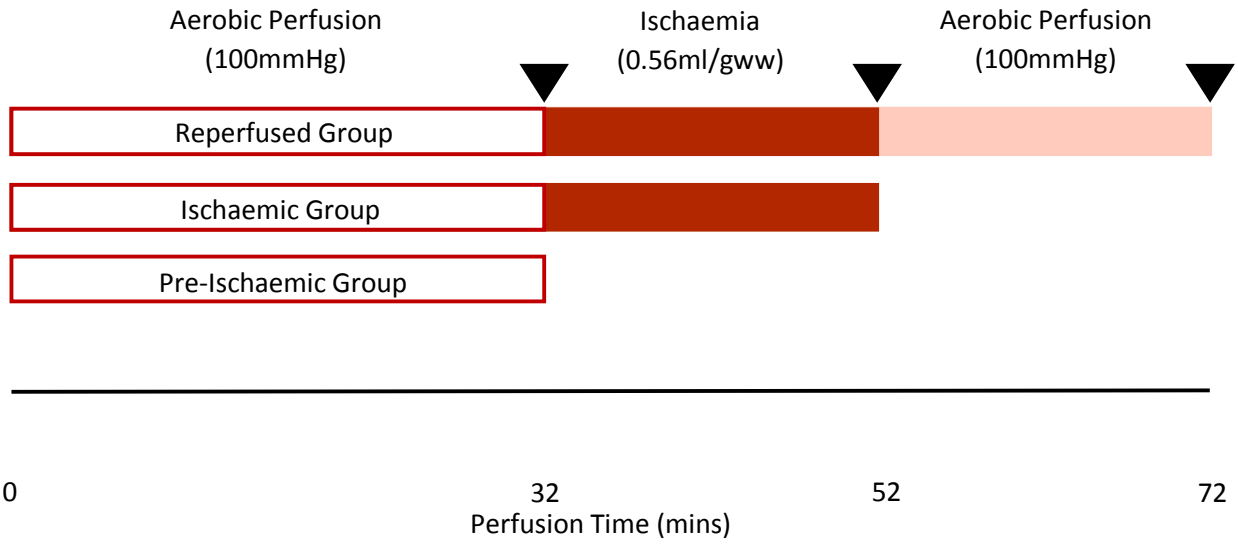

Figure 5.2: Timeline depicting the perfusion protocol for each group

This ischaemic flow rate was chosen because it resulted in 100% recovery of function following reperfusion at 100mmHg; the intention of this was to establish that any alterations to metabolism and ketogenesis which were observed would be due to the ischaemic conditions and not due to functional damage caused to the tissue.

The perfusion medium was 250 mL of recirculated KH buffer (118 mM NaCl, 4.7 mM KCl, 1.2 mM $MgSO_4$, 1.3 mM $CaCl_2$, 0.5mM EDTA, 25 mM $NaHCO_3$, 1.2 mM KH_2PO_4; pH 7.4) containing 8.25 mM glucose, 2.75 mM U-^{13}C labelled glucose (Cambridge Isotopes Ltd) and 0.4 mM equivalent intralipid (n=7 for each of the reperfused, ischaemic and pre-ischaemic groups).

Following the end of the perfusion protocol, the left ventricle was rapidly sectioned in transverse and snap frozen with the exception of ~10 mg which was placed on ice-cold biopsy preservation solution (BIOPS) before being permeabilised for respirometry.

Further groups were perfused in the absence of intralipid where A) the NAD+ precursor nicotinamide mononucleotide (NMN; 200 µM) was added to the buffer at the beginning of the protocol and B) the LDH inhibitor sodium oxamate (50mM) were added to the perfusion buffer 12 min before the induction of the 20 min low flow ischaemic period. These hearts were sectioned and snap frozen, along with controls where the compound was not added, at the end of the ischaemic period.

Protocol for the Assessment of Impact upon Recovery of Function Post-Reperfusion

A second perfusion protocol was employed in order to investigate the impact of ketogenesis on functional recovery from ischaemia/reperfusion. Hearts were perfused at 100 mmHg for 32 min following an acclimatisation period, before being subjected to 32 min of 0.3 ml.min^{-1}gww^{-1} low flow ischaemia. This flow rate was chosen because it resulted in 65% recovery of pre-ischaemic function in pilot studies, therefore allowing scope for treatments to either improve or further impair contractile recovery. A reperfusion period was then initialised whereby 100 mmHg perfusion was restored for 32 min. 80 µg/ml hymeglusin in 80 µl DMSO vector (n=5), 80 µl DMSO vehicle injection (n=5) or 50 mM sodium oxamate (n=5) were added to the perfusion buffer 12 min before the ischaemic period in their respective groups, while a control group (n=5) with no additions was performed for comparison with the sodium oxamate group. The perfusion medium was 250 mL of recirculated KH buffer (118 mM NaCl, 4.7 mM KCl, 1.2 mM $MgSO_4$, 1.3 mM $CaCl_2$, 0.5 mM EDTA, 25 mM $NaHCO_3$, 1.2 mM KH_2PO_4; pH 7.4) containing 11 mM glucose, gassed with 95% O_2 and 5% CO_2. The hearts were sectioned and frozen following the end of the reperfusion period for future analysis.

For all groups, samples of coronary effluent were taken every four minutes and immediately frozen.

5.2.2 High-Resolution Respirometry

Permeabilision of LV fibres and measurement of respiration rates was conducted as described in **Chapter 2 (Section 2.2).** The ratio of fatty acid oxidation preference (FAO) was calculated by dividing the octanoyl carnitine supported oxphos rate by the octanoyl carnitine plus pyruvate supported oxphos rate. The respiratory control ratio (RCR) was calculated as an indicator of mitochondrial coupling by dividing the rate of oxygen consumption supported by malate and octanoyl carnitine in the oxphos state by that supported by the same substrates in the leak state.

5.2.3 Measurement of Metabolite Levels Using Liquid Chromatography-Coupled Mass Spectrometry (LC-MS/MS and LC-MS)

Metabolites were extracted from frozen left ventricle using a Bligh-Dyer method as described in **Chapter 2 (2.3.2)**. Levels of metabolites (Krebs cycle intermediates, amino acids and malonyl-CoA) were assessed using the C18pfp chromatography method coupled to the Thermo Quantiva, while levels of β-hydroxybutyrate and lactate were assessed using the C18pfp method coupled to the Thermo Elite, all as described in sections **2.3.3** and **2.3.4**.

Coronary effluent samples (20 µl plus 80 µl 10 mM ammonium acetate/internal standard mix) were also analysed for β-hydroxybutyrate using the c18pfp chromatography method coupled to the Thermo Elite.

5.2.4 Measurement of Cardiac Triolein Uptake Using LC-MS

For measurement of the rate of cardiac triolein consumption, buffer samples collected before and after the heart were extracted using the tissue extraction method described in **Chapter 2 (2.3.2)**. Metabolites were reconstituted in a small volume of methanol/chloroform (1:1) and then diluted into isopropyl alcohol/acetonitrile/water (2:1:1), with a dilution of 1 in 10.

Chromatography parameters

5 µL of sample was injected onto a C18 CSH column, 75 µM x 100 mm (Thermo Scientific), which was maintained at 55°C within an Ultimate 3000 UHPLC system (Thermo Scientific). The mobile phase comprised of solvents A (acetonitrile/water 60:40, plus 10 mM ammonium formate) and B (acetonitrile/isopropanol 10:90, plus 10 mM ammonium formate). Total run time was 20 minutes, with a flow rate of 0.400 µL/min. The initial proportion of solvent B in the run buffer was 40%, which was incrementally increased to 43% after 2 min, 50% at 2.1 min, 54% at 12 min, 70% at 12.1 min and 99% at 18 min, at which point it was returned to 40% for 2 min.

Mass spectrometry parameters

Mass spectrometry was then carried out using the Orbitrap Elite Mass Spectrometer (Thermo Scientific) in positive mode. Metabolites were ionised by heated electrospray before entering the spectrometer. The source temperature was set to 420 °C, and the capillary temperature to 380 °C. The full scan was performed across an m/z range of 110-2000.

Data processing using R

For processing, spectra were converted from Xcalibur .raw files into .mzML files using MS Convert (Proteowizard) for analysis by XCMS within R studio. XCMS software was used to process data and identify peaks. Peaks were annotated by accurate mass, using an automated R script and comparison to the LipidMaps database. Intensity was normalised to internal standards. Cardiac triolein uptake at each time point was calculated by subtracting the concentration of triolein in the coronary effluent from that in the reservoir.

5.2.5 Caspase-1 Activity Assay and ELISA for IL-1β

Preparation of Tissue Homogenates

Approximately 10 mg of frozen LV from each of the ischaemic hymeglusin-treated and control hearts was homogenised with an Eppendorf pestle in an Eppendorf tube containing 300 µl of ice cold homogenisation buffer 2 **(Appendix V)**. The samples were then centrifuged (380 × g, 30 s, 4°C) and supernatant was collected. This was then centrifuged for a second time (380 × g, 30 s, 4°C) and the supernatant collected to obtain a homogeneous suspension.

Protein Quantification

Protein concentration of chamber and tissue homogenates was measured using the Quick Start Bradford protein assay (Bio Rad) with a standard curve of a range of concentrations (8 standards from

0 to 2 mg ml^{-1} in triplicate) of bovine serum albumin (BSA). The assay works on the principle that Coomassie Blue is deprotonated in the presence of proteins, leading to a detectable colour change with maximal absorbance at 595 nm. A 5 µl volume of homogenates diluted 25 and 50 × in homogenisation buffer was added in triplicate to a 96-well microplate. Bradford reagent (200 µl) was added to all standards and samples and incubated at room temperature for 5 min. Absorbance at a wavelength of 595 nm was then quantified using a microplate reader (ELx800, BioTek). Sample protein concentrations were then calculated using the equation generated from the linear line of best fit through the readings from the standard curve.

Caspase-1 Activity Assay

Caspase-1 activity was quantified using a Caspase-1 Activity Assay kit (BioVision Incorporated, US). Briefly, 150µg of tissue lysate was resuspended in 50 µl cell lysis buffer and combined with 50 µl 2X reaction buffer (containing 10mM DTT) and 200 µM YVAD-pNA substrate before a 1.5hr incubation at 37°C. Absorbance at a wavelength of 405 nm was then quantified using a microplate reader (ELx800, BioTek).

ELISA for Il-1β

Il-1β concentration was determined using an ELISA kit (Cloud Clone Corp) according to the manufacturers' instructions.

5.2.6 Presentation and Statistics

Where relevant, results are presented as mean ± SEM and Student's T-test was employed to determine statistical significance of differences relative to levels of respiration or metabolites either pre-ischaemia or in the control group. Significance was denoted as * $p < 0.05$, ** $p < 0.01$, *** $p < 0.001$.

For levels of metabolites in the coronary effluent, significance relative to control is denoted on the graph at each time point where there is significance.

For cardiac function, T-test significance was calculated for the mean LVDP or RPP over a four minute period, and the four minute periods where a significant difference was detected were then denoted on the graph by

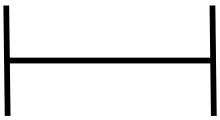

, and the level of significance

Key to Results

Pre-Ischaemic Group

Ischaemic Group

Reperfused Group

5.3 RESULTS

5.3.1 Contractile Function

Cardiac contractile function was fully recovered following reperfusion at 100 mmHg from the 20 min 0.56 ml.min^{-1}gww^{-1} ischaemic period **(Figure 5.3)**. Both LVDP and RPP re-attained pre-ischaemic levels of function following reperfusion, and maintained this for the full 20 min reperfusion time.

Table 5.1: Pre-Ischaemic Cardiac Function

LVDP (mmHg)	*Heart Rate (bpm)*	*RPP (mmHg.min)*
119 ± 7	300 ± 12	35500 ± 2500

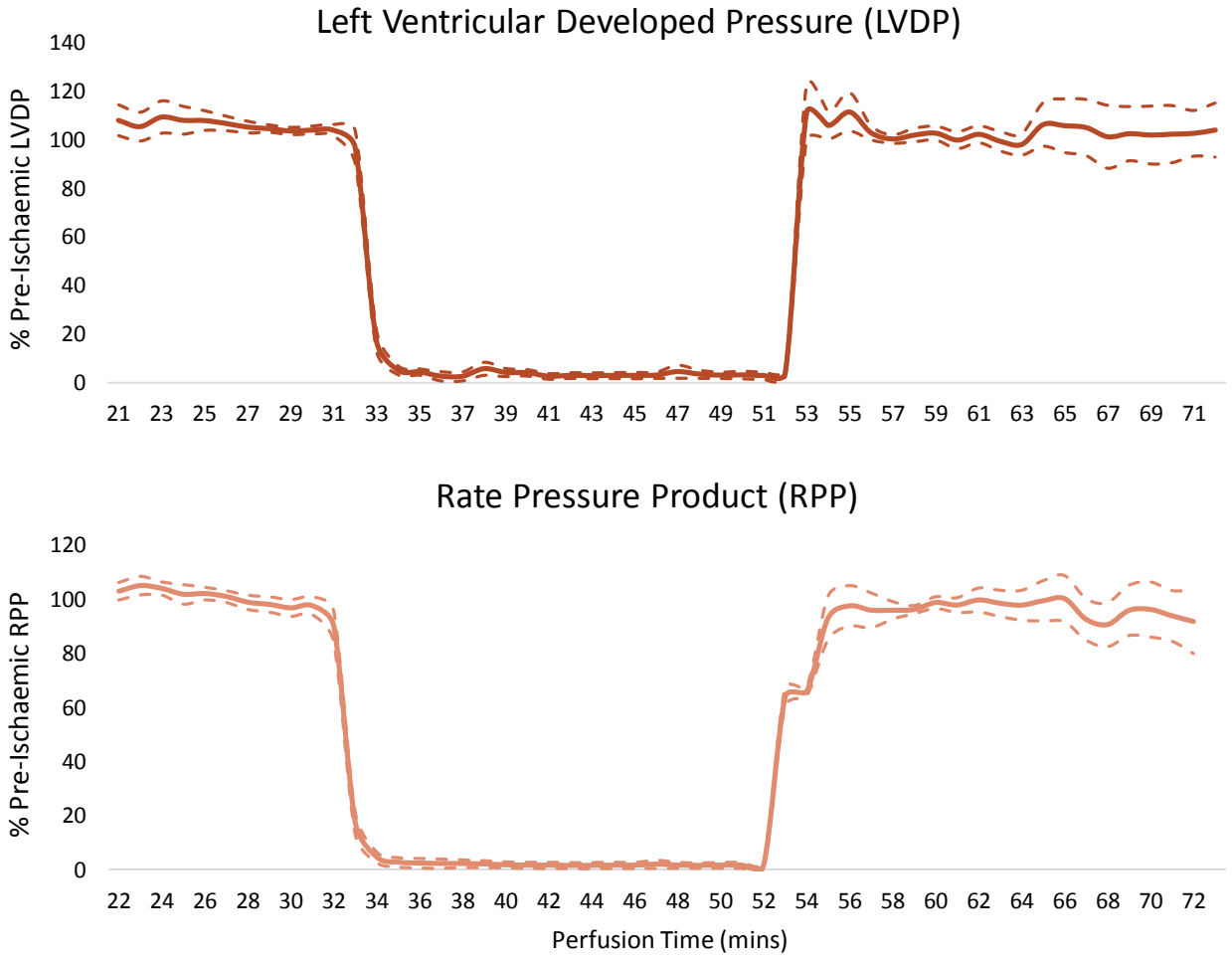

Figure 5.3: Cardiac Contractile Function. Left Ventricular Developed Pressure (LVDP) and Rate Pressure Product (RPP) in hearts subjected to a 20 min 0.56 ml.min^{-1}gww^{-1} ischaemic period then reperfused at 100 mmHg for 20 min following an initial 32 min pre-ischaemic perfusion period. Results displayed as mean ± SEM

5.3.2 Ketone Accumulation

The ketone body β-hydroxybutyrate accumulated in the ischaemic myocardium, despite being at a negligible concentration pre-ischaemia **(Figure 5.4A)**. Following 20 min reperfusion, levels dropped to just over the pre-ischaemic concentration, suggesting that the accumulated β-hydroxybutyrate was either metabolised or lost from the tissue following restoration of oxygen supply.

β-hydroxybutyrate was produced to such levels that it was also detectable in the coronary effluent **(Figure 5.4B)**. During the ischaemic period (32-52 min), the concentration of β-hydroxybutyrate in the coronary effluent was dramatically raised, and continued to increase as the ischaemic period progressed, before returning rapidly to pre-ischaemic levels post-reperfusion.

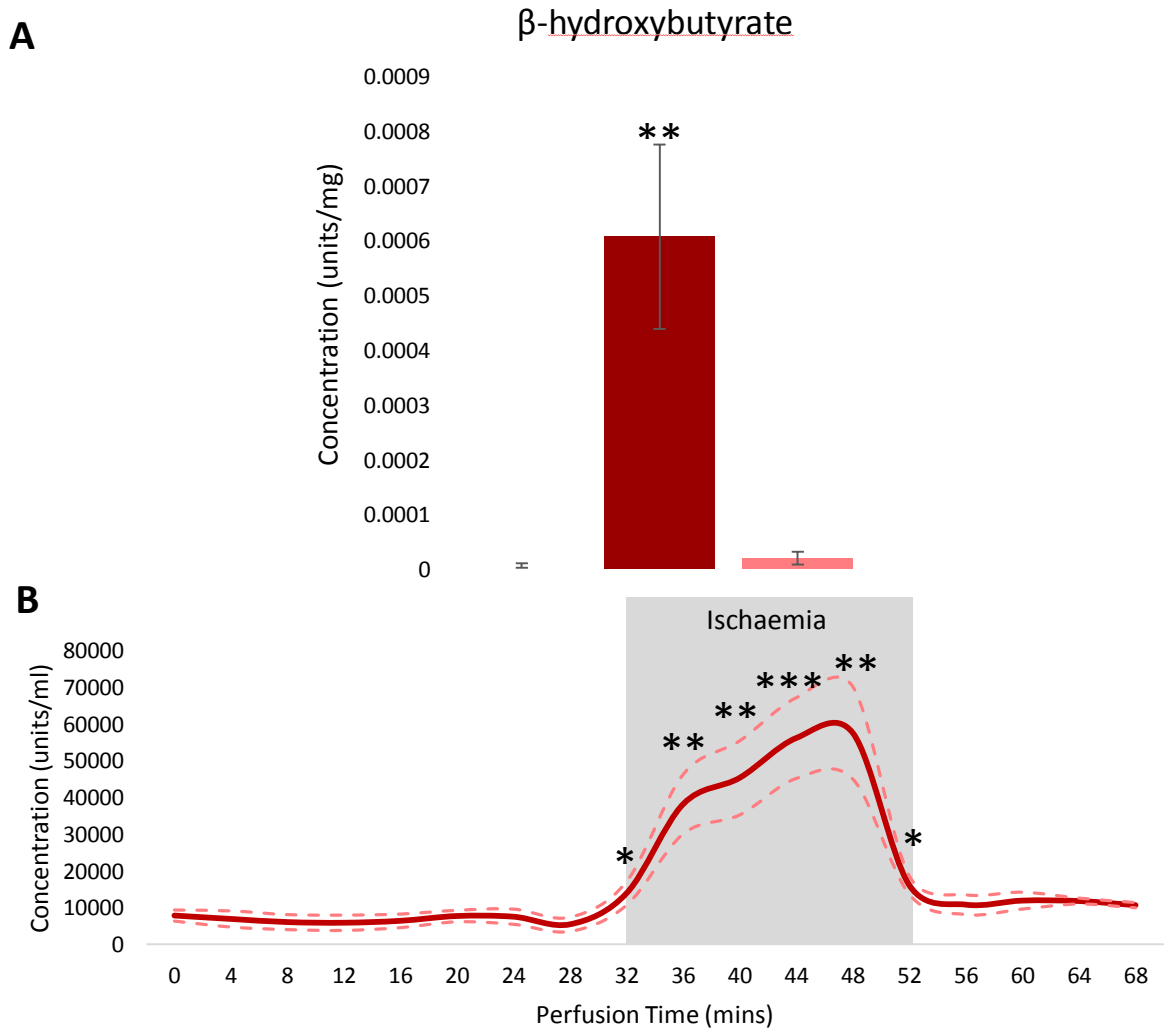

Figure 5.4: Concentrations of β-hydroxybutyrate in rat heart (A), and in the coronary effluent (B). All displayed as mean ± SEM. * = $p < 0.05$, **= $p < 0.01$ and *** $p < 0.001$ relative to pre-ischaemic levels.

5.3.3 Mitochondrial Function

To determine whether damage to the electron transport chain or a change in substrate oxidation preference during ischaemia may contribute to cardiac ketogenesis, high-resolution respirometry was employed **(Figure 5.5A)**.

Complex I supported respiration was broadly conserved across the 20 min period of 0.56 $ml.min^{-1}gww^{-1}$ ischaemia, with significant reduction of oxygen consumption visible only following a subsequent 20 min reperfusion at 100 mmHg.

Meanwhile, complex II supported respiration was significantly decreased ($p<0.01$) following the ischaemic period, with a further reduction in capacity following reperfusion ($p<0.001$).

The FAO ratio was 6% lower in the ischaemic group compared to control ($p<0.05$, **Figure 5.5 B**), while the RCR was not significantly different between the groups **(Figure 5.5 C)**

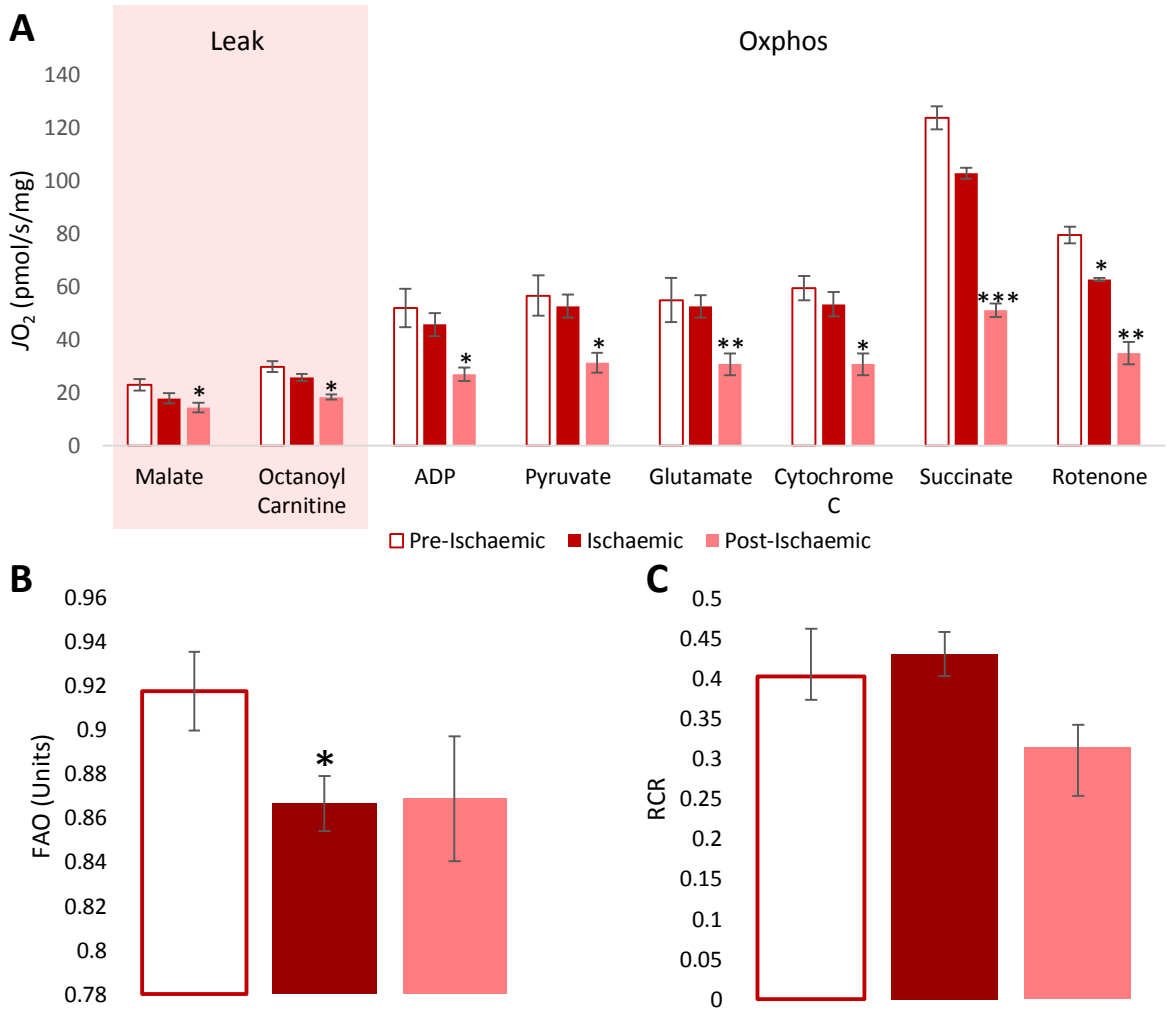

Figure 5.5: Respiration rates corrected for wet mass (A). Malate and octanoyl carnitine were added initially to stimulate leak respiration, ADP to stimulate β-oxidation supported Oxphos, glutamate to saturate complex I, cytochrome *c* as a test of membrane integrity, succinate to activate complex II, and rotenone to inhibit complex I. The ratio between octanoyl carnitine and octanoyl carnitine plus pyruvate-supported respiration (FAO) as a marker of preference for fatty acid oxidation (B); respiratory control ratio (RCR) (C). All displayed as mean ± SEM. * $p < 0.05$, ** $p < 0.01$, *** $p < 0.001$ relative to pre-ischaemic levels.

5.3.4 Cardiac and Mitochondrial Fat Uptake

In order to further investigate whether the lower FAO preference seen in the ischaemic and post-ischaemic groups was reflected by rates of cardiac triglyceride uptake, the rate of triglyceride uptake from the buffer and the tissue concentration of malonyl-CoA (which inhibits uptake of acyl-carnitines to the mitochondria) were measured, using LC-MS and LC-MS/MS respectively.

Cardiac uptake of triolein (the predominant component of intralipid) from the perfusion buffer was almost completely ablated during the ischaemic period **(Figure 5.6)**. Whilst it was partially restored following reperfusion, triolein uptake reached only 28.7% of its pre-ischaemic rates.

Myocardial malonyl-CoA concentrations were 2.3-fold higher in the ischaemic heart relative to pre-ischaemia ($p<0.01$, **Figure 5.7**). This may limit mitochondrial acyl-carnitine uptake and therefore β-oxidation, and is in contrast to previous suggestions of a drop in levels, which are thought to underpin increased fat oxidation in ischaemia.

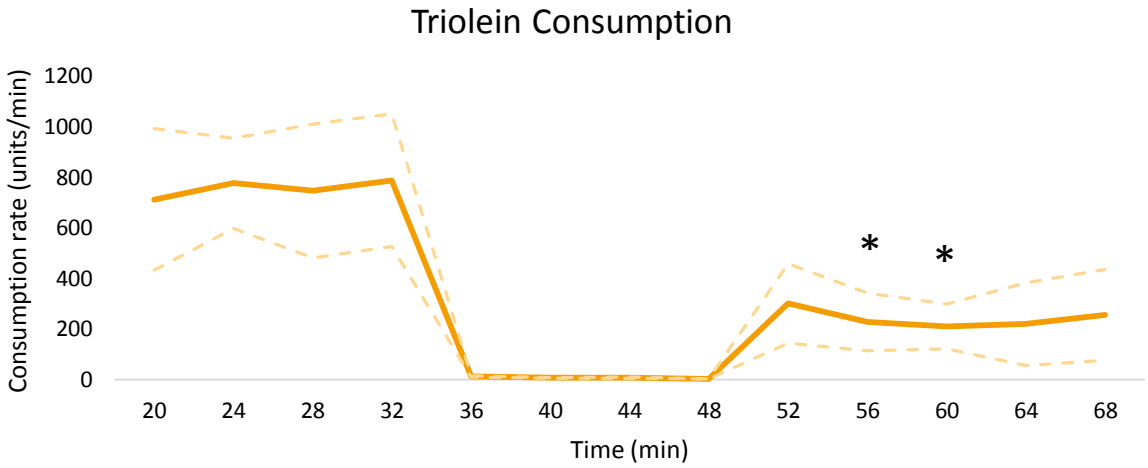

Figure 5.6: Rate of cardiac triglyceride consumption, mean ± SEM. * $p < 0.05$ relative to pre-ischaemia.

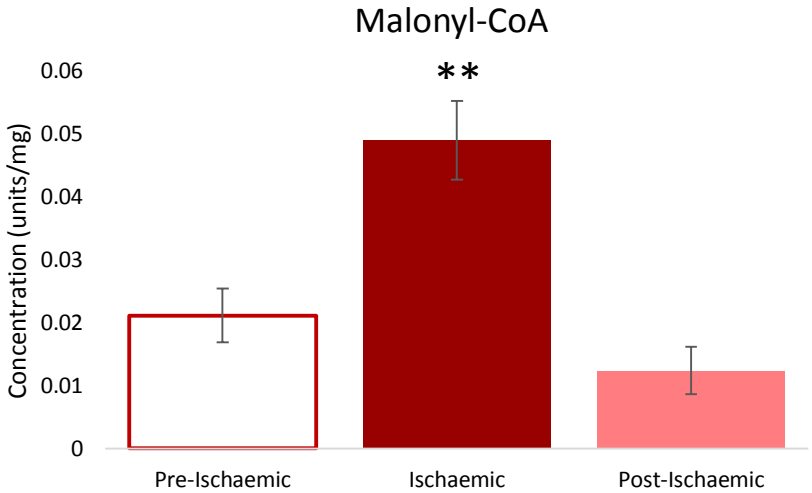

Figure 5.7: Concentration of malonyl-CoA in heart tissue displayed as mean ± SEM. ** $p < 0.01$ relative to pre-ischaemic levels.

5.3.5 The Krebs Cycle in the Ischaemic Heart

Ketogenesis has been linked to the presence of key Krebs cycle intermediates, including succinate. To investigate whether this might correspond to a mechanism for ketogenesis, cardiac concentrations of Krebs cycle intermediates were measured **(Figure 5.8)**, as well as their isotopic distributions to determine whether the proportion of triglyceride or glucose oxidation increased during ischaemia.

Levels of early-cycle Krebs cycle intermediates (citrate and isocitrate) were depleted relative to pre-ischaemia at the end of the ischaemic period (both $p<0.05$).

In contrast, concentrations of malate were 1.4-fold higher than their pre-ischaemic concentration ($p<0.05$), and those of succinate increased 4.5 fold ($p<0.001$). Upon reperfusion, concentrations of all Krebs cycle intermediates were found to have returned towards pre-ischaemic levels.

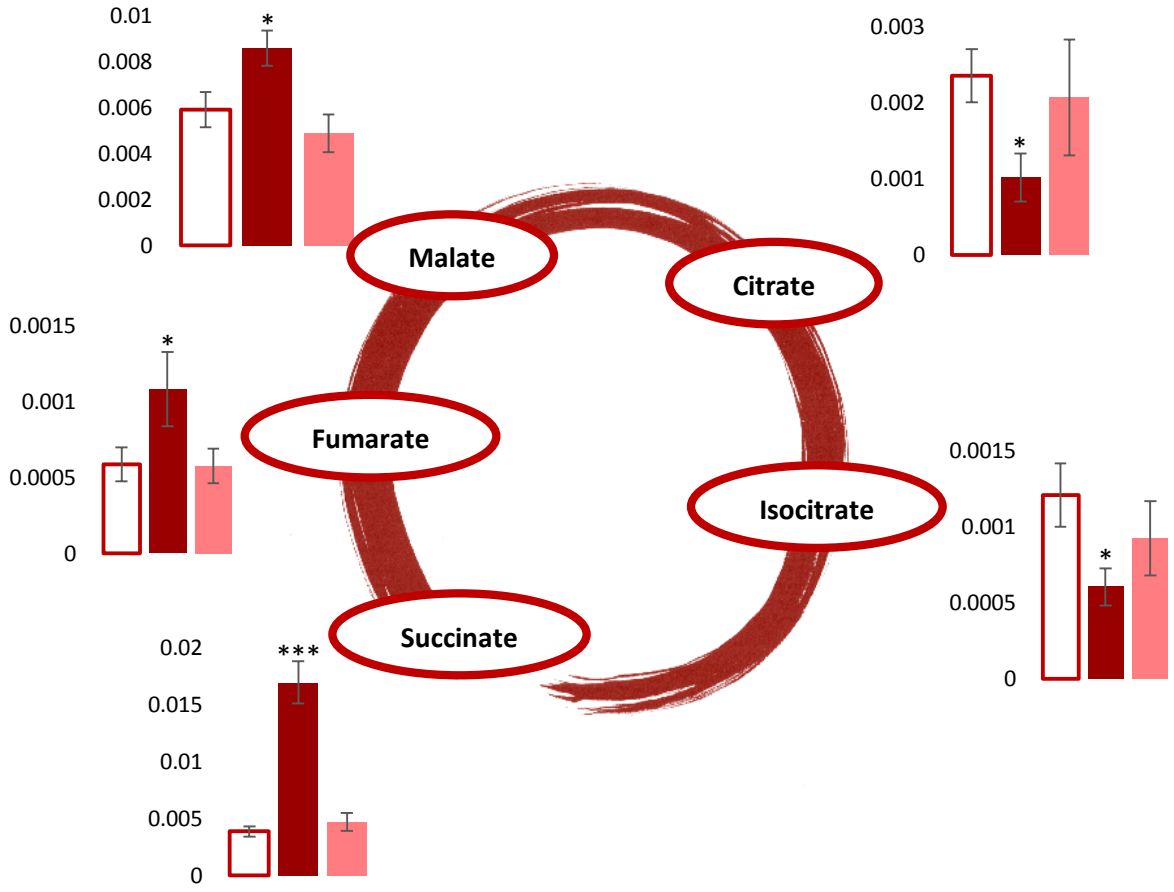

Figure 5.8: Concentrations of Krebs cycle intermediates (units, corrected for tissue mass) displayed as mean ± SEM. * $p < 0.05$, ** $p < 0.01$, *** $p < 0.001$ relative to pre-ischaemic levels.

5.3.6 Krebs Cycle Intermediate Isotopologue Distributions

The isotopic distributions of the Krebs cycle intermediates when 25% of the glucose supplied in the perfusion buffer was $U^{13}C$ labelled did not change between the pre-ischaemic, ischaemic and post-ischaemic myocardium. The implication of this is that the proportion of oxidised acetyl-CoA stemming from FAO, relative to glucose oxidation, did not increase in ischaemia **(Figure 5.9)**.

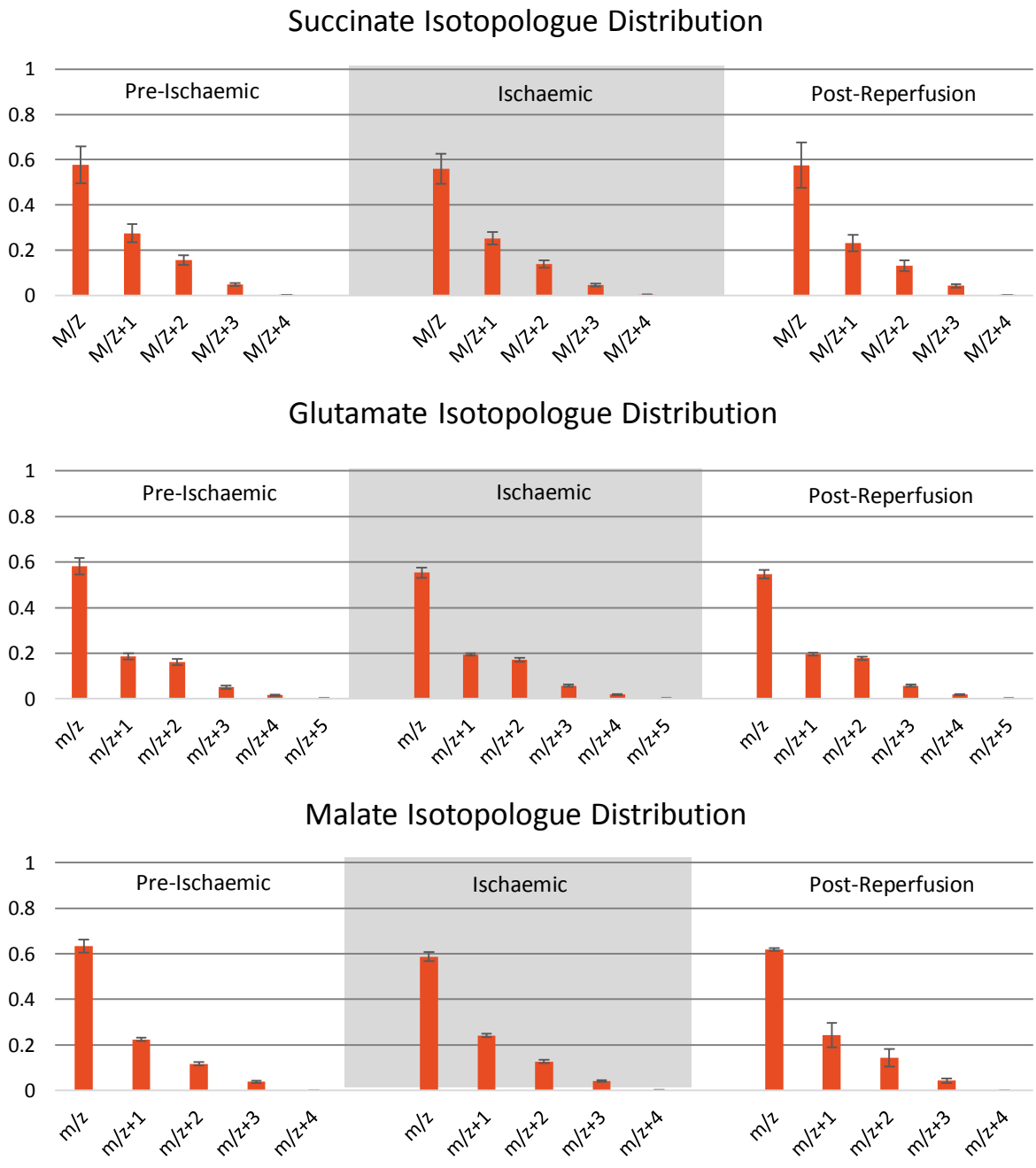

Figure 5.9: Isotopologue distributions of Succinate, Glutamate and Malate in pre-ischaemic, ischaemic and post-ischaemic hearts. Displayed as mean ± SEM.

5.3.7 α Values Before, During and After Ischaemia

Values for α, the proportion of acetyl-CoA entering the Krebs cycle, were calculated from the isotopologue distributions of Succinate, Glutamate and Malate (**Figure 5.9)** by use of the model outlined in **Chapter 3 (Table 5.2)**. These values further support the conclusion that there was no change in the percentage contribution of glucose to the acetyl-CoA oxidised during ischaemia relative to pre-ischaemic or post-ischaemic conditions.

Table 5.2: *α values Calculated for the Pre-Ischaemic, Ischaemic and Post-Ischaemic Myocardium*

	Pre-Ischaemic	***Ischaemic***	***Post-Ischaemic***
α	*0.145±0.009*	*0.142±0.005*	*0.143±0.008*

5.3.8 Labelling of β-hydroxybutyrate

When 25% of the glucose delivered in the perfusion buffer was $U^{13}C$ labelled, ~28% of the total β-hydroxybutyrate concentration in the ischaemic heart tissue was $U^{13}C$ labelled **(Figure 5.10)**. This meant 13.8% of the acetyl-CoA monomers incorporated into β-hydroxybutyrate were amu 2+ labelled with ^{13}C **(Figure 5.11)**, a value which closely corresponds to the value for α of 0.145±0.009 obtained from the Krebs cycle intermediate labelling data. This suggests that there is no greater contribution from either glycolysis or FAO towards ketogenesis, but rather that the process incorporates acetyl-CoA from either source indiscriminately under these conditions.

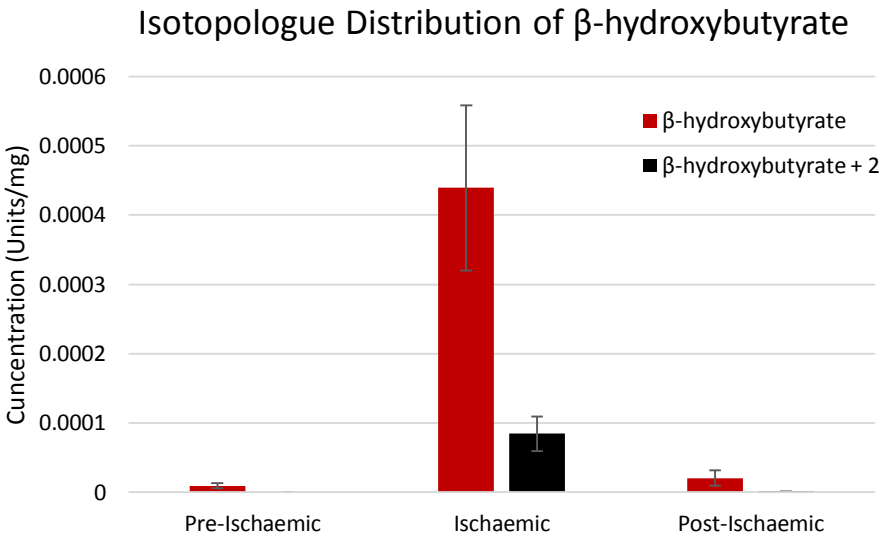

Figure 5.10: Isotopologue distribution of β-hydroxybutyrate in pre-ischaemic, ischaemic and post-ischaemic hearts. Displayed as mean ± SEM.

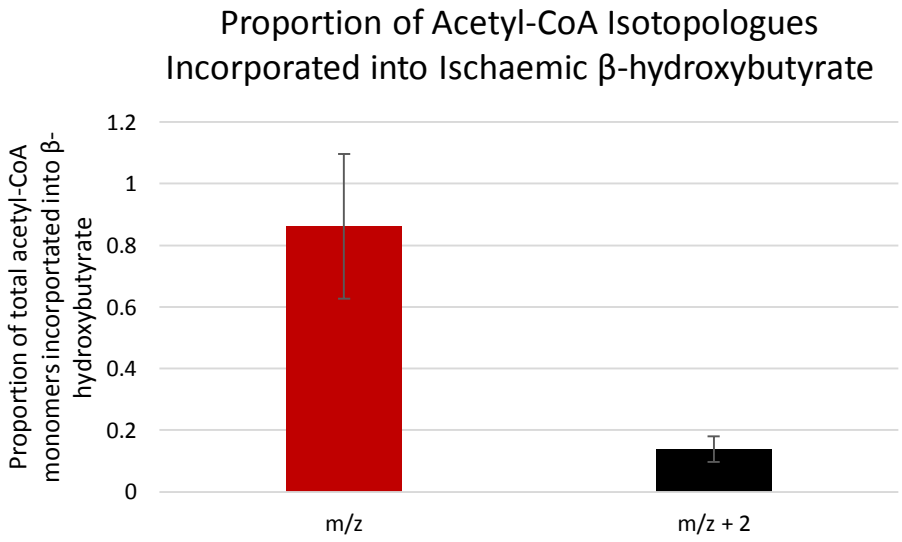

Figure 5.11: Proportional incorporation of unlabelled and m/z+2 isotopologues of acetyl-CoA into β-hydroxybutyrate during ischaemia. Displayed as mean ± SEM.

BOX A

Alanine -> Aspartate -> Succinate?

Previous studies have suggested a shuttle between aspartate and succinate as a source of the succinate accumulation during ischaemia, bypassing the early part of the Krebs cycle (Chouchani et al., 2014; Drake et al., 2013). Alanine, which may be converted to aspartate, is elevated in the ischaemic heart, and offers a possible source of carbon flux to the Krebs cycle through aspartate (Sookoian and Pirola, 2012). However, the isotopic distribution of aspartate did not vary in ischaemia **(Figure 5.12)**. Nor did it align with that of alanine, which is a glycolytic product of pyruvate and therefore ~75% unlabelled, 25% $U^{13}C$ labelled in line with the glucose intake. Aspartate displayed a higher concentration of 1+ labelling, a distribution which also did not match that of succinate **(Figure 5.9)**, suggesting a limited role for both alanine -> aspartate and aspartate -> succinate fluxes in either the aerobic or ischaemic heart.

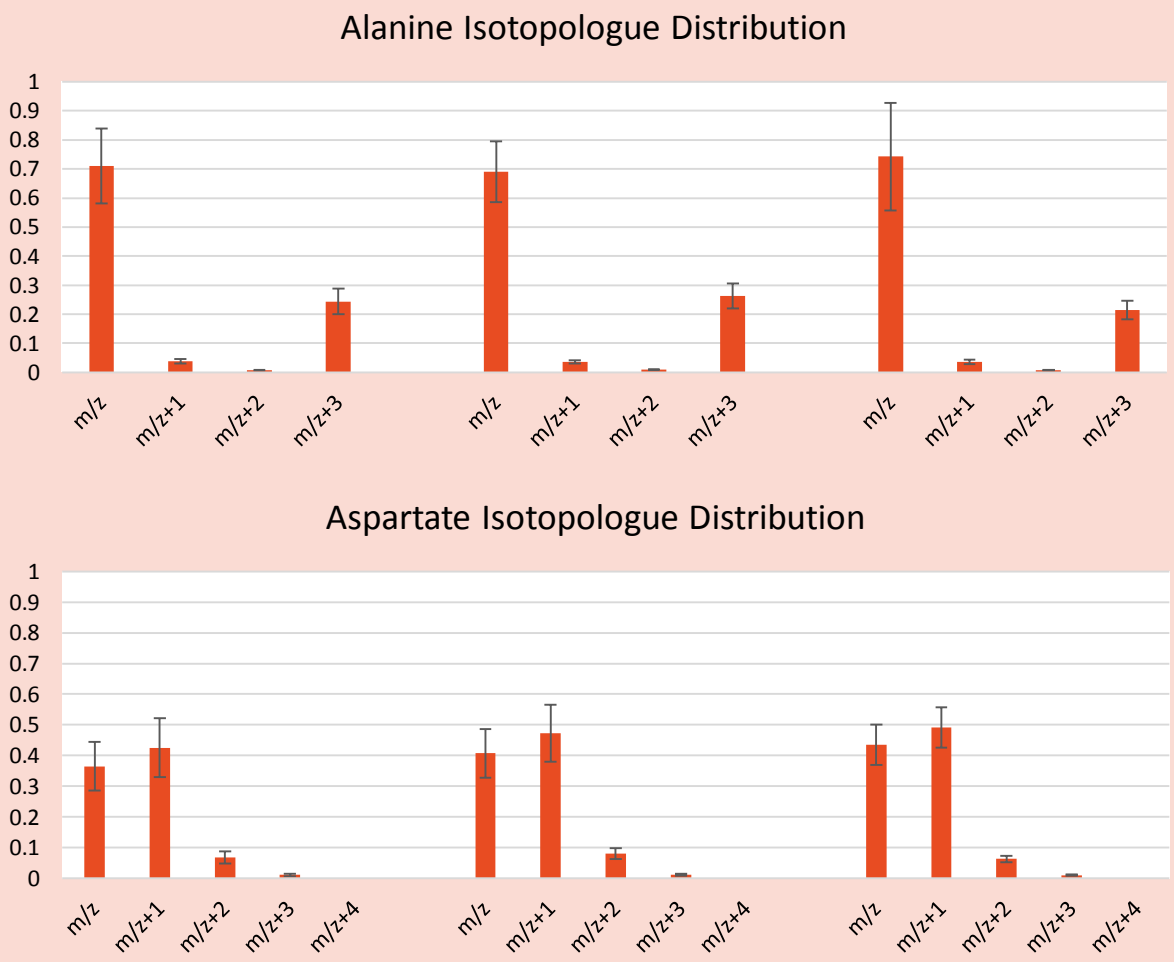

Figure 5.12: Isotopologue distributions of Alanine and Aspartate in pre-ischaemic, ischaemic and post-ischaemic hearts. Displayed as mean ± SEM.

5.3.9 NAD/NADH Levels Influence Rate of Ketogenesis

Nicotinamide mononucleotide (NMN), an NAD+ precursor shown to boost levels of available NAD in the heart, was added to the perfusion buffer 32 min prior to onset of ischaemia. In frozen LV tissue, analysed for β-hydroxybutyrate at the end of the ischaemic period using LC-MS, levels were 37% higher than in control hearts (**Figure 5.13;** p<0.01). This suggests that ketogenesis could be driven by the reductive environment during ischaemia, with greater levels of NAD+ resulting in greater accumulation of NADH in ischaemia and greater reduction of acetoacetate to β-hydroxybutyrate; however, the ratio of NADH/NAD+ in the ischaemic heart was not found to be different between groups.

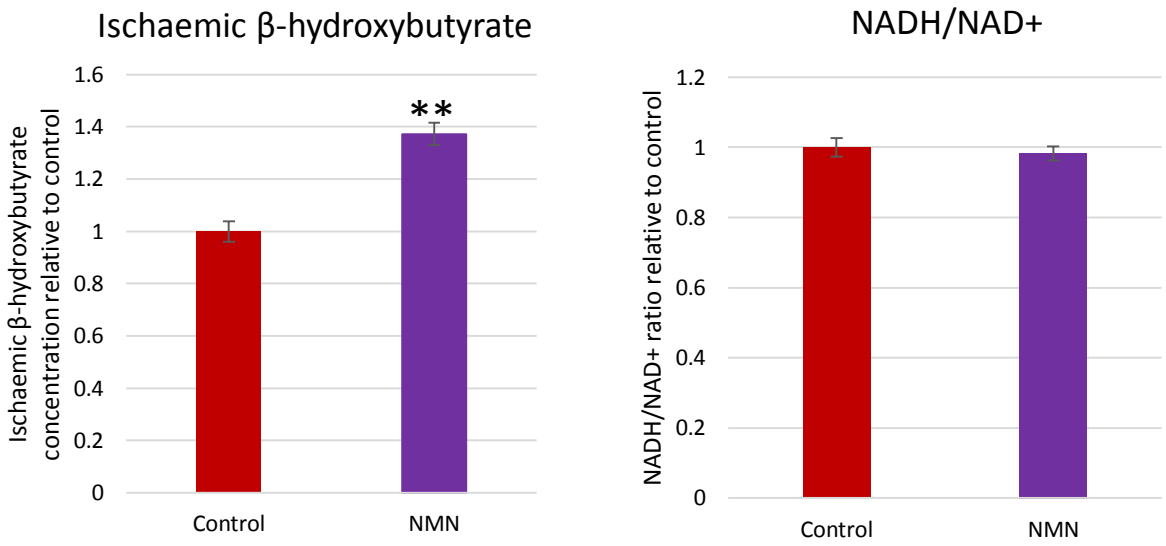

Figure 5.13: Concentration of β-hydroxybutyrate and the ratio of NADH/NAD+ in ischaemic heart tissue perfused with and without 200 µM nicotinamide mononucleotide (NMN) relative to control, displayed as mean ± SEM. ** $p < 0.01$ relative to control.

5.3.10 LDH Inhibition

Inhibition of LDH Boosts Ketogenesis

Administration of 50 mM sodium oxamate via the perfusion buffer 12 min before the onset of ischaemia led to 5.3-fold greater accumulation of β-hydroxybutyrate following the ischaemic period **(Figure 5.14)**. Sodium oxamate is a competitive LDH inhibitor which prevents the diversion of pyruvate to lactate, allowing more to be converted to acetyl-CoA. This finding suggests that ischaemic ketogenesis proceeds at a rate proportional to the available concentration of acetyl-CoA.

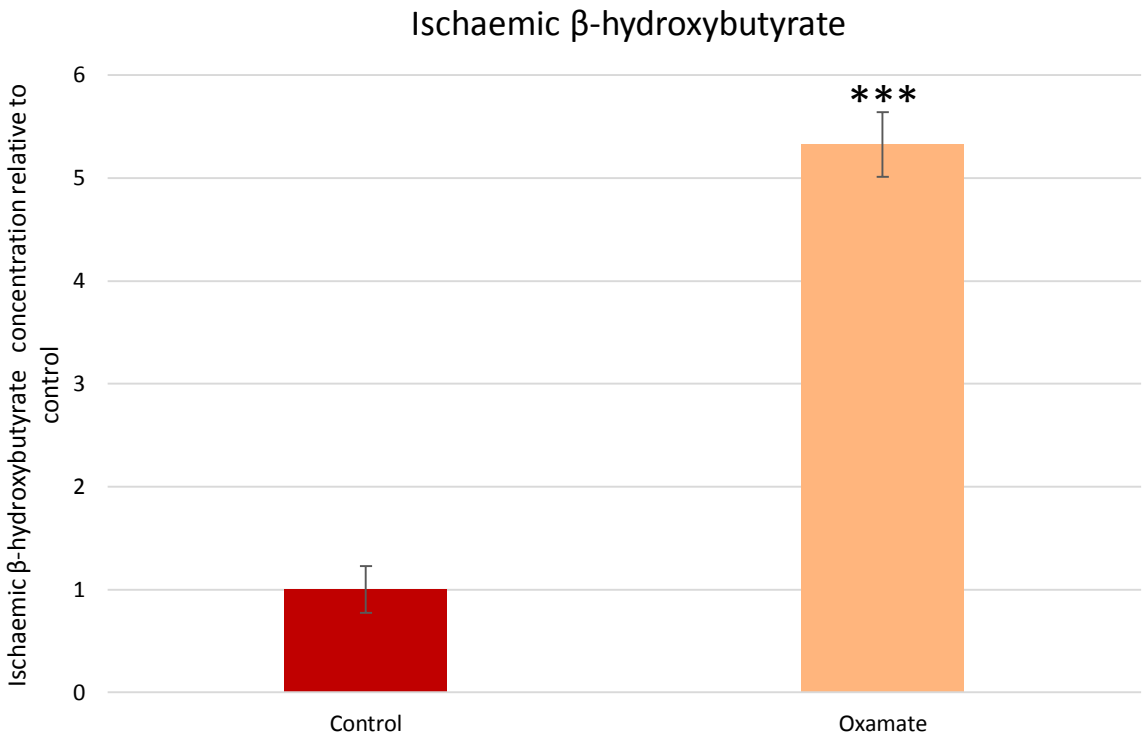

Figure 5.14: Concentration of β-hydroxybutyrate in ischaemic heart tissue perfused with and without 50 mM Sodium Oxamate relative to control, displayed as mean ± SEM. *** $p < 0.001$ relative to control.

LDH Inhibition Influenced Ischaemic Secretion of Lactate and β-hydroxybutyrate

During the ischaemic period, hearts given sodium oxamate secreted less lactate into the coronary effluent than control hearts **(Figure 5.15)**. Peak secretion of lactate reached only 60% of the levels released by the control group ($p<0.01$), and this rate was not maintained.

Meanwhile, β-hydroxybutyrate secretion was initially 3.3-fold higher in the oxamate treated group (**Figure 5.16,** $p<0.01$). This rate of release then dropped away rapidly, while the rate of control group β-hydroxybutyrate release was maintained throughout the ischaemic period.

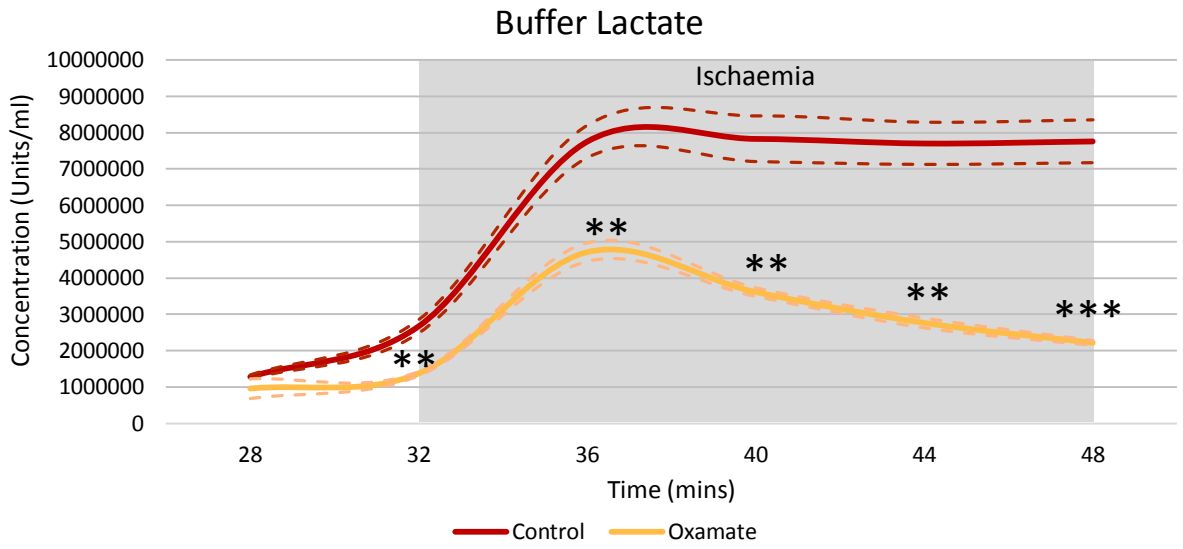

Figure 5.15: Concentrations of lactate in the coronary effluent during the ischaemic period. Displayed as mean ± SEM. ** $p < 0.01$, *** $p < 0.001$ relative to control.

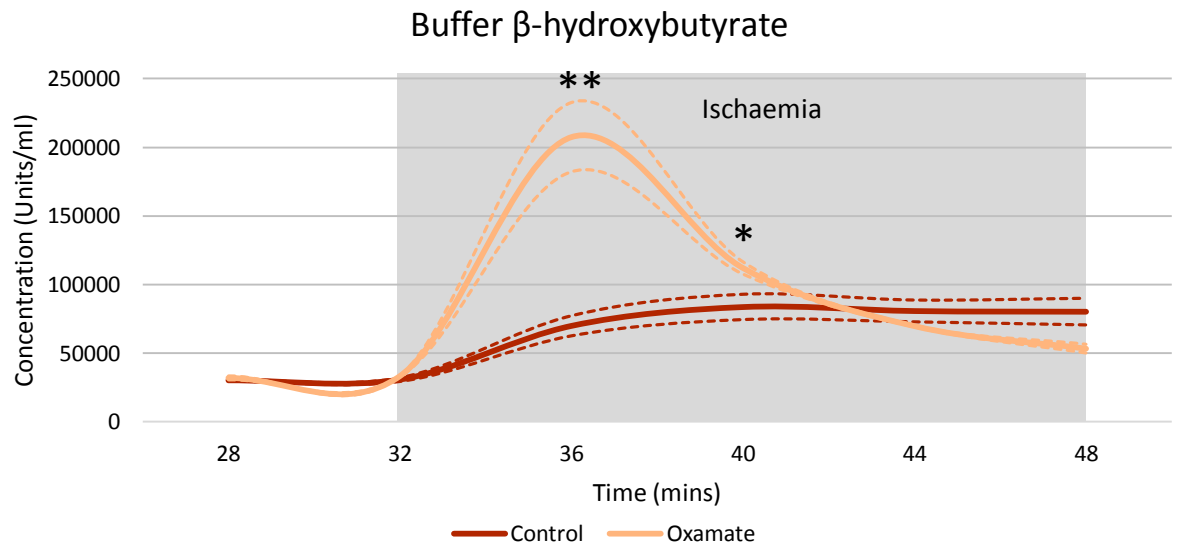

Figure 5.16: Concentrations of β-hydroxybutyrate in the coronary effluent during the ischaemic period. Displayed as mean ± SEM. * $p < 0.05$, ** $p < 0.01$ relative to control.

LDH Inhibition Impaired Cardiac Function

Following addition of sodium oxamate (50mM) to the perfusion buffer at 20 min, cardiac LVDP and RPP were decreased while heart rate remained steady **(Figure 5.17)** .

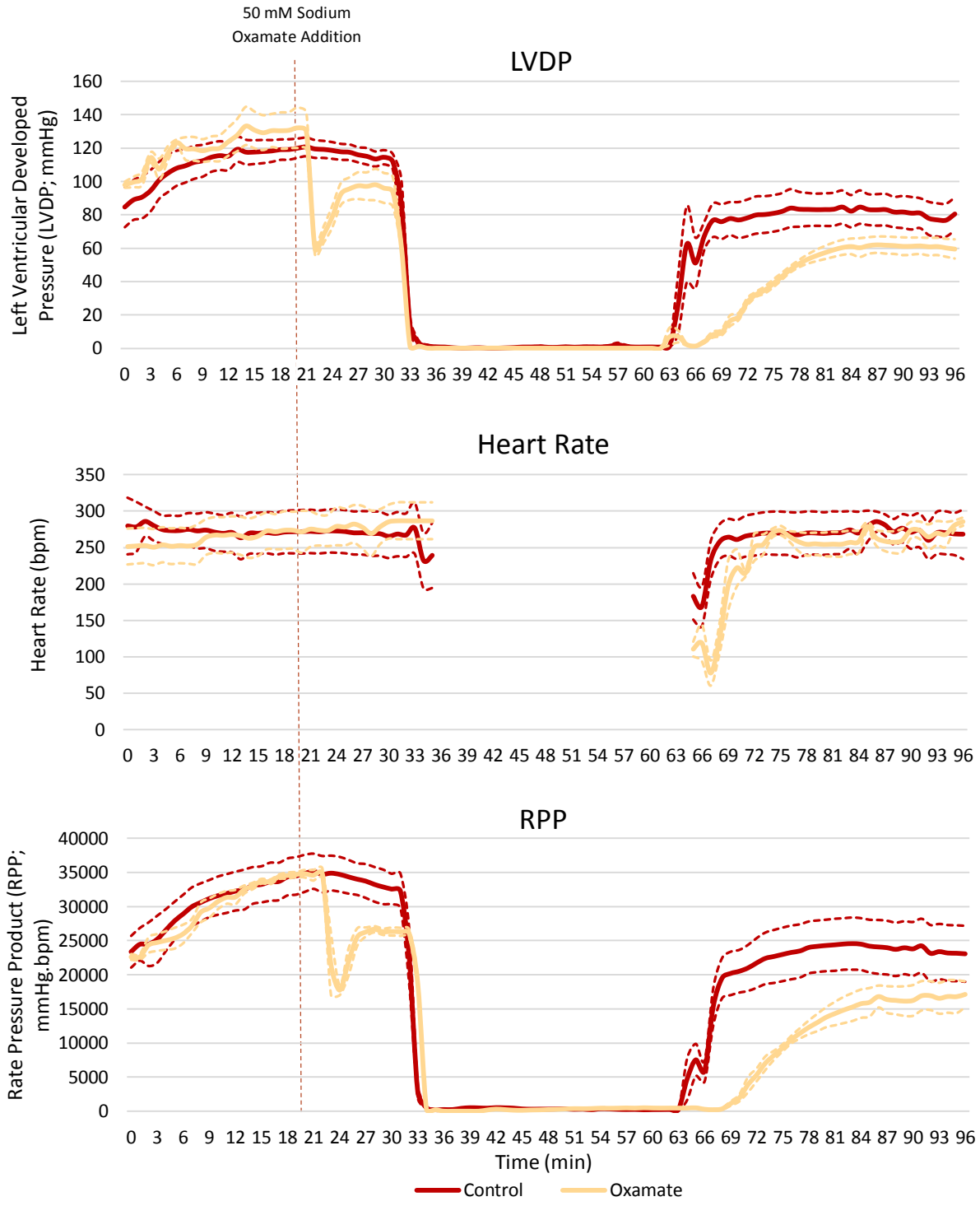

Figure 5.17: Cardiac Contractile Function. Left Ventricular Developed Pressure (LVDP), Heart Rate and Rate Pressure Product (RPP) in hearts subjected to a 32 min 0.3 ml.min^{-1}gww^{-1} ischaemic period before reperfusion at 100 mmHg for 32 min, following an initial 32 min pre-ischaemic perfusion period. Sodium oxamate (50mM) was added to the perfusion buffer at 20 min in the oxamate group. Results displayed as mean ± SEM

Impact of LDH Inhibition on Functional Recovery

Following 32 min reperfusion, control hearts and those given 50 mM sodium oxamate recovered the same percentage of their pre-ischaemic LVDP and RPP (both p>0.05, **Figure 5.18**). However, to recover to the LVDP and RPP they displayed at 32 min reperfusion, the sodium oxamate hearts took 13 and 14 minutes longer than controls (p<0.001 and p<0.01 respectively).

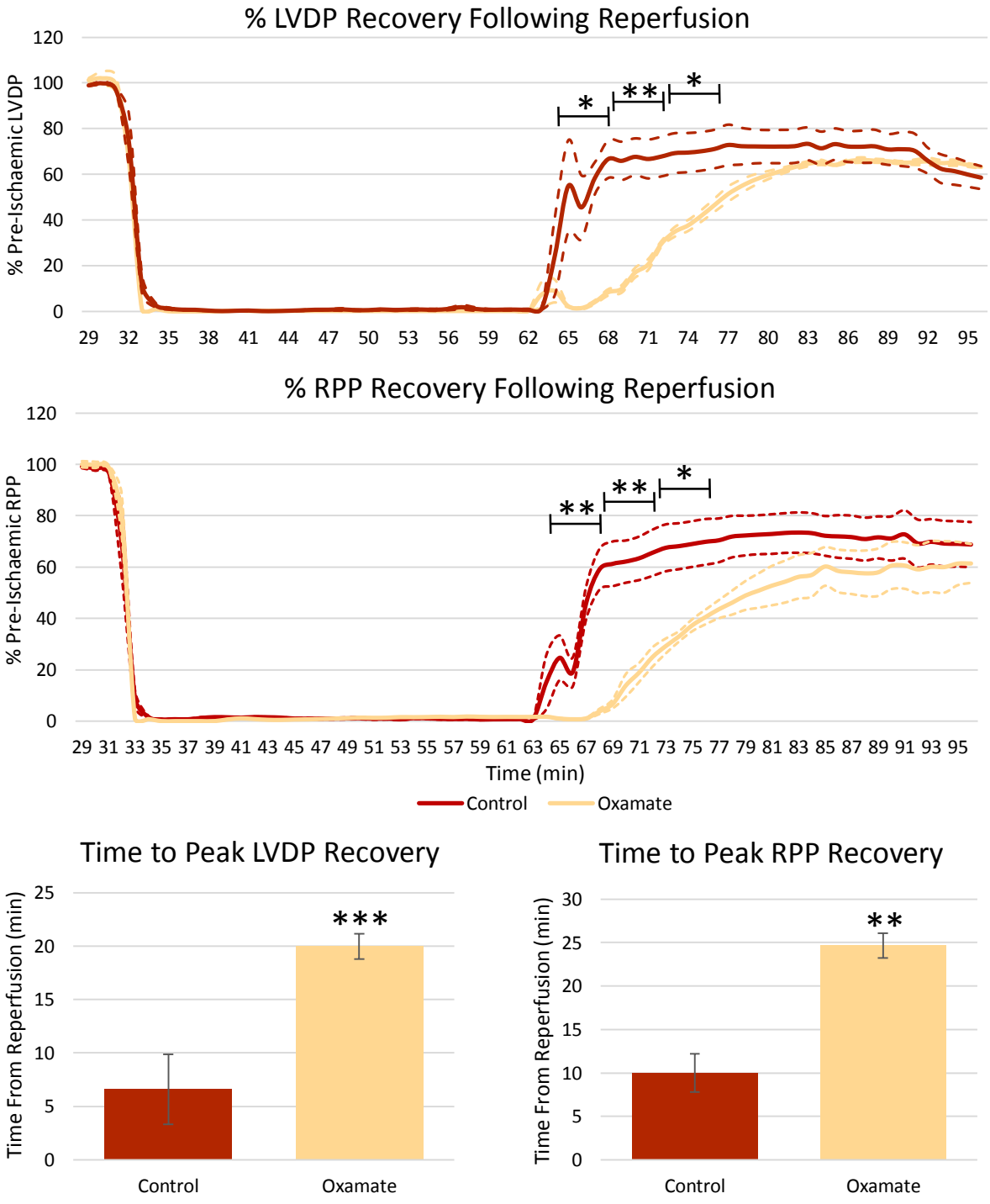

Figure 5.18: Left-ventricular developed pressure and rate pressure product as a percentage of pre-ischaemic levels following 32 min 0.3 ml.min^{-1}gww^{-1} low flow ischaemia, and the time taken to attain final recovery. All presented as mean ± SEM. * p < 0.05, ** p < 0.01, *** *p* < 0.001 relative to control.

LDH Inhibition Increased Contracture of the Heart During Ischaemia

During an ischaemic period, hearts undergo contracture due to the loss of ion homeostasis. After being in ischaemia for 8 min, hearts given sodium oxamate underwent a sudden contraction with a force of 76 mmHg, which control hearts did not ($p<0.0001$). The contracture of the sodium oxamate hearts remained greater at the end of the ischaemic period ($p<0.001$), a fact which may go some way towards explaining the longer time they took to recover contractile function following reperfusion.

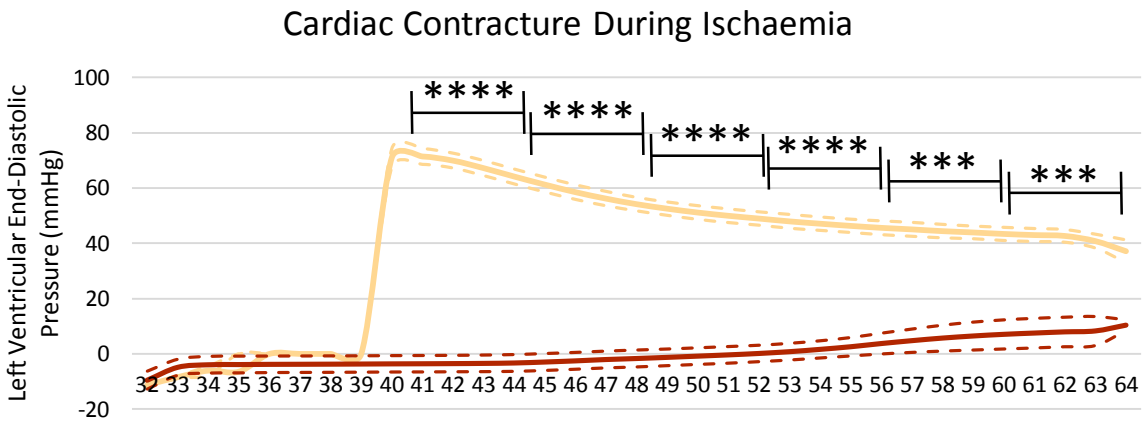

Figure 5.19: Left-ventricular end-diastolic pressure during 32 min of 0.3 ml.min^{-1}gww^{-1} low flow ischaemia, presented as mean ± SEM. *** $p < 0.001$, **** $p < 0.0001$ relative to control.

5.3.11 Inhibition of HMG-CoA Synthase with Hymeglusin

Ketone Accumulation

At the end of a 32 minute period of 0.3 ml.min^{-1}gww^{-1} low flow ischaemia, the accumulated concentration of β-hydroxybutyrate was 32% lower when 80 µg.L^{-1} of the HMG-CoA Synthase inhibitor hymeglusin was added to the perfusion buffer 10 min before the onset of ischaemia ($p<0.05$, **Figure 5.20**). This verified A) that some, though not all, ischaemic ketogenesis was due to flux through HMG-CoA synthase, and B) that 80 µg.L^{-1} hymeglusin in the perfusion buffer was sufficient to achieve at least partial inhibition of the ketogenic pathway.

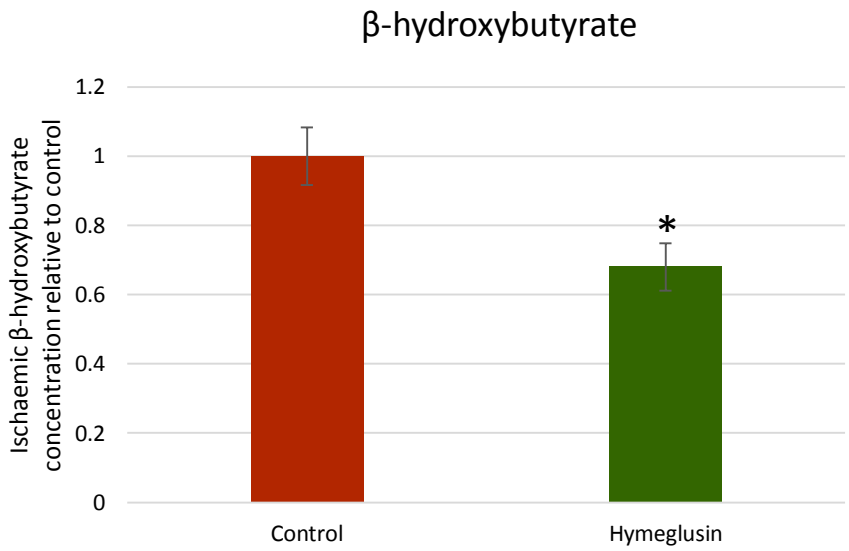

Figure 5.20: Concentration of β-hydroxybutyrate in ischaemic heart tissue perfused with and without hymeglusin, relative to control. Displayed as mean ± SEM. * $p < 0.05$ relative to control.

Functional Recovery

Inhibition of HMG-CoA Synthase with hymeglusin resulted in a 23% greater recovery of left ventricular developed pressure following 32 min reperfusion at 100 mmHg from 32 min 0.3 ml.min^{-1}gww^{-1} ischaemia **(Figure 5.21**, $p<0.05$**)**. Recovery of rate pressure product was also 34% greater in the hearts administered hymeglusin ($p<0.05$). Hymeglusin administration had no effect upon pre-ischaemic LVDP, heart rate or RPP **(Table 5.3)**.

Table 5.3: *Pre-Ischaemic LVDP, Heart Rate and RPP*

	LVDP (mmHg)	***Heart Rate (bpm)***	***RPP (mmHg.bpm)***
Control	120.2 ± 14.1	305 ± 15	36900 ± 4800
Hymeglusin	107.3 ± 7.5	284.9 ± 9.2	29700 ± 3300

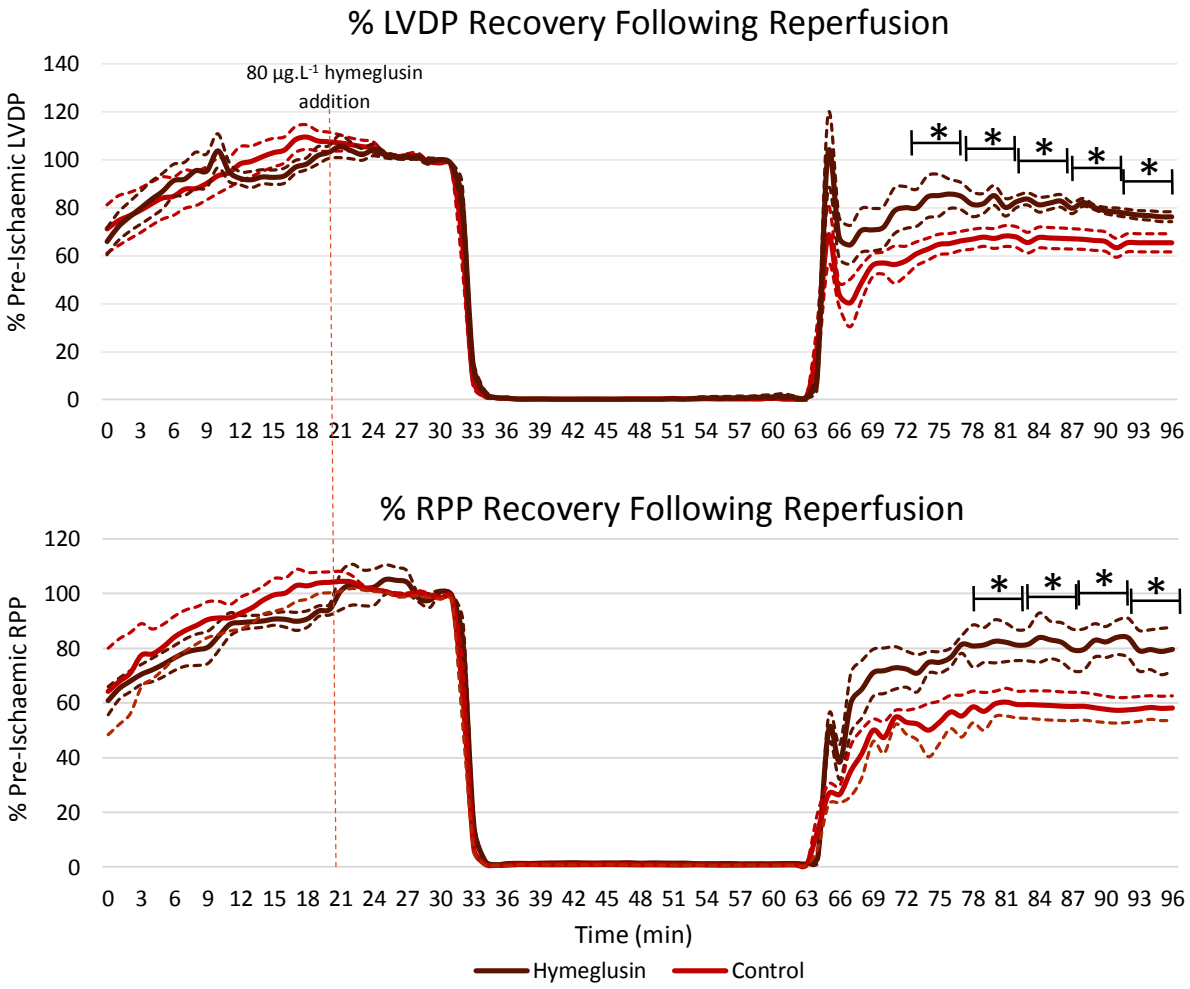

Figure 5.21: Left-ventricular developed pressure as a percentage of pre-ischaemic levels following 32 min 0.3 ml.min^{-1}gww^{-1} low flow ischaemia, presented as mean ± SEM. * $p < 0.05$ relative to control.

The Ischaemic Inflammasome

β-hydroxybutyrate has been demonstrated to inhibit the formation of the inflammasome, a process which occurs in the ischaemic heart (Yamanashi et al., 2017; Youm et al., 2015) and has previously been reported to be cardioprotective (Sandanger et al., 2016). To determine whether this might be a mechanism for the influence of β-hydroxybutyrate upon cardiac recovery from ischaemia/reperfusion, the activation of Caspase-1, the end effector of the inflammasome, and the concentration of its substrate, IL-1β, were assayed **(Figure 5.22)**. Caspase-1 activity was 1.85 fold higher in the hymeglusin treated ischaemic heart relative to control ($p<0.05$), suggesting that β-hydroxybutyrate does indeed inhibit the inflammasome. Meanwhile, concentrations of IL-1β were reduced by around 77% ($p<0.05$), probably due to increased cleavage by caspase-1.

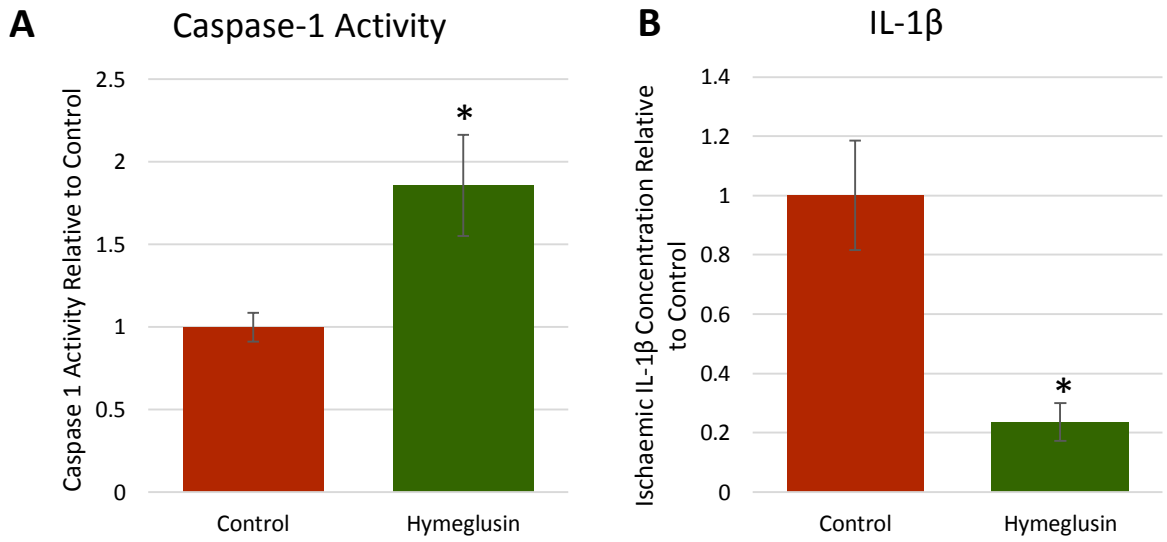

Figure 5.22: (A) Activity of Caspase-1 and (B) Concentration of IL-1β in ischaemic heart tissue perfused with and without hymeglusin, relative to control. Displayed as mean ± SEM. * $p < 0.05$ relative to control.

5.4 DISCUSSION

In the rat heart, the ketone body β-hydroxybutyrate accumulates during ischaemia in a process which is not specifically linked to FAO. The ischaemic accumulation of β-hydroxybutyrate can be increased through inhibition of LDH by sodium oxamate addition, in association with delayed recovery of contractile function following reperfusion. Meanwhile, inhibition of HMG-CoA synthase resulted in lower ischaemic accumulation of β-hydroxybutyrate, and greater functional recovery following reperfusion, suggesting that cardiac ketogenesis could be a detrimental process during ischaemia.

5.4.1 Strengths and Limitations of the Study

Use of Langendorff perfusion was a strength of this study which enabled establishment of reproducible intensities of ischaemia in which cardiac supply of metabolic substrates could be carefully controlled. This was a big advantage in comparison to *in vivo* studies in which the degree of ischaemia is more variable or β-hydroxybutyrate produced and consumed by other tissues would have complicated the picture. For example, Bedi *et al.*, (2016), and Aubert *et al.*, (2016) have both documented increased BDH1 & 2 expression and β-hydroxybutyrate levels in failing human hearts and those of mice with transverse aortic constriction (TAC). However, since these studies were conducted in whole organisms the source of the β-hydroxybutyrate was not clear, and it was assumed to be coming from the liver since ketogenesis has only previously been documented in the heart following pharmacological inhibition of complex I with amytal. Knowing now that ketogenesis can occur in the heart, their papers do not exclude the possibility that it may have been cardiac ketogenesis, rather than ketolysis, which was occurring. The experiments presented in this chapter have the advantage that, with no β-hydroxybutyrate being delivered to the hearts in the perfusion buffer, it can clearly be seen that ketogenesis is occurring in the heart.

It would have been more ideal to be able to investigate the functional implications of ischaemic ketogenesis with the use of a more established and better characterised pharmacological agent. However, there are no such commercially available compounds with a direct action, and so the more experimental compound hymeglusin was employed. Hymeglusin has been developed and used in the inhibition of cholesterol synthesis (Le Foll et al., 2014; Greenspan et al., 1987), which shares a common enzyme (HMG-CoA synthase) with the ketogenesis pathway, and so was identified as a potential inhibitor to investigate ischaemic ketogenesis. Its use here, in concentrations calculated to approximate or exceed that which prevented cholesterol synthesis in the aforementioned studies, has achieved only partial inhibition of the ketogenesis which occurs during ischaemia. Nonetheless, it has succeeded in lowering the amount of β-hydroxybutyrate synthesised during ischaemia, and this was

enough to see a functional effect upon cardiac recovery. This has been a success in that it has suggested that ketogenesis is a detrimental process during cardiac ischaemia, which is potentially surprising due to the well documented oxygen-efficient properties of β-hydroxybutyrate as a cardiac substrate (Sato et al., 1995; Veech et al., 2001), but perhaps less so when considering that it can form poly- β-hydroxybutyrate, which can permeabilise membranes and stabilise the opening of the mtPTP (Dedkova and Blatter, 2014; Newman et al., 2015). Unanswered questions are still present due to hymeglusin not achieving full inhibition of ketogenesis however: how much of the β-hydroxybutyrate synthesis which still occurs stems from flux through HMG-CoA synthase, and might some of it stem from other routes such as reverse flux through SCOT? Would total ablation of ischaemic ketogenesis have an enhanced protective effect or might some level of ketogenesis be beneficial? It would be good to have been able to address these questions through full inhibition of HMG-CoA synthase, as well as inhibitors of other ketogenic/ketolytic enzymes such as SCOT, but unfortunately these were not commercially available. Knockout models such as the SCOT knockout mice used by Cotter *et al.*, (2013) and Schugar *et al.*, (2014) could also be of help in more totally ablating a potential arm of ketogenesis to determine its effect upon cardiac recovery; yet it is worth noting that such knockout models may also exhibit altered overall metabolism.

However, while the Langendorff could be used to consistently impose an ischaemic environment, when the fresh or frozen ischaemic tissue was used for other analyses these exact conditions could not necessarily be maintained. It is possible for example that with the permeabilised fibre respirometry some of the oxygen sensitive post-translational modifications which can affect the ETC (Papanicolaou et al., 2014) were lost due to the ready availability of oxygen in the Oxygraph chamber. Some ischaemic loss of complex II supported respiration was observed, but how much of this was due to damage, how much to post-translational modification and how much to alterations we cannot visualise because respirometry cannot be conducted in ischaemic conditions will remain unclear. The capabilities are not currently available for these experiments, but it would be good in future to be able to conduct proteomic analysis of the ETC, Krebs cycle and ketogenic enzymes to see whether post-translational modifications affect the ketogenic pathway during ischaemia and aid the diversion of acetyl-CoA to β-hydroxybutyrate.

5.4.2 Significance of Results

At the less severe ischaemic flow rate employed in this chapter, cardiac mitochondrial function was broadly preserved during the ischaemic period, with ETC damage only sustained upon reperfusion. The only complex to show decreased activity at the end of the ischaemic period itself was complex II,

and this loss of function was still less severe than that seen after reperfusion. That mitochondrial damage was detected upon reperfusion in itself is nothing surprising – it is well documented that most reactive oxygen species are produced upon reperfusion (Raedschelders et al., 2012). However, what is interesting is that this loss of mitochondrial capacity occurred despite 100% recovery of cardiac contractile function. The 20 min 0.56 $ml.min^{-1}gww^{-1}$ ischaemic protocol was used since this protocol allowed full recovery of pre-ischaemic function in pilot studies, and as such the observation of the metabolic response to the ischaemic and post-ischaemic states was not complicated by damage to the myocardium. It seems though that flux capacity of the electron transport chain does not directly correlate to cardiac function in this scenario, with impaired complex I and complex II supported respiration alongside anaerobic respiration apparently still sufficient to produce enough ATP for contractile function to remain unaffected.

During ischaemia, late-stage Krebs cycle intermediates accumulated at the expense of early intermediates. Malate, fumarate and succinate were present in higher concentrations at the end of ischaemia, while citrate and isocitrate were depleted. This could be due to lower acetyl-CoA flux into the mitochondria, with less citrate being generated and thus greater accumulation of the later intermediates. This corresponds with the respirometry data since the only mitochondrial difference between the ischaemic and pre-ischaemic hearts was a loss of complex II function. If there is reduced utilisation of oxaloacetate and subsequent accumulation of malate, this may feedback upon complex II to limit oxidative metabolism and result in the more dramatic accumulation of succinate. Malonylation of complex II is known to occur (Papanicolaou et al., 2014), and could represent a mechanism through which mitochondrial metabolism adapts to hypoxic conditions. Meanwhile, the accumulation of succinate could contribute towards ketogenesis.

There are two mechanisms through which accumulation of succinate in ischaemia may drive ketogenesis. The first is that SCOT generates succinate from succinyl-CoA during ketolysis, a process which may be reversed if the concentration of succinate becomes large enough to begin driving the reaction kinetics. The second relates to NADH levels, as Krebs postulated, driving a reduction of acetoacetate to β-hydroxybutyrate (Krebs et al., 1961; Schönfeld et al., 2010). The potential of this as a driving factor for the reaction was tested here through the addition of NMN. When perfused into rats it had taken only 30 min for the NAD precursor to be converted to NAD (Birrell and Hirst, 2013; Karamanlidis et al., 2013; Yano et al., 2015), and so addition to the perfusion buffer 32 min before ischaemia would be sufficient to determine whether greater availability of NAD^+ would enable a greater level of reduction to NADH during ischaemia and drive more β-hydroxybutyrate production. Increased availability of NAD^+ precursors did appear to lead to increased ketogenesis, suggesting that the increased NAD^+ may become reduced in reductive ischaemic conditions and drive ketogenesis –

increased NAD^+/NADH ratios would drive the reaction in the other direction. The implication is that NADH levels and reduction of acetoacetate to β-hydroxybutyrate plays a large part in ischaemic ketogenesis. However, the ratio of NADH/NAD+ in the ischaemic heart tissue was not found to be altered by NMN. This could be because the majority of NAD+ is reduced during ischaemia, and therefore there was no detectable difference; it may have been more enlightening to have measured this prior to onset of ischaemia in order to visualise the effect of NMN upon cardiac NAD+ pools.

Are Fatty Acids the Source of Ischaemic β-hydroxybutyrate?

Whilst in the liver, β-hydroxybutyrate synthesis is thought to come from excess fat oxidation (McGarry and Foster, 1976) although this may reflect the fact that more fatty acid than glucose is metabolised in the liver. In **Chapter 4** I demonstrated that the presence of fat in the perfusion buffer does not affect the level of β-hydroxybutyrate produced in ischaemia. The results in this chapter suggest that a higher ratio of fat to glucose oxidation during ischaemia does not underpin ketogenesis, but also call into question whether there is increased preference for fat oxidation in ischaemia.

Fatty acid uptake to both cell and mitochondria appeared to be limited during ischaemia. Cardiac fatty acid uptake was 200-fold lower during the ischaemic period, even accounting for the decreased flow of buffer through the heart. This suggests that fatty acid uptake is actively limited during ischaemia, and is no longer under the influence of concentration in the blood/perfusate only. Further, malonyl CoA levels are seen here to be raised during ischaemia, rather than lowered as claimed previously (Kantor et al., 1999; Lopaschuk et al., 2009; Wall and Lopaschuk, 1989). Rather than a decrease in malonyl-CoA levels enhancing FAO capacity as these papers claim, this would suggest that fatty acid uptake to the mitochondria is inhibited. This is further supported by the lower fraction of complex I activity which can be accounted for by FAO in the ischaemic heart. Since fatty acid uptake during the ischaemic period is lower, it suggests that cardiac ketogenesis (which only occurs during the ischaemic period) may not be driven by fatty acid uptake and oxidation exceeding capacity for oxidation of the resultant acetyl-CoA in the Krebs cycle.

Carbon labelling analysis of Krebs cycle intermediates and of β-hydroxybutyrate itself also demonstrated no reliance of ischaemic ketogenesis upon FAO. The proportion of acetyl-CoA which was incorporated into the Krebs cycle and arose from either fatty acids or from glucose does not change in ischaemia. β-hydroxybutyrate labelling suggests that the proportional contribution of fatty acid- and glucose-derived acetyl-CoA to ketogenesis is also matched to the generation of acetyl-CoA from each in the system. The conclusion which can be drawn from this is that ketogenesis is dependent upon acetyl-CoA alone, with no preference for its metabolic precursor.

Knowing this, the aim of using sodium oxamate was to divert more pyruvate into the mitochondria rather than allowing it to be metabolised anaerobically, and determine the effect on ketogenesis. Sodium oxamate is a competitive inhibitor of LDH which has previously been used in the Langendorff preparation (Yoshioka et al., 2012). Its addition twelve minutes before the onset of ischaemia resulted in a 530% increase in the amount of β-hydroxybutyrate which had accumulated in the heart at the end of the ischaemic period, as well as higher levels initially being lost in coronary effluent. Ischaemic ketogenesis seems therefore perfectly capable of utilising carbon derived from glycolysis – so much so that it may even constitute a mechanism for lowering acetyl-CoA levels when it cannot be oxidised in ischaemia, performing a similar function to that which lactate production performs with pyruvate. It would be of interest to investigate whether activation of the PDC with dichloroacetate (DCA) had an impact upon the rate of β-hydroxybutyrate synthesis, as this would increase the amount of acetyl-CoA available for ketogenesis, and DCA has been shown to improve cardiac functional recovery following a hypoxic insult in animals previously exposed to chronic hypoxia (Handzlik et al., 2018). Another potential avenue for exploration would be to measure the relative oxidation of glucose and fatty acids immediately following reperfusion; it may be that LDH inhibition is affecting glucose oxidation as well as anaerobic glycolysis, and the availability of glucose upon reperfusion has been reported by some to be critical to functional recovery (Lopaschuk et al., 1990).

Is Ketogenesis Beneficial or Detrimental to Recovery From I/R?

It is difficult to draw conclusions on the functional repercussions of ischaemic ketogenesis from the oxamate study. Hearts given sodium oxamate eventually recovered contractile function to the same extent as control hearts. However, there was a delay in this occurring, with these hearts taking 15 minutes longer to reach the same level of RPP recovery. This could have been due to the increased concentration of ketone bodies present or flux through the ketogenic pathway preventing ketolysis; however, these conclusions cannot conclusively be drawn given the effects of oxamate upon lactate production. The slower recovery could be a result of the greater contracture exhibited by hearts given oxamate during ischaemia, with a longer recovery time required for the tissue to relax. Contracture is the contraction of the heart during ischaemia, onset of which is thought to relate to depletion of cardiac ATP levels (Hearse et al., 1977; Piper et al., 2004) – as would happen when the ischaemic heart can no longer gain energy from glycolysis. The onset and magnitude of contracture are thought to be related to the influx of calcium to the cell, which can no longer be reversed due to the inactivity of the ATP dependent Ca^{2+} pumps (Hearse et al., 1977). Since the ATP for ion homeostasis is thought to be supplied by cytosolic glycolysis (Mcnulty et al., 2000; Weiss and Hiltbrand, 1985), it could be that the contracture observed to be associated with oxamate treatment in this chapter is a result of LDH inhibition preventing glycolytic ATP production. It could take time following ischaemia to restore this

energy deficit, offering a possible explanation for the longer time taken to recover contractile function. Lactate itself is also normally utilised by the heart early upon reperfusion (Aquaro et al., 2015; de Groot et al., 1995), so its absence may compromise recovery by limiting the heart's access to an easily oxidisable substrate. A cleaner investigation was therefore needed to draw conclusions about the functional effects of ischaemic ketogenesis.

Hymeglusin, a HMG-CoA Synthase inhibitor, was used to inhibit ketogenesis and resulted in a 33% greater recovery of RPP following 32 mins reperfusion. The concentration of hymeglusin used may have been sub-optimal as it was based on studies of its effects upon cholesterol synthesis (Greenspan et al., 1987) and on brain ketogenesis (Le Foll et al., 2014) in-vivo in the rat, yet it did result in a decrease of ischaemic β-hydroxybutyrate accumulation of 32%, achieving the aim of inhibiting ketogenesis. It therefore appears that ischaemic ketogenesis may be detrimental to cardiac function. This is interesting given the myriad beneficial effects that β-hydroxybutyrate has been reported to possess, such as antioxidant activity and inhibition of inflammasome formation which could all be hypothesised to be beneficial during ischaemia (Kashiwaya et al., 1994; Newman and Verdin, 2017; Veech et al., 2001). Perhaps it is the fact that ketogenic flux inhibits the reverse reaction of β-hydroxybutyrate consumption as a fuel during ischaemia, or formation of the potentially pro-apoptotic poly-β-hydroxybutyrate (Dedkova and Blatter, 2014) which are the mechanisms for this. Either way, it seems that inhibition of ketogenesis might be a beneficial strategy in the treatment of ischaemia.

One possible explanation for the adverse effects of ketogenesis is its inhibitory effect upon the inflammasome. β-hydroxybutyrate has been shown to inhibit the formation of the NLRP3 inflammasome, which acts through caspase-1 mediated cleavage of IL-1β (Yamanashi et al., 2017; Youm et al., 2015). In this chapter, this is also shown, with greater caspase-1 activity and cleavage/excretion of IL-1β in hymeglusin treated hearts where β-hydroxybutyrate levels are lower. Inflammasome formation has previously been reported to be cardioprotective (Sandanger et al., 2016), so this could underpin any detrimental effects of β-hydroxybutyrate upon recovery of contractile function.

In conclusion, ischaemic ketogenesis occurs in the rat heart, indiscriminately of whether the source carbon is derived from glucose or fatty acid catabolism. Data presented in this chapter suggests that this process may be detrimental to the functional recovery of the heart following reperfusion.

5.4.3 Future Directions

This study has suggested that ketogenesis occurs in, and is detrimental to, the heart during ischaemia, and it would be interesting to further investigate the process in other cardiac conditions where metabolic substrate supply might exceed mitochondrial oxidative capacity. In particular, metabolism in both the diabetic and failing hearts is limited at the ETC, which could potentially stimulate cardiac ketogenesis. The type 1 diabetic heart exhibits higher capacity for FAO (Bayeva et al., 2013; Friederich et al., 2009), yet a decreased ETC capacity compared with non-diabetic controls (Duicu et al., 2017; Kiebish et al., 2012; Loiselle et al., 2014; MacDonald et al., 2011; Pham et al., 2014). Further, and making the model of particular interest, the expression of ketogenic enzymes is enhanced (Cook *et al.*, 2017; and see **Chapter 6**). In the failing heart, the heart cannot supply itself with enough blood (and oxygen) to meet its own energetic demand, leading to a decreased ETC rate of activity which could result in diversion of acetyl-CoA away from the Krebs cycle and towards β-hydroxybutyrate. TAC models of the failing heart have also exhibited greater expression of BDH1, and while this was linked to greater oxidation of β-hydroxybutyrate (Aubert et al., 2016; Bedi et al., 2016), the enzyme catalyses a bidirectional reaction so this is likely to potentiate ketogenesis. These investigations would be best carried out in the *ex vivo* heart, as *in vivo* there would be uncertainty as to which organ any β-hydroxybutyrate detected in the heart had originated from. Perfusion of type 1 diabetic hearts and failing hearts in the Langendorff mode would allow certainty that any β-hydroxybutyrate was indeed being produced in the heart, and would also allow investigation of whether these hearts were capable of producing more β-hydroxybutyrate than controls during ischaemia.

A proteomic study would also be of interest, in order to determine whether the point at which the heart switches from oxidising to producing ketone bodies during ischaemia is controlled by post-translational modification. Accumulation of various metabolic intermediates such as succinate, malate and acetyl-CoA may lead to post-translational modification of ketogenic enzymes during ischaemia (Papanicolaou et al., 2014; Quant et al., 1990). If this were detected, further enzyme activity assays could potentially be conducted to investigate whether the modification had an effect upon enzyme activity; although it would be difficult to maintain ischaemic conditions during these assays so these assays would be enlightening only if the modifications were robust enough to withstand tissue preparation.

If ketogenesis is a response of the myocardium to glucose and FAO exceeding mitochondrial oxidative capacity, it could be interesting to see the effects upon rate of ketogenesis if the heart were not supplied with any exogenous substrate just before and during ischaemia. Excess supply of substrates to the Krebs cycle during ischaemia could be detrimental, and leads to diversion of glucose-derived

pyruvate to lactate and alanine (Lloyd et al., 2004), with both glucose and FAO derived acetyl-CoA also now shown to be diverted to β-hydroxybutyrate during ischaemia. Limiting metabolic substrate supply to the heart could perhaps lead to a more manageable amount of substrate metabolism being derived from endogenous sources only. The experiment should be easy to conduct in the Langendorff perfused heart, as internal triglyceride and glycogen stores are capable of sustaining a rat heart for up to thirty minutes without external supply of metabolic substrate, a process which is evinced during the experimental process of glycogen depletion (Nakao et al., 1993).

CHAPTER 6

Isoprenaline Mediated Stimulation of Cardiac Metabolism in the Pancreatectomised Rat

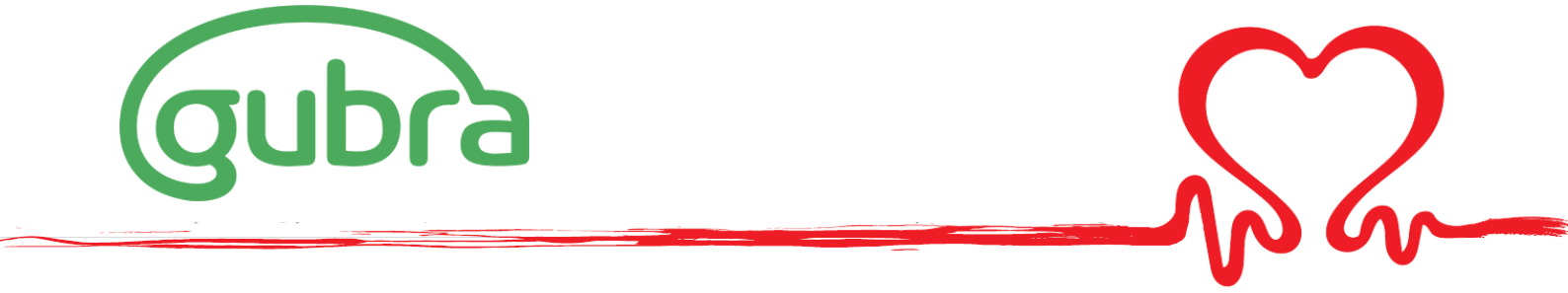

ABSTRACT

BACKGROUND The type 1 diabetic heart is characterised by metabolic remodelling, including a loss of metabolic flexibility, which may alter the response to stress. It is unknown whether any impaired ability to respond to stress may result in the higher rates of mortality from cardiovascular complications seen in diabetic patients.

OBJECTIVE This study aimed to determine how the type 1 diabetic heart responds to chronic stimulation with the β-agonist isoprenaline (Iso).

METHODS Partially pancreatectomised (90% removal, Px) and sham-operated rats were administered Iso daily (10x1 mg/kg) or vehicle *i.p.* between 5 and 7 wks post-operation. Respirometry, mass spectrometry and RNAseq were performed on left ventricle following termination at 10 wks.

RESULTS Rodent mortality following the first dose of isoprenaline was 43% in the sham rats, while there was no loss of life in the Px rats. Mitochondrial respiratory capacity was impaired following Px, with a substrate switch towards fatty acid oxidation (FAO) alongside greater expression of FAO-related enzymes and evidence of oxidative stress. Iso treatment also impaired respiratory capacity, but enhanced flux through glycolysis with increased aldolase expression ($p<0.001$). In the hearts of Iso-treated Px rats ($p<0.0001$), mitochondrial respiratory capacity was preserved, and whilst myocardial PCr was depleted following Px, this too was conserved in Iso-treated Px rats. Uncoupling of adrenergic signalling through repression of adenylyl cyclase by both Iso and Px may underpin this apparent protection.

CONCLUSION Isoprenaline administration conserved mitochondrial respiratory capacity and energetics in the type 1 diabetic heart.

6.1 BACKGROUND

Increasingly referred to as an epidemic in the western world, diabetes mellitus can exert a direct effect upon the myocardium to cause diabetic cardiomyopathy (Bugger and Abel, 2014). Diabetes stems from an inability to regulate blood glucose through response to insulin, whether this be through decreased cellular sensitivity to insulin as in type 2 diabetes, or the pancreatic inability to produce sufficient insulin which defines type 1 diabetes and is the strata of disease which will be addressed in this chapter.

6.1.1 Type 1 Diabetes Mellitus

Type 1 diabetes mellitus results from impaired pancreatic function, meaning that lack of insulin secretion prevents efficient cellular uptake of glucose (Katsarou et al., 2017). It is characterised by elevated concentrations of blood glucose, which also lead to heightened blood lipid levels. While type 2 diabetes is a state which stems from poor diet control and a sedentary lifestyle, type 1 diabetes is a consequence of a destruction of pancreatic cells by an auto-immune response (Van Belle et al., 2011). Insulin produced in the pancreas stimulates uptake of glucose in non-diabetic humans and rats, and when its production is impaired in type 1 diabetes this leads to an inability to regulate blood glucose levels. This hyperglycaemia and hyperlipidaemia which characterise type 1 diabetes generate a state of nutrient excess, which leads to the perturbation of cardiac metabolism (Stanley et al., 1997a).

Type 1 diabetes is associated with an increased risk of developing heart failure. Type 1 diabetic men were 9.4 times as likely and type 1 diabetic women 39.1 times as likely to develop heart failure than their non-diabetic counterparts in the under 40 age group of the Diabetes UK cohort (Laing et al., 2003). In addition, 40% of those presenting with acute heart failure syndrome have a history of diabetes (Gheorghiade and Pang, 2009). The outcome of this heart failure was also worsened by diabetes, with diabetic heart failure patients twice as likely to die from or be hospitalised by their condition as non-diabetic heart failure patients (Macdonald et al., 2008). There are arguments that this mortality is correlated with levels of blood glucose (Lehto et al., 1999), and some that this is not the case, but that instead increased resistance to insulin stimulation increases risk of death from CVD (Orchard et al., 2003). Moreover, some of the mortality and incidence of heart failure arising from type 1 diabetes does not stem from an intermediary cardiovascular complication such as infarction (Bertoni et al., 2003; Schilling and Mann, 2012).

6.1.2 Diabetic Cardiomyopathy

Such cases have been hypothesised to be a condition termed diabetic cardiomyopathy, a direct diabetic instigation of left ventricular dysfunction in the absence of intermediary effectors such as myocardial infarction (Rubler et al., 1972; Schilling and Mann, 2012). The molecular mechanisms behind this are not yet fully understood, yet many factors have been proposed to contribute. In particular, mitochondrial dysfunction, oxidative stress, lipotoxicity, increased fatty acid oxidation, hyperglycaemia and advanced glycation end products are thought to feature strongly in the development of the disease (Bugger and Abel, 2014) **(Figure 6.1)**.

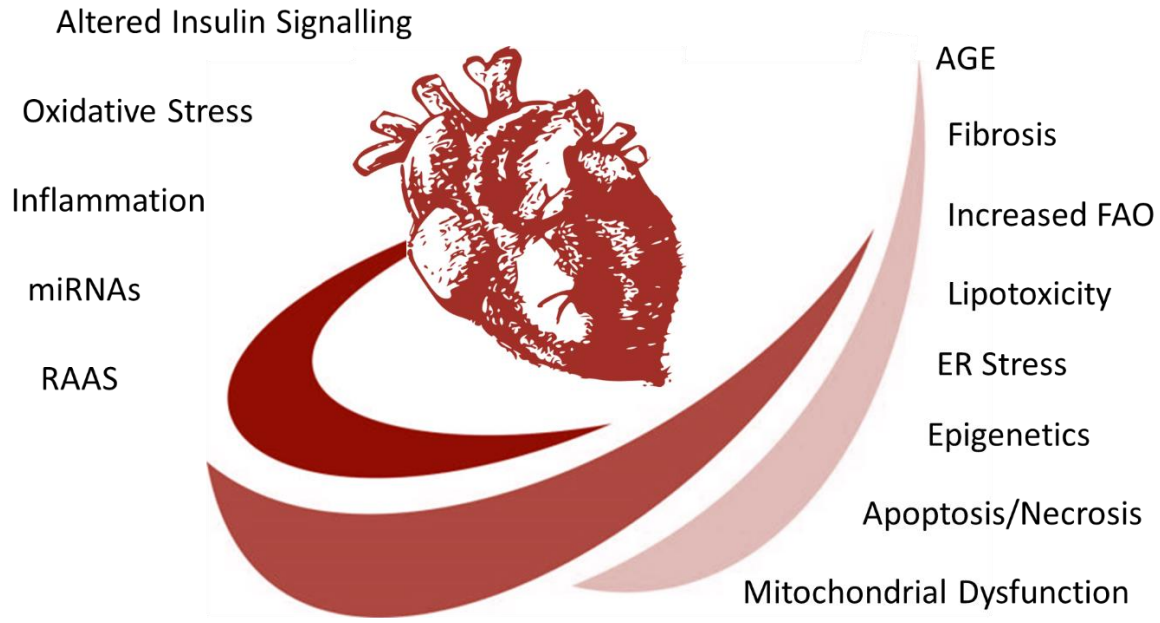

Figure 6.1: Pathways and factors which have been implicated in the genesis of diabetic cardiomyopathy

Hyperglycaemia

Hyperglycaemia induced ROS production has the potential to elicit a state of oxidative stress which, amongst other complications, engenders impaired contractile function. ROS production has been documented to arise from both the polyol and hexosamine pathways during hyperglycaemia (Wold et

al., 2005), yet the principal source is thought to lie at the mitochondrial inner membrane with the ETC (Nishikawa et al., 2000). Prolonged exposure to high glucose levels causes the mitochondria to undergo rapid morphological fission, which is necessary if not sufficient for the generation of ROS (Yu et al., 2006, 2009). It is mooted that there is a certain threshold of mitochondrial proton gradient above which the half-life of ROS-producing components such as ubisemiquinone is prolonged, and that hyperglycaemia pushes the proton gradient above this level through over-generation of electron donors to the ETC (Szabo, 2009). Whether or not this the underlying mechanism, collapsing this gradient through over-expression of UCP-1 in human aortic endothelial cells prevented hyperglycaemia-induced ROS production, while over-expression of MnSOD, the mitochondrial form of superoxide dismutase, prevented ROS signalling and increased PKC activation (Yao and Brownlee, 2010). This ROS production from hyperglycaemia in the type 1 diabetic heart has been found to impair contractile function, and hence the dysfunctional metabolism of glucose may underlie diabetic cardiomyopathy (Ceylan-Isik et al., 2006)

Metabolic Substrate Preference

Over-reliance upon fatty acid oxidation is a hallmark of the diabetic heart, and can also be responsible for ROS generation and loss of efficiency. The primary cause for this is a combination of increased circulating levels of fatty acids coupled with an impaired ability to take up and oxidise glucose in the absence of insulin (Bayeva et al., 2013). Fatty acid uptake contrasts with that of glucose because it is not primarily under hormonal control, instead being transported into the cell via the CD36 transporter in proportion to plasma fatty acid concentrations (Stanley et al., 1997a). Myocardial levels of CD36 are increased in the diabetic heart, whilst plasma free fatty acid levels are also elevated since insulin-mediated inhibition of lipolysis no longer occurs (Stanley et al. 1997; Heather et al. 2006).

Modulation of PDH activity also contributes to a loss of metabolic flexibility in the diabetic heart. Accumulation of acetyl-CoA, as a product of β-oxidation, feeds back to inhibit PDH (Hansford and Cohen, 1978), whilst increased levels of the inhibitory PDH kinase (PDK) isoform 4, which is suppressed by insulin, are also seen the diabetic heart (Kim et al., 2006; Wu et al., 1998). Crucially, even if hearts from type 1 diabetic rats are perfused in the absence of any lipids, glucose oxidation rates remain low and supply less than 20% of the heart's energy requirements (Wall and Lopaschuk, 1989). This suggests that reduced PDH flux is due to metabolic remodelling and not purely the balance of mitochondrial substrate availability.

TCA cycle activity appears unaffected in the diabetic heart, so the shift in origin of acetyl-CoA appears to be the major effect upon mitochondrial metabolism. There is no difference in activity of TCA cycle

enzymes (Chen et al., 1984; Glatz et al., 1994), but total ATP production is depressed (Wall and Lopaschuk, 1989).

Lipotoxicity

The increased uptake of fatty acids, coupled with mismanagement of their storage, is thought to lead to lipotoxic damage which may drive development of cardiomyopathy. Lipid content and steatosis increases in the type 1 diabetic heart, preceding the onset of left ventricular dysfunction (Ritchie et al., 2017). FAO is less oxygen efficient than glucose oxidation and results in greater ROS production (Hinkle, 2005), however it appears that any lipotoxic effects are a symptom of mismanagement and cytosolic accumulation rather than oxidation (Scherer et al., 2016). Accumulation of lipid droplets and associated disruption of cardiomyocyte function could impair contractility leading to cardiomyopathy.

Mitochondrial Dysfunction

Mitochondrial dysfunction may be the unifying factor between these hallmarks of diabetic cardiomyopathy and the development of contractile dysfunction. Overall mitochondrial respiratory capacity is depressed in the streptozotocin (STZ) type 1 diabetic heart (Flarsheim et al., 1996; Lashin et al., 2006). This is associated with an increased ratio of FAO to glucose oxidation (Chatham and Forder, 1997; Depre et al., 2000; Finck et al., 2002; Flarsheim et al., 1996; How et al., 2007). Meanwhile, the ROS production associated with both hyperglycaemia (Yao and Brownlee, 2010) and increased FAO is mitochondrial and has been associated with the loss of ETC function (Lashin et al., 2006). Furthermore metabolic dysfunction precedes the onset of the loss of contractile function and its reversal prevents the onset of contractile dysfunction (Nielsen et al., 2002), and it therefore seems likely that metabolism and the mitochondria are central effectors of diabetic cardiomyopathy.

6.1.3 The Need for More Representative Animal Models

Reported features of type 1 diabetic cardiomyopathy can vary quite widely, and a consideration worth taking into account is that this may be due to inconsistencies in animal models. STZ models of type 1 diabetes are widely used, easy to implement and allow diabetes to be instigated at different timepoints during the study (Bugger and Abel, 2009). The model involves administration of the genotoxic glucose analogue streptozotocin, which causes destruction of the insulin secreting pancreatic β cells following selective uptake by GLUT2 transporters which are most highly expressed in β cells. However, STZ has a number of off-target effects including genotoxicity (Bolzán and Bianchi, 2002), influence upon liver metabolism of glucose and lipids (Kume et al., 2005), and depression of

cardiac contractile function (Wold and Ren, 2004), all of which may lead to misinformative findings in the heart. A more reliable animal model is needed to fully investigate type 1 diabetic cardiomyopathy; because if cardiomyopathy is defined as a direct impact of diabetes upon contractile function and streptozotocin also impacts cardiac contractility, how may the effects of the diabetes be discerned from those of the drug?

6.1.4 Objectives

Diabetic patients have an increased risk of mortality from cardiovascular causes, which potentially stems from diabetic cardiomyopathy and a loss of metabolic flexibility (Bugger and Abel, 2014). The purpose of this chapter was therefore to test the hypothesis that this increased mortality rate originated from decreased ability to respond to metabolic stimuli by challenging the type 1 diabetic rat with the β-adrenergic agonist isoprenaline.

A secondary objective was to characterise a 90% pancreatectomy rat model of type 1 diabetes, which was chosen for this study to discount the off target effects of the more commonly used STZ induced model. 90% pancreatectomy has been used previously as a model for pancreatic regeneration (Yu et al., 2015), and resulted in a stable hyperglycaemic phenotype. However, it had not yet been characterised metabolically. In choosing to utilise this model, the aim was also to test the hypothesis that it would also induce a metabolic phenotype of type 1 diabetes.

6.2 METHODS

6.2.1 Animal Housing and Treatment

All treatment of live animals discussed in this chapter was carried out by and at Gubra ApS, Horsholm, Denmark under their licence. Termination of the animals, tissue collection, respirometry analysis, mass spectrometry and the analysis of data collected through RNAseq was conducted by myself.

6.2.2 Experimental Design

Sprague-Dawley rats were either 90% pancreatectomised (Px) or sham operated. Following an overnight full-fast with grids installed in the cages, the rats were operated upon under isofluorane induced anaesthesia by Dr Philip Pedersen at Gubra ApS. Pancreatectomy (90%) was performed by ligation and then removal of the tail, body and a part of the pancreatic head by gentle abrasion with dental applicator. The 10% of the pancreas which remained was the portion between the duodenal loop and the pancreatic duct. The major blood vessels to the stomach, spleen and gut were left intact so no other organs are compromised. The sham operation consisted of anaesthesia and ligation of the portion of the pancreas described above, a ligature which was then removed in order to leave behind a fully functional pancreas. The rats were not offered food from one day before until one day after the surgery, whereupon they were offered 5 g of chow. From the second day after surgery food was provided *ad libitum*.

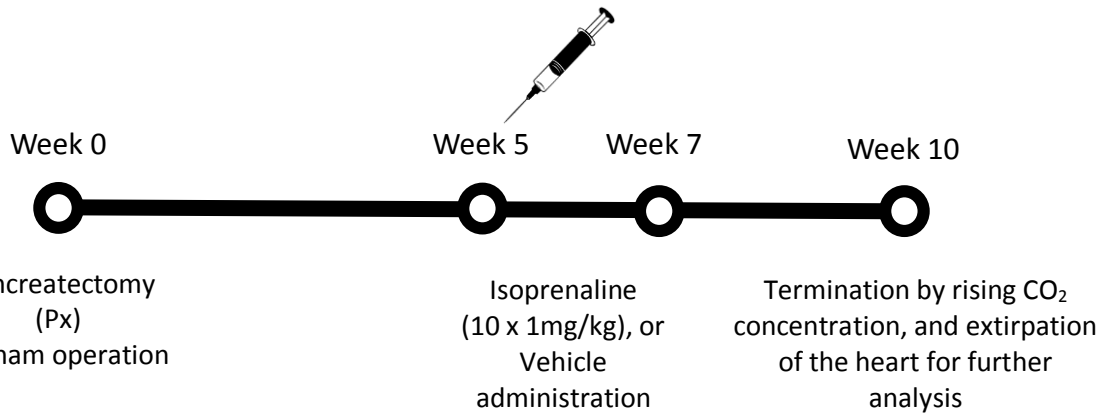

Figure 6.2: Timeline of Key Events in the Experimental Protocol

Animals from each group then underwent a daily subcutaneous administration of either isoprenaline (1 mg/kg) or vehicle (saline solution) for 10 days, commencing 5 weeks post-operation. Blood glucose and bodyweight were monitored throughout. At 10 weeks post-operation, rats were euthanised with rising concentrations of CO_2 followed by cervical dislocation. Hearts were extracted, and the left ventricle sectioned before being either snap frozen for further analysis (RNAseq and Mass Spectrometry) or transferred fresh into ice cold BIOPS solution **(Appendix 2.2)** for immediate analysis of mitochondrial respiratory function with high-resolution respirometry.

6.2.4 Blood Glucose Measurement

Performed by the Animal Technician Staff at Gubra ApS

Blood samples were collected weekly from tongue blood in heparinized glass capillary tubes, and immediately suspended in glucose/lactate system solution buffer (EKF-diagnostics, Germany). Blood Glucose was then measured using a BIOSEN c-Line glucose meter (EKF-diagnostics, Germany).

6.2.5 Echocardiography

Performed by Louise Thisted and Dr. Nora Zois, with assistance from the author

Echocardiography was performed on the rats 9 weeks post-operation by use of a Philips iE33 Ultrasound echocardiograph and a 12-4 MHz probe (Philips S12-4 sector array transducer). The rat was lightly anaesthetized using 1.5-3% isofluorane, and the chest of the rat was shaved. The rat was then placed on a hot water pad in the supine position. Ultrasound gel was preheated to 37°C in a warm water bath and applied to the rat's chest. The rat underwent echocardiography under continuous electrocardiographic measurements and a minimum of 5 heart cycles were saved in each projection (parasternal and apical positions, respectively). Echocardiographic images were saved and processed off-line in order to quantify left ventricular function and dimensions. Fractional shortening was calculated by subtracting the left ventricular diameter in systole (LVIDs) from the left ventricular diameter in diastole (LVIDd) and expressing this as a fraction of LVIDd. A measure of ejection fraction was derived by dividing the stroke volume by the end-diastolic volume.

6.2.6 High-Resolution Respirometry

Permeablision of LV fibres and measurement of respiration rates was conducted as described in **Chapter 2 (Section 2.2).** The ratio of fatty acid oxidation preference (FAO) was calculated by dividing the octanoyl carnitine supported oxphos rate by the octanoyl carnitine plus pyruvate supported oxphos rate.

6.2.7 Liquid Chromatography-Coupled Mass Spectrometry (LC-MS/MS and LC-MS)

Metabolites were extracted from frozen left ventricle using a Bligh-Dyer method as described in **Chapter 2 (2.3.2)**. Levels of glycolytic intermediates and energetic compounds (ATP and PCr) were assessed using the BEH amide column chromatography method as described in sections 2.3.3 and 2.3.4. Levels of oxidative stress markers (LysOH and Glutathione) were assessed using the C18pfp chromatography method coupled to the Thermo Quantiva, while levels of β-hydroxybutyrate and lactate were assessed using the C18pfp method coupled to the Thermo Elite, all as described in the aforementioned chapters.

6.2.8 RNAseq

RNA extraction, cDNA generation and next-generation sequencing was performed at Gubra ApS as follows:

RNA was purified from homogenized tissue using the NucleoSpin RNA Plus kit (MACHEREY-NAGEL GmbH). 500ng purified RNA from each sample was used to generate a cDNA library using the NEBNext® Ultra™ II Directional RNA Library Prep Kit from Illumina (New England Biolabs). The cDNA library was then sequenced on a NextSeq 500 using NextSeq 500/550 High Output Kit V2 (Illumina). Sequencing was carried out for 75 cycles and 2 x 8 index cycles.

The sequencing data was aligned to the genome of the rat obtained from the Ensembl database using the Spliced Transcripts Alignment to a Reference (STAR) software. For the bioinformatic analysis, the quality of the data was evaluated using the standard RNA-sequencing quality control parameters, the inter- and intra-group variability was evaluated using principal component analysis and hierarchical clustering. Analysis of the data was then performed by the present author.

6.2.9 LV Histology

Performed by the histology group at Gubra ApS

The half of the ventricle designated for histological staining was fixed in 4 % paraformaldehyde, embedded in paraffin and cut into 3-4 µm sections. Slides with paraffin embedded sections were de-paraffinated in xylene and rehydrated in a series of graded ethanol. The slides were incubated in Weigert's iron hematoxylin (Sigma-Aldrich), washed in tap water, then stained with Picro-sirius red (Sigma-Aldrich) and washed twice in acidified water. Excess water was removed by shaking the slides and the slides were then dehydrated using three washes of 100% ethanol, cleared in xylene and mounted with Pertex to be allowed to dry before scanning. Histological scoring was performed on Picro-Sirius Red stained sections by a trained histopathologist. All histological assessments were performed by a pathologist blind to treatment. Imaging analysis for quantitation of collagen levels were performed using HDevelop Image Analysis Toolbox (MVTec, Munich, Germany) or Visiomorph (Visiopharm, Hørsholm, Denmark) software. Area fraction was calculated as by calculating the staining area as a percentage of the whole-sectional area (area fraction).

6.2.10 Statistical Analysis

Unless otherwise stated, all statistical analysis was performed using two-way ANOVA with Isoprenaline treatment and Pancreatectomy as the variables. Significant effects and interactions were further examined using Tukey's post-hoc test.

Graphically, the following representations were used for significant effects:

Effect of pancreatectomy

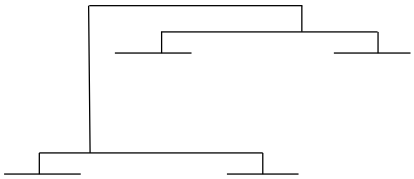

Effect of isoprenaline

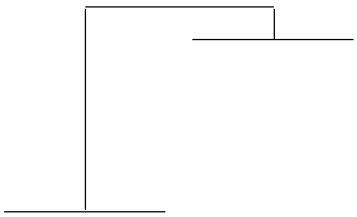

Interaction

For data where there was more than one significant effect, both are instead written upon the graph. Significance was represented as * = p<0.05, ** = p<0.01, *** = p<0.001 and **** = p<0.0001

Group Key

Sham/ Vehicle | Px/ Vehicle | Sham/ Iso | Px/ Iso

6.3 RESULTS

6.3.1 Core Dataset

Blood Glucose Levels

Blood glucose levels remained constant throughout in sham operated rats. An initial rise to a plateau around 25 mM in both Px groups clearly demonstrated hyperglycaemia and an inability to regulate blood glucose **(Figure 6.3)**. There was no noticeable effect of isoprenaline treatment upon blood glucose concentrations.

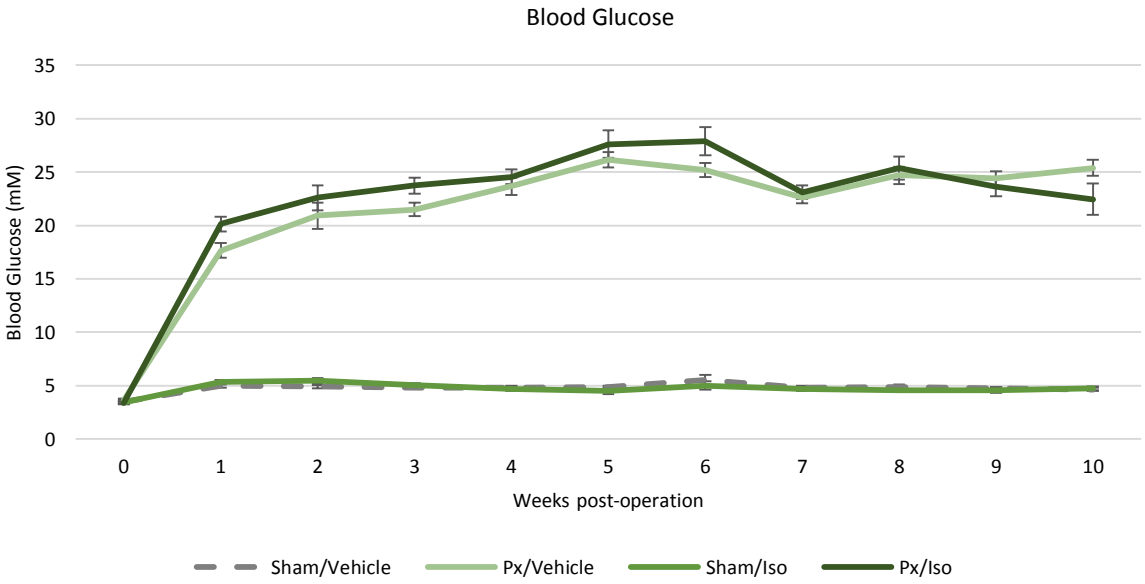

Figure 6.3: Concentration of glucose in the blood for the 10 weeks between Px or sham operation and termination.

Body and Heart Weight

On termination, bodyweight was 33% lower in the pancreatectomised rats than in the sham-operated rats (**Figure 6.4B**, p<0.0001). This bodyweight difference was due to slower growth rather than weight loss **(Figure 6A)**. Total heart weight on termination was 25% lower as an effect of pancreatectomy (**Figure 6C,** p<0.0001), whilst the ratio of LV mass to total heart weight was the same across all groups (**Figure 6D)**. This showed that isoprenaline administration had not induced lasting cardiac hypertrophy.

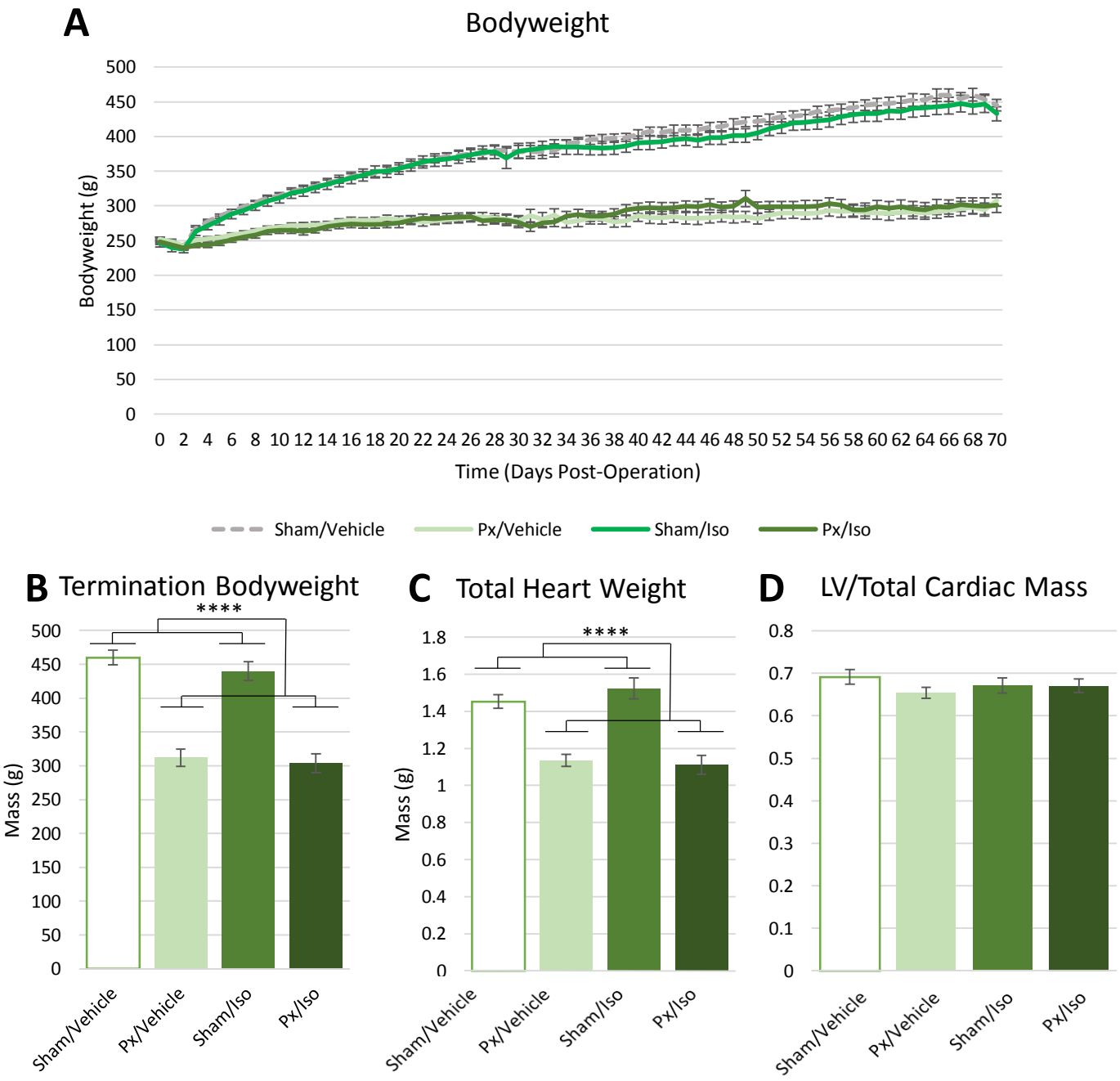

Figure 6.4: (A) Rat bodyweight measured daily following surgery; (B) Mass of rat upon termination; (C) Total heart weight on termination; (D) Ratio of LV mass to total heart weight. Masses and ratios displayed as mean ± SEM. 2-way ANOVA, **** p<0.0001

Food Intake

Following a period of lower food intake immediately following pancreatectomy, the Px rats consumed around 40% more food than Sham–operated rats over the ten weeks following the operation (Px Effect, p<0.0001) **(Figure 6.5)**. When coupled with the fact that these animals had a lower bodyweight than the Sham operated group, and grew at a slower rate **(Figure 6.4)**, this suggests that the Px rats were less effective at extracting nutrients from the food and had to eat more in an attempt to compensate.

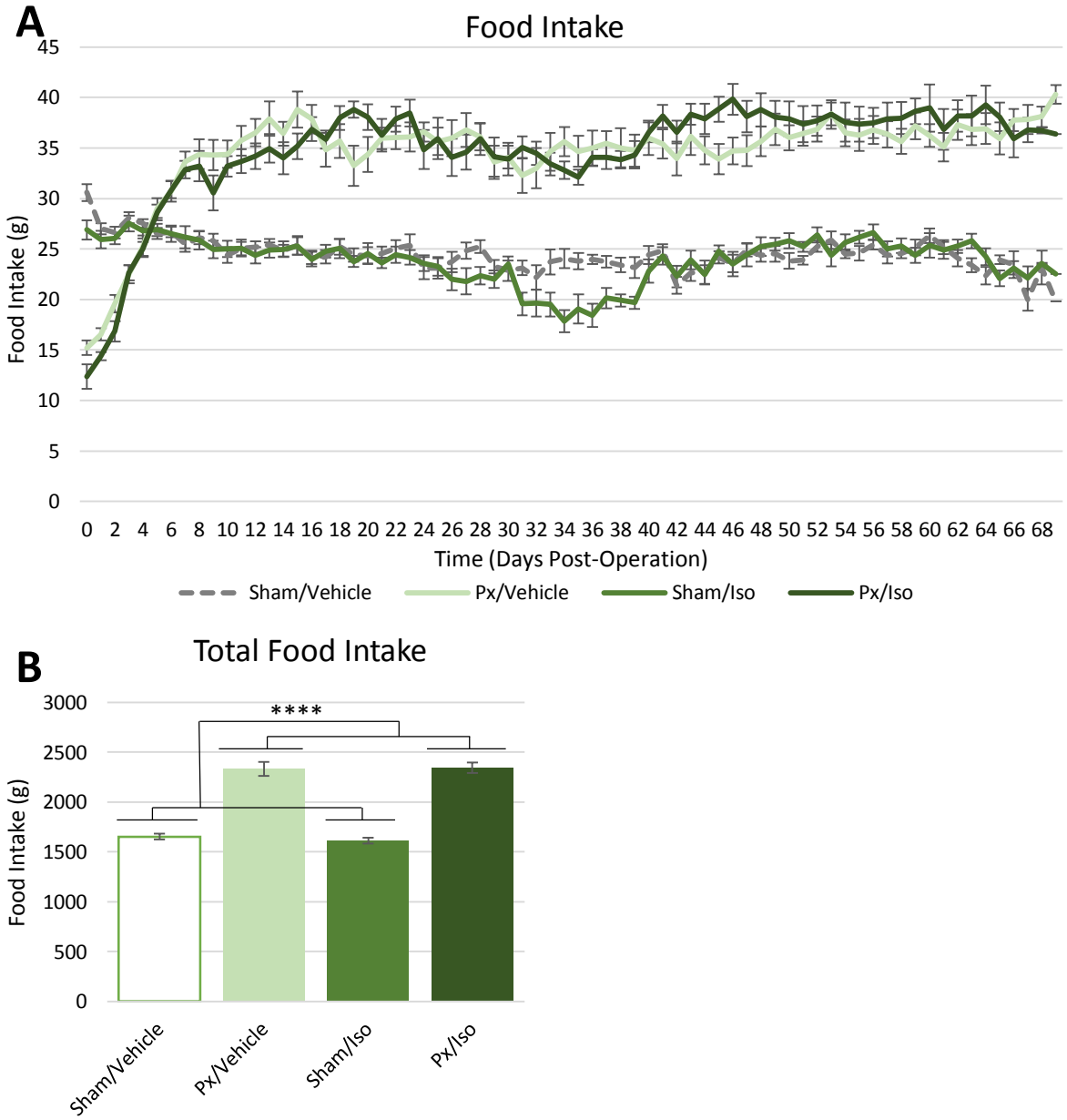

Figure 6.5: (A) Daily food intake following surgery; (B) Total food intake. Masses displayed as mean ± SEM. 2-way ANOVA, **** p<0.0001

6.3.2 Mortality

Of the total cohort of rats which underwent isoprenaline administration (n=43), including those destined for other experimental endpoints at Gubra ApS than those detailed in this chapter, there were 9 deaths following administration of the first dose of isoprenaline **(Figure 6.6)**. All 9 of these deaths occurred in the Sham/Iso group, meaning that of the 21 animals originally destined for this group, 43% succumbed to the initial administration of isoprenaline. By contrast, there were no fatalities sustained by the 22 rats comprising the Px/Iso group. This indicated two things: firstly, that the 1 mg/kg dose of isoprenaline represented a severe insult; and secondly that the pancreatectomised group were more resilient to this stimulus, whether through a lower contractile ability to respond or a desensitisation to adrenergic stimulation.

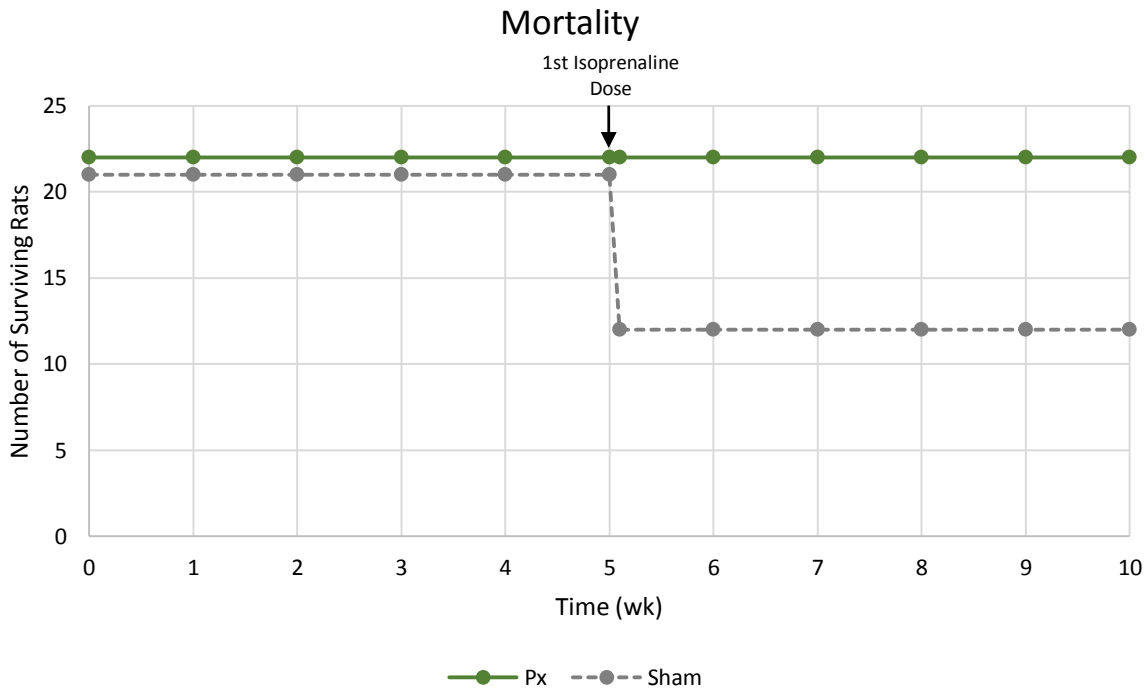

Figure 6.6: Survival rate over the experimental period

6.3.3 Tissue Fibrosis

Left ventricles were stained with picro-sirius red by the histology department at Gubra ApS for imaging of tissue fibrosis **(Figure 6.7 A)**.

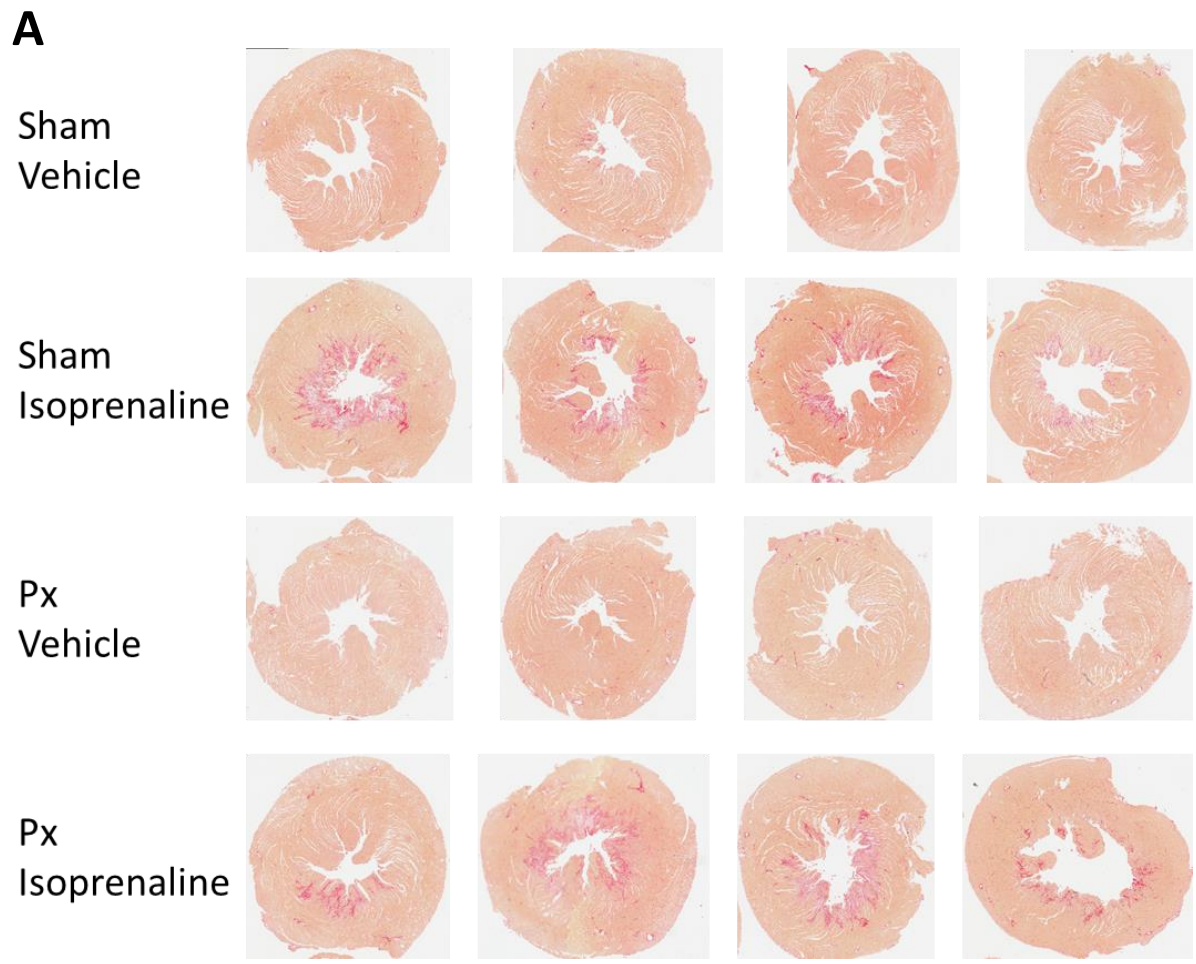

Figure 6.7: Transverse sections of LV stained with picro-sirius red.

Cardiac tissue taken from the groups administered isoprenaline was more fibrotic than the vehicle treated groups **(Figure 6.7 B&C)**. Picro-sirius red staining showed a greater mass of collagen (Iso effect, p<0.0001) and a greater area fraction of collagen in the isoprenaline treated groups (Iso effect, p<0.0001). Collagen mass was also lowered as an effect of pancreatectomy (p<0.01).

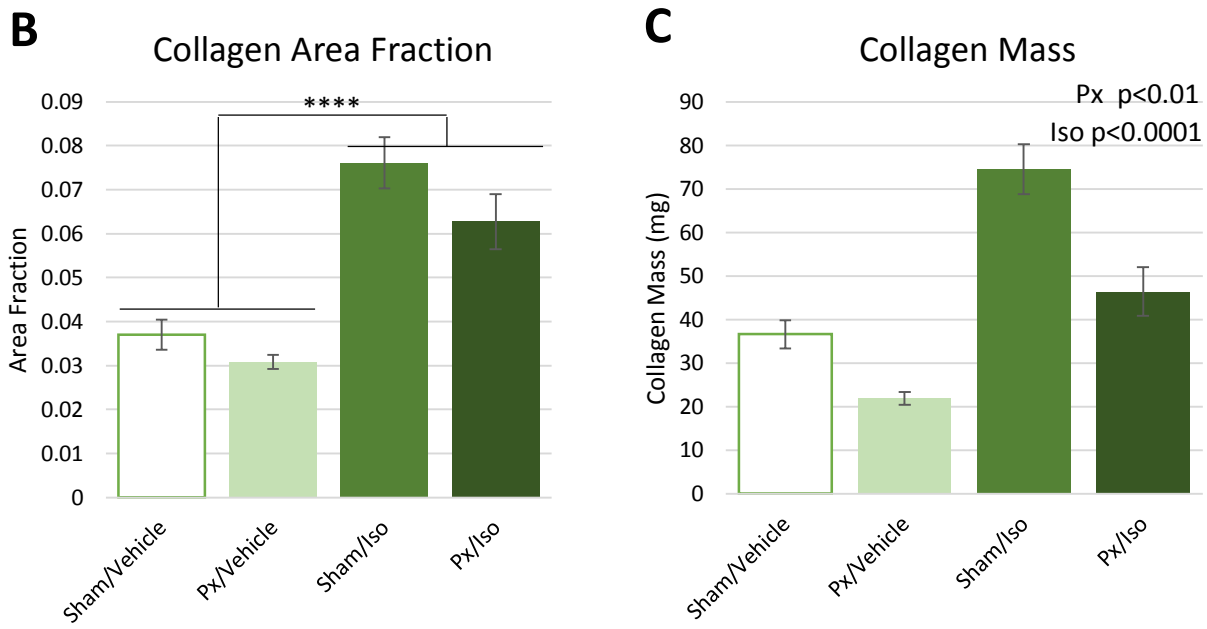

Figure 6.7: (B) Collagen area fraction and (C) collagen mass measured by quantification of Picro-sirius Red staining. Displayed as mean ± SEM. 2-way ANOVA **** = p<0.0001

6.3.4 Echocardiography

Isoprenaline administration also impacted upon cardiac contractile function as measured using echocardiography by Louise Thisted **(Figure 6.8)**. Fractional shortening and ejection fraction were compromised in the Iso treated groups relative to those administered vehicle (Effect of Iso, $p<0.0001$ for both parameters). This suggests that the fibrosis incurred following chronic isoprenaline administration **(Figure 6.7)** may impede the ability of the heart to contract fully or as vigorously as in those not administered isoprenaline.

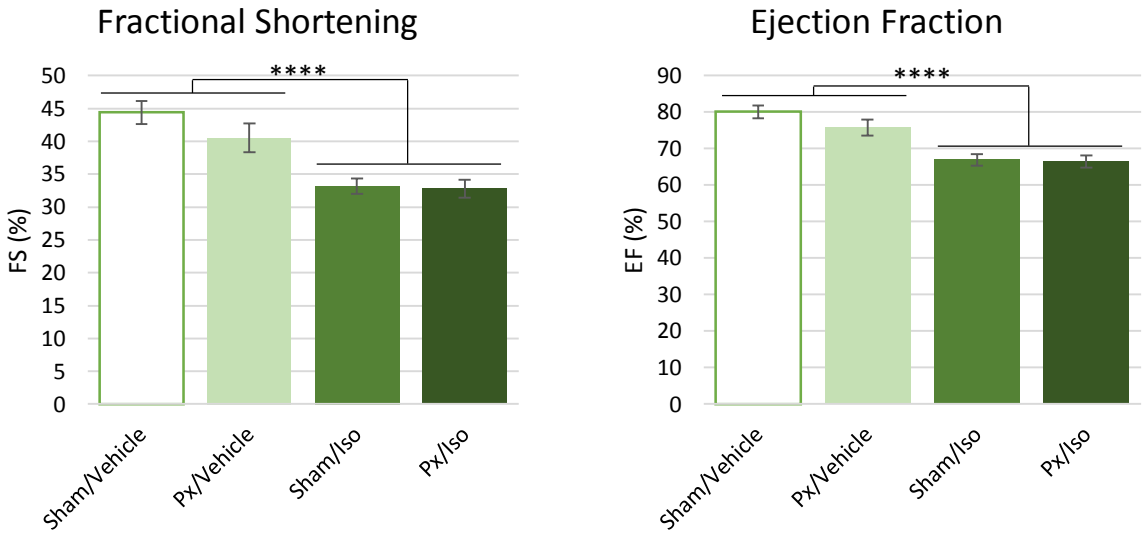

Figure 6.8: Fractional shortening, FS (LVIDd – LVIDs/LVIDd *100) and ejection fraction, EF (Teichholz formula). Displayed as mean ± SEM. 2-way ANOVA **** = $p<0.0001$

6.3.5 Mitochondrial Function

Leak state β-oxidation limited oxygen consumption, measured using high-resolution respirometry, revealed a significant interaction between isoprenaline administration and pancreatectomy ($p<0.01$). Explicitly, the Px/Vehicle group displayed significantly lower oxygen consumption than the Sham/Vehicle group (Tukey's, $p<0.05$), and the Sham/Iso group was also lower than the Sham/Vehicle group. The two factors combined in the Px/Iso group however displayed a rate of oxygen consumption significantly greater than the Sham/Iso group (Tukey's, $p<0.05$), and not significantly different to Sham/Vehicle, suggesting a reversal of the effects seen with Px or Iso alone.

The same broad pattern and interaction continued to be exhibited in the Oxphos state, for β-oxidation limited oxygen consumption, β-Oxidation plus Pyruvate, Complex I activity, Total Oxphos and Complex II activity (Interactions $p<0.01$, $p<0.001$, $p<0.001$, $p<0.0001$ and $p<0.0001$ respectively), such that both Px and Iso decreased mitochondrial respiratory capacity, whilst the two factors in combination at least partially reversed this decline.

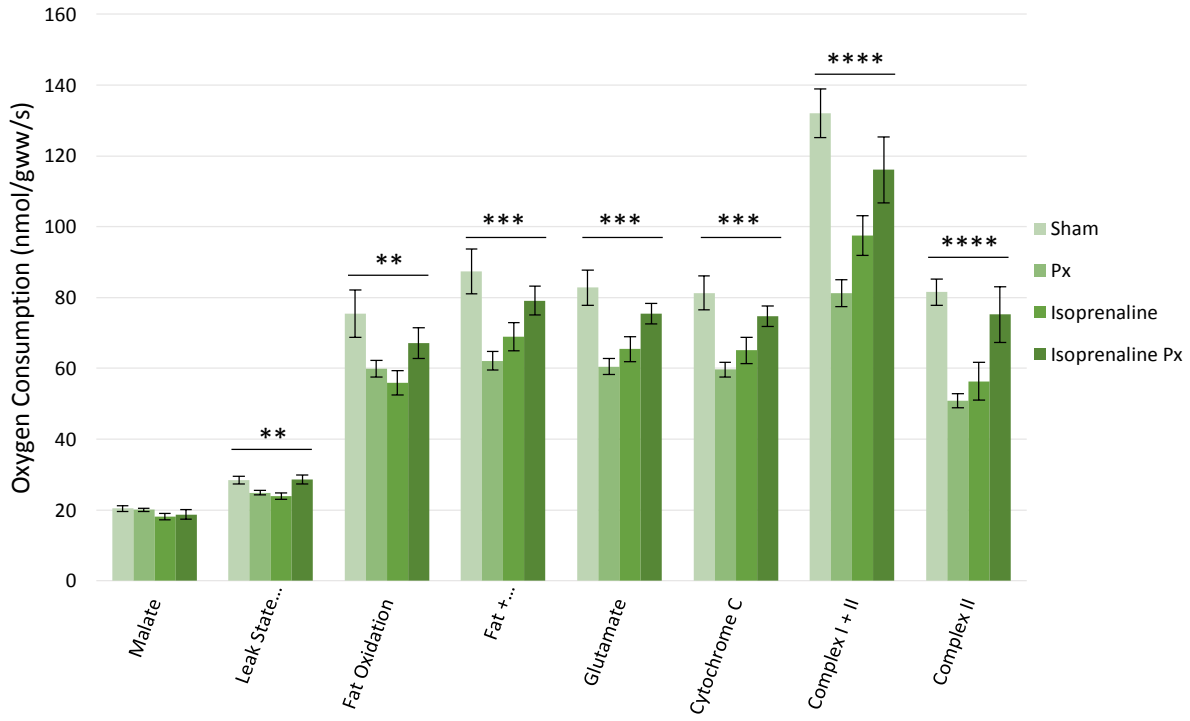

Figure 6.9: Respiration rates corrected for wet mass. Rates displayed as mean ± SEM. 2-way ANOVA ** = $p<0.01$, *** = $p<0.001$ and **** = $p<0.0001$

Of particular note was the difference in the FAO ratio, or the proportion of complex I activity accounted for by β-oxidation **(Figure 6.10)**. The Px/Vehicle group had a significantly higher FAO ratio than the Sham/Vehicle group (Tukey's, $p<0.01$). This was also higher than in the Sham/Iso group (Tukey's, $p<0.0001$), and the Px/Iso group (Tukey's, $p<0.001$). This was an effect of pancreatectomy ($p<0.01$) and an effect of isoprenaline ($p<0.001$). There was no effect of either pancreatectomy or isoprenaline upon the respiratory control ratio (RCR).

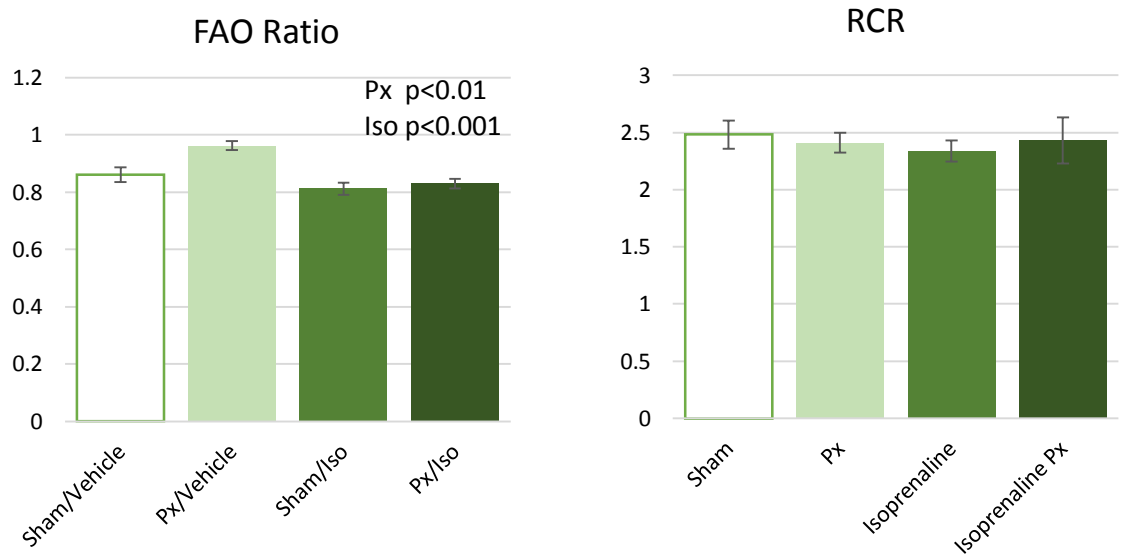

Figure 6.10: The ratio between octanoyl carnitine and octanoyl carnitine plus pyruvate supported respiration (FAO) as a marker of preference for fatty acid oxidation; and the respiratory control ratio (RCR). Ratios displayed as mean ± SEM. 2-way ANOVA effects denoted on graph.

6.3.6 Tissue Energetics

To further understand the implications of the altered mitochondrial capacity, high energy phosphate levels were investigated.

Tissue levels of ATP were 80% higher in the Sham/Iso group relative to control, and 140% higher in the Px/Iso group. Statistically, there was an effect of Isoprenaline treatment ($p<0.01$), with no Px effect **(Figure 6.11)**.

Phosphocreatine levels were lower in the Px/Vehicle group relative to Sham/Vehicle, with only 60% of the levels present in the non-pancreatectomised heart. This effect was nullified by isoprenaline administration, which preserved PCr concentrations ($p<0.05$, effect of isoprenaline administration).

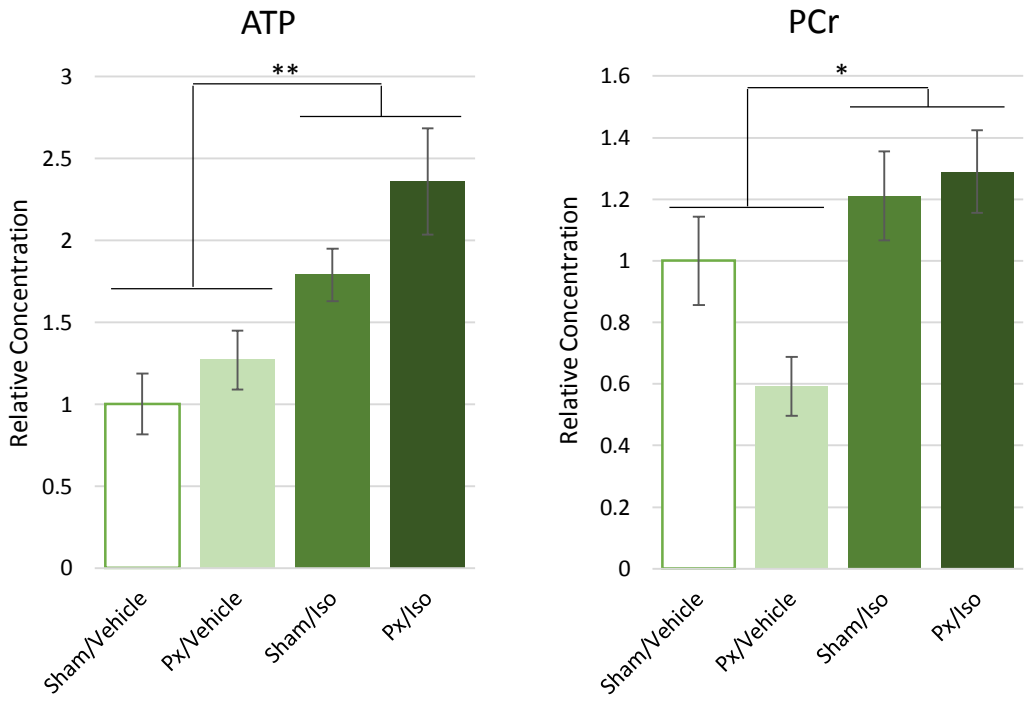

Figure 6.11: Concentrations of ATP and PCr in cardiac tissue relative to control. Concentrations displayed as mean ± SEM. 2-way ANOVA * = $p<0.05$, ** = $p<0.01$.

6.3.7 Oxidative Stress

Levels of oxidised glutathione were 1.6 times greater in the two Px groups relative to those which were sham operated ($p<0.001$, **Figure 6.12 overleaf**).

This change was reflected in another oxidative stress marker, LysOH, where concentrations were approximately three- and two-fold greater in the Px/Vehicle and Px/Iso groups than in the Sham/Vehicle group ($p<0.05$, **Figure 6.12 B**).

Mitochondrial Amidoxime Reducing Complex 1 on the other hand, a mitochondrial antioxidant enzyme, was expressed at ~1.5 times higher levels in the isoprenaline treated groups than in the vehicle treated groups ($p<0.001$, **Figure 6.12 C**).

Isoprenaline administration also increased expression of the mitochondrial superoxide generator NADPH Oxidase 4 **(Figure 6.12 D,** $p<0.01$), also ameliorating a 2.9 fold loss of expression in the Px/Vehicle group (Px effect, $p<0.001$).

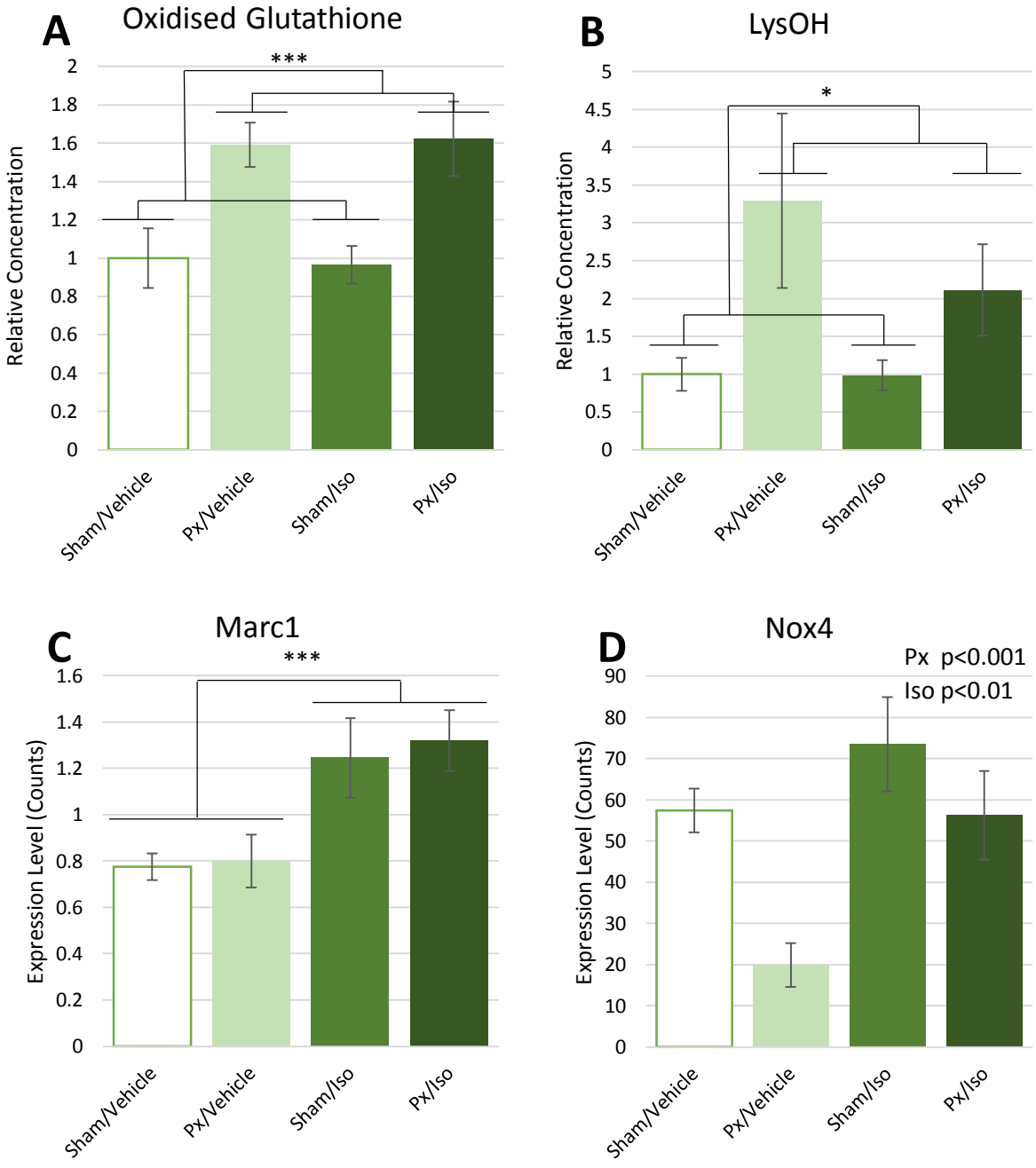

Figure 6.12: Concentrations of (A) Glutathione and (B) LysOH in cardiac tissue relative to control. Expression levels of (C) Mitochondrial Amidoxime Reducing Complex 1 and (D) NADPH Oxidase 4. Concentrations and expression levels displayed as mean ± SEM. 2-way ANOVA * = p<0.05, ** = p<0.01, *** = p<0.001 and **** = p<0.0001

6.3.8 Glucose Uptake Related Gene Expression

Expression of the glucose transporter, GLUT1, was decreased in Px/Vehicle animals relative to Sham/Vehicle, enhanced in the Sham/Iso group and decreased to a lesser extent in the Px/Iso group. This was an effect of both Iso and Px ($p<0.01$ and $p<0.0001$).

Insulin receptor transcripts were lower only in the Sham/Iso group relative to control, displaying both and effect of isoprenaline administration and an effect of pancreatectomy (both $p<0.05$).

TBC1D4, a GTPase which inhibits the translocation of glucose transporters to the cellular membrane, displayed lower levels of transcripts again only in the Sham/Iso group relative to Sham/Vehicle (Px effect, $p<0.05$, and Iso effect, $p<0.01$).

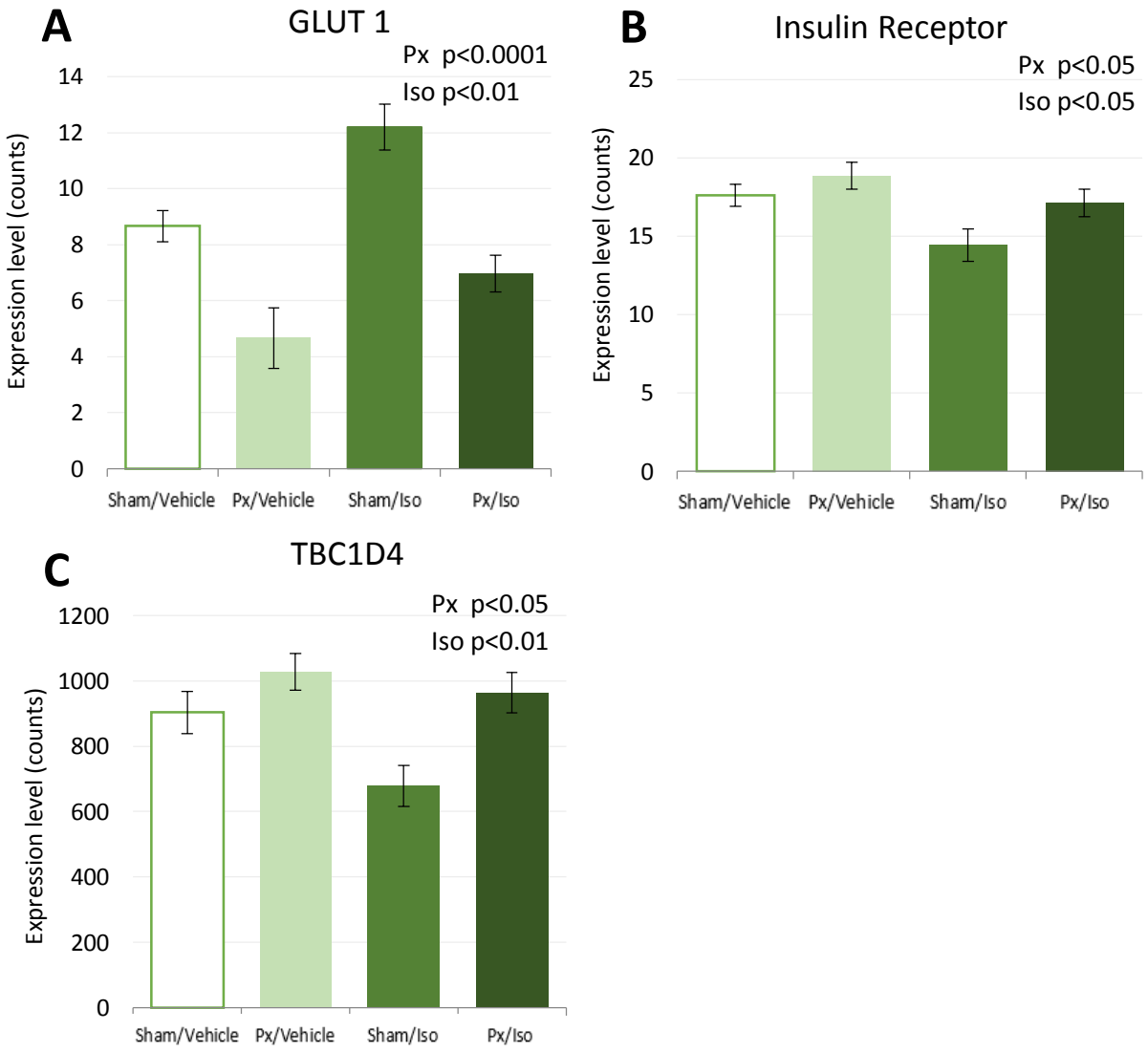

Figure 6.13: Expression levels of (A) GLUT1, (B) the Insulin Receptor and (C) TBC1D4 in cardiac tissue. Expression levels displayed as mean ± SEM. 2-way ANOVA * = $p<0.05$, ** = $p<0.01$, *** = $p<0.001$ and **** = $p<0.0001$

6.3.9 Fat Oxidation Enzymes

In order to investigate the mechanism behind the altered mitochondria fatty acid oxidation preference, gene expression levels of FAO related genes were examined.

Expression levels of CPT1b, HOADa and ACADvl were greater as an effect of pancreatectomy (~1.2 fold $p<0.0001$, ~1.65 fold $p<0.0001$ and ~1.4 fold $p<0.0001$ respectively).

Conversely, ACADs expression was repressed by around 20%, also as an effect of pancreatectomy ($p<0.0001$)

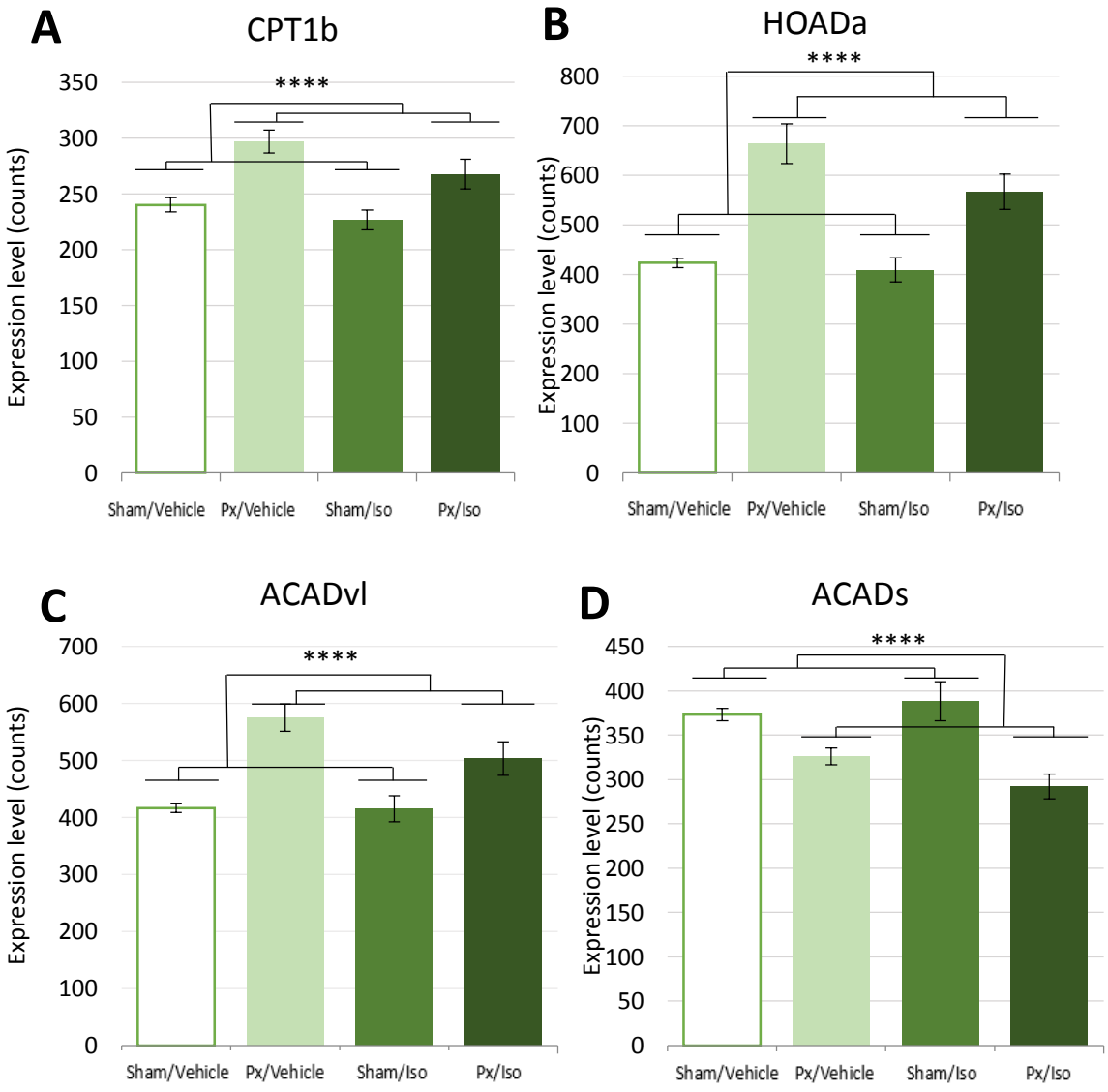

Figure 6.14: Expression levels of (A) CPT1b, (B) HOADa, (C) ACADvl and (D) ACADs in cardiac tissue. Expression levels displayed as mean ± SEM. 2-way ANOVA * = $p<0.05$, ** = $p<0.01$, *** = $p<0.001$ and **** = $p<0.0001$

6.3.10 PPAR Expression

Fat oxidation comes under the control of the Peroxisome Proliferator Activated Receptors (PPAR), the expression of which was thus examined.

Expression of the three main PPAR isoforms, α, β/δ and γ, was analysed employing RNAseq. PPAR β/δ was only expressed in the diabetic myocardium to 75% of the levels present in the Sham/Vehicle hearts. A similar but more pronounced expression shift was exhibited with PPAR α, with only 63% of the levels of Sham/Vehicle RNA transcribed in the Px/Vehicle group. In contrast, PPAR γ was expressed at 1.45 fold higher levels in the Px/Vehicle hearts than in the Sham/Vehicle ones, although this change was less pronounced in the Px/Iso hearts (1.15 x Sham/Vehicle).

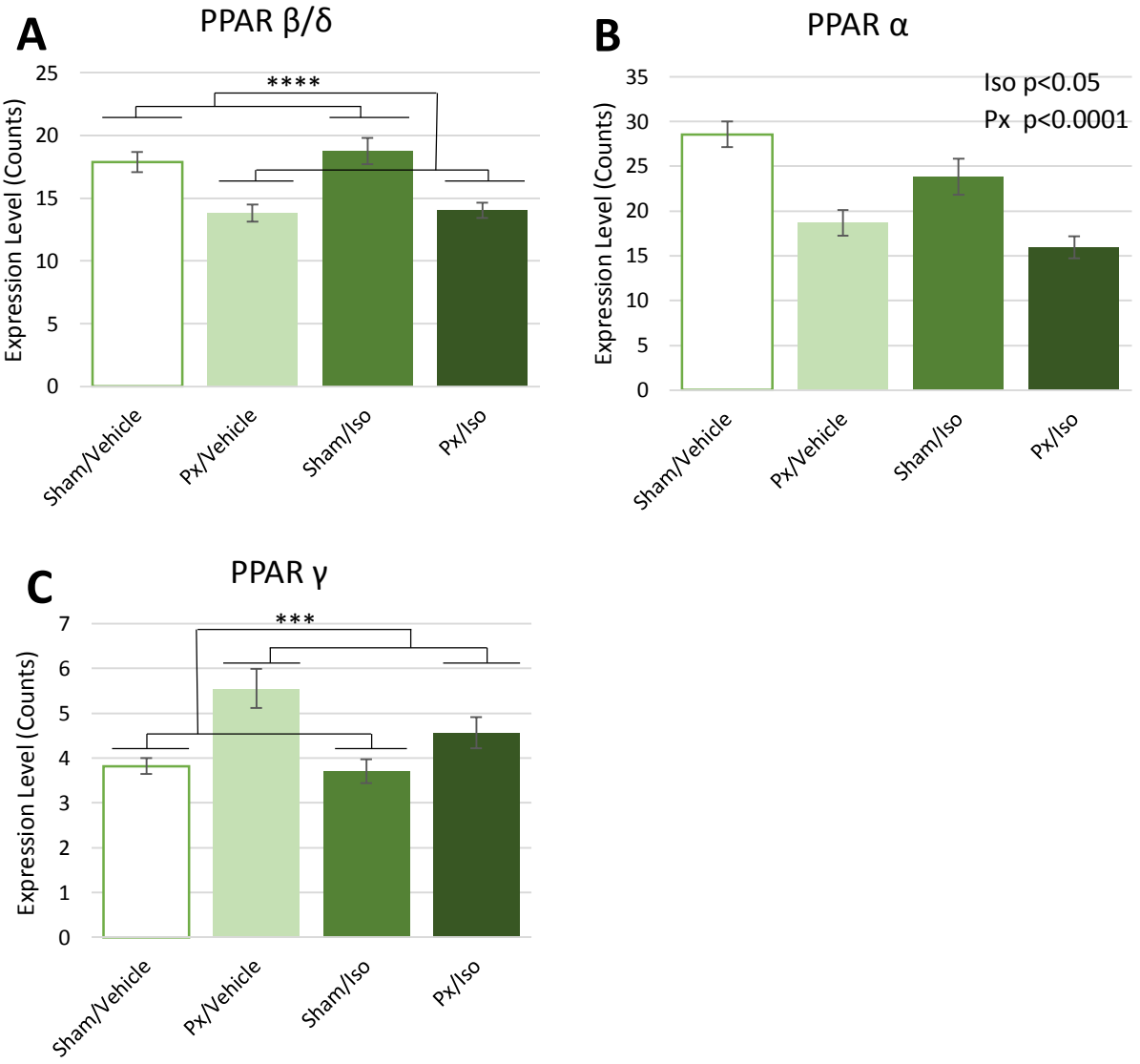

Figure 6.15: Expression levels of (A) PPAR β/δ, (B) PPARα and (C) PPAR γ in cardiac tissue. Expression levels displayed as mean ± SEM. 2-way ANOVA * = p<0.05, ** = p<0.01, *** = p<0.001 and **** = p<0.0001

6.3.11 Myotype Switching and Uncoupling Proteins

Expression of myosin Heavy Chain 7 increased in pancreatectomised hearts ($p<0.0001$; ~1.6 fold) when interrogated with RNAseq. Meanwhile, Myosin Heavy Chain 6 expression was suppressed ($p<0.0001$; ~2.4 fold).

The uncoupling proteins UCP2 and UCP3 both displayed greater levels of expression in the Px/Vehicle heart than in the Sham/Vehicle hearts (3.8 fold and 1.7 fold respectively). While this was an overall effect of diabetes with both ($p<0.0001$ and $p<0.01$ respectively), UCP2 was not expressed to a greater extent in the Px/Iso group than in the Sham/Iso group.

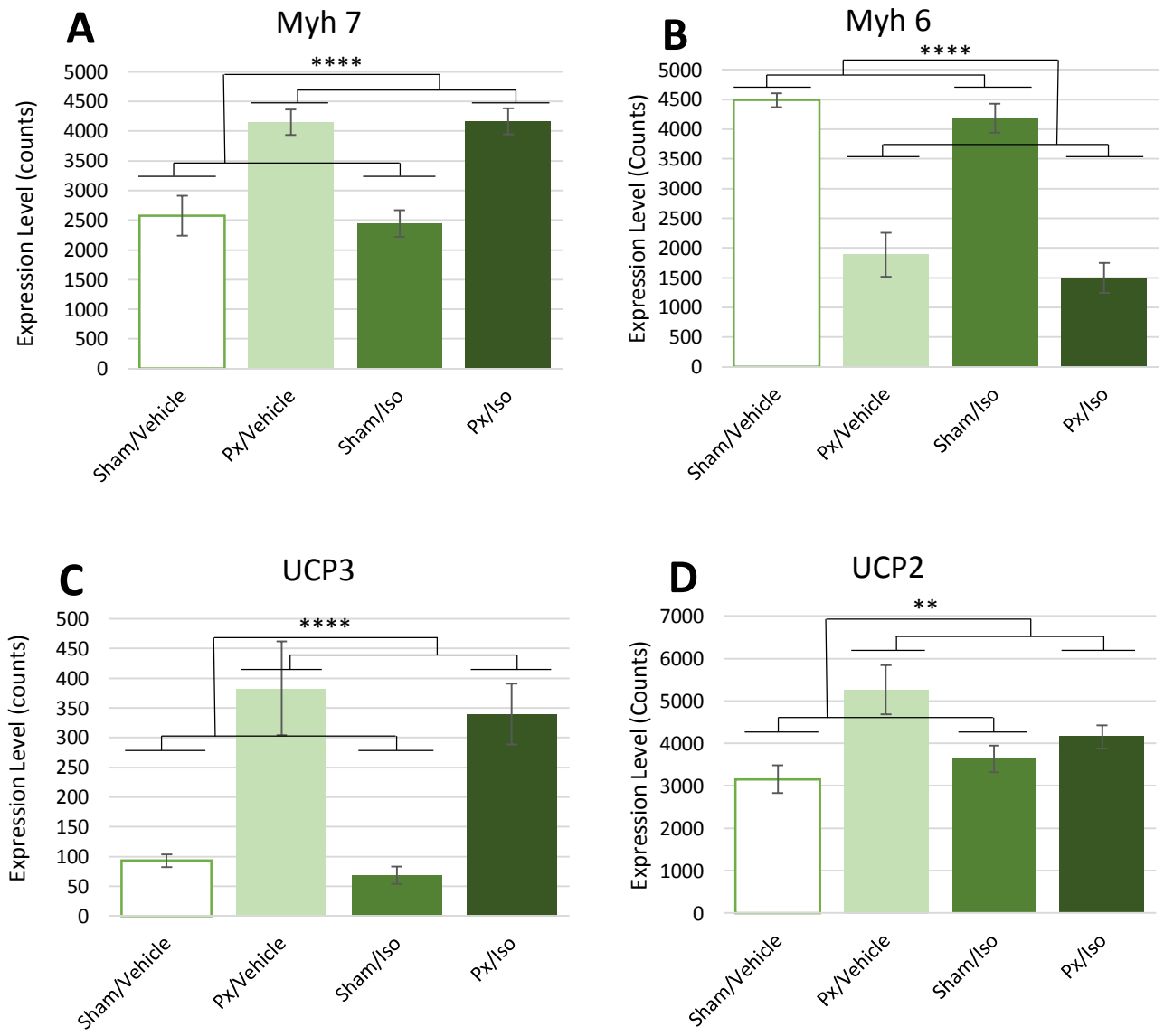

Figure 6.16: Expression levels of (A) Myosin Heavy Chain 7, (B) Myosin Heavy Chain 6, (C) Uncoupling Protein 3 and (D) Uncoupling Protein 2 in cardiac tissue. Expression levels displayed as mean ± SEM. 2-way ANOVA * = $p<0.05$, ** = $p<0.01$, *** = $p<0.001$ and **** = $p<0.0001$

6.3.12 Glycolytic Alterations

Levels of glycolytic intermediates were measured using LC-MS. Those intermediates prior to the enzyme aldolase were found to be increased as an effect of pancreatectomy (glucose-6-phosphate $p<0.01$; Fructose-1,6-bisphosphate $p<0.05$) (**Figure 6.17,** overleaf). Transcript levels for the initial enzyme involved in glycolysis, hexokinase (HK), were also found to be greater in the pancreatectomised groups (Px effect, $p<0.001$).

Transcript levels of the enzyme aldolase, however, were greater in the groups which had been administered isoprenaline (Iso effect, $p<0.001$). This was especially true for the Px/Iso group, which had aldolase (Aldol) transcript levels 1.75 times higher than those observed in the Px/Vehicle group.

Following aldolase, glycolytic intermediates were more prevalent in the Isoprenaline-treated groups than the vehicle treated groups. Expression of dihydroxyacetone phosphate, glyceraldehyde-3-phosphate and 2-phosphoglycerate/3-phosphoglycerate (chemically indistinguishable using this detection method because they have an identical molecular mass) were all observed to be higher (Iso effect, $p<0.05$, $p<0.01$ and $p<0.01$ respectively).

This suggests that despite higher flux through the early part of glycolysis in the pancreatectomised groups, induction of aldolase expression by isoprenaline administration serves to increase glycolytic flux in the Iso groups, potentially acting to help restore metabolic flexibility in the Px/Iso group.

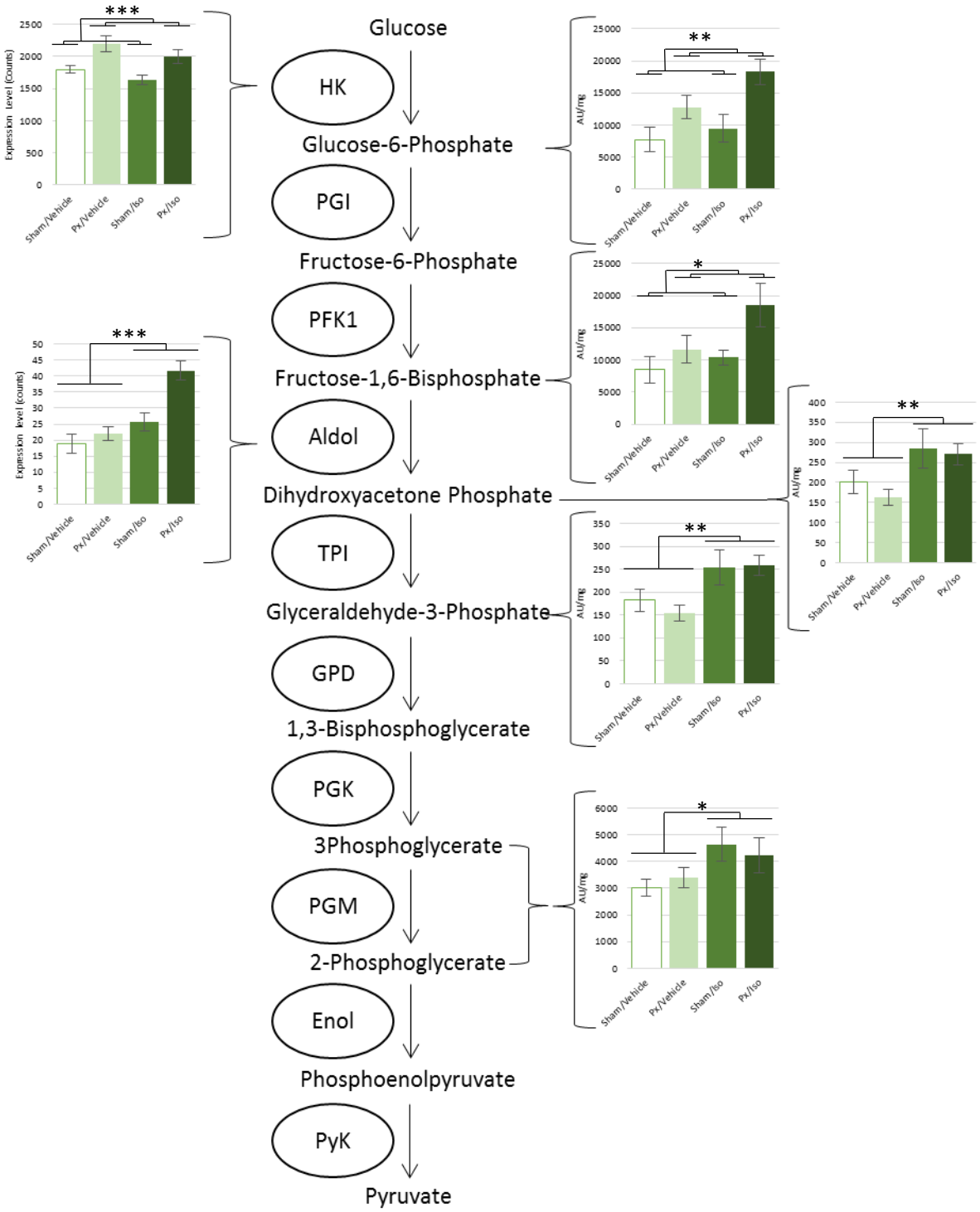

Figure 6.17: Concentrations of glycolytic intermediates (right) and expression levels of selected glycolytic enzymes (left) in cardiac tissue. Levels displayed as mean ± SEM. 2-way ANOVA * = p<0.05, ** = p<0.01, *** = p<0.001 and **** = p<0.0001

6.3.13 Regulation of Pyruvate Metabolism

Transcript levels of PDH Kinase 1, PDH Phosphatase Regulatory Subunit, Alanine Transaminase 2 and PDH Kinase 2 were each depressed in the groups subjected to Isoprenaline administration (all $p<0.05$)

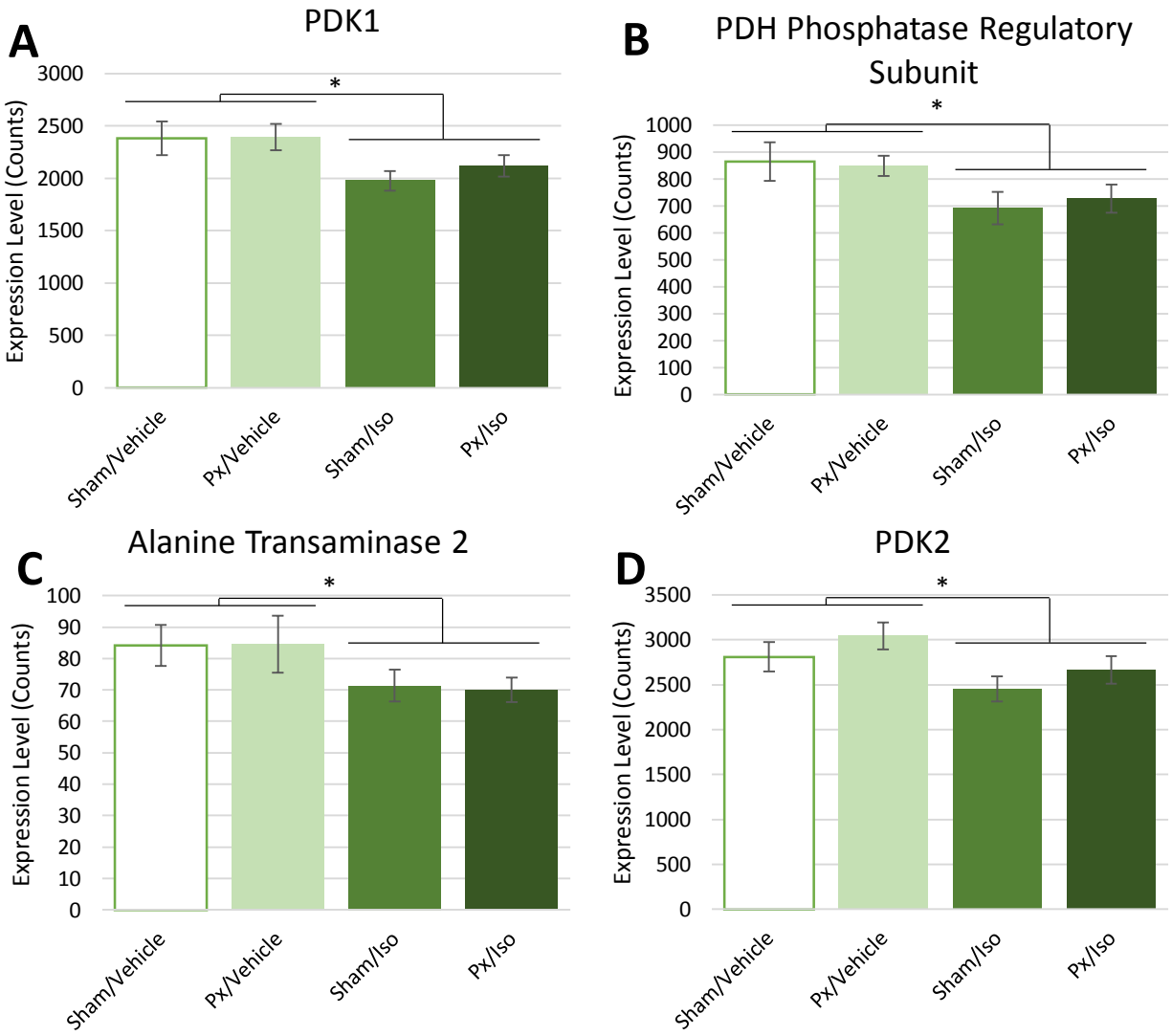

Figure 6.18: Expression levels of (A) Pyruvate Dehydrogenase Kinase 1, (B) Pyruvate Dehydrogenase Phosphatase Regulatory Subunit, (C) Alanine Transaminase 2, and (D) Pyruvate Dehydrogenase Kinase 2 in cardiac tissue. Expression levels displayed as mean ± SEM. 2-way ANOVA * = $p<0.05$, ** = $p<0.01$, *** = $p<0.001$ and **** = $p<0.0001$

6.3.14 Adrenergic Signalling

Expression of β-adrenoceptor 1A was decreased by 28% in the Sham/Iso group compared to Sham/Vehicle yet not in any other groups, manifesting as an effect of both Px and Iso (both $p<0.05$).

Meanwhile, Adenylyl Cyclase transcript levels were decreased in both the Px/Vehicle and Sham/Iso groups relative to Sham/Vehicle, with an even greater decrease visible in the Px/Iso group. Again both Px and Iso demonstrated an effect with 2-way ANOVA (both $p<0.05$).

Phosphodiesterase 3a expression was 1.28 fold greater in the Px/Vehicle group relative to Sham/Vehicle. However, isoprenaline administration decreased expression by around 20%, leading to a dual effect of isoprenaline ($p<0.05$) and pancreatectomy ($p<0.01$).

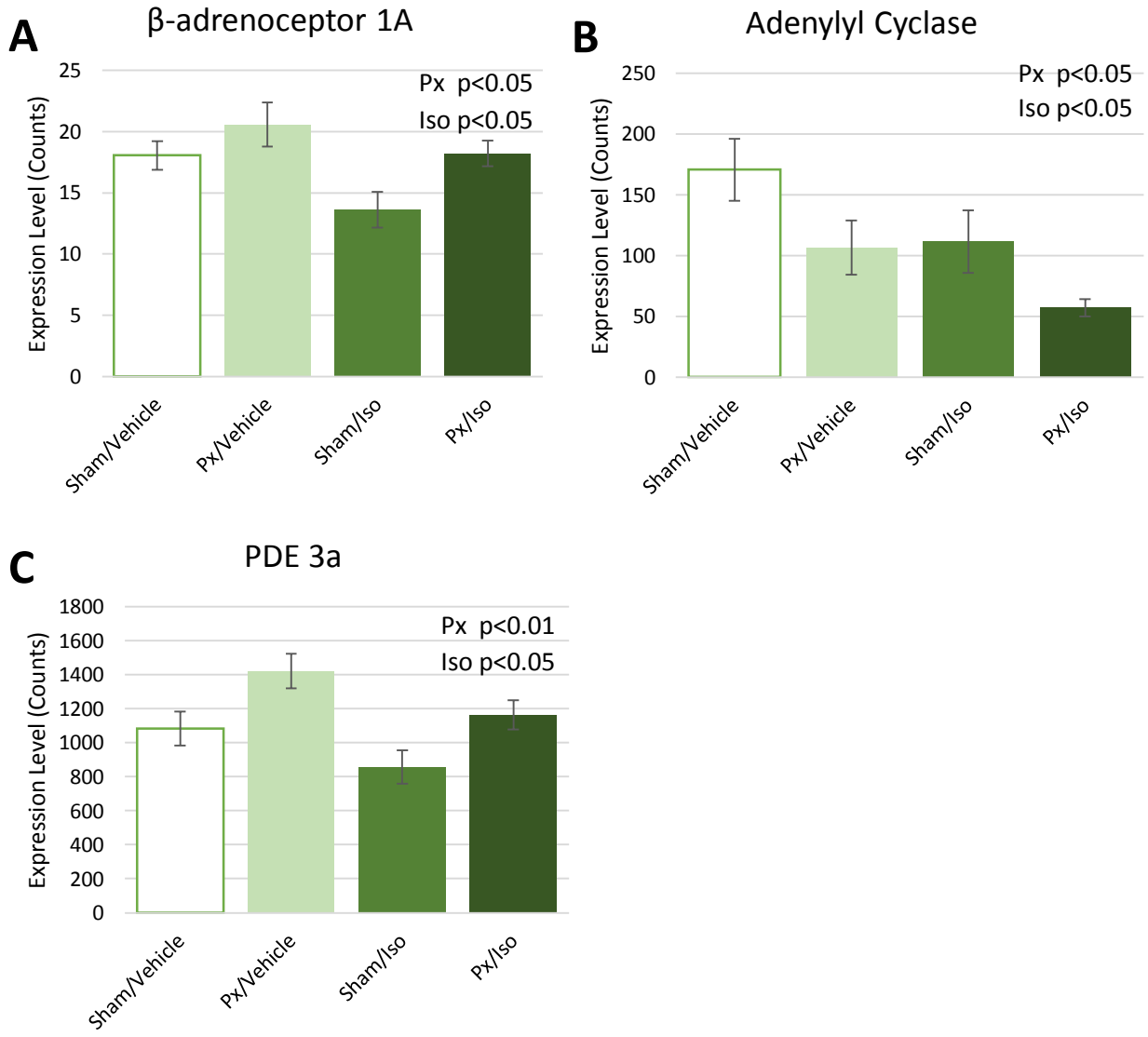

Figure 6.19: Expression levels of (A) β adrenoceptor 1A, (B) Adenylyl Cyclase and (C) Phosphodiesterase 3a in cardiac tissue. Expression levels displayed as mean ± SEM. 2-way ANOVA * = $p<0.05$, ** = $p<0.01$, *** = $p<0.001$ and **** = $p<0.0001$

BOX A

Ketogenesis in the Type 1 Diabetic Heart?

It was demonstrated in **Chapter 4** and **Chapter 5** that ketogenesis occurs in the ischaemic rat heart. In the type 1 diabetic heart, where oxidation capacity for fatty acids is higher and mitochondrial respiratory capacity lower than in the Sham/Vehicle group, a similar process may occur. Certainly, transcript levels for the "ketogenic" enzymes HMG-CoA lyase and synthase is higher as an effect of pancreatectomy (Figure 6.20, both $p<0.0001$), and that for the "ketolytic" enzyme SCOT is lower (px effect, $p<0.0001$). Tissue levels of β-hydroxybutyrate are higher in the hearts of pancreatectomised rats ($p<0.01$). However, it cannot be concluded from this that ketogenesis is occurring, as the enzymes involved are bidirectional and the β-hydroxybutyrate may have originated in other tissues.

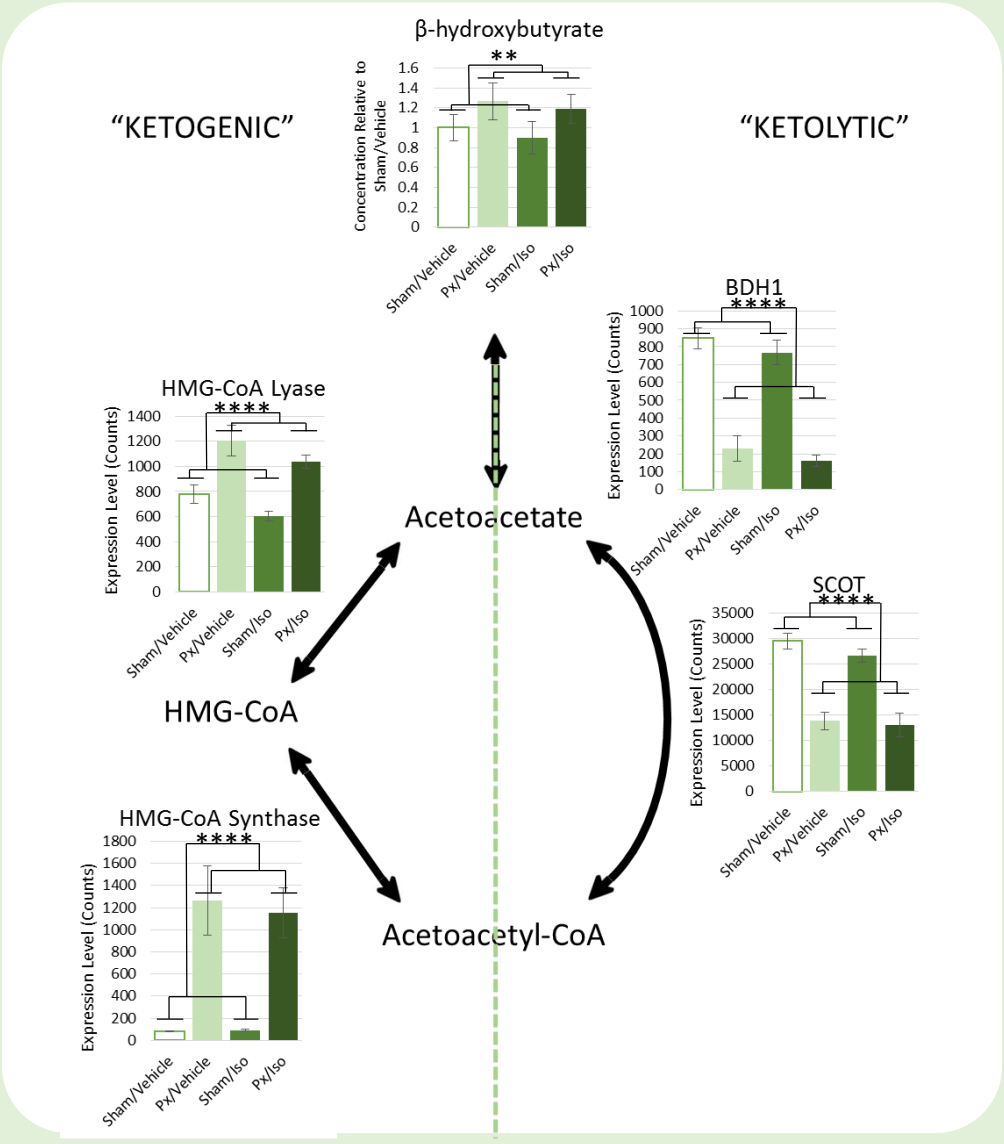

Figure 6.17: Concentration of β-hydroxybutyrate and expression levels of β-hydroxybutyrate dehydrogenase 1 (BDH1), HMG-CoA lyase, HMG-CoA synthase and succinyl-CoA-3-oxaloacid CoA transferase (SCOT) in cardiac tissue. Expression levels displayed as mean ± SEM. 2-way ANOVA ** = $p<0.01$ and **** = $p<0.0001$

6.4 DISCUSSION

Both isoprenaline administration and pancreatectomy impaired mitochondrial respiratory capacity in the rat heart. Further, pancreatectomy enhanced gene expression of FAO related enzymes, and meant that a greater proportion of maximal complex I supported respiration was accounted for by FAO. However, in combination pancreatectomy and isoprenaline administration interacted to result in preserved respiratory capacity and tissue energetics relative to the states engendered by either pancreatectomy or isoprenaline administration individually.

6.4.1 Strengths and Limitations of the Study

A great strength of this study came from the fact that it employed a combination of gold standard techniques which complemented each other well. The RNAseq gene expression data offered valuable insight into the metabolomics data, as particularly well exemplified by the identification of aldolase as the glycolytic gene which was expressed to a greater extent in the isoprenaline treated groups. This offered a great mechanistic explanation as to why the later glycolytic intermediates were present in greater concentrations in these groups. Likewise, data obtained from both techniques played a great part in elucidating the functional changes observed through the use of respirometry: for example, the gene expression data showed greater expression of FAO related genes which is likely to underlie the greater FAO preference which respirometry revealed in the Px/Vehicle group, despite an overall suppressed capacity. Metabolite data meanwhile revealed that a possible mechanism for restoration of metabolic flexibility in the Px/Iso group came from enhanced glycolytic flux, and that the higher mitochondrial respiratory capacity preserved the concentration of PCr produced.

Something which would have further complimented the dataset would have been the measurement of rates of metabolic flux as they occur *in vivo* or *ex vivo.* Respirometry offers a great insight into the maximal capacity of the mitochondria to sustain oxygen consumption supported by the different fluxes and pathways; however, these measurements are made under saturating concentrations of substrates and oxygen, and in the absence of physiological regulation, meaning that these measurements consider maximal capacity for flux through the pathways rather than the rates which occur in vivo. Gene expression data has similar shortcomings, with transcript levels not necessarily corresponding to actual protein levels, which in turn do not necessarily correspond to enzyme activity levels. Metabolite measurements using mass spectrometry do offer insight into the total pool sizes present in vivo at the time of termination, but not into the rate at which those metabolites are being turned over. It would therefore be good to investigate the rates of metabolic fluxes occurring in these animals when metabolism is not frozen, perhaps using hyperpolarised metabolites to trace flux *in vivo*

using MRI as employed by Le Page *et al.* (2015), or $U^{13}C$ labelling to assess contribution of glucose and fatty acid oxidation to the Krebs cycle using the model described in **Chapter 3**.

6.4.2 Consistency of the Physiological Models

Pancreatectomy as a Model of Type 1 Diabetes

Partial pancreatectomy rapidly induced hyperglycaemia, with fasted blood sugar levels plateauing at around 25 mM from four weeks post-operation. This was similar to that reported in a previous study of the 90% pancreatectomised rat (Yu et al., 2015). The greater levels of early glycolysis seen here were also observed in pancreatectomised humans (Del Prato et al., 1983), and this also correlates with patients with type 1 diabetes. Greater dependence upon FAO and loss of metabolic flexibility has also been reported in STZ models of type 1 diabetes (Arikawa et al., 2007; King et al., 2001; Le Page et al., 2015; Ritchie et al., 2017). It appears therefore that the 90% pancreatectomised rat model generated at Gubra ApS is a robust metabolic model of type 1 diabetes.

However, in this model no loss of contractile function resulted from the pancreatectomy alone **(Figure 6.8)** despite this being regularly reported in STZ models (Joffe et al., 1999; Nielsen et al., 2002). It is worth noting that in two other non-STZ models of type 1 diabetes, the partial insulin gene knockout Akita mice and the OVE2 knockout (Bugger et al., 2008; Liang et al., 2002; Lu et al., 2007), impaired contractile function was also either not noticeable or mild. There are therefore two possibilities: The first is that the 90% pancreatectomised rat was simply measured too early for contractile function alterations to have manifested, which would be addressable by running another study in which contractile function was assessed later; and the second is that the contractile effects of type 1 diabetes observed with the STZ models are in fact an effect of STZ not diabetes *per se* (Wold and Ren, 2004), and that true contractile dysfunction does not occur in the type 1 diabetic rodent heart.

Repetitive Isoprenaline Administration as a Metabolic Stressor

This study generated a model of isoprenaline induced cardiac dysfunction with similarities and differences to those reported previously. Jin *et al.* (2006) observed a similar loss of contractile function (impaired ejection fraction and fractional shortening) in dogs infused subcutaneously with isoprenaline. However, Desrois *et al.* (2014) delivered 5 mg/kg isoprenaline to rats daily via subcutaneous infusion, and observed an enhanced ejection fraction and ventricular mass over a 7 day period, which contrasts with the identical ventricular mass and decreased ejection fraction seen here. This data was obtained at the point of isoprenaline infusion though, while in this chapter the isoprenaline administration last occurred 4.5 weeks prior to termination, so if ventricular hypertrophy had occurred it could have subsided to be replaced by fibrosis and impaired ejection fraction by the

time of termination. Desrois et al. also observed no alterations to blood glucose concentration and bodyweight between isoprenaline and control groups, which corroborates the finding that Iso affected neither of these parameters in this chapter. In a similar model to Desrois et al., Heather *et al* (2009) observed fibrosis in the isoprenaline treated group similar to that reported in this study, as well as decreased FAO and decreased sensitivity to insulin which could corroborate the decreased insulin receptor expression **(Figure 6.13)** observed in this study. Cardiac fibrosis alongside contractile dysfunction following isoprenaline administration has also been reported in Sprague Dawley rats (Zhou et al., 2017) and mice (Brooks and Conrad, 2009). Death rate following subcutaneous isoprenaline injection had previously been reported at 10% for a single 100 mg/kg dose (Grimm et al., 1998), which is lower than the 43% mortality rate observed in this study; albeit in female rats rather than the male ones used here. Acikel *et al.* (2005) reported 33% mortality following a 150 mg/kg dose, although this is a greater dose than that employed in this chapter.

Pancreatectomy and Repetitive Isoprenaline Stimulation

The model of combining 90% pancreatectomy with 10 days of isoprenaline administraton has never been reported before. While possessing some characteristics previously reported in both models of type 1 diabetes and isoprenaline induced heart failure, it possesses some characteristics which set it apart from both. In line with both the Px/Vehicle group and a previous 90% pancreatectomy paper (Yu et al., 2015), the Px/Iso rats were hyperglycaemic with a fasted blood glucose concentration around 25 mg/L. However, unlike the Px/Vehicle rats and previously reported STZ type 1 diabetes models (Arikawa et al., 2007; King et al., 2001; Le Page et al., 2015; Ritchie et al., 2017)., they did not appear to have lost metabolic flexibility.

6.4.3 Significance of Results

Mitochondrial Capacity and Energetics

Total mitochondrial respiratory capacity and the function of complexes I and II was impaired in both the Px/Vehicle and Sham/Iso groups relative to Sham/Vehicle. Respiratory capacity has not previously been characterised in 90% pancreatectomised rats, yet the STZ model has in multiple cases been found to exhibit lower total respiratory capacity than that of controls (Duicu et al., 2017; Kiebish et al., 2012; Loiselle et al., 2014; MacDonald et al., 2011; Pham et al., 2014). The results in this chapter show that the 90% pancreatectomy model generated at Gubra ApS displays a similar impairment of respiration capacity to this other established model of type 1 diabetes. A further insight into the metabolic impairment of the type 1 diabetic rat was also offered: the FAO preference ratio, or the proportion of

complex 1 activity which could be saturated by fat oxidation alone, was significantly higher in the diabetic rats, indicating greater reliance on fat oxidation.

The Sham/Iso groups also displayed diminished mitochondrial oxygen consumption capacity compared with Sham/Vehicle, suggesting they too had compromised mitochondrial function. While the mitochondrial oxygen consumption following chronic administration of isoprenaline is not well characterised, it has previously been shown that ETC complexes and Krebs cycle enzymes are less active (Punithavathi et al., 2010). In combination with the depressed respiratory capacity seen here, this suggests that isoprenaline administration instigated mitochondrial dysfunction.

However, the reduction in mitochondrial function observed in both the Px/Vehicle and Sham/Iso groups was partially abolished in the Px/Iso rat hearts. Leak state and oxphos respiration, along with the capacity of both complex I and complex II, were not significantly different in the Px/Iso group compared with Sham/Vehicle hearts. This suggests that whatever the source of the stress which causes loss of mitochondrial function in Px/Vehicle and Sham/Iso hearts, the two counteract each other in combination. An interesting lead into the mechanism behind this is the fact that the FAO ratio was not increased (and was if anything decreased) between the Sham/Vehicle and Sham/Iso groups, suggesting the possibility that isoprenaline administration also reverses the dependency of type 1 diabetic hearts upon fat oxidation.

Metabolic Flexibility

Examination of FAO enzyme expression helps give insight into the mechanism behind the higher proportion of mitochondrial respiratory capacity accounted for by FAO in the Px/Vehicle heart. Transcripts encoding the majority of enzymes and proteins involved in the importation of fats to the mitochondria and the β-oxidation of fats (ACADs and HOAD) were upregulated in the Px groups; although perhaps less so in the Px/Iso group. This upregulation may explain the increased FAO ratio in the Px/Vehicle group, as the extra facility for β-oxidation allows it to account for more of the mitochondrial ETC capacity. Nevertheless, the Px/Iso groups still exhibit an upregulation of fatty acid oxidation genes. This suggests that if they have a greater metabolic flux through the fat oxidation pathways and yet the mitochondrial capacity is not as saturated by this as in the Px/Vehicle group, then other metabolic pathways may also be upregulated in the Px/Iso animals in order to balance out the fluxes.

This is best demonstrated in the glycolytic pathway, where an upregulation of aldolase appears to underpin enhanced glycolytic flux in the Iso treated hearts. Prior to aldolase, the early glycolytic

intermediates appear in greater concentrations in the Px groups; yet following aldolase, which is a hypoxia regulated enzyme, there is greater flux through glycolysis in the isoprenaline treated groups. Others have indicated that adrenergic stimulation induces an increased glycolytic rate (Clark and Patten, 1984; Depre et al., 1998), and it appears that this may be allowing the Px/Iso group to counterbalance enhanced expression of FAO enzymes relative to Sham/Vehicle with similarly higher glycolytic flux, restoring some metabolic flexibility and allowing for conservation of mitochondrial function..

This case is further supported by the expression of enzymes which control entrance of pyruvate into the mitochondria and oxidative phosphorylation. Inhibitory enzymes, such as PDH kinases 1&2 which phosphorylate and inactivate PDH, and the subunit by which PDH phosphatase (which reverses this inhibition) is itself phosphorylated and inactivated, are downregulated in hearts which underwent isoprenaline administration. PDH flux has previously been reported to be enhanced by isoprenaline (Hiraoka et al., 1980), and this lower expression of PDH kinases 1 and 2 may underlie a mechanism. This suggests that the enhancement of glycolytic flux does not purely support anaerobic metabolism, and that the pyruvate is fated to be oxidised in the mitochondria.

A further glucose metabolism related gene of interest is the glucose transporter, GLUT1. GLUT1 is responsible for glucose uptake from the blood, and has also been reported to be downregulated in an STZ model of diabetes (Šoltésová et al., 2013). However, in the Sham/Iso group, GLUT1 transcripts were higher than in Sham/Vehicle, suggesting that isoprenaline stimulates a greater uptake of glucose and corroborating a previous finding that isoprenaline led to greater expression of GLUT1 in the heart (Egert et al., 1999). The insulin receptor is also downregulated in the Sham/Iso group alone, which is an indicator that perhaps control of glucose uptake is wrested from insulin signalling by a response to isoprenaline. In the Px/Iso group, these two stimuli appear to balance each another out, with isoprenaline stimulation reducing the amount that GLUT1 expression is downregulated by pancreatectomy.

Adrenergic Signalling

The mechanism for this apparent protection of the diabetic heart is therefore intriguing. Previous studies have demonstrated that the diabetic heart is less responsive to β-adrenergic stimulation (and specifically with isoprenaline) than the healthy heart (Roth et al., 1995), which would help explain the lack of mortality in the Px/Iso group compared with the sham-operated rats. Adrenoceptors can be desensitised, either at the membrane or at the expression level in response to prolonged and

excessive stimulation. B-adrenoceptor A1 is expressed to a lesser extent than Sham/Vehicle in the Sham/Iso but not the Px/Iso group. This mirrors findings that β-adrenoceptors are downregulated in the isoprenaline induced failing heart (Yin et al., 2016), and suggests that isoprenaline stimulation of the β-adrenoceptor may not be having the same intensity of effect in the pancreatectomised animals. It has been reported before both *ex vivo* and *in vivo* that diabetic hearts are less sensitive to isoprenaline stimulation than their non-diabetic counterparts (Gtzsche, 1983; Roth et al., 1995). While β-adrenoceptor levels themselves have remained unchanged in the diabetic heart, a functional uncoupling between the β-adrenoceptor and downstream effectors including adenylyl cyclase has been reported (Bockus and Humphries, 2015; Gtzsche, 1983). This would appear to be evident in the findings of this study too, given that while β-adrenoceptor expression remains unchanged in the Px/Vehicle heart relative to Sham/Vehicle, adenylyl cyclase expression is suppressed. This suppression is further exhibited in the Sham/Iso group, presumably as a continuation of the isoprenaline mediated desensitisation, and in the Px/Iso group the effects are additive. It is therefore probable that decreased sensitivity of the Px heart to isoprenaline, coupled with the phenomenon that isoprenaline stimulation is augmented by insulin (Almira and Misbin, 1989) means that isoprenaline does not exert such a damaging effect upon Px hearts as it does upon the sham operated ones. This would explain the lack of mortality in the Px/Iso group as well as the observation that the Px/Iso group exhibits better preserved cardiac mitochondrial function and energetics than the Sham/Iso group. Further, the extra adenylyl cyclase downregulation from isoprenaline administration could then protect the diabetic heart from subsequent progression of the disease through chronic adrenergic stimulation.

6.4.4 Future Directions

The exact mechanism through which isoprenaline and pancreatectomy mutually protect the heart from the detrimental effects of the other is of great interest and deserving of further investigation. It would be interesting to conduct an experiment in which Px and Sham hearts were perfused in Langendorff mode and then exposed to isoprenaline stimulation in order to directly establish the acute effects of isoprenaline in each situation upon both contractility and substrate oxidation, perhaps again using U-^{13}C labelled substrates. Similarly, use of increasing doses of dobutamine as used by Choi *et al.* (1997) would allow a dose response curve and assessment of β-receptor desensitisation to be conducted, an assessment which could also be used to analyse whether the Iso administered groups were less susceptible to chronic β-adrenergic stimulation

Another potential follow up experiment would be to terminate the experiment and assess the hearts immediately after Isoprenaline administration. The insights gained from this would be twofold. Firstly, if the Px groups displayed similar respiratory capacity and energetics to those of the Px/Iso group at ten weeks, it could be that isoprenaline administration arrested the progression of type 1 diabetes in the heart. If, on the other hand, respiratory capacity and energetics were already further deteriorated than observed here in the Px/Iso group, then the implication would be that Iso reversed the process. Secondly, it would show how the results presented here sit on the timeline of recovery from isoprenaline administration, determining whether they initially manifested the hypertrophy seen in previous papers (Desrois et al., 2014; Grimm et al., 1998; Heather et al., 2009), but over the following 4.5 weeks returned to a normal heart weight.

CHAPTER 7

DISCUSSION

7.1 SUMMARY OF FINDINGS

The studies presented in this thesis aimed to investigate the manipulation of cardiac metabolism in various pathological states. Initially, the effects of dietary nitrate and intralipid on the recovery of the heart from ischaemia/reperfusion were examined. When this revealed that ketogenesis occurred in the ischaemic heart, the next step was to interrogate this the mechanism underlying this process, and the implications for cardiac recovery. In the final chapter, metabolism was investigated in the diabetic heart, examining how the type 1 diabetic heart responded to metabolic stress.

In **Chapter 3,** a method was developed for the interpretation of ^{13}C labelling patterns in the Krebs cycle, in order to determine the proportional oxidation of different substrates.

Chapter 4 presented a study into the effects of dietary nitrate supplementation upon the heart's capacity to recover from ischaemia/reperfusion. Sodium nitrate supplementation enhanced the functional recovery of the heart following reperfusion in the absence of triglyceride in the perfusion buffer. However, when triglyceride was added to the perfusion mix, nitrate supplementation impaired the recovery of the heart. The intralipid by itself had cardioprotective effects. Neither the effects of dietary nitrate supplementation nor intralipid protected mitochondrial respiratory capacity, which was the same in all groups following reperfusion. However, a surprising effect of nitrate supplementation appeared to be the enhancement of levels of the ketone body β-hydroxybutyrate present in the ischaemic myocardium, despite none being present in the initial composition of the buffer. This suggested that ketogenesis had occurred in the ischaemic heart

Ischaemic ketogenesis was further investigated in **Chapter 5**. Unlike in the liver, ischaemic ketogenesis in the heart was not a result of fat metabolism exceeding metabolic demand, with the proportion of fatty acid to glucose oxidation remaining unaltered during ischaemia. It appeared instead that ketogenesis in the heart was driven by a combination of the reductive environment and accumulation of acetyl-CoA induced by ischaemia. Diverting greater levels of pyruvate to acetyl-CoA through the inhibition of LDH increased the concentration of β-hydroxybutyrate. Furthermore, inhibition of ketogenesis, using the HMG-CoA synthase inhibitor hymeglusin, improved functional recovery of the heart following reperfusion, suggesting that the accumulated of β-hydroxybutyrate is detrimental. This comes despite the observation that β-hydroxybutyrate suppresses inflammasome activation, with hymeglusin engendering an increased inflammatory state in the ischaemic heart tissue.

Chapter 6 investigated the resilience of the type-1 diabetic heart against chronic stimulation with Isoprenaline. Mitochondrial respiratory capacity was impaired in the rat heart following 90% pancreatectomy, with a substrate switch towards fatty acid oxidation being observed alongside greater expression of FAO-related enzymes and evidence of oxidative stress. Isoprenaline treatment

also impaired respiratory capacity, but enhanced flux through glycolysis through increased aldolase expression. In the hearts of Isoprenaline treated pancreatectomised rats, mitochondrial respiratory capacity was preserved, and whilst myocardial PCr was depleted following pancreatectomy, this too was conserved when pancreatectomised rats had been administered isoprenaline. Uncoupling of adrenergic signalling through repression of adenylyl cyclase by both isoprenaline and pancreatectomy may underpin this apparent protection.

7.2 CRITIQUE OF EXPERIMENTAL TECHNIQUES

7.2.1 Langendorff Perfusion

Control over supply of metabolic substrates

In this thesis, the Langendorff method of heart perfusion has conferred the great advantage that it has allowed the control of substrate supply to the heart. By varying the supply of substrates in the buffer supplied to the Langendorff heart, the capacity to study how metabolite supply influences cardiac function and metabolism in a controlled manner was gained. This kind of study is not practical in the *in vivo* heart, given the impossibility of removing all fatty acids from the circulating blood supply, or precisely regulating the concentration of fats in the blood. It is a strength of several studies which have examined *ex vivo* cardiac function with and without various fats in the buffer (King et al., 2001; Lou et al., 2014a), allowing determination of the effect upon the heart, and in this thesis allowed the elucidation of the interaction between dietary nitrate supplementation and cardiac triglyceride use **(Chapter 4)**. It also allowed measurement of cardiac triglyceride uptake, as we know the concentration of lipid entering and leaving the heart varies, and the identification of cardiac ketogenesis because it was possible to say with certainty that no β-hydroxybutyrate was being supplied to the heart from other tissues. Perfusion with oxygenated KH buffer is removed from a physiological situation however. Aside from being less effective at transporting oxygen than blood, the 11 mM glucose used here in the buffer in order to ensure cardiac glucose uptake must be high compared to blood glucose levels, in part to overcome the lack of insulin to stimulate glucose uptake. All manners of other substrates and cardio-effective hormones circulate in the blood, and it is both a disadvantage and an advantage to exclude these from the system: reproducibility and simplicity of the experiment confer greater power to see metabolic alterations, yet the system is further removed from the conditions present *in vivo* and this caveat must be considered when drawing conclusions from the Langendorff perfused heart.

Pharmacological Manipulation

The Langendorff heart preparation also offers a reproducible framework for investigating the effects of drugs and other compounds on the heart (Lateef et al., 2015). In a similar manner to metabolites, pharmacological compounds could be added to the perfusion buffer at any point during the perfusion protocol. This allowed effects on the function and metabolism to be taken into account, as well as more subtle effects such as how they influence the heart's ability to recover from a period of ischaemia. Introducing these compounds to the Langendorff preparation had several other advantages; it negated the effect of any systemic effects the compound may have, allowing characterisation of the cardiac effects alone; and it meant that the concentration of the drug administered could be much more easily controlled without the influence of pharmacokinetic effects. The setup also allowed easy use of non-clinically approved compounds, such as hymeglusin, as there could be no off-target side effects (Verdouw et al., 1998).

Low-Flow Ischaemia

In contrast to total global ischaemia, during which all supply of buffer to the heart ceases, the ischaemia reperfusion protocols used in this thesis involved low-flow ischaemia. It is rare during a clinical case of ischaemia that all blood flow to the heart is removed; more usually the vessel is partially occluded with a diminished supply of blood still and low-flow ischaemia replicates this (Verdouw et al., 1998). During aerobic perfusion at 100 mmHg the rate of coronary flow was as high as 40 ml/min, however during low-flow ischaemia this could fall to 0.5 ml/min. However, this low flow rate still allows delivery of some substrate, whilst ischaemic products and biomarkers are washed out, and can be detected using LC-MS allowing insight into the metabolic response to ischaemia.

Strengths and Limitations of the Langendorff Heart as a Model of Ischaemia/Reperfusion

Investigation of Ischaemia/Reperfusion using the Langendorff preparation is common. Whilst there are other models for investigating ischaemia/reperfusion including *in vivo* ligation of the coronary arteries, Langendorff perfusion offers clear advantages. In the *in vivo* scenario, an anaesthetised rat has its chest opened and one of the coronary arteries is ligated. This could be argued to be more physiological than the Langendorff ischaemia/reperfusion model, however the presence of anaesthetic plus the severe physiological stress of having the chest cavity opened could have a large influence upon results. Presence of actual blood rather than perfusion buffer could be considered an advantage or a disadvantage, being more physiological and having a greater oxygen carrying capacity than KH buffer yet offering less control over its constituents. Low flow ischaemia in the Langendorff heart also allows the infliction of a more consistent degree of ischaemia than is possible *in vivo*,

allowing more consistent results to be obtained and offering more power to see differences between experimental groups. The fact that the heart is still part of a closed circulation and under the influence of anaesthetic and the nervous system *in vivo* also makes it harder to interpret measurements of cardiac function than the more comprehensively analysable Langendorff heart. The Langendorff perfused heart therefore has limitations, but represents a more controlled experimental platform for investigation of ischaemia/reperfusion.

7.2.2 High Resolution Respirometry

Suitability of Preparation of the Biological Samples for Respirometry

Although the most physiological quantitation of respirometry in biological samples would be *in vivo* or in intact tissue, in practice this is less practical and does not have the resolution to see alterations in the mitochondrial machinery. Measurement of oxygen consumption in the whole animal cannot distinguish between tissues and does not allow the use of compounds like mitochondrial complex inhibitors to investigate ETC flux in more depth. Meanwhile, intact cells enable the investigator to distinguish which tissue they originate from, but are not permeable to certain inhibitors and substrates, limiting the number of assays which can be used. Both methods also fail to account for the concentration of endogenous metabolites, ADP and other metabolically active components, meaning it is difficult to accurately quantitate what the limiting factor on mitochondrial function is.

For these reasons, permeabilisation of cardiac fibres was chosen as the method through which to measure mitochondrial oxygen consumption in this thesis. Conducting respirometry upon isolated mitochondria has other advantages, including the ability to quantify the mitochondrial density of the tissue, isolate separate sub-populations of mitochondria and offer a direct measurement of how many molecules of ADP are consumed per oxygen atom. However, mitochondria are not isolated organelles within the cell, operating in a system with the cytoskeleton and cytoplasmic enzymes to effect transportation of substrates and products into and out of the mitochondria. Isolation of mitochondria can result in both deformation of their structure and destruction of the network they operate in within the cell, while the choice to use permabilised LV fibres meant that these systems remained intact (Kuznetsov et al., 2008). Washing the permeabilised tissue preparation in this state also removed endogenous substrates and ADP, meaning that measurements could be made in the confidence that leftover metabolites from before the preparation would not affect respiration.

Strengths and Limitations of the Measurement of Mitochondrial Oxygen Consumption

Since oxygen consumption at the ETC is a function of electron flux, it offers a reliable way to observe respiratory capacity, flux through various metabolic pathways and the function of different ETC complexes. However, given that it was measured *ex vivo*, and in the presence of saturating concentrations of experimentally administered substrates, the respirometry employed in this thesis indicates maximal cellular capacity for respiration rather reflecting respiration *in vivo*. Oxygen level was also maintained in the oxygraph chambers throughout the protocol, which is a necessity of measuring oxygen consumption to overcome diffusion gradients yet means that limitations of oxygen concentration which occur *in vivo* or in conditions such as ischaemia are not replicated. Further, post translational modifications such as the phosphorylation of PDH may be lost outside of the physiological system. Given all of the above, it is important to note that the respirometry data presented in this thesis represents the maximal capacity of the system for oxygen consumption in the given conditions, and that it has the caveat of not necessarily being a representation of the rates which occur *in vivo*.

7.2.3 Mass Spectrometry

Metabolic profiling using liquid chromatography coupled mass spectrometry has worked well combined with both langendorff perfusion and high resolution respirometry in this thesis. Mass spectrometry allows assessment of levels of metabolites present in a tissue at the point the sample was frozen, so metabolite levels following, for example, the imposition of ischaemic conditions using the Langendorff protocol, can be directly assessed at the point of analysis. Measurement of compounds in this way allows only the measurement of metabolite levels, and not of the flux through the pathway under those conditions. Thus a metabolite may be present in higher levels due to greater flux through the pathway, or because inhibition of an enzyme has led to its accumulation. Combination of this technique with measurements of maximal metabolic rates, such as those obtained through respirometry, or with carbon labelling flux analysis such as that used in **Chapter 3**, can help to overcome this issue.

A potential drawback of using this kind of mass spectrometry is that it is a semi-quantitative technique rather than one which allows easy quantitation of metabolite levels. Due to variations between sample batches, it is possible to directly compare levels of metabolites between samples run at the same time, but not with those run at different time points. This means the results may be assessed

relative to those in a control sample, but that for quantification of metabolites and comparison of concentrations between different metabolites a concentration ladder of known concentrations would have to be run for each compound on each experimental run in order to make the technique quantitative. Owing to the sheer number of metabolites assessed in each sample, alongside the number of extra sample runs this would represent, this would be prohibitive. However, in this thesis the semi-quantitative analysis was not a limitation, as I was assessing how different experimental conditions altered metabolite levels relative to those in control samples.

7.3 THIS THESIS IN THE CONTEXT OF THE WIDER FIELD

7.3.1 Fat Oxidation in the Ailing Heart

Pathological, Beneficial or is the Key a Balanced Diet?

While there have been some papers pronouncing the benefits of FAO in ischaemia, there is also a large volume of work indicating that excess FAO is detrimental (Lopaschuk et al., 2009). Controversy therefore remains.

The work presented in **Chapters 4 and 5** appears to contradict the school of thought that FAO occurs excessively and is pathological during ischaemia on several counts. Hearts perfused with intralipid in the buffer appeared to recover contractile function to a greater extent than those given only glucose in the perfusion buffer upon reperfusion from ischaemia, and while exhibiting increased mitochondrial uncoupling they also appeared to have enhanced ATP production. This suggests a cardioprotective effect of circulating triglycerides, which has also been observed in several other studies involving FAO during ischaemia (King et al., 2001; Li et al., 2013; Lou et al., 2014c, 2014a; Rahman et al., 2012)

Meanwhile, despite claims that FAO increases during ischaemia due to decreased malonyl-CoA production (Fillmore et al., 2014), in **Chapter 5** malonyl-CoA was seen to be increased in the ischaemic heart. This would suggest a decrease in capacity for FAO through inhibition of CPT-1 (Hue et al., 2009), which was supported by the finding that cardiac uptake of triolein was almost completely attenuated during ischaemia, and that the proportional contribution of acetyl-CoA derived from glucose oxidation relative to that derived from FAO was unchanged. A lack of increase in FAO during ischaemia is a finding mirrored in older studies (Opie et al., 1973; Whitmer et al., 1978), and makes sense when considering that with oxygen as a limiting factor during ischaemia, there is a benefit to a switch towards more oxygen-efficient substrates.

This discrepancy may be due to experimental differences. Kudo et al. (1995) observed decreased malonyl-CoA concentrations during ischaemia, and then a further fall after reperfusion. They did however use a more severe ischaemic protocol than that used during this thesis (30 min total global ischaemia), which immediately presents two possible reasons as to why they observed decreased ischaemic malonyl-CoA levels. The first is that they may simply have caused more damage to the myocardium, which would reduce the overall oxidative capacity of the heart and therefore ability to synthesise malonyl-CoA. Secondly, through obstructing all substrate delivery to the heart during the ischaemic period, they would have removed the supply of the substrates from which malonyl-CoA is synthesised. This also limited their ability to measure cardiac fatty acid uptake during ischaemia, and extrapolated from the increased rate of fatty acid uptake upon reperfusion to assume that FAO had

also increased in the ischaemic heart. Notably, they also observed no difference in either CPT-1 or ACC activity levels at the end of ischaemia relative to pre-ischaemia. The low-flow ischaemia used in this thesis offers a different capacity to observe metabolism in the ischaemic heart, with a severe reduction in flow rate resulting in an ischaemic heart, yet not denying the myocardium the metabolic substrates which would be available to it in the physiological setting and allowing measurement of metabolic flux and substrate uptake throughout the ischaemic period.

Taken together, it seems that FAO may have become an unfairly maligned villain during cardiac ischaemia. While the data presented in this thesis cannot contest that which has been observed in total global ischaemia, in the model of low-flow ischaemia employed here and previously (King et al., 2001; Li et al., 2013; Lou et al., 2014c, 2014a; Opie et al., 1973; Rahman et al., 2012; Whitmer et al., 1978), FAO during ischaemia has been found not only to not be increased, but also to be conducive to enhanced functional recovery. The implications of this are that clinically reperfusing patients with fatty acids or pharmacologically attempting to enhance FAO may in fact be beneficial in cases presenting with ischaemic heart disease.

Separately, in the diabetic myocardium, increased FAO capacity was only associated with impaired mitochondrial respiration and energetics when glycolytic flux was not increased in tandem. In **Chapter 6** it was demonstrated that in the 90% pancreatectomised rat increased FAO capacity was observed through both mitochondrial oxygen consumption rates and FAO associated gene expression. This correlated with impaired mitochondrial respiratory capacity and energetics. Yet in pancreatectomised rats which were repetitively administered isoprenaline between 5 and 7 weeks post-operation, overall mitochondrial respiratory capacity was conserved whilst FAO associated gene expression and oxygen consumption were still enhanced. Suggestion that enhanced capacity for, and rate of, FAO results in lipotoxicity and associated pathology (Bayeva et al., 2013) may therefore only hold if there is a concurrent loss of metabolic flexibility. Restoration of flexibility may be an important avenue to explore in terms of treatment of diabetes mellitus, and therefore future exploration using tools such as inducible knockout models for both the glycolytic and FAO pathways to further establish the importance of flexibility over one pathway or the other could offer much insight.

7.3.2 The Heart as a Setting for Ketogenesis

Net ketogenesis has never before been reported to occur in the intact heart. The work I present in this thesis is the first to my knowledge to do so, and goes further yet in attempting to establish the mechanism for this ketogenesis, and whether it is beneficial or detrimental to recovery from ischaemia/reperfusion. The requisite enzymes are all known to have been present in the heart, so why has nobody observed cardiac ketogenesis before?

Most probably, nobody has thought to look. Krebs et al. (1961) came close when homogenised ovine heart tissue to observe that sodium amytal, a mitochondrial complex I inhibitor, resulted in the reduction of acetoacetate to β-hydroxybutyrate. They did not, however, investigate whether this process occurred in any pathophysiological situations in the intact heart.

Conversely, Fink et al. (1988) demonstrated that there was bidirectional flux through the ketogenic pathway in the perfused working rat heart through measuring dilution of a (3R)-hydroxybutyrate tracer pool, yet did not observe any net accumulation of ketone bodies in the heart. The conclusion this paper drew was therefore that this process was negligible, and reflected the fact that the capacity of the reversible enzyme SCOT was 60 times greater than cardiac uptake of β-hydroxybutyrate could account for. While they speculate that the rate of what they term "pseudoketogenesis" is not necessarily the same under all experimental conditions, they did not attempt to manipulate these conditions to investigate whether the acetoacetate to β-hydroxybutyrate direction of the reaction could become dominant in some scenarios.

My work in **Chapter 5** is based on novel observations, but addresses the gaps in both of these studies. Like Krebs et al. I demonstrate that net ketogenesis can occur in cardiac tissue; yet unlike that study I also demonstrate that net ketogenesis does occur in the intact, perfused, heart, without pharmacological stimulation, and is therefore a relevant process to ischaemic heart disease. Like Fink et al. meanwhile, I demonstrate flux through the ketogenic pathway in a perfused (but not working) heart model; yet unlike them I have manipulated the conditions of the heart both pharmacologically and through the induction of ischaemia to demonstrate that ketogenesis can become significant in certain conditions. Because of these points of difference, I can conclude for the first time that net ketogenesis can and does occur in the ischaemic heart, without any pharmacological stimulation being necessary.

The Physiological Implications of Ischaemic Ketogenesis

No work has ever before been done to attempt to establish whether ischaemic ketogenesis is beneficial or detrimental to recovery following reperfusion. Whilst there are papers which have sought to address whether exogenous β-hydroxybutyrate could protect the heart against ischaemia/ reperfusion (Goodwin and Taegtmeyer, 1994; King et al., 2001; Liu et al., 2016; Zou et al., 2002), there are none which examine the capacity of endogenously produced ketone bodies to do so. It may have been reasonable to expect that the increased availability of an oxygen efficient substrate upon reperfusion might aid recovery, yet several studies have shown that exogenous provision is not cardioprotective unless previous fasting has upregulated ketolytic enzymes in the heart (Goodwin and Taegtmeyer, 1994; Zou et al., 2002). These studies were performed without the awareness that

ketogenesis actually occurs during ischaemia, and my work in **Chapter 5** addresses functional recovery in the knowledge that this does occur for the first time. It demonstrates that increased availability of endogenously produced β-hydroxybutyrate upon reperfusion in the presence of sodium oxamate is associated with worsened recovery from ischaemia reperfusion, whilst partial inhibition of ketogenesis enhances functional recovery. This thesis therefore presents the novel finding that ketogenesis during ischaemia is likely detrimental to recovery. While there is not yet evidence upon which to base a hypothesis that this ketogenesis may be significant to human health, this finding is certainly worthy of further examination in the attempt to develop treatment of ischaemic heart disease.

7.3.3 Does Impairment of Contractile Function Truly Occur in the Type 1 Diabetic Rodent Heart?

A 90% pancreatectomy model of the type 1 diabetic heart has been described before (Yu et al., 2015), but the work presented in Chapter 6 of this thesis is the first ever to characterise its metabolic phenotype and assess its mitochondrial function. As with the well characterised streptozotocin induced model of type 1 diabetes (Flarsheim et al., 1996; Lashin et al., 2006; Chatham and Forder, 1997; Depre et al., 2000; Finck et al., 2002; How et al., 1904; Nielsen et al., 2002), there is severe impairment of mitochondrial respiratory capacity, and a greater reliance upon FAO. Unlike some of these cases of streptozotocin induced type 1 diabetes though, over a period of 10 weeks the 90% pancreatectomised model did not develop contractile impairment, or cardiomyopathy. There are several possible reasons for this discrepancy; one being that 90% removal of the pancreas is a very harsh treatment, and that the condition of the rats deteriorates too swiftly for them to develop cardiomyopathy. However, there is a distinct lack of any evidence that cardiomyopathy has been developed in any rodent model other than those induced by streptozotocin. Since streptozotocin is known to have direct effects upon cardiac contractility (Wold and Ren, 2004), I believe it likely that most rodent incidence of diabetic cardiomyopathy are in fact the result of direct off target effects of streptozotocin. Diabetic cardiomyopathy in the rodent heart may well be a myth.

7.3.4 Structural Effects of Isoprenaline Administration upon the Heart

Several papers have previously examined the potential of isoprenaline administration to induce heart failure (Jin et al., 2006; Desrois et al., 2014; Heather et al., 2009; Zhou et al., 2017). However, the work presented in this thesis is the first to my knowledge to investigate this from a number of angles. No other work has previously subjected rats to daily bolus injections of isoprenaline over a ten day period;

no other work has then allowed the rats 3.5 weeks without injection to recover; and no other work has examined the mitochondrial and metabolic effects of this administration to such depth.

The hearts examined in this thesis show similar induction of fibrosis to those seen in studies where isoprenaline was delivered through continuous infusion via an osmotic pump for 7 days (Desrois et al., 2014; Heather et al., 2009). There was no evidence though, of the ventricular hypertrophy observed in these studies, which both examined the hearts immediately following the end of the 7 day infusion period. This suggests that either constant infusion of isoprenaline leads to greater wall stress and remodelling than repetitive bolus dose administration which may allow the heart to recuperate between doses rather than develop hypertrophy, or that the 3.5 weeks between isoprenaline administration and termination in this study was long enough for hypertrophy to be reversed. Desrois et al. (2014) and Heather et al. (2009) also infused 5mg.kg bodyweight^{-1}day^{-1} isoprenaline, a greater overall dose of isoprenaline than the 1mg.kg bodyweight^{-1}day^{-1} injections detailed in this thesis which could also explain our study not replicating the hypertrophy they observe. The delivery of isoprenaline was also spread out across the whole day in these papers, which may lessen the systemic shock and help explain how they record lower initial mortality than that observed with the bolus doses administered in this thesis.

7.4 FUTURE DIRECTIONS

The work presented in this thesis has presented several novel discoveries which are worth expanding further, not least the finding that ketogenesis occurs in the ischaemic rat heart and that isoprenaline preserves mitochondrial function in the type 1 diabetic rat heart.

If a year's further funding and time were available to these projects, I would identify further investigation of β-hydroxybutyrate metabolism in the type 1 diabetic heart as a priority, as these experiments could elucidate several of the unanswered questions presented by the findings of this thesis. Firstly, catheterisation of the rat heart and sampling of blood would allow investigation of whether the type 1 diabetic heart produced β-hydroxybutyrate under physiological conditions. Secondarily, mounting of the hearts for Langendorff perfusion would allow further verification of whether this occurred in normoxic conditions, and interrogation of how rates of ketogenesis were altered during ischaemia. Given that the data in **Figure 6.17** suggests HMG-CoA synthase expression is increased in the 90% pancreatectomised rat heart and SCOT expression is decreased this observation should also cast further insight into which of the two enzymes contributes most greatly to cardiac ketogenic flux. Conducting these investigations whilst $U^{13}C$ glucose is present in the perfusion buffer would also be revealing in terms of further characterising how the ratio of FAO to glucose oxidation is altered in the type 1 diabetic heart; findings produced with this data could also be used to further validate the model presented in **Chapter 3**.

Hearts perfused in Langendorff mode could also be further stimulated with isoprenaline to investigate how the responses of sham and pancreatectomised hearts to the agent differs in real time. One of the biggest unanswered questions in **Chapter 6** is why none of the pancreatectomised rats succumbed to isoprenaline when so many of the sham operated ones did; there are many possible answers to this including that desensitisation of β adrenoceptors in the pancreatectomised heart may reduce the stimulatory effect of isoprenaline, or that the energetically impaired state renders the pancreatectomised heart less able to respond to said stimulation. Investigation of the effects of isoprenaline stimulation on the two groups with and without β blockers in the perfusion buffer would establish whether or not desensitisation contributes to the difference.

If a greater length of time, and further resources were available, a priority would be to confirm whether the observation of ischaemic ketogenesis extends to the *in vivo* heart and to humans. In the rat, this could be done by cannulation of the heart followed by in vivo partial occlusion of the descending coronary artery. Blood samples taken before and after the heart could be examined using LC-MS in order to determine the rate of ketogenesis. Following reperfusion, the whole heart could be removed, fixed and stained to assess whether ketogenesis had any impact upon infarct size, given that

in vivo immune cells play a part in the process and the inhibitory effects of β-hydroxybutyrate upon the inflammasome would have a greater effect upon the outcome than in the Langendorff perfused heart.

Given ethical considerations, attempts to confirm ischaemic ketogenesis in humans would be difficult given that initiating ischaemic periods in live humans is frowned upon. If the earlier suggested study into ketogenesis in type 1 diabetes bore fruition, this would be much easier to follow up in humans and would take priority given that it would involve only blood samples from across the heart catheterisation of patients, a routine operation which many of these patients already undergo. With the ischaemic heart however, unless relying on tissue from patients who have passed away from their ischaemic incident (which would be difficult to find controls for), a proxy would be required. One possibility here is to attempt to obtain tissue samples from ex vivo transplant hearts which are kept in cold ischaemia.

Further work to be done expanding on the findings of this thesis could centre around establishing the heart's status of substrate supply during ischaemia/reperfusion, and whether supplementation or deprivation of substrate to the heart could improve prognosis. In **Chapter 4**, presence of intralipid in the perfusion buffer was cardioprotective, yet while there is an argument that this could be due to cardioprotective effects of triglycerides, it could also be argued that when more substrate is available to a heart which is potentially nutrient deprived it will recover better. Reperfusing hearts from ischaemia while increasing the concentration of glucose and intralipid available to them without varying the proportions at which they are present in the buffer would be a good way to address whether this had any impact upon functional recovery. If a greater functional benefit were to be gained by instead varying the proportion of triglyceride to glucose in the buffer, it may be concluded to be an effect of intralipid rather than substrate availability; otherwise, substrate supply itself may be limiting.

7.5 CONCLUDING REMARKS

This thesis has studied metabolic aspects of ischaemic and diabetic heart that have not previously been explored. The emergence of ketogenesis as a process which occurs not only in the liver, but also in the ischaemic heart is a novel finding which may hold potential both as an avenue for easily effected metabolic interventions, and as an insight into the ischaemic metabolism. FAO appears to be less detrimental in either ischaemic or diabetic heart disease than previously projected, with its occurrence potentially beneficial to the ischaemia/reperfusion recovery process and not so damaging if elevated in a type 1 diabetic heart so long as metabolic flexibility is maintained. These findings, coupled with a novel method of analysing stable isotope labelling data from the Krebs cycle, represent a novel contribution to our understanding of cardiac metabolism under conditions of metabolic stress.

References

REFERENCES

Acikel, M., Buyukokuroglu, M.E., Erdogan, F., Aksoy, H., Bozkurt, E., and Senocak, H. (2005). Protective effects of dantrolene against myocardial injury induced by isoproterenol in rats: Biochemical and histological findings. Int. J. Cardiol. *98*, 389–394.

Aldakkak, M., Stowe, D.F., Chen, Q., Lesnefsky, E.J., and Camara, A.K.S. (2008). Inhibited mitochondrial respiration by amobarbital during cardiac ischaemia improves redox state and reduces matrix Ca2+overload and ROS release. Cardiovasc. Res. *77*, 406–415.

Almira, E.C., and Misbin, R.I. (1989). Effects of Insulin and Streptozotocin-Diabetes on Isoproterenol-Stimulated Cyclic AMP Production in Myocytes Isolated from Rat Heart. Metabolism *38*, 102–103.

An, H.J., Lee, B., Kim, S.M., Kim, D.H., Chung, K.W., Ha, S.G., Park, K.C., Park, Y.J., Kim, S.J., Yun, H.Y., et al. (2018). A PPAR Pan Agonist, MHY2013 Alleviates Age-Related Hepatic Lipid Accumulation by Promoting Fatty Acid Oxidation and Suppressing Inflammation. Biol. Pharm. Bull. *41*, 29–35.

An, Y., Xu, W., Li, H., Lei, H., Zhang, L., Hao, F., Duan, Y., Yan, X., Zhao, Y., Wu, J., et al. (2013). High-Fat Diet Induces Dynamic Metabolic Alterations in Multiple Biological Matrices of Rats. J. Proteome Res. *12*, 3755–3768.

Aquaro, G.D., Frijia, F., Positano, V., Menichetti, L., Santarelli, M.F., Lionetti, V., Giovannetti, G., Recchia, F.A., and Landini, L. (2015). Cardiac metabolism in a pig model of ischemia-reperfusion by cardiac magnetic resonance with hyperpolarized 13C-pyruvate. IJC Metab. Endocr. *6*, 17–23.

Arikawa, E., Ma, R.C.W., Isshiki, K., Luptak, I., He, Z., Yasuda, Y., Maeno, Y., Patti, M.E., Weir, G.C., Harris, R.A., et al. (2007). Angiotensin , and PKC ^{N_L} ' s Actions to Normalize Cardiac Gene Expression and Fuel Metabolism in Diabetic Rats. Diabetes *56*, 1410–1420.

Ashmore, T., Fernandez, B.O., Branco-price, C., West, J.A., Cowburn, A.S., Heather, L.C., Griffin, J.L., Johnson, R.S., Feelisch, M., and Murray, A.J. (2014a). Dietary nitrate increases arginine availability and protects mitochondrial complex I and energetics in the hypoxic rat heart. J Physiol *21*, 4715–4731.

Ashmore, T., Fernandez, B.O., Evans, C.E., Huang, Y., Branco-price, C., Grif, J.L., Johnson, R.S., Feelisch, M., and Murray, A.J. (2014b). Suppression of erythropoiesis by dietary nitrate. FASEB J. 1–11.

Ashmore, T., Roberts, L.D., Morash, A.J., Kotwica, A.O., Finnerty, J., West, J.A., Murfitt, S.A., Fernandez, B.O., Branco, C., Cowburn, A.S., et al. (2015). Nitrate enhances skeletal muscle fatty acid

oxidation via a nitric oxide-cGMP-PPAR- mediated mechanism. BMC Biol. 1–17.

Astrazeneca (2009). The burden of acute coronary syndromes in the United Kingdom.

Atherton, H.J., Schroeder, M.A., Dodd, M.S., Heather, L.C., Carter, E.E., Cochlin, L.E., Nagel, S., Sibson, N.R., Radda, G.K., Clarke, K., et al. (2011). Validation of the in vivo assessment of pyruvate dehydrogenase activity using hyperpolarised 13C MRS. NMR Biomed. *24*, 201–208.

Aubert, G., Martin, O.J., Horton, J.L., Lai, L., Vega, R.B., Leone, T.C., Koves, T., Gardell, S.J., Krüger, M., Hoppel, C.L., et al. (2016). The Failing Heart Relies on Ketone Bodies as a Fuel. Circulation *115*, CIRCULATIONAHA.115.017355.

Barry, W.H. (1991). Calcium and Ischemic Injury. Trends Cardiovasc. Med. *1*, 162–166.

Bayeva, M., Sawicki, K.T., and Ardehali, H. (2013). Taking Diabetes to Heart — Deregulation of Myocardial Lipid. J Am Hear. Assoc *2*, e000433.

Becker, L.B. (2018). New concepts in reactive oxygen species and cardiovascular reperfusion physiology. Cardiovasc Res *61*, 461–470.

Becker, L.B., Hoek, T.L. Vanden, Shao, Z., Li, C., Schumacker, P.T., Lance, B., Hoek, T.L. Vanden, Li, C., and Genera-, P.T.S. (1999). Generation of superoxide in cardiomyocytes during ischemia before reperfusion. Am. J. Physiol. 2240–2246.

Bedi, K.C., Snyder, N.W., Brandimarto, J., Aziz, M., Mesaros, C., Worth, A., Wang, L., Javaheri, A., Blair, I.A., Margulies, K., et al. (2016). Evidence for Intramyocardial Disruption of Lipid Metabolism and Increased Myocardial Ketone Utilization in Advanced Human Heart Failure. Circulation *133*, 706–716.

Bell, R.M., Mocanu, M.M., and Yellon, D.M. (2011). Retrograde heart perfusion : The Langendorff technique of isolated heart perfusion. J. Mol. Cell. Cardiol. *50*, 940–950.

Le Belle, J.E., Harris, N.G., Williams, S.R., and Bhakoo, K.K. (2002). A comparison of cell and tissue extraction techniques using high-resolution 1H-NMR spectroscopy. NMR Biomed. *15*, 37–44.

Van Belle, T.L., Coppetiers, K.T., and Von Herrath, M.G. (2011). Type 1 Diabetes: Etiology, Immunology, and Therapeutic Strategies. Physiol Rev *91*, 79–118.

Bertoni, A.G., Tsai, A., Kasper, E.K., and Brancati, F.L. (2003). Diabetes and idiopathic cardiomyopathy: a nationwide case-control study. Diabetes Care *26*, 2791–2795.

BHF (2018b). CVD Statistics 2018 - Morbidity.

BHF (2018a). CVD Statistics 2018 - Mortality.

Birrell, J.A., and Hirst, J. (2013). Investigation of NADH binding, hydride transfer, and NAD+ dissociation during NADH oxidation by mitochondrial complex i using modified nicotinamide nucleotides. Biochemistry *52*, 4048–4055.

Bittl, J. a, and Shine, K.I. (1983). Protection of ischemic rabbit myocardium by glutamic acid. Am. J. Physiol. *245*, H406-12.

Bleier, L., and Dröse, S. (2013). Superoxide generation by complex III: From mechanistic rationales to functional consequences. Biochim. Biophys. Acta - Bioenerg. *1827*, 1320–1331.

Bockus, L.B., and Humphries, K.M. (2015). cAMP-dependent protein kinase (PKA) Signaling is Impaired in the Diabetic Heart. J. Biol. Chem. *Online*, e1-22.

Bolzán, A.D., and Bianchi, M.S. (2002). Genotoxicity of Streptozotocin. Mutat. Res. - Rev. Mutat. Res. *512*, 121–134.

Bonora, M., Bononi, A., De Marchi, E., Giorgi, C., Lebiedzinska, M., Marchi, S., Patergnani, S., Rimessi, A., Suski, J.M., Wojtala, A., et al. (2013). Role of the c subunit of the FOATP synthase in mitochondrial permeability transition. Cell Cycle *12*, 674–683.

Boudina, S., Sena, S., O'Neill, B.T., Tathireddy, P., Young, M.E., and Abel, E.D. (2005). Reduced mitochondrial oxidative capacity and increased mitochondrial uncoupling impair myocardial energetics in obesity. Circulation *112*, 2686–2695.

Boudina, S., Sena, S., Theobald, H., Sheng, X., Wright, J.J., Hu, X.X., Aziz, S., Johnson, J.I., Bugger, H., Zaha, V.G., et al. (2007). Mitochondrial Energetics in the Heart in Obesity-Related. Diabetes *56*, 2457–2466.

Brinkmann, J.F.F., Abumrad, N.A., Ibrahimi, A., Van Der Vusse, G.J., and Glatz, J.F.C. (2002). New insights into long-chain fatty acid uptake by heart muscle: a crucial role for fatty acid translocase/CD36a crucial role for fatty acid translocase / CD36. Biochem J *570*, 561–570.

Brooks, W.W., and Conrad, C.H. (2009). Isoproterenol-induced myocardial injury and diastolic dysfunction in mice: structural and functional correlates. Comp Med *59*, 339–343.

Bryan, N.S., Calvert, J.W., Elrod, J.W., Gundewar, S., Ji, S.Y., and Lefer, D.J. (2007a). Dietary nitrite supplementation protects against myocardial ischemia-reperfusion injury. Proc. Natl. Acad. Sci. *104*, 19144–19149.

Bryan, N.S., Calvert, J.W., Elrod, J.W., Gundewar, S., Ji, S.Y., and Lefer, D.J. (2007b). Dietary nitrite

supplementation protects against myocardial ischemia-reperfusion injury. Proc. Natl. Acad. Sci. *104*, 19144–19149.

Bugger, H., and Abel, E.D. (2009). Rodent models of diabetic cardiomyopathy. Dis. Model. Mech. *2*, 454–466.

Bugger, H., and Abel, E.D. (2014). Molecular mechanisms of diabetic cardiomyopathy. Diabetologia *57*, 660–671.

Bugger, H., Boudina, S., Hu, X.X., Tuinei, J., Zaha, V.G., Theobald, H.A., Yun, U.J., McQueen, A.P., Wayment, B., Litwin, S.E., et al. (2008). Type 1 diabetic akita mouse hearts are insulin sensitive but manifest structurally abnormal mitochondria that remain coupled despite increased uncoupling protein 3. Diabetes *57*, 2924–2932.

Burgess, S.C., Babcock, E.E., Je, F.M.H., Sherry, A.D., and Malloy, C.R. (2001). NMR indirect detection of glutamate to measure citric acid cycle £ ux in the isolated perfused mouse heart. FEBS Lett. *505*, 163–167.

Canoso, R., Rodvien, R., Scoon, K., and Levine, P. (2018). Hydrogen Peroxide and Platelet Function. Blood *43*, 645–656.

Carlström, M., Larsen, F.J., Nyström, T., Hezel, M., Borniquel, S., and Weitzberg, E. (2010). Dietary inorganic nitrate reverses features of metabolic syndrome in endothelial nitric oxide synthase-deficient mice. PNAS *107*, 17716 – 17720.

Ceylan-Isik, A.F., Wu, S., Li, Q., Li, S.-Y., and Ren, J. (2006). High-dose benfotiamine rescues cardiomyocyte contractile dysfunction in streptozotocin-induced diabetes mellitus. J. Appl. Physiol. *100*, 150–156.

Chatham, J.C., and Forder, J.R. (1997). Relationship between cardiac function and substrate oxidation in hearts of diabetic rats. Am. J. Physiol. *273*, H52-8.

Chegary, M., Ruiter, J.P.N., Wijburg, F.A., Stoll, M.S.K., Minkler, P.E., Weeghel, M. Van, Schulz, H., Hoppel, C.L., Wanders, R.J.A., and Houten, S.M. (2009). Mitochondrial long chain fatty acid β -oxidation in man and mouse. BBA - Mol. Cell Biol. Lipids *1791*, 806–815.

Chen, Q., Vazquez, E.J., Moghaddas, S., Hoppel, C.L., and Lesnefsky, E.J. (2003). Production of Reactive Oxygen Species by Mitochondria. J. Biol. Chem. *278*, 36027–36031.

Chen, Q., Moghaddas, S., Hoppel, C.L., and Lesnefsky, E.J. (2007). Ischemic defects in the electron transport chain increase the production of reactive oxygen species from isolated rat heart

mitochondria. Am J Physiol Cell Physiol *111*, 460–466.

Chen, V., Ianuzzo, C.D., Fong, B.C., and Spitzer, J.J. (1984). The Effects of Acute and Chronic Diabetes on Myocardial Metabolism in Rats. Diabetes *33*, 1078–1084.

Chiari, P.C., Bienengraeber, M.W., Pagel, P.S., Krolikowski, J.G., Kersten, J.R., and Warltier, D.C. (2005). Isoflurane protects against myocardial infarction during early reperfusion by activation of phosphatidylinositol-3-kinase signal transduction: Evidence for anesthetic-induced postconditioning in rabbits. Anesthesiology *102*, 102–109.

Choi, D.J., Koch, W.J., Hunter, J.J., and Rockman, H.A. (1997). Mechanism of beta-adrenergic receptor desensitization in cardiac hypertrophy is increased beta-adrenergic receptor kinase. J Biol Chem *272*, 17223–17229.

Chouchani, E.T., Pell, V.R., Gaude, E., Aksentijević, D., Sundier, S.Y., Robb, E.L., Logan, A., Nadtochiy, S.M., Ord, E.N.J., Smith, A.C., et al. (2014). Ischaemic accumulation of succinate controls reperfusion injury through mitochondrial ROS. Nature *515*, 431–435.

Clark, M.G., and Patten, G.S. (1984). Adrenergic Regulation of Glucose Metabolism in Rat Heart. J. Biol. Chem. *259*, 15204–15211.

Cole, M.A., Murray, A.J., Cochlin, L.E., Heather, L.C., McAleese, S., Knight, N.S., Sutton, E., Jamil, A.A., Parassol, N., and Clarke, K. (2011). A high fat diet increases mitochondrial fatty acid oxidation and uncoupling to decrease efficiency in rat heart. Basic Res. Cardiol. *106*, 447–457.

Cole, M.A., Jamil, A.H.A., Heather, L.C., Murray, A.J., Sutton, E.R., Slingo, M., Sebag-Montefiore, L., Tan, S.C., Aksentijevíc, D., Gildea, O.S., et al. (2016). On the pivotal role of PPARa in adaptation of the heart to hypoxia and why fat in the diet increases hypoxic injury. FASEB J. *30*, 2684–2697.

Cook, G.A., King, M.T., and Veech, R.L. (1978). Ketogenesis and Malonyl Coenzyme A Content of Isolated Rat Hepatocytes. J. Biol. Chem. *253*, 2529–2531.

Cook, G.A., Lavrentyev, E.N., Pham, K., and Park, E.A. (2017). Streptozotocin diabetes increases mRNA expression of ketogenic enzymes in the rat heart. Biochim. Biophys. Acta - Gen. Subj. *1861*, 307–312.

Cotter, D.G., Schugar, R.C., Wentz, A.E., Andre d'Avignon, D., and Crawford, P.A. (2013). Successful adaptation to ketosis by mice with tissue-specific deficiency of ketone body oxidation. AJP Endocrinol. Metab. *304*, E363–E374.

Cotter, D.G., Ercal, B., Huang, X., Leid, J.M., D'Avignon, D.A., Graham, M.J., Dietzen, D.J., Brunt, E.M.,

Patti, G.J., and Crawford, P.A. (2014). Ketogenesis prevents diet-induced fatty liver injury and hyperglycemia. J. Clin. Invest. *124*.

Dargie, H. (2005). Heart failure post-myocardial infarction: a review of the issues. Heart *91*, 3–6.

Darvey, I.G. (1998). Biochemical Education How does the ratio of ATP yield from the complete oxidation of palmitic acid to that of glucose compare with the relative energy contents of fat and carbohydrate ? Biochem. Educ. *26*, 22–23.

Debrunner, M., Schuiki, E., Minder, E., Straumann, E., Naegli, B., Mury, R., Bertel, O., and Frielingsdorf, J. (2008). Proinflammatory cytokines in acute myocardial infarction with and without cardiogenic shock. Clin Res Cardiol *305*, 298–305.

Dedkova, E.N., and Blatter, L.A. (2014). Role of β -hydroxybutyrate , its polymer poly- β -hydroxybutyrate and inorganic polyphosphate in mammalian health and disease. *5*, 1–22.

Depre, C., Rider, M.H., and Hue, L. (1998). Mechanisms of control of heart glycolysis. Eur. J. Biochem. *258*, 277–290.

Depre, C., Young, M.E., Ying, J., Ahuja, H.S., Han, Q., Garza, N., Davies, P.J.A., and Taegtmeyer, H. (2000). Streptozotocin-induced changes in cardiac gene expression in the absence of severe contractile dysfunction. J. Mol. Cell. Cardiol. *32*, 985–996.

Desrois, M., Kober, F., Lan, C., Dalmasso, C., Cole, M., Clarke, K., Cozzone, P.J., and Bernard, M. (2014). Effect of isoproterenol on myocardial perfusion, function, energy metabolism and nitric oxide pathway in the rat heart - a longitudinal MR study. NMR Biomed. *27*, 529–538.

Drake, K.J., Sidorov, V.Y., McGuinness, O.P., Wasserman, D.H., and Wikswo, J.P. (2013). Amino Acids as Metabolic Substrates during Cardiac Ischemia. Exp Biol Med *237*, 1–17.

Duicu, O.M., Privistirescu, A., Wolf, A., Petruş, A., Dănilă, M.D., Raţiu, C.D., Muntean, D.M., and Sturza, A. (2017). Methylene blue improves mitochondrial respiration and decreases oxidative stress in a substrate-dependent manner in diabetic rat hearts. Can. J. Physiol. Pharmacol. *95*, 1376–1382.

Dyck, J.R.B., Cheng, J., Stanley, W.C., Barr, R., Chandler, M.P., Brown, S., Wallace, D., Arrhenius, T., Harmon, C., Yang, G., et al. (2004). Malonyl Coenzyme A Decarboxylase Inhibition Protects the Ischemic Heart by Inhibiting Fatty Acid Oxidation and Stimulating Glucose Oxidation. Circ. Res. *94*, e78–e84.

Echtay, K.S., Murphy, M.P., Smith, R.A.J., Talbot, D.A., and Brand, M.D. (2002). Superoxide Activates Mitochondrial Uncoupling Protein 2 from the. Biochemistry *277*, 47129–47135.

Edlund, A., and Wennmalm, Å. (1981). Oxygen consumption in rabbit Langendorff hearts perfused with a saline medium. Acta Physiol. Scand. *113*, 117–122.

Egert, S., Nguyen, N., and Schwaiger, M. (1999). GLUT1 Translocation in the Isolated Perfused Rat Heart. Circ. Res. *84*, 1407–1415.

Fang, J., Mensah, G.A., Croft, J.B., and Keenan, N.L. (2008). Heart Failure-Related Hospitalization in the U . S ., 1979 to 2004. J. Am. Coll. Cardiol. *52*, 428–434.

Ferrannini, E., Mark, M., and Mayoux, E. (2016). CV Protection in the EMPA-REG OUTCOME Trial : A " Thrifty Substrate " Hypothesis. Diabetes Care *39*, 1108–1114.

Ferrari, R., Censi, S., Mastrorilli, F., Boraso, A., and Ferrara, U. (2018). Prognostic benefits of heart rate reduction in cardiovascular disease. Circulation *5*, 10–14.

Fillmore, N., Mori, J., and Lopaschuk, G.D. (2014). Mitochondrial fatty acid oxidation alterations in heart failure, ischaemic heart disease and diabetic cardiomyopathy. Br. J. Pharmacol. *171*, 2080–2090.

Finck, B.N., Lehman, J.J., Leone, T.C., Welch, M.J., Bennett, M.J., Kovacs, A., Han, X., Gross, R.W., Kozak, R., Lopaschuk, G.D., et al. (2002). The cardiac phenotype induced by PPARα overexpression mimics that caused by diabetes mellitus. J. Clin. Invest. *109*, 121–130.

Fink, G., Desrocherss, S., Rosiersp, C. Des, Garneaus, M., David, F., Landau, B.R., and Brunengraber, H. (1988). Pseudoketogenesis in the Perfused Rat Heart *. J. Biol. Chem. *263*, 18036–18042.

Fisher, B.R.B., and Williamson, J.R. (1961). The Oxygen Uptake of the Perfused Rat Heart. J Physiol *158*, 86–101.

Flarsheim, C.E., Grupp, I.L., and Matlib, M.A. (1996). Mitochondrial dysfunction accompanies diastolic dysfunction in diabetic rat heart. Am J Physiol Hear. Circ Physiol *271*, H192-202.

Folbergrová, J., Ljunggren, B., Norberg, K., and Siesjö, B.K. (1974). Influence of complete ischemia on glycolytic metabolites, citric acid cycle intermediates, and associated amino acids in the rat cerebral cortex. Brain Res. *80*, 265–279.

Le Foll, C., Dunn-Meynell, A.A., Miziorko, H.M., and Levin, B.E. (2014). Regulation of hypothalamic neuronal sensing and food intake by ketone bodies and fatty acids. Diabetes *63*, 1259–1269.

Francis, S.D., Jesus, N.M. De, Lindsey, M.L., and Ripplinger, C.M. (2016). Journal of Molecular and Cellular Cardiology The crossroads of in fl ammation , fi brosis , and arrhythmia following myocardial infarction. J. Mol. Cell. Cardiol. *91*, 114–122.

Frangogiannis, N.G. (2015). The inflammatory response in myocardial injury, repair and remodeling. Nat Rev Cardiol *11*, 255–265.

Friederich, M., Hansell, P., and Palm, F. (2009). Diabetes, oxidative stress, nitric oxide and mitochondria function. Curr. Diabetes Rev. *5*, 120–144.

Gheorghiade, M., and Pang, P.S. (2009). Acute Heart Failure Syndromes. JAC *53*, 557–573.

Glatz, J.F.C., van Breda, E., Keizer, H.A., de Jong, Y.F., Lakey, J.R.T., Rajotte, R. V, Thompson, A., Van Der Vusse, G.J., and Lopaschuk, G.D. (1994). Rat Heart Fatty Acid Binding Protein.pdf. Biochem. Biophys. Res. Commun. *199*, 639–646.

Gnaiger, E. (2008). Polarographic Oxygen Sensors, the Oxygraph and High-Resolution Respirometry to Assess Mitochondrial Function. In Drug-Induced Mitochondrial Dysfunction, pp. 327–347.

Goodwin, G.W., and Taegtmeyer, H. (1994). Metabolic recovery of isolated working rat heart after brief global ischemia. Am. Physiol. Soc. *94*, 467–470.

Gormsen, L.C., Svart, M., Thomsen, H.H., Sondergaard, E., Vendelbo, M., Christensen, N., Tolbod, L.P., Harms, H.J., Nielsen, R., Wiggers, H., et al. (2017). Ketone Body Infusion With 3-Hydroxybutyrate Reduces Myocardial. J. Am. Heart Assoc. *6*, e005066.

Gottlieb, R.A. (2011). Cell Death Pathways in Acute Ischemia / Reperfusion Injury. J. Cardiovasc. Pharmacol. Ther. *16*, 233–238.

Grabacka, M., Pierzchalska, M., Dean, M., and Reiss, K. (2016). Regulation of ketone body metabolism and the role of PPARα. Int. J. Mol. Sci. *17*.

Granger, D.N., and Kvietys, P.R. (2015). Reperfusion injury and reactive oxygen species : The evolution of a concept. Redox Biol. *6*, 524–551.

Greenspan, M.D., Yudkovitz, J.B., Lo, C.Y., Chen, J.S., Alberts, A.W., Hunt, V.M., Chang, M.N., Yang, S.S., Thompson, K.L., and Chiang, Y.C. (1987). Inhibition of hydroxymethylglutaryl-coenzyme A synthase by L-659,699. Proc Natl Acad Sci U S A *84*, 7488–7492.

Grimm, D., Elsner, D., Schunkert, H., Pfeifer, M., Griese, D., Bruckschlegel, G., Muders, F., Riegger, G.A., and Kromer, E.P. (1998). Development of heart failure following isoproterenol administration in the rat: role of the renin-angiotensin system. Cardiovasc. Res. *37*, 91–100.

de Groot, M.J.M., van Helden, M.A.B., de Jong, Y.F., Coumans, W.A., and van der Vusse, G.J. (1995). The influence of lactate, pyruvate and glucose as exogenous substrates on free radical defense mechanisms in isolated rat hearts during ischaemia and reperfusion. Mol. Cell. Biochem. *146*, 147–

155.

Gtzsche, O.L.E. (1983). The Adrenergic β-Receptor Adenylate Cyclase System in Heart and Lymphocytes from Streptozotocin-Diabetic Rats: In Vivo and In Vitro Evidence for a Desensitized Myocardial β-Receptor. Diabetes *32*, 1110–1116.

Guo, Z. (2015). Pyruvate dehydrogenase , Randle cycle , and skeletal muscle insulin resistance. PNAS *112*, 2854.

Guzy, R.D., and Schumacker, P.T. (2006). Oxygen sensing by mitochondria at complex III : the paradox of increased reactive oxygen species during hypoxia. Exp Physiol 807–819.

Halestrap, A.P. (1998). Elucidating the molecular mechanism of the permeability transition pore and its role in reperfusion injury of the heart. Biochim. Biophys. Acta *1366*, 79.94.

Handzlik, M.K., Constantin-Teodosiu, D., Greenhaff, P.L., and Cole, M.A. (2018). Increasing cardiac pyruvate dehydrogenase flux during chronic hypoxia improves acute hypoxic tolerance. J. Physiol. *15*, 3357–3369.

Hansford, R.G., and Cohen, L. (1978). Relative Importance Inhibition of Pyruvate Dehydrogenase Interconversion and in the Effect of Fatty Acids on Pyruvate Oxidation by Rat Heart Mitochondria of fatty acids , ketones , results in an inhibition of pyruvate oxidation (4). These of products of. Biochem. Biophys. *191*, 65–81.

Hasin, Y., and Barry, H. (1984). Myocardial metabolic inhibition and membrane potential , contraction , and potassium uptake. Am. J. Physiol. *247*, 322–329.

Hearse, D.J., Garlick, P.B., and Humphrey, S.M. (1977). Ischemic contracture of the myocardium: Mechanisms and prevention. Am. J. Cardiol. *39*, 986–993.

Heather, L.C., and Clarke, K. (2011). Metabolism, hypoxia and the diabetic heart. J. Mol. Cell. Cardiol. *50*, 598–605.

Heather, L.C., Cole, M.A., Lygate, C.A., Evans, R.D., Stuckey, D.J., Murray, A.J., Neubauer, S., and Clarke, K. (2006). Fatty acid transporter levels and palmitate oxidation rate correlate with ejection fraction in the infarcted rat heart. Cardiovasc. Res. *72*, 430–437.

Heather, L.C., Catchpole, A.F., Stuckey, D.J., Cole, M.A., Carr, C.A., and Clarke, K. (2009). Isoproterenol induces in vivo functional and metabolic abnormalities; similar to those found in the infarcted rat heart. J. Physiol. Pharmacol. *60*, 31–39.

Heather, L.C., Carr, C.A., Stuckey, D.J., Pope, S., Morten, K.J., Carter, E.E., Edwards, L.M., and Clarke,

K. (2010). Critical role of complex III in the early metabolic changes following myocardial infarction. Cardiovasc. Res. *85*, 127–136.

Heather, L.C., Cole, M.A., Tan, J.J., Ambrose, L.J.A., Pope, S., Abd-Jamil, A.H., Carter, E.E., Dodd, M.S., Yeoh, K.K., Schofield, C.J., et al. (2012). Metabolic adaptation to chronic hypoxia in cardiac mitochondria. Basic Res. Cardiol. *107*.

Heather, L.C., Wang, X., West, J.A., and Griffin, J.L. (2013). A practical guide to metabolomic profiling as a discovery tool for human heart disease. J. Mol. Cell. Cardiol. *55*, 2–11.

Hendgen-Cotta, U.B., Luedike, P., Totzeck, M., Kropp, M., Schicho, A., Stock, P., Rammos, C., Niessen, M., Heiss, C., Lundberg, J.O., et al. (2012). Dietary nitrate supplementation improves revascularization in chronic ischemia. Circulation *126*, 1983–1992.

Herr, D.J., Aune, S.E., and Menick, D.R. (2015). Induction and Assessment of Ischemia-reperfusion Injury in Langendorff- perfused Rat Hearts. J. Vis. Exp. *101*.

Heusch, G., and Gersh, B.J. (2018). The pathophysiology of acute myocardial infarction and strategies of protection beyond reperfusion : a continual challenge. Eur. Heart J. *38*, 774–784.

Heusch, G., Libby, P., Gersh, B., Yellon, D., Böhm, M., Lopaschuk, G., Opie, L., and Saar, H. (2014). Cardiovascular remodelling in coronary artery disease and heart failure. Lancet *383*, 1933–1943.

Hex, N., Bartlett, C., Wright, D., Taylor, M., and Varley, D. (2012). Health Economics Estimating the current and future costs of Type 1 and Type 2 diabetes in the UK , including direct health costs and indirect societal and productivity costs. Diabet. Med. 855–862.

Hezel, M.P., Liu, M., Schiffer, T.A., Larsen, F.J., Checa, A., Wheelock, C.E., Carlström, M., Lundberg, J.O., and Weitzberg, E. (2015). Effects of long-term dietary nitrate supplementation in mice. Redox Biol. *5*, 234–242.

Hinkle, P.C. (2005). P / O ratios of mitochondrial oxidative phosphorylation. Biochim. Biophys. Acta *1706*, 1–11.

Hiraoka, T., DeBuysere, M., and Olson, M.S. (1980). Studies of the effects of beta-adrenergic agonists on the regulation of pyruvate dehydrogenase in the perfused rat heart. J. Biol. Chem. *255*, 7604–7609.

Hohl, C., Oestreich, R., Rösen, P., Wiesner, R., and Grieshaber, M. (1987). Evidence for succinate production by reduction of fumarate during hypoxia in isolated adult rat heart cells. Arch. Biochem. Biophys. *259*, 527–535.

Home, P. (2011). Safety of PPAR Agonists. Diabetes Treat. *34*, s215–s219.

Horscroft, J.A., Burgess, S.L., Hu, Y., and Murray, A.J. (2015). Altered Oxygen Utilisation in Rat Left Ventricle and Soleus after 14 Days , but Not 2 Days , of Environmental Hypoxia. PLoS One *2*, 1–16.

Houten, S.M., and Wanders, R.J.A. (2010). A general introduction to the biochemistry of mitochondrial fatty acid β -oxidation. J Inherit Metab Dis. *33*, 469–477.

Houten, S.M., Violante, S., Ventura, F. V, and Wanders, R.J.A. (2018). The Biochemistry and Physiology of Mitochondrial Fatty Acid β -Oxidation and Its Genetic Disorders. Annu Rev Physiol *78*, 23–44.

How, O.-J., Larsen, T.S., Hafstad, a D., Khalid, A., Myhre, E.S.P., Murray, a J., Boardman, N.T., Cole, M., Clarke, K., Severson, D.L., et al. (2007). Rosiglitazone treatment improves cardiac efficiency in hearts from diabetic mice. Arch. Physiol. Biochem. *113*, 211–220.

Huang, Y., Powers, C., Moore, V., Schafer, C., Ren, M., Phoon, C.K.L., James, J.F., Glukhov, A. V., Javadov, S., Vaz, F.M., et al. (2017). The PPAR pan-agonist bezafibrate ameliorates cardiomyopathy in a mouse model of Barth syndrome. Orphanet J. Rare Dis. *12*, 1–9.

Hue, L., Taegtmeyer, H., Randle, P., Garland, P., and Hales, N. (2009). The Randle cycle revisited : a new head for an old hat. Am J Physiol Endocrinol Metab *297*, 578–591.

Hugli, O., Braun, J.E., Kim, S., Pelletier, A.J., and Jr, C.A.C. (2001). United States Emergency Department Visits for Acute Decompensated Heart Failure , 1992 to 2001. Am. J. Cardiol. 1537–1342.

Von Hundelshausen, P., and Weber, C. (2007). Platelets as Immune Cells Bridging Inflammation and Cardiovascular Disease. Circ. Res. *100*, 27–40.

Jaswal, J.S., Keung, W., Wang, W., Ussher, J.R., and Lopaschuk, G.D. (2011). Targeting fatty acid and carbohydrate oxidation — A novel therapeutic intervention in the ischemic and failing heart. BBA - Mol. Cell Res. *1813*, 1333–1350.

Jeddi, S., Khalifi, S., Ghanbari, M., Bageripour, F., and Ghasemi, A. (2016a). Effects of Nitrate Intake on Myocardial Ischemia-Reperfusion Injury in Diabetic Rats. Arq. Bras. Cardiol. 339–347.

Jeddi, S., Khalifi, S., Ghanbari, M., Bageripour, F., and Ghasemi, A. (2016b). Effects of Nitrate Intake on Myocardial Ischemia-Reperfusion Injury in Diabetic Rats. Arq. Bras. Cardiol. 339–347.

Jin, Y.-T., Hasebe, N., Matsusaka, T., Natori, S., Ohta, T., Tsuji, S., and Kikuchi, K. (2006). Magnesium attenuates isoproterenol-induced acute cardiac dysfunction and beta-adrenergic desensitization. AJP

Hear. Circ. Physiol. *292*, H1593–H1599.

Joffe, I.I., Travers, K.E., Perreault-Micale, C.L., Hampton, T., Katz, S.E., Morgan, J.P., and Douglas, P.S. (1999). Abnormal cardiac function in the streptozotocin-induced, non-insulin- dependent diabetic rat: Noninvasive assessment with Doppler echocardiography and contribution of the nitric oxide pathway. J. Am. Coll. Cardiol. *34*, 2111–2119.

Johnston, D.L., and Lewandowski, E.D. (1991). Fatty Acid Metabolism and Contractile Function in the Reperfused Myocardium Multinuclear NMR Studies of Isolated Rabbit Hearts. Circ. Res. *68*, 714–726.

Jonckheere, A.I., Smeitink, J.A.M., and Rodenburg, R.J.T. (2012). Mitochondrial ATP synthase : architecture , function and pathology. J Inherit Metab Dis. *35*, 211–225.

Jones, J.G. (2014). Identifying Sources of Hepatic Lipogenic Acetyl-CoA Using Stable Isotope Tracers and NMR. Adv. Radiol. *2014*, 1–8.

Kalogeris, T., Bao, Y., and Korthuis, R.J. (2014). Mitochondrial reactive oxygen species : A double edged sword in ischemia / reperfusion vs preconditioning. Redox Biol. *2*, 702–714.

Kantor, P.F., Dyck, J.R.B., and Lopaschuk, G.D. (1999). Fatty Acid Oxidation in the Reperfused Ischemic Heart. Am. J. Med. Sci. *318*, 3–14.

Karamanlidis, G., Lee, C.F., Garcia-Menendez, L., Kolwicz, S.C., Suthammarak, W., Gong, G., Sedensky, M.M., Morgan, P.G., Wang, W., and Tian, R. (2013). Mitochondrial complex i deficiency increases protein acetylation and accelerates heart failure. Cell Metab. *18*, 239–250.

Kashiwaya, Y., Satos, K., Tsuchiya, N., Thomas, S., Fells, D.A., and Veechn, R.L. (1994). Control of Glucose Utilization in Working Perfused Rat Heart. J. Biol. Chem. *269*, 25502–25514.

Katsarou, A., Gudbjörnsdottir, S., Rawshani, A., Dabelea, D., Bonifacio, E., Anderson, B.J., Jacobsen, L.M., Schatz, D.A., and Lernmark, A. (2017). Type 1 diabetes mellitus. Nat. Rev. Dis. Prim. *3*, 1–18.

Katzs, J., Walss, P., and Lee, W.N. (1993). Isotopomer Studies of Gluconeogenesis and the Krebs Cycle with 13C-Labeled Lactate. J. Biol. Chem. *268*, 25509–25521.

Kiebish, M.A., Yang, K., Sims, H.F., Jenkins, C.M., Liu, X., Mancuso, D.J., Zhao, Z., Guan, S., Abendschein, D.R., Han, X., et al. (2012). Myocardial regulation of lipidomic flux by cardiolipin synthase: Setting the beat for bioenergetic efficiency. J. Biol. Chem. *287*, 25086–25097.

Kim, J., Jin, Y., Lemasters, J.J., Jin, Y., and Reactive, J.J.L. (2018). Reactive oxygen species , but not Ca 2 ε overloading , trigger pH- and mitochondrial permeability transition-dependent death of adult rat myocytes after ischemia-reperfusion. Am J Physiol Hear. Circ Physiol *7090*, 2024–2034.

Kim, Y.I., Lee, F.N., Choi, W.S., Lee, S., and Youn, J.H. (2006). Insulin regulation of skeletal muscle PDK4 mRNA expression is impaired in acute insulin-resistant states. Diabetes *55*, 2311–2317.

King, L.M., and Opie, L.H. (1998). Glucose delivery is a major determinant of glucose utilisation in the ischemic myocardium with a residual coronary flow. Cardiovasc. Res. *39*, 381–392.

King, L.M., Sidell, R.J., Wilding, J.R., Radda, G.K., Clarke, K., Linda, M., Sidell, R.J., Wilding, J.R., Radda, G.K., and Clarke, K. (2001). Free fatty acids , but not ketone bodies , protect diabetic rat hearts during low-flow ischemia. 1173–1181.

Kornberg, H. (2000). Krebs and his trinity of cycles. Nat. Rev. *1*, 5–8.

Kowalski, G.M., Souza, D.P. De, Risis, S., Burch, M.L., Hamley, S., Kloehn, J., Selathurai, A., Lee-young, R.S., Tull, D., Callaghan, S.O., et al. (2015). In vivo cardiac glucose metabolism in the high-fat fed mouse : Comparison of euglycemic e hyperinsulinemic clamp derived measures of glucose uptake with a dynamic metabolomic fl ux pro fi ling approach. Biochem. Biophys. Res. Commun. *463*, 818–824.

Kraut, J.A., and Madias, N.E. (2014). Lactic Acidosis. N. Engl. J. Med. *371*, 2309–2319.

Krebs, H.A., and Johnson, W.A. (1937). LXXXVII . METABOLISM OF KETONIC ACIDS IN ANIMAL TISSUES. Biochem J. 645–660.

Krebs, H.A., and Johnson, W.A. (1980). The role of citric acid in intermediate metabolism in animal tissues BY. FEBS Lett. *117*, 148–156.

Krebs, B.Y.H.A., Eggleston, L. V, and Alessandro, A.D. (1961). The Effect of Succinate and Amytal on the Reduction of Acetoacetate in Animal Tissues. Biochem. J. *79*.

Krebs, H.A., Salvin, E., and Johnson, W. (1938). The Formation of Citric Acid and a-Ketoglutaric Acids in the Mammalian Body. Biochem. J. *32*, 113–117.

Kudo, N; Barr, A. J.; Barr, R. L.; Desai, S.; Lopaschuk, G.D. (1995). High Rates of Fatty Acid Oxidation during Reperfusion of Ischemic Hearts Are Associated with a Decrease in Malonyl-CoA Levels Due to an Increase in 5’-AMP-activated Protein Kinase Inhibition of Acetyl-CoA Carboxyl. J. Biol. Chem. *270*, 17513–17520.

Kume, E., Aruga, C., Ishizuka, Y., Takahashi, K., Miwa, S., Itoh, M., Fujimura, H., Toriumi, W., Kitamura, K., and Doi, K. (2005). Gene expression profiling in streptozotocin treated mouse liver using DNA microarray. Exp. Toxicol. Pathol. *56*, 235–244.

Kuznetsov, A. V, Veksler, V., Gellerich, F.N., Saks, V., Margreiter, R., and Kunz, W.S. (2008). Analysis

of mitochondrial function in situ in permeabilized muscle fibers , tissues and cells. Nat. Protoc. *3*, 965–976.

Laflamme, M.A., and Murry, C.E. (2005). Regenerating the heart. Nat. Biotechnol. *23*, 845–856.

Lahey, R., Wang, X., Carley, A.N., and Lewandowski, Douglas, E. (2014). Dietary Fat Supply to Failing Hearts Determines Dynamic Lipid Signaling for Nuclear Receptor Activation and Oxidation of Stored Triglyceride. Circulation *130*, 1790–1799.

Laing, S.P., Swerdlow, A.J., Slater, S.D., Burden, A.C., Morris, A., Waugh, N.R., Gatling, W., Bingley, P.J., and Patterson, C.C. (2003). Mortality from heart disease in a cohort of 23,000 patients with insulin-treated diabetes. Diabetologia *46*, 760–765.

Lakshminarayanan, V., Lewallen, M., Frangogiannis, N.G., Evans, A.J., Wedin, K.E., Michael, L.H., and Entman, M.L. (2001). Reactive Oxygen Intermediates Induce Monocyte Chemotactic Protein-1 in Vascular Endothelium after Brief Ischemia. Am. J. Pathol. *159*, 1301–1311.

Lammerant, J., Huynh-thu, T., Kolanowski, J., and Inhibitory, J.K. (1985). Inhibitory Effects o f the D (-) Isomer of 3-hydroxybutyrate on Cardiac Non-esterified Fatty Acid Uptake and Oxygen Demand Induced by Norepinephrine in the Intact Dog. J Mol Cell Cardiol *433*, 421–433.

Larsen, F.J., Weitzberg, E., Lundberg, J.O., and Carlstro, M. (2011a). Roles of dietary inorganic nitrate in cardiovascular health and disease. 525–532.

Larsen, F.J., Schiffer, T.A., Borniquel, S., Sahlin, K., Ekblom, B., Lundberg, J.O., and Weitzberg, E. (2011b). Dietary inorganic nitrate improves mitochondrial efficiency in humans. Cell Metab. *13*, 149–159.

Lashin, O.M., Szweda, P.A., Szweda, L.I., and Romani, A.M.P. (2006). Decreased complex II respiration and HNE-modified SDH subunit in diabetic heart. Free Radic. Biol. Med. *40*, 886–896.

Lateef, R.U., Al-masri, A.A., and Alyahya, A.M. (2015). Langendorff ' s isolated perfused rat heart technique : a review. Int. J. Basic Clin. Pharmacol. *4*, 1314–1322.

Lee, J.A., and Allen, D.G. (2006). Mechanisms of Acute Ischemic Contractile Failure of the Heart. Role of Intracellular Calcium. J. Clin. Investig. *88*, 361–367.

Lehto, S., Rönnemaa, T., Pyörälä, K., and Laakso, M. (1999). Poor glycemic control predicts coronary heart disease events in patients with type 1 diabetes without nephropathy. Arterioscler. Thromb. Vasc. Biol. *19*, 1014–1019.

Li, J., Iorga, A., Sharma, S., Youn, J.-Y., Partow-Navid, R., Umar, S., Cai, H., Rahman, S., and Eghbali, M.

(2013). Intralipid, a Clinically Safe Compound, Protects the Heart Against Ischemia-Reperfusion Injury More Efficiently Than Cyclosporine-A. Anesthesiology *117*, 836–846.

Li, X., Gu, J., and Zhou, Q. (2015). Review of aerobic glycolysis and its key enzymes – new targets for lung cancer therapy. Thorac. Cancer *6*, 17–24.

Liang, Q., Carlson, E.C., Donthi, R. V, Kralik, P.M., Shen, X., and Epstein, P.N. (2002). Overexpression of metallothionein reduces diabetic cardiomyopathy. Diabetes *51*, 174–181.

Liao, R., Podesser, B.K., and Lim, C.C. (2012). The continuing evolution of the Langendorff and ejecting murine heart : new advances in cardiac phenotyping. Am J Physiol Hear. Circ Physiol *303*, 156–167.

Liedtke, A.J., Demaison, L., Eggleston, A.M., Cohen, L.M., and Nellis, S.H. (1988). Changes in Substrate Metabolism and Effects of Excess Fatty Acids in Reperfiised Myocardium. Circ. Res. *62*, 535–542.

Linn, T., Santosa, B., Grönemeyer, D., Aygen, S., Scholz, N., Busch, M., and Bretzel, R.G. (2000). Effect of long-term dietary protein intake on glucose metabolism in humans. Diabetologia *43*, 1257–1265.

Liu, J., Wang, P., Douglas, S.L., Tate, J.M., Sham, S., Lloyd, S.G., Liu, J., Wang, P., Sl, D., Jm, T., et al. (2016). Impact of high-fat , low-carbohydrate diet on myocardial substrate oxidation , insulin sensitivity , and cardiac function after ischemia-reperfusion. 1–10.

Liu, J.L.Y., Maniadakis, N., Gray, A., and Rayner, M. (2002). The economic burden of coronary heart disease in the. Heart *88*, 597–603.

Lloyd, S., Brocks, C., and Chatham, J.C. (2003). Differential modulation of glucose , lactate , and pyruvate oxidation by insulin and dichloroacetate in the rat heart. Am J Physiol Hear. Circ Physiol *285*.

Lloyd, S.G., Wang, P., Zeng, H., Chatham, J.C., Steven, G., Wang, P., Zeng, H., and John, C. (2004). Impact of low-flow ischemia on substrate oxidation and glycolysis in the isolated perfused rat heart. *0005*.

Loiselle, D.S., Han, J.-C., Mellor, K.M., Phamm, T., Tran, K., Goo, S., Taberner, A.J., and Hickey, A.J.R. (2014). Assessing the Efficiency of the Diabetic Heart at Subcellular, Tissue and Organ Level. J. Gen. Pract. *02*.

Lomax, P. (1966). Measurement of Core Temperature in the Rat. Nature *209*, 694–696.

Lopaschuk, G.D. (1997). Advantages and limitations of experimental techniques used to measure

cardiac energy metabolism. J. Nucl. Cardiol. *4*, 316–2328.

Lopaschuk, G.D., Spafford, M.A., Davies, N.J., and Wall, S.R. (1990). Glucose and Palmitate Oxidation in Isolated Working Rat Hearts Reperfused After a Period of Transient Global Ischemia. Circ. Res. *66*, 546–553.

Lopaschuk, G.D., Wambolt, R.B., and Barr, R.L. (1993). An Imbalance between Glycolysis and Glucose Oxidation Is a Possible Explanation for the Detrimental Effects of High Levels of Fatty Acids during Aerobic Reperfusion of Ischemic Hearts. J. Pharmacol. Exp. Ther. *264*, 135–144.

Lopaschuk, G.D., Ussher, J.R., Folmes, C.D.L., Jaswal, J.S., and Stanley, W.C. (2009). Myocardial Fatty Acid Metabolism in Health and Disease. Physiol Rev *90*, 207–258.

Lopaschuk, G.D., Ussher, J.R., Folmes, C.D.L., Jaswal, J.S., and Stanley, W.C. (2010). Myocardial Fatty Acid Metabolism in Health and Disease. Physiol Rev 207–258.

Lou, P.H., Lucchinetti, E., Zhang, L., Affolter, A., Schaub, M.C., Gandhi, M., Hersberger, M., Warren, B.E., Lemieux, H., Sobhi, H.F., et al. (2014a). The mechanism of intralipid®-mediated cardioprotection complex IV inhibition by the active metabolite, palmitoylcarnitine, generates reactive oxygen species and activates reperfusion injury salvage kinases. PLoS One *9*.

Lou, P.H., Lucchinetti, E., Zhang, L., Affolter, A., Gandhi, M., Hersberger, M., Warren, B.E., Lemieux, H., Sobhi, H.F., Clanachan, A.S., et al. (2014b). Loss of Intralipid®- but not sevoflurane-mediated cardioprotection in early type-2 diabetic hearts of fructose-fed rats: Importance of ROS signaling. PLoS One *9*, 1–13.

Lou, P.H., Lucchinetti, E., Zhang, L., Affolter, A., Gandhi, M., Hersberger, M., Warren, B.E., Lemieux, H., Sobhi, H.F., Clanachan, A.S., et al. (2014c). Loss of Intralipid®- but not sevoflurane-mediated cardioprotection in early type-2 diabetic hearts of fructose-fed rats: Importance of ROS signaling. PLoS One *9*.

Lu, Z., Jiang, Y., Xu, X., Ballou, L.M., Cohen, I.S., and Lin, R.Z. (2007). Decreased L-Type Ca2+ Current in Cardiac Myocytes of Type 1 Diabetic Akita Mice Due to Reduced Phosphatidylinositol 3-Kinase signalling. Diabetes *56*, 2780–2789.

Lunt, S.Y., and Heiden, M.G. Vander (2011). Aerobic Glycolysis : Meeting the Metabolic Requirements of Cell Proliferation. Annu. Rev. Cell Dev. Biol. *27*, 441–464.

Macdonald, M.R., Petrie, M.C., Varyani, F., Jan, O., Michelson, E.L., Young, J.B., Solomon, S.D., Granger, C.B., Swedberg, K., Yusuf, S., et al. (2008). Impact of diabetes on outcomes in patients with low and preserved ejection fraction heart failure Reduction in Mortality and morbidity (CHARM)

programme. Eur. Heart J. *29*, 1377–1385.

MacDonald, J.R., Oellermann, M., Rynbeck, S., Chang, G., Ruggiero, K., Cooper, G.J.S., and Hickey, A.J.R. (2011). Transmural differences in respiratory capacity across the rat left ventricle in health, aging, and streptozotocin-induced diabetes mellitus: evidence that mitochondrial dysfunction begins in the subepicardium. AJP Cell Physiol. *300*, C246–C255.

Mamou, Z., Descotes, J., Chevalier, P., Bui-Xuan, B., Romestaing, C., and Timour, Q. (2015). Electrophysiological, haemodynamic, and mitochondrial alterations induced by levobupivacaine during myocardial ischemia in a pig model: Protection by lipid emulsions? Fundam. Clin. Pharmacol. *29*, 439–449.

Manninen, A.H. (2004). Metabolic Effects of the Very-Low- Carbohydrate Diets : Misunderstood "Villains" of Human Metabolism. J. Int. Soc. Sports Nutr. *1*, 7–11.

Mansor, L.S., Gonzalez, E.R., Cole, M. a, Tyler, D.J., Beeson, J.H., Clarke, K., Carr, C. a, and Heather, L.C. (2013). Cardiac metabolism in a new rat model of type 2 diabetes using high-fat diet with low dose streptozotocin. Cardiovasc. Diabetol. *12*, 136.

Marcinek, D.J., Kushmerick, M.J., and Conley, K.E. (2010). Lactic acidosis in vivo : testing the link between lactate generation and H ƨ accumulation in ischemic mouse muscle. J Appl Physiol *108*, 1479–1486.

Mccommis, K.S., and Finck, B.N. (2016). Mitochondrial pyruvate transport: a historical perspective and future research directions. Biochem. J. *466*, 443–454.

McGarry, J.D., and Foster, D.W. (1976). Ketogenesis and its regulation. Am. J. Med. *61*, 9–13.

Mcnulty, P.H., Jagasia, D., Cline, G.W., Ng, C.K., Whiting, J.M., Garg, P., Shulman, G.I., and Soufer, R. (2000). Persistent Changes in Myocardial Glucose Metabolism In Vivo During Reperfusion of a Limited-Duration Coronary Occlusion. Circulation *101*, 917–922.

Mitchel, P. (1961). Coupling of Phosphorylation to Electron and Hydrogen Transfer by a Chemiosmotic Type of Mechanism. Nature *191*, 144–148.

Monaco, C.M.F., Miotto, P.M., Huber, J.S., Van Loon, L.J.C., Simpson, J.A., and Holloway, G.P. (2018). Sodium nitrate supplementation alters mitochondrial H2O2 emission but does not improve mitochondrial oxidative metabolism in the heart of healthy rats. J Physiol.

Murray, A.J., Panagia, M., Hauton, D., Gibbons, G.F., and Clarke, K. (2005). Plasma free fatty acids and peroxisome proliferator-activated receptor alpha in the control of myocardial uncoupling

protein levels. Diabetes *54*, 3496–3502.

Murray, A.J., Cole, M.A., Lygate, C.A., Carr, C.A., Stuckey, D.J., Little, S.E., Neubauer, S., and Clarke, K. (2008). Increased mitochondrial uncoupling proteins, respiratory uncoupling and decreased efficiency in the chronically infarcted rat heart. J. Mol. Cell. Cardiol. *44*, 694–700.

Myears, D.W., Sobel, E., and Bergmann, R. (1987). Substrate use in ischemic and reperfused canine myocardium : quantitative considerations. Am. Physiol. Soc. *87*, 107–114.

Nakao, M., Matsubara, T., and Sakamoto, N. (1993). Effects of diabetes on cardiac glycogen metabolism in rats. Heart Vessels *8*, 171–175.

Neely, J.R., Liebermeister, H., Battersby, E.J., and Morgan, H.E. (1967). Effect of pressure development on oxygen consumption by isolated rat heart. Am. J. Physiol. *212*, 804–814.

Nellis, S.H., Liedtke, A.J., and Renstrom, B. (1991). Distribution of Carbon Flux Within Fatty Acid Utilization During Myocardial Ischemia and Reperfusion. Circ. Res. *69*, 779–790.

Neubauer, S. (2007). The Failing Heart — An Engine Out of Fuel.

Newman, J.C., and Verdin, E. (2017). β-Hydroxybutyrate: A Signaling Metabolite. Annu. Rev. Nutr. *37*.

Newman, J.C., Verdin, E., Francisco, S., and Francisco, S. (2015). β -hydroxybutyrate : Much more than a metabolite. *106*, 173–181.

Nguyen, T.P., Qu, Z., and Weiss, J.N. (2014). Cardiac fibrosis and arrhythmogenesis The road to repair is paved. J. Mol. Cell. Cardiol. *70*, 83–91.

NHS (2017). National Diabetes Audit , 2015-16 Report 2a : Complications and Mortality.

Nielsen, L.B., Bartels, E.D., and Bollano, E. (2002). Overexpression of apolipoprotein B in the heart impedes cardiac triglyceride accumulation and development of cardiac dysfunction in diabetic mice. J. Biol. Chem. *277*, 27014–27020.

Nishikawa, T., Edelstein, D., Du, X.L., Yamagishi, S., Matsumura, T., Kaneda, Y., Yorek, M.A., Beebe, D., Oates, P.J., Hammes, H., et al. (2000). Normalizing mitochondrial superoxide production blocks three pathways of hyperglycaemic damage. Nature *404*, 787–790.

Nohl, H., and Werner, J. (1986). The mitochondrial site of superoxide formation. Biochem. Biophys. Res. Commun. *138*, 533–539.

Onay-Besikci, A. (2006). Regulation of cardiac energy metabolism in newborn. Mol. Cell. Biochem. *287*, 1–11.

Opie, L.H., and Sack, M.N. (2002). Metabolic Plasticity and the Promotion of Cardiac Protection in Ischemia and Ischemic Preconditioning. J Mol Cell Cardiol *1089*, 1077–1089.

Opie, L.H., Owen, P., and Riemersma, R.A. (1973). Relative Rates of Oxidation of Glucose and Free Fatty Acids by Ischaemic and Non-Ischaemic Myocardium after Coronary Artery Ligation in the Dog. Eur. J. Clin. Invest. *3*, 419–435.

Orchard, T.J., Olson, J.C., Erbey, J.R., Williams, K., Forrest, K.Y.Z., Kinder, L.S., Ellis, D., and Becker, D.J. (2003). Insulin resistance-related factors, but not glycemia, predict coronary artery disease in type 1 diabetes: 10-year follow-up data from the Pittsburgh epidemiology of diabetes complications study. Diabetes Care *26*, 1374–1379.

Owen, O.E., Kalhan, S.C., and Hanson, R.W. (2002). The Key Role of Anaplerosis and Cataplerosis for Citric Acid Cycle Function *. J. Biol. Chem. *34*, 30409–30412.

Le Page, L.M., Rider, O.J., Lewis, A.J., Ball, V., Clarke, K., Johansson, E., Carr, C. a, Heather, L.C., and Tyler, D.J. (2015). Increasing Pyruvate Dehydrogenase Flux as a Treatment for Diabetic Cardiomyopathy: A Combined 13C Hyperpolarized Magnetic Resonance and Echocardiography Study. Diabetes *64*, 2735–2743.

Pannala, A.S., Mani, A.R., Spencer, J.P.E., Skinner, V., Bruckdorfer, K.R., Moore, K.P., and Rice-Evans, C.A. (2003). The Effect of Dietary Nitrate on Salivary, Plasma, and Urinary Nitrate Metabolism in Humans. Free Radic. Biol. Med. *34*, 576–584.

Panth, N., Paudel, K.R., and Parajuli, K. (2016). Reactive Oxygen Species : A Key Hallmark of Cardiovascular Disease. Adv. Med. 1–12.

Paoli, A., Rubini, A., Volek, J.S., and Grimaldi, K.A. (2013). Beyond weight loss : a review of the therapeutic uses of very-low-carbohydrate (ketogenic) diets. Eur. J. Clin. Nutr. *67*, 789–796.

Papandreou, I., Cairns, R.A., Fontana, L., Lim, A.L., and Denko, N.C. (2006). HIF-1 mediates adaptation to hypoxia by actively downregulating mitochondrial oxygen consumption. 187–197.

Papanicolaou, K.N., Rourke, B.O., and Foster, D.B. (2014). Metabolism leaves its mark on the powerhouse : recent progress in post-translational modifications of lysine in mitochondria. Front. Physiol. *5*, 1–22.

Patton, K.T., and Thibodeau, G.A. (2013). Anatomy and Physiology (St. Louis: Mosby).

Pham, T., Loiselle, D., Power, A., and Hickey, A.J.R. (2014). Mitochondrial inefficiencies and anoxic ATP hydrolysis capacities in diabetic rat heart. AJP Cell Physiol. *307*, C499–C507.

Piper, H.M., and Ovize, M. (1998). A fresh look at reperfusion injury. Cardiovasc. Res. *38*, 291–300.

Piper, H.M., Abdallah, Y., and Schäfer, C. (2004). The first minutes of reperfusion: A window of opportunity for cardioprotection. Cardiovasc. Res. *61*, 365–371.

Pironti, G., Ivarsson, N., Yang, J., Farinotti, A.B., Jonsson, W., Zhang, S.J., Bas, D., Svensson, C.I., Westerblad, H., Weitzberg, E., et al. (2016). Dietary nitrate improves cardiac contractility via enhanced cellular Ca2+ signaling. Basic Res. Cardiol. *111*.

Del Prato, S., Tiengo, A., Baccaglini, U., Tremolada, C., Duner, E., Marescotti, M.C., Avogaro, A., Valverde, I., Nosadini, R., and Assan, R. (1983). Effect of insulin replacement on intermediary metabolism in diabetes secondary to pancreatectomy. Diabetologia *25*, 252–259.

Pride, C.K., Mo, L., Quesnelle, K., Dagda, R.K., Murillo, D., Geary, L., Corey, C., Portella, R., Zharikov, S., St Croix, C., et al. (2014). Nitrite activates protein kinase A in normoxia to mediate mitochondrial fusion and tolerance to ischaemia/reperfusion. Cardiovasc. Res. *101*, 57–68.

Prondzinsky, R., Unverzagt, S., and Lemm, H. (2012). Interleukin-6 , -7 , -8 and -10 predict outcome in acute myocardial infarction complicated by cardiogenic shock. Clin Res Cardiol *101*, 375–384.

Punithavathi, V.R., Shanmugapriya, K., and Stanely Mainzen Prince, P. (2010). Protective effects of rutin on mitochondrial damage in isoproterenol- induced cardiotoxic rats: An in vivo and in vitro study. Cardiovasc. Toxicol. *10*, 181–189.

Quant, P.A., Tubbs, P.K., and Brand, M.D. (1990). Glucagon activates mitochondrial 3-hydroxy-3-methylglutaryl-CoA synthase in vivo by decreasing the extent of succinylation of the enzyme. Eur. J. Biochem. *187*, 169–174.

Raedschelders, K., Ansley, D.M., and Chen, D.D.Y. (2012). Pharmacology & Therapeutics The cellular and molecular origin of reactive oxygen species generation during myocardial ischemia and reperfusion. Pharmacol. Ther. *133*, 230–255.

Rahman, S., Jingyuan, L., Chrisostome Bopassa, J., Umar, S., Iorga, A., Partownavid, P., and Eghbali, M. (2012). Phosphorylation of GSK-3β mediates Intralipid-induced cardioprotection against Ischemia/Reperfusion injury. Anesthesiology *115*, 242–253.

Randle, P., Garland, M., Hales, C., and Newsholme, E. (1963). The Glucose Fatty-Acid Cycle: Its Role in Insulin Sensitivity and the Metabolic Disturbances of Diabetes Mellitus. Lancet *281*, 785–789.

Ravingerova, T., Adameova, A., Carnicka, S., Nemcekova, M., Kelly, T., Matejikova, J., Galatou, E., Barlaka, E., and Lazou, A. (2011). The role of PPAR in myocardial response to ischemia in normal and

diseased heart. 329–341.

Reed, M.A.C., Ludwig, C., Bunce, C.M., Khanim, F.L., and Günther, U.L. (2016). Malonate as a ROS product is associated with pyruvate carboxylase activity in acute myeloid leukaemia cells. Cancer Metab. *4*, 1–8.

Richmond, W., Ambrosio, G., Pike, M., Jacobus, W., and Becker, L. (1992). The functional recovery of post-ischemic myocardium requires glycolysis during early reperfusion.pdf. J Mol Cell Cardiol *25*, 261–276.

Ripplinger, C.M., Lou, Q., Li, W., Hadley, J., and Efimov, I.R. (2009). Panoramic imaging reveals basic mechanisms of induction and termination of ventricular tachycardia in rabbit heart with chronic infarction: Implications for low-voltage cardioversion. HeartRhythm *6*, 87–97.

Risa, Ø., Henry, D.K.P., and Sonnewald, U. (2011). Tricarboxylic Acid Cycle Activity Measured by 13 C Magnetic Resonance Spectroscopy in Rats Subjected to the Kaolin Model of Obstructed Hydrocephalus. *i*, 1801–1808.

Ritchie, R.H., Zerenturk, E.J., Prakoso, D., and Calkin, A.C. (2017). Lipid metabolism and its implications for type 1 diabetes-associated cardiomyopathy. J. Mol. Endocrinol. *58*, R225–R240.

Roberts, L.D., Murray, A.J., Menassa, D., Ashmore, T., Nicholls, A.W., and Griffin, J.L. (2011). The contrasting roles of PPAR δ and PPAR g in regulating the metabolic switch between oxidation and storage of fats in white adipose tissue. Genome Biol. *12*, R75.

Roberts, L.D., Ashmore, T., Kotwica, A.O., and Mur, S.A. (2015). Inorganic Nitrate Promotes the Browning of White Adipose Tissue Through the Nitrate- Nitrite-Nitric Oxide Pathway. *64*, 471–484.

Ross, T., Szczepanek, K., Bowler, E., Hu, Y., Larner, A., Lesnefsky, J., and Chen, Q. (2013). Reverse electron flow-mediated ROS generation in ischemia- damaged mitochondria: Role of complex I inhibition vs. depolarization of inner mitochondrial membrane. Biochim. Biophys. Acta *1830*, 4537–4542.

Roth, D.A., White, C.D., Hamilton, C.D., Hall, J.L., and Stanley, W.C. (1995). Adrenergic Desensitization in Left Ventricle from Streptozotocin Diabetic Swine. J Mol Cell Cardiol *27*, 2315–2325.

Rubler, S., Dlugash, J., Yuceoglu, Y.Z., Kumral, T., Branwood, A.W., and Grishman, A. (1972). New type of cardiomyopathy associated with diabetic glomerulosclerosis. Am. J. Cardiol. *30*, 595–602.

Ruparelia, N., Chai, J.T., Fisher, E.A., and Choudhury, R.P. (2016). Inflammatory processes in

cardiovascular disease: a route to targeted therapies. Nat. Publ. Gr. *14*, 133–144.

Sandanger, Gao, E., Ranheim, T., Bliksøen, M., Kaasbøll, O.J., Alfsnes, K., Nymo, S.H., Rashidi, A., Ohm, I.K., Attramadal, H., et al. (2016). NLRP3 inflammasome activation during myocardial ischemia reperfusion is cardioprotective. Biochem. Biophys. Res. Commun. *469*, 1012–1020.

Sato, K., Kashiwaya, Y., Keaon, C.A., Tsuchiya, N., King, M.T., Radda, G.K., Chance, B., Clarke, K., and Veechn, R.L. (1995). Insulin ketone bodies and mitochondrial energy transduction.pdf. FASEB *9*, 651–658.

Schell, J.C., and Rutter, J. (2013). The long and winding road to the mitochondrial pyruvate carrier. Cancer Metab. *1*, 1–9.

Schenkman, K.A., Beard, D.A., Ciesielski, W.A., Feigl, E.O., Kenneth, A., and Wayne, A. (2003). Comparison of buffer and red blood cell perfusion of guinea pig heart oxygenation. Am J Physiol Hear. Circ Physiol *285*, H1819–H1825.

Scherer, P.E., Hill, J.A., Schulze, P.C., Drosatos, K., and Goldberg, I.J. (2016). Lipid Use and Misuse by the Heart. Circ. Res. *118*, 1736–1752.

Schilling, J.D., and Mann, D.L. (2012). Diabetic Cardiomyopathy: Bench to Bedside. Hear. Fail Clin *8*, 619–631.

Schönfeld, P., and Reiser, G. (2013). Why does brain metabolism not favor burning of fatty acids to provide energy-Reflections on disadvantages of the use of free fatty acids as fuel for brain. J. Cereb. Blood Flow Metab. *33*, 1493–1499.

Schönfeld, P., Wi, M.R., Lebiedzi, M., and Wojtczak, L. (2010). Mitochondrial fatty acid oxidation and oxidative stress : Lack of reverse electron transfer-associated production of reactive oxygen species. Biochim. Biophys. Acta *1797*, 929–938.

Schugar, R.C., Moll, A.R., André d'Avignon, D., Weinheimer, C.J., Kovacs, A., and Crawford, P.A. (2014). Cardiomyocyte-specific deficiency of ketone body metabolism promotes accelerated pathological remodeling. Mol. Metab. *3*, 754–769.

Schulz, H. (1991). Beta oxidation of fatty acids. Biochim. Biophys. Acta *1081*, 109–120.

Shimazu, T., Hirschey, M.D., Newman, J., He, W., Moan, N. Le, Grueter, C.A., Lim, H., Laura, R., Stevens, R.D., Newgard, C.B., et al. (2013). Suppression of Oxidative Stress by β-Hydroxybutyrate, an Endogenous Histone Deacetylase Inhibitor. Science (80-.). *339*, 211–214.

Shinde, A. V, and Frangogiannis, N.G. (2014). Fibroblasts in myocardial infarction : A role in

inflammation and repair. J. Mol. Cell. Cardiol. *70*, 74–82.

Shiva, S., and Gladwin, M.T. (2009). Nitrite mediates cytoprotection after ischemia/reperfusion by modulating mitochondrial function. Basic Res. Cardiol. *104*, 113–119.

Shiva, S., Sack, M.N., Greer, J.J., Duranski, M., Ringwood, L.A., Burwell, L., Wang, X., Macarthur, P.H., Shoja, A., Raghavachari, N., et al. (2007). Nitrite augments tolerance to ischemia / reperfusion injury via the modulation of mitochondrial electron transfer. JEM *204*, 2089–2102.

Simonson, T.S., Yang, Y., Huff, C.D., Yun, H., Qin, G., Witherspoon, D.J., Bai, Z., Lorenzo, F.R., Xing, J., Jorde, L.B., et al. Genetic Evidence for High-Altitude Adaptation in Tibet.

Šoltésová, D., Veselá, A., Mravec, B., and Herichová, I. (2013). Daily profile of glut1 and glut4 expression in tissues inside and outside the blood-brain barrier in control and streptozotocin-treated rats. Physiol. Res. *62*.

Sookoian, S., and Pirola, C.J. (2012). Alanine and aspartate aminotransferase and glutamine-cycling pathway: Their roles in pathogenesis of metabolic syndrome. World J. Gastroenterol. *18*, 3775–3781.

Stanley, W.C., Lopaschuk, G.D., and Mccormack, J.G. (1997a). Regulation of energy substrate metabolism in the diabetic heart. Cardiovasc. Res. *34*, 25–33.

Stanley, W.C., Lopaschuk, G.D., Hall, J.L., and Mccormack, J.G. (1997b). Regulation of myocardial carbohydrate metabolism under normal and ischaemic conditions Potential for pharmacological interventions. Cardiovasc. Res. *33*, 243–257.

Stanley, W.C., Meadows, S.R., Kivilo, K.M., Roth, B.A., Lopaschuk, G.D., William, C., Meadows, S.R., Krista, M., Roth, B.A., and Lopaschuk, G.D. (2003). [illegible] -Hydroxybutyrate inhibits myocardial fatty acid oxidation in vivo independent of changes in malonyl-CoA content. *4970*, 1626–1631.

Stanley, W.C., Recchia, F.A., and Lopaschuk, G.D. (2005). Myocardial Substrate Metabolism in the Normal and Failing Heart. 1093–1129.

Stone, G.W., Selker, H.P., Thiele, H., Patel, M.R., Udelson, J.E., Ohman, E.M., Maehara, A., Eitel, I., Granger, C.B., Jenkins, P.L., et al. (2016). Relationship Between Infarct Size and Outcomes Following Primary PCI. J. Am. Coll. Cardiol. *67*, 1674–1683.

Szabo, C. (2009). Role of nitrosative stress in the pathogenesis of diabetic vascular dysfunction. Br. J. Pharmacol. *156*, 713–727.

Taegtmeyer, H., and Lubrano, G. (2014). Rethinking cardiac metabolism : metabolic cycles to refuel

and rebuild the failing heart. F1000 Prime Reports *9*, 1–9.

Taegtmeyer, H., and Stanley, W.C. (2011). Journal of Molecular and Cellular Cardiology Too much or not enough of a good thing ? Cardiac glucolipotoxicity versus lipoprotection. J. Mol. Cell. Cardiol. *50*, 2–5.

Taegtmeyer, H., and de Villalobos, D.H. (1995). Metabolic support for the postischaemic heart. Lancet *345*, 1552–1555.

Taegtmeyer, H., Peterson, M.B., Ragavan, V. V, Ferguson, A.G., and Lesch, M. (1977). De Novo Alanine Synthesis in Isolated Oxygen-deprived Rabbit Myocardium. J. Biol. Chem. *252*, 5010–5018.

Talman, V., and Ruskoaho, H. (2016). Cardiac fibrosis in myocardial infarction — from repair and remodeling to regeneration. Cell Tissue Res. 563–581.

Tran-dinh, S., Beganton, F., Ncuyen, T., Bouet, F., and Herve, M. (1996). Mathematical model for evaluating the Krebs cycle flux with non-constant glutamate-pool size by I3C-NMR spectroscopy Evidence for the existence of two types of Krebs cycles in cells. Eur. J. Biochem. *242*, 220–227.

Transonic (2018). Technical Note Ex-vivo Isolated Langendorff Heart Model for Cardiac Assessment using Pressure Measurements. 1–9.

Turrens, J.F. (2003). Mitochondrial formation of reactive oxygen species. J Physiol *2*, 335–344.

Veech, R.L. (2004). The therapeutic implications of ketone bodies : the effects of ketone bodies in pathological conditions : ketosis , ketogenic diet , redox states , insulin resistance , and mitochondrial metabolism. Prostaglandins, Leukot. Essent. Fat. Acids *70*, 309–319.

Veech, R.L., Chance, B., Kashiwaya, Y., Lardy, H.A., and Cahill, G.F. (2001). Ketone Bodies, Potential Therapeutic Uses. Life *51*, 241–247.

Verdouw, P.D., Doel, M.A. Van Den, Zeeuw, S. De, and Duncker, D.J. (1998). Animal models in the study of myocardial ischaemia and ischaemic syndromes. Cardiovasc Res *39*, 121–135.

Wall, S.R., and Lopaschuk, G.D. (1989). Glucose oxidation rates in fatty acid-perfused isolated working hearts from diabetic rats. Biochim. Biophys. Acta *1006*, 97–103.

Webb, A.J., Patel, N., Loukogeorgakis, S., Okorie, M., Aboud, Z., Misra, S., Rashid, R., Miall, P., Deanfield, J., Benjamin, N., et al. (2008). Acute blood pressure lowering, vasoprotective, and antiplatelet properties of dietary nitrate via bioconversion to nitrite. Hypertension *51*, 784–790.

Weihrauch, D., Krolikowski, J.G., Bienengraeber, M., Kersten, J.R., Warltier, D.C., and Pagel, P.S.

(2005). Morphine enhances isoflurane-induced postconditioning against myocardial infarction: The role of phosphatidylinositol-3-kinase and opioid receptors in rabbits. Anesth. Analg. *101*, 942–949.

Weiss, J., and Hiltbrand, B. (1985). Functional Compartmentation of Glycolytic Versus Oxidative Metabolism in Isolated Rabbit Heart. J. Clin. Investig. *75*, 436–447.

Wengrowski, A.M., Kuzmiak-Glancy, S., Jaimes, R., and Kay, M.W. (2014). NADH changes during hypoxia, ischemia, and increased work differ between isolated heart preparations. Am. J. Physiol. Circ. Physiol. *306*, H529–H537.

Wentz, A.E., D'Avignon, D.A., Weber, M.L., Cotter, D.G., Doherty, J.M., Kerns, R., Nagarajan, R., Reddy, N., Sambandam, N., and Crawford, P.A. (2010). Adaptation of myocardial substrate metabolism to a ketogenic nutrient environment. J. Biol. Chem. *285*, 24447–24456.

Whitmer, J.T., Idell-Wenger, J.A., Rovetto, M.J., and Neely, J.R. (1978). Control of fatty acid metabolism in ischemic and hypoxic hearts. J. Biol. Chem. *253*, 4305–4309.

Wier, W.G. (1990). Cytoplasmic [Ca2+] In Mammalian Ventricle: Dynamic Control By Cellular Processes. Annu Rev Physiol *52*, 467–485.

Wold, L.E., and Ren, J. (2004). Streptozotocin directly impairs cardiac contractile function in isolated ventricular myocytes via a p38 map kinase-dependent oxidative stress mechanism. Biochem. Biophys. Res. Commun. *318*, 1066–1071.

Wold, L.E., Ceylan-isik, A.F., and Ren, J. (2005). Oxidative stress and stress signaling : menace of diabetic cardiomyopa- thy. Acta Pharmacol. Sin. *26*, 908–917.

Wu, P., Sato, J., Zhao, Y., Jaskiewicz, J., Popov, K.M., and Harris, R. a (1998). Starvation and diabetes increase the amount of pyruvate dehydrogenase kinase isoenzyme 4 in rat heart. Biochem. J. *329*, 197–201.

Yamanashi, T., Iwata, M., Kamiya, N., Tsunetomi, K., Kajitani, N., Wada, N., Iitsuka, T., Yamauchi, T., Miura, A., Pu, S., et al. (2017). Beta-hydroxybutyrate, an endogenic NLRP3 inflammasome inhibitor, attenuates stress-induced behavioral and inflammatory responses. Sci. Rep. *7*, 1–11.

Yang, L., Kasumov, T., Kombu, R.S., Zhu, S., Cendrowski, A. V, David, F., Anderson, V.E., Kelleher, J.K., and Brunengraber, H. (2008). Metabolomic and Mass Isotopomer Analysis of Liver Gluconeogenesis and Citric Acid Cycle. J. Biol. Chem. *283*, 21988–21996.

Yano, M., Akazawa, H., Oka, T., Yabumoto, C., Kudo-Sakamoto, Y., Kamo, T., Shimizu, Y., Yagi, H., Naito, A.T., Lee, J.K., et al. (2015). Monocyte-derived extracellular Nampt-dependent biosynthesis of

NAD + protects the heart against pressure overload. Sci. Rep. *5*, 1–14.

Yao, D., and Brownlee, M. (2010). Hyperglycemia-Induced Reactive Oxygen Species Increase Expression of the Receptor for Advanced Glycation End Products (RAGE) and RAGE Ligands. Diabetes *59*, 249–255.

Yao, X., Li, Y., Tao, M., Wang, S., Zhang, L., Lin, J., Xia, Z., and Liu, H. (2015). Effects of Glucose Concentration on Propofol Cardioprotection against Myocardial Ischemia Reperfusion Injury in Isolated Rat Hearts. J. Diabetes Res. 1–10.

Yin, Q., Yang, C., Wu, J., Lu, H., Zheng, X., and Zhang, Y. (2016). Downregulation of β -Adrenoceptors in Isoproterenol-Induced Cardiac Remodeling through HuR. 1–14.

Yoshioka, J., Chutkow, W.A., Lee, S., Kim, J.B., Yan, J., Tian, R., Lindsey, M.L., Feener, E.P., Seidman, C.E., Seidman, J.G., et al. (2012). Deletion of thioredoxin-interacting protein in mice impairs mitochondrial function but protects the myocardium from ischemia-reperfusion injury. J. Clin. Invest. *122*, 267–279.

Youm, Y., Nguyen, K.Y., Grant, R.W., Goldberg, E.L., Bodogai, M., Kang, S., Horvath, T.L., Fahmy, T.M., and Crawford, P.A. (2015). Ketone body β-hydroxybutyrate blocks the NLRP3 inflammasome-mediated inflammatory disease. Nat. Med. *21*, 263–269.

Yu, T., Robotham, J.L., and Yoon, Y. (2006). Increased production of reactive oxygen species in hyperglycemic conditions requires dynamic change of mitochondrial morphology. PNAS *103*, 2653–2658.

Yu, T., Sheu, S.-S., Robotham, J.L., and Yoon, Y. (2009). Mitochondrial fission mediates high glucose-induced cell death through elevated production of reactive oxygen species. Medicine (Baltimore). *79*, 341–351.

Yu, X., White, L.T., Lewandowski, E.D., Damico, L.A., Kathryn, F., and Alpert, N.M. (1995). Kinetic Analysis of Dynamic 13C NMR Spectra : Metabolic Flux , Regulation , and Compartmentation in Hearts. Biophys. J. *69*, 2090–2102.

Yu, Y. Bin, Bian, J.M., and Gu, D.H. (2015). Transplantation of insulin-producing cells to treat diabetic rats after 90% pancreatectomy. World J. Gastroenterol. *21*, 6582–6590.

Zhao, Z.-Q., Corvera, J.S., Halkos, M.E., Kerendi, F., Wang, N.-P., Guyton, R.A., and Vinten-Johansen, J. (2003). Inhibition of myocardial injury by ischemic postconditioning during reperfusion: comparison with ischemic preconditioning. Am. J. Physiol. - Hear. Circ. Physiol. *285*, H579–H588.

Zhao, Z., Nelson, A.R., Betsholtz, C., and Zlokovic, B. V. (2015). Establishment and Dysfunction of the Blood-Brain Barrier. Cell *163*, 1064–1078.

Zhou, L., Stanley, W.C., Saidel, G.M., Yu, X., and Cabrera, M.E. (2005). Regulation of lactate production at the onset of ischaemia is independent of mitochondrial NADH / NAD + : insights from in silico studies. J Physiol *3*, 925–937.

Zhou, R., Ma, P., Xiong, A., Xu, Y., Wang, Y., and Xu, Q. (2017). Protective effects of low-dose rosuvastatin on isoproterenol-induced chronic heart failure in rats by regulation of DDAH-ADMA-NO pathway. Cardiovasc. Ther. *35*, 1–8.

Zhu, X., and Zuo, L. (2013). Characterization of oxygen radical formation mechanism at early cardiac ischemia. Cell Death Dis. *4*, e787-7.

Zorov, D.B., Juhaszova, M., and Sollott, S.J. (2014). Mitochondrial Reactive Oxygen Species (ROS) and ROS-Induced ROS Release. Physiol. Rev. *94*, 909–950.

Zou, Z., Sasaguri, S., Rajesh, K.G., Suzuki, R., Sasaguri, S., Gopalrao, K., and Suzuki, R. (2002). dl -3-Hydroxybutyrate administration prevents myocardial damage after coronary occlusion in rat hearts. Am J Physiol Hear. Circ Physiol *283*, 1968–1974.

Appendices

APPENDIX II

II.1 Composition of the Krebs-Henseleit Buffer

Table 1: ***The basic composition of the Krebs-Henseleit buffer (KH) used to sustain the heart.*** The buffer is composed at pH 7.4, and may contain additional substrates/components depending upon the experiment.

Constituent	**Concentration (mM)**	**Function**
Sodium Chloride (NaCl)	118	Controlling buffer osmolarity; Source of Na^+ for ion homeostasis
Potassium Chloride (KCl)	4.7	Source of K^+ for ion homeostasis
Magnesium Sulphate ($MgSO_4$)	1.2	Source of Mg^{2+} for ion homeostasis
EDTA	0.5	Ion chelator Anticoagulant
Glucose	11	Metabolic substrate
Sodium Bicarbonate ($NaHCO_3$)	25	pH buffer
Calcium Chloride	1.3	Provides Ca^{2+} for cardiac contractile function

II.2 Composition of Buffers Used for Respirometry

BIOPS

Table 2: ***Composition of BIOPS for the preservation of biological samples and permeabilisation of fibres.*** pH 7.1

Constituent	**Concentration (mM)**	**Function**
CaK_2EGTA	2.77	Source of Ca^{2+} and K^+ for regulation of ion gradients EGTA functions as an ion chelator
K_2EGTA	7.23	Further source of K^+ and EGTA
Na_2ATP	5.77	Source of ATP to allow survival of tissue
$MgCl_2.6H2O$	6.56	Source of Mg^{2+} to augment enzyme function
Taurine	20	Muscle relaxant – depresses action potentials ROS scavenger
Na2PCr	15	Source of PCr for tissue energetics
Imidazole	20	Interferes with protein interactions to preserve tissue state
Dithiothreitol	0.5	Reduces disulphide bonds, further preventing protein-protein interaction
MES Hydrate	50	pH buffer

MiR05

Table 3: ***Composition of MiR05, the mitochondrial respiration medium.*** A muscle relaxant void of substrates; pH 7.1

Constituent	**Concentration (mM unless otherwise stated)**	**Function**
EGTA	0.5	Ion chelator
$MgCl_2.6H_2O$	3	Mg^{2+} to augment enzyme function
K-Lactobionate	60	Source of K+ for intracellular ion homeostasis
Taurine	20	Muscle relaxant – depresses action potentials ROS scavenger
KH_2PO_4	10	Phosphate source for ADP phosphorylation
HEPES	20	pH buffer
D-Sucrose	110	Impermeant for maintenance of osmolarity
BSA	1g/l	Ion chelator; binds free fatty acids

II.3 Measured SRM Transitions

C18Pfp Method

Table 4: *SRM Transitions measured using the C18pfp method*

Compound	Start Time (min)	End Time (min)	Polarity	Precursor (m/z)	Product (m/z)	Collision Energy (V)	RF Lens (V)
MDA	0	6.5	Positive	73.152	45.222	10.253	125
Alanine	0	6.5	Positive	90.1	44.275	11	30
[$^{13}C_1$]Alanine_1	0	6.5	Positive	91.1	44.275	11	30
[$^{13}C_1$]Alanine_2	0	6.5	Positive	91.1	45.275	11	30
[$^{13}C_2$]Alanine_1	0	6.5	Positive	92.1	45.275	11	30
[$^{13}C_2$]Alanine_2	0	6.5	Positive	92.1	46.275	11	30
[$^{13}C_3$]Alanine	0	6.5	Positive	93.1	46.275	11	30
Crn	0	6.5	Positive	114.1	86.141	11	49
ProIS	0	6.5	Positive	121.15	74.188	17	46
NicAm	0	6.5	Positive	123.152	80.165	19.556	30
NicAc	0	6.5	Positive	124.07	80.111	20.82	168
Vald8	0	6.5	Positive	126.1	80.2	10	41
Cr	0	6.5	Positive	131.975	43.111	29.972	30
Asn	0	6.5	Positive	133.1	116.049	8	42
Asn_2	0	6.5	Positive	133.2	60	20	44
Asn_1	0	6.5	Positive	133.2	74.12	16	44
Aspartate	0	6.5	Positive	134.175	74.175	15	31
[$^{13}C_1$]Aspartate_1	0	6.5	Positive	135.175	74.175	15	31
[$^{13}C_1$]Aspartate_2	0	6.5	Positive	135.175	75.175	15	31
[$^{13}C_2$]Aspartate_2	0	6.5	Positive	136.175	74.175	15	31
[$^{13}C_2$]Aspartate_1	0	6.5	Positive	136.175	75.175	15	31
[$^{13}C_2$]Aspartate_3	0	6.5	Positive	136.175	76.175	15	31
[$^{13}C_3$]Aspartate_2	0	6.5	Positive	137.175	75.175	15	31
[$^{13}C_3$]AspartateC3	0	6.5	Positive	137.175	76.175	15	31
[$^{13}C_4$]Aspartate	0	6.5	Positive	138.175	76.175	15	31
Leud10	0	6.5	Positive	142.025	96.2	8	35
Glutamate	0	6.5	Positive	148	84.15	16	46

[$^{13}C_1$]Glutamate_1	0	6.5	Positive	149	84.15	16	46
[$^{13}C_1$]Glutamate_2	0	6.5	Positive	149	85.15	16	46
[$^{13}C_2$]Glutamate_1	0	6.5	Positive	150	85.15	16	46
[$^{13}C_2$]Glutamate_2	0	6.5	Positive	150	86.15	16	46
Methionine	0	6.5	Positive	150.05	61.16	23	36
[$^{13}C_3$]Glutamate_1	0	6.5	Positive	151	86.15	16	46
[$^{13}C_3$]Glutamate_2	0	6.5	Positive	151	87.15	16	46
[$^{13}C_4$]Glutamate_1	0	6.5	Positive	152	87.15	16	46
[$^{13}C_4$]Glutamate_2	0	6.5	Positive	152	88.15	16	46
[$^{13}C_5$]Glutamate	0	6.5	Positive	153	88.15	16	46
Glu13C515NP	0	6.5	Positive	154.1	89.094	15	47
LysOH	0	6.5	Positive	163.2	100.1	16	48
MetSO	0	6.5	Positive	166	149.109	12	48
GuaO	0	6.5	Positive	168	151.1	19	84
Phed5	0	6.5	Positive	171.1	125.15	13	41
TyrOH	0	6.5	Positive	198.1	152.1	12	57
TyrNO2	0	6.5	Positive	227.1	181.1	12	83
GSH	0	6.5	Positive	308.1	233.104	13	68
cAMP	0	6.5	Positive	330.1	136.21	25	91
NsoGSH	0	6.5	Positive	337.13	307.054	10.253	122
cGMP	0	6.5	Positive	346	152.108	21	86
AMP	0	6.5	Positive	348.1	136.123	20	82
Ribofl	0	6.5	Positive	377.161	243.071	21.73	249
GSSG	0	6.5	Positive	613.2	355.161	22	106
NAD	0	6.5	Positive	664.1	136.237	43	103
FAD	0	6.5	Positive	786.2	348.153	20	146
Pyr	0	6.5	Negative	87	43	10	43
PyrNF	0	6.5	Negative	87	87	0	43
PyrU13C	0	6.5	Negative	90	45	10	43
PyrNFU13C	0	6.5	Negative	90	90	0	43
2OHBA	0	6.5	Negative	103.025	57.169	12	44
3OHBA	0	6.5	Negative	103.025	73.143	10	40
[$^{13}C_1$]3OHBA_1	0	6.5	Negative	104.025	73.143	10	40

[$^{13}C_1$]3OHBA_2	0	6.5	Negative	104.025	74.143	10	40
[$^{13}C_2$]3OHBA_1	0	6.5	Negative	105.025	74.143	10	40
[$^{13}C_2$]3OHBA_2	0	6.5	Negative	105.025	75.143	10	40
[$^{13}C_3$]3OHBA_1	0	6.5	Negative	106.025	75.143	10	40
[$^{13}C_3$]3OHBA_2	0	6.5	Negative	106.025	76.143	10	40
[$^{13}C_4$]3OHBA	0	6.5	Negative	107.025	76.143	10	40
Fum/kVal	0	6.5	Negative	115	71.172	7	50
[$^{13}C_1$]Fumarate_1	0	6.5	Negative	116	71.172	7	50
[$^{13}C_1$]Fumarate_2	0	6.5	Negative	116	72.172	7	50
[$^{13}C_2$]Fumarate_1	0	6.5	Negative	117	72.172	7	50
Succinate	0	6.5	Negative	117	73	10.2	45
[$^{13}C_2$]Fumarate_2	0	6.5	Negative	117	73.172	7	50
[$^{13}C_1$]Succinate_1	0	6.5	Negative	118	73	10.2	45
[$^{13}C_3$]Fumarate_1	0	6.5	Negative	118	73.172	7	50
[$^{13}C_1$]Succinate_2	0	6.5	Negative	118	74	10.2	45
[$^{13}C_3$]Fumarate_2	0	6.5	Negative	118	74.172	7	50
[$^{13}C_2$]Succinate_1	0	6.5	Negative	119	74	10.2	45
[$^{13}C_4$]Fumarate	0	6.5	Negative	119	74.172	7	50
[$^{13}C_2$]Succinate_2	0	6.5	Negative	119	75	10.2	45
[$^{13}C_3$]Succinate_1	0	6.5	Negative	120	75	10.2	45
[$^{13}C_3$]Succinate_2	0	6.5	Negative	120	76	10.2	45
[$^{13}C_4$]Succinate	0	6.5	Negative	121	76	10.2	45
Oxaloacetate	0	6.5	Negative	131	87.084	10	33
[$^{13}C_1$]Oxaloacetate_1	0	6.5	Negative	132	87.084	10	33
[$^{13}C_1$]Oxaloacetate_2	0	6.5	Negative	132	88.084	10	33
Pyr + formic	0	6.5	Negative	133	87	5	30
[$^{13}C_2$]Oxaloacetate_1	0	6.5	Negative	133	88.084	10	33
[$^{13}C_2$]Oxaloacetate_2	0	6.5	Negative	133	89.084	10	33
Malate	0	6.5	Negative	133	115.081	12	51
[$^{13}C_4$]MalateC4	0	6.5	Negative	133	119.081	12	51
[$^{13}C_3$]Oxaloacetate_1	0	6.5	Negative	134	89.084	10	33
[$^{13}C_3$]Oxaloacetate_2	0	6.5	Negative	134	90.084	10	33
[$^{13}C_1$]Malate	0	6.5	Negative	134	116.081	12	51

[$^{13}C_4$]Oxaloacetate	0	6.5	Negative	135	90.084	10	33
[$^{13}C_2$]Malate	0	6.5	Negative	135	117.081	12	51
[$^{13}C_3$]Malate	0	6.5	Negative	136	118.081	12	51
AKG	0	6.5	Negative	145	101.123	8	42
[$^{13}C_5{}^{15}NN$]Glu	0	6.5	Negative	152.1	134.102	13	55
Suc+formic	0	6.5	Negative	163	117	5	30
Aco	0	6.5	Negative	173.05	85.129	15	39
AscA	0	6.5	Negative	175.304	115	12.629	127
Oxal+formic	0	6.5	Negative	177	131	5	30
Mal+formic	0	6.5	Negative	179	133	5	30
Cit/Icit	0	6.5	Negative	191	111	15	53
AKG+formic	0	6.5	Negative	191	145	5	30
[$^{13}C_1$]Citrate_1	0	6.5	Negative	192	111	15	53
[$^{13}C_1$]Citrate_2	0	6.5	Negative	192	112	15	53
[$^{13}C_2$]Citrate _1	0	6.5	Negative	193	112	15	53
[$^{13}C_2$]Citrate _2	0	6.5	Negative	193	113	15	53
[$^{13}C_3$]Citrate _1	0	6.5	Negative	194	113	15	53
[$^{13}C_3$]Citrate _2	0	6.5	Negative	194	114	15	53
[$^{13}C_4$]Citrate _1	0	6.5	Negative	195	114	15	53
[$^{13}C_4$]Citrate _2	0	6.5	Negative	195	115	15	53
[$^{13}C_5$]Citrate _1	0	6.5	Negative	196	115	15	53
[$^{13}C_5$]Citrate _2	0	6.5	Negative	196	116	15	53
[$^{13}C_6$]Citrate	0	6.5	Negative	197	116	15	53
PCr	0	6.5	Negative	210	79.028	16	50
Aco+formic	0	6.5	Negative	219	173.1	5	30

BEH Amide Method

Table 4. ***SRM Transitions measured using the BEH Amide method.***

Compound	Start Time (min)	End Time (min)	Polarity	Precursor (m/z)	Product (m/z)	Collision Energy (V)	RF Lens (V)
Putr1	0	6	Positive	89.252	30.333	20.264	68
Putr2	0	6	Positive	89.252	48.151	10.253	68
Putr3	0	6	Positive	89.252	72.169	10.253	68
AlphaKBA_3	0	6	Positive	103.639	43.986	38.719	56
AlphaKBA_1	0	6	Positive	103.639	58	13.944	56
AlphaKBA_2	0	6	Positive	103.639	62.875	10.253	56
gammaANBA_2	0	6	Positive	104.039	40.986	19.91	30
gammaANBA_3	0	6	Positive	104.039	42.857	27.494	30
DMG_2	0	6	Positive	104.039	44	39.579	54
gammaANBA_1	0	6	Positive	104.039	58	10.253	30
DMG_1	0	6	Positive	104.039	58	14.146	54
DMG_3	0	6	Positive	104.039	62.889	10.253	54
HTaur_2	0	6	Positive	110.122	30.058	11.365	51
HTaur_3	0	6	Positive	110.122	44.986	18.444	51
HTaur_1	0	6	Positive	110.122	91.946	10.253	51
AcPutr1	0	6	Positive	131.23	72.097	16.017	108
AcPutr2	0	6	Positive	131.23	90.556	10.253	108
AcPutr3	0	6	Positive	131.23	114.111	10.253	108
Asp	0	6	Positive	134.175	74.175	15	31
Hypx	0	6	Positive	137.07	119.058	20.315	88
Lys/Gln	0	6	Positive	147.1	84.169	16	48
Glu	0	6	Positive	148	84.15	16	46
Gua	0	6	Positive	152.1	135.077	19	84
Glu13C515NP	0	6	Positive	154.1	89.094	15	47
SAla_2	0	6	Positive	154.122	71.889	14.5	132
SAla_1	0	6	Positive	154.122	112.889	10.253	132

SAla_3	0	6	Positive	154.122	133.373	10.253	132
gammaGluCys_3	0	6	Positive	251.191	98.875	25.169	82
gammaGluCys_2	0	6	Positive	251.191	168.903	14.096	82
gammaGluCys_1	0	6	Positive	251.191	210.071	10.253	82
78DHNP1	0	6	Positive	256.161	165.04	22.135	249
78DHNP2	0	6	Positive	256.161	208.04	16.118	249
78DHNP3	0	6	Positive	256.161	238.071	10.253	249
Ads	0	6	Positive	268.1	136.1	18	68
Ins	0	6	Positive	269.152	137.111	10.253	104
Guas	0	6	Positive	284.1	152.102	15	80
CMP	0	6	Positive	324.1	112.194	15	62
UMP	0	6	Positive	325	97.179	15	64
cAMP	0	6	Positive	330.1	136.21	25	91
cGMP	0	6	Positive	346	152.108	21	86
AMP	0	6	Positive	348.1	136.123	20	82
AMP_IS	0	6	Positive	363.1	146.123	20	82
GMP	0	6	Positive	364.1	152.197	16	67
SAH	0	6	Positive	385.1	136.132	20	73
SAM	0	6	Positive	399.1	250.147	16	79
CDP	0	6	Positive	404	112.132	19	71
UDP	0	6	Positive	405	97.062	16	74
TPP	0	6	Positive	426.061	304.96	16.522	249
ADP	0	6	Positive	428	136.174	24	91
Fol_2	0	6	Positive	442.1	176.071	37.86	83
Fol_1	0	6	Positive	442.1	295.071	16.876	83
Fol_3	0	6	Positive	442.1	401.04	11.517	83
GDP	0	6	Positive	444	152.08	18	83
DHF_2	0	6	Positive	444.026	324.889	19.101	97
DHF_3	0	6	Positive	444.026	365.946	13.994	97
DHF_1	0	6	Positive	444.026	402.889	10.253	97
MeTHF_3	0	6	Positive	460.109	179.986	37	88

MeTHF_1	0	6	Positive	460.109	313.04	19.708	88
MeTHF_2	0	6	Positive	460.109	418.942	10.253	88
CTP	0	6	Positive	484	112.234	21	91
UTP	0	6	Positive	485	378.973	20	73
CDP-ch	0	6	Positive	489.1	184.111	38	89
ATP	0	6	Positive	508	136.189	32	102
ATP_IS	0	6	Positive	513	141.189	32	102
GTP	0	6	Positive	524	152.106	24	95
UDP-glcNAC	0	6	Positive	608.1	99	16	90
NAD	0	6	Positive	664.1	136.237	43	103
NADH_3	0	6	Positive	666.183	301.929	37.961	100
NADH_2	0	6	Positive	666.183	513.942	25.118	100
NADH_1	0	6	Positive	666.183	649.014	15.966	100
NADP	0	6	Positive	744.1	136.2	46	121
NADPH_2	0	6	Positive	746.057	301.929	34.826	126
NADPH_3	0	6	Positive	746.057	427.929	24.966	126
NADPH_1	0	6	Positive	746.057	728.942	17.129	126
CoA	0	6	Positive	768.374	261.111	28.051	249
FAD	0	6	Positive	786.2	348.153	20	146
AcCoA	0	6	Positive	810.225	303.049	33.41	147
IBCoA	0	6	Positive	838.178	331.154	30.427	145
IVCoA	0	6	Positive	852.087	345.222	30.629	145
AcAcCoA	0	6	Positive	852.1	345.2	34	142
MalCoA	0	6	Positive	854.1	347.201	27	161
SucCoA	0	6	Positive	868.1	361.214	34	163
HMGCoA	0	6	Positive	912.191	405.222	33.309	249
Pyr	0	6	Negative	87	43	10	43
Pyr	0	6	Negative	87	87	0	43
AlphaKBA_N1	0	6	Negative	101.213	56.986	10.253	47
AlphaKBA_N2	0	6	Negative	101.213	59.952	10.253	47
AlphaKBA_N3	0	6	Negative	101.213	73.058	10.506	47

HTaur_N1	0	6	Negative	108.213	63.946	15.865	45
Fum	0	6	Negative	115	71.172	7	50
Suc	0	6	Negative	117	73	15	60
SucIS	0	6	Negative	121	76	10.2	45
Oxal	0	6	Negative	131	87.084	10	33
Mal	0	6	Negative	133	115.081	12	51
AKG	0	6	Negative	145	101.123	8	42
MelA	0	6	Negative	147.152	59.111	12.022	84
Glu13C515NN	0	6	Negative	152.1	134.102	13	55
PEP	0	6	Negative	167	79.081	14	45
DHAP	0	6	Negative	169	97.143	12	48
GA3p	0	6	Negative	169.009	97	10.253	54
Aco	0	6	Negative	173.05	85.129	14.5	39
2PG/3PG	0	6	Negative	185	97.065	16	53
Cit/Icit	0	6	Negative	191	111	15	53
Ery4p	0	6	Negative	199.009	97	10.253	98
PCr	0	6	Negative	210	79.028	16	50
MelA5p	0	6	Negative	227.122	97	17.23	141
Ribo5p	0	6	Negative	228.948	97	14.854	151
Ribu5p	0	6	Negative	229.283	97	10.253	121
DMApp	0	6	Negative	244.939	79	22.135	124
IPpp	0	6	Negative	245.252	79.058	22.084	135
G6P/F6P	0	6	Negative	259	97.077	17	60
BPG	0	6	Negative	265	97.084	22	80
6pGlcA	0	6	Negative	275.039	97	17.584	187
MelApp	0	6	Negative	307.039	209	14.348	217
CMPN	0	6	Negative	322.1	97.005	24	102
UMPN	0	6	Negative	323	97.034	23	94
cAMPN	0	6	Negative	328.1	134.115	26	108
FBPN	0	6	Negative	339	97.084	22	83
cGMPN	0	6	Negative	344	150.099	25	124

AMPN	0	6	Negative	346.1	134.111	34	108
AMPN_IS	0	6	Negative	361.1	144.111	34	108
GMPN	0	6	Negative	362.1	211.079	20	98
CDPN	0	6	Negative	402	158.926	27	115
UDPN	0	6	Negative	403	158.971	28	103
TPP_N	0	6	Negative	424.03	303.111	15.36	168
ADPN	0	6	Negative	426	134.136	25	120
GDPN	0	6	Negative	442	150.096	27	120
DHF_N1	0	6	Negative	442.183	176.044	26.382	133
DHF_N2	0	6	Negative	442.183	265.03	19.253	133
DHF_N3	0	6	Negative	442.183	313.097	18.848	133
MeTHF_N2	0	6	Negative	458.109	278.014	18.393	142
MeTHF_N1	0	6	Negative	458.109	279.04	18.596	142
MeTHF_N3	0	6	Negative	458.109	329.032	26.382	142
CTPN	0	6	Negative	482	158.921	30	110
UTPN	0	6	Negative	483	158.986	31	117
ATPN	0	6	Negative	506	158.983	32	123
ATPN_IS	0	6	Negative	511	158.983	32	123
GTPN	0	6	Negative	522	158.999	35	129
UDPglc	0	6	Negative	565.078	323	23.449	249
UDP-glcNACN	0	6	Negative	606.1	159	28	103

Appendix III

III.1 Intralipid and U-^{13}C Triglyceride Mixture Compositions

Table III.1: ***Composition of Intralipid.***

Constituent	% of Intralipid Represented
Egg Yolk Phopholipids	**1.2**
Glycerin	**2.25**
Soybean Oil (Lipid composition of which is as follows:)	**20%**
Linoleic Acid	44-62
Oleic Acid	19-30
Palmitic Acid	7-14
Linolenic Acid	4-11
Stearic Acid	1.4-5.5

Table III.2: ***Composition of U-13C Triglyceride Mixture (Cambridge Isotopes).***

Fatty Acid	Relative Area	Carbon Number	Sites of Unsaturation
palmitolenic	8.3%	16	2
hiragonic	6.4%	16	3
palmitoleic	5.7%	16	1
	1.0%	16	0
palmitic	19.6%	16	0
margaric	1.5%	17	0
linoleic	23.2%	18	2
oleic	25.6%	18	1
eliadic	1.9%	18	1
	3.6%	18	0
stearic	2.9%	18	0

Appendix V

V.1 Homogenisation Buffer Composition

Table V.1: ***Homogenisation Buffer Composition.***

Constituent	Concentration
HEPES	20 mM
EDTA	1 mM
Triton	0.1%